Evaluating growth patterns and element-to-calcium ratios of *Arctica islandica* (Bivalvia) shells as environmental proxies

Dissertation
zur Erlangung des akademischen Grades
„Doktor der Naturwissenschaften“
im Promotionsfach Geologie/Paläontologie

am Fachbereich 09 für Chemie, Pharmazie und Geowissenschaften
der Johannes Gutenberg-Universität in Mainz

von
Soraya Marali-Djame-Khiabani
geb. in Lingen (Ems)

Mainz 2016
(D77)

Dekan: Not displayed for reasons of data protection.
1. Berichterstatter: Not displayed for reasons of data protection.
2. Berichterstatter: Not displayed for reasons of data protection.
Datum der mündlichen Prüfung: 22. Februar 2017

Hiermit erkläre ich, dass ich die vorliegende Arbeit selbstständig verfasst und keine anderen als die angegebenen Quellen und Hilfsmittel benutzt habe.

Soraya Marali-Djame-Khiabani
Mainz, 30. November 2016

„Die Natur muss uns leiten.
Wer woanders sucht, als in der Natur,
verschwendet nur seine Zeit.

Die Natur beginnt mit einer Ursache
und am Ende steht dann die Erfahrung,

also beginne ich mit der Erfahrung
und erforsche die Ursache."

Leonardo da Vinci

Abstract

Long-term, coherent, multi-regional records of environmental parameters are needed to quantify the rapidity, persistence and geographic extent of climatic phenomena and/or (extreme) weather events. The aragonitic shell of the long-lived marine bivalve mollusk *Arctica islandica* records past environmental conditions in the climate-sensitive, extra-tropical North Atlantic Ocean over decades to centuries at an annual or even higher resolution. Due to synchronous shell growth, individual growth records can be stacked together to form so-called composite chronologies. These chronologies provide uninterrupted annual to sub-annual environmental proxy data over several centuries or even millennia. Although previous studies demonstrated that *A. islandica* shells are reliable paleoclimate archives, there are still research questions. The present study addresses the following issues: (1) Are shells from shallow water specimens also suitable to construct stacked chronologies? (2) Can chronology construction be facilitated and increment-based crossdating be tested by means of geochemical properties? (3) Are environmental factors driving the growth and trace element-to-calcium ratios of *A. islandica* shells?

In the first manuscript of this thesis, it has been demonstrated that the shell growth patterns of *A. islandica* from shallow (ca. 9 – 23 m), unpolluted waters off northeastern Iceland (1) grew synchronously over discrete time intervals and (2) shell growth responded to the local oceanographic conditions. (3) The degree to which the environmental signals are expressed in the chronology (i.e. the degree of growth synchrony between the specimens) is high, when the environmental year-to-year variability reaches a critical level, the strength of which needs to be determined in future studies. variability reaches a critical level, the strength of which needs to be determined in future studies. The second and third manuscript explored the trace element-to-calcium ratios of *A. islandica* shells by means of laser ablation-inductively coupled plasma-mass spectrometry (LA-ICP-MS) in line scan mode. The second article focused on shell barium-to-calcium (Ba/Ca) ratios of specimens from four distinct habitats (Iceland, Faroe Islands, Isle of Man, Gulf of Maine), showing that (4) shell Ba/Ca ratios were highly synchronous among coeval specimens from the same habitat and (5) may be related to marked increases in oceanic primary productivity. (6) The synchrony in shell Ba/Ca time-series was not influenced by changes in increment widths (as long as the sampling resolution is adequate, e.g., increment widths are not below the laser spot-size). Therefore, (7) shell Ba/Ca time-series can be used to double-check the temporal alignment of contemporaneous shells from the same locality. The last article examined additional means for assessing the reliability of shell element-to-calcium ratios, measured by laser ablation-inductively coupled plasma-mass

spectrometry (LA-ICP-MS) line scans, as proxies of environmental parameters. To do so, the reproducibility of trace element time-series was tested within specimens and between coeval shells from the same site. (8) Na/Ca time-series of this species were largely irreproducible and therefore likely contained no environmental information. (9) Sr/Ca and Mg/Ca time-series were well-reproducible within specimens and were synchronous among coeval *A. islandica* as long as shell growth patterns were similar. Thus, these ratios may function as growth line tracers (when studied with the techniques applied in the present article). (10) The degree to which Mn/Ca time-series were reproducible within each specimen were potentially lowered, because the Mn/Ca ratios of the shells were close to detection limits. Still, Mn/Ca time-series were running synchronous among coeval specimens from the same site over certain time intervals, which may indicate that shell Mn/Ca ratios are potentially influenced by environmental parameters. (11) Shell Ba/Ca ratios were the most reproducible both within and between specimens and thus probably contain a strong environmental signal.

Zusammenfassung

Lange, kontinuierliche, überregionale Zeitreihen von Umweltparametern sind wichtig, um die Geschwindigkeit, die Dauer und die geographische Dimension von klimatischen Phänomenen und/oder (extremen) Wettereignissen zu quantifizieren. Die aragonitische Schale der langlebigen marinen Muschel *Arctica islandica* zeichnet die Umweltbedingungen vergangener Zeiten im klima-sensitiven, außertropischen Nordatlantischen Ozean über mehrere Jahrzehnte bis Jahrhunderte mit einer jährlichen oder höheren zeitlichen Auflösung auf. Aufgrund des synchronisierten Schalenwachstums, können die Wachstumsmuster verschiedener Individuen zu sogenannten zusammengesetzten Chronologien kombiniert werden. Diese Chronologien liefern über mehrere Jahrhunderte oder sogar Jahrtausende annuell bis sub-annuell aufgelöste Proxy-Daten für die Rekonstruktion von Umweltparametern. Obwohl frühere Studien gezeigt haben, dass die Schalen von *A. islandica* verlässliche Paläo-Umwelt-Archive darstellen, sind noch immer Forschungsfragen offen, von denen die Folgenden in der vorliegenden Studie behandelt werden: (1) Sind die Schalen von Exemplaren aus dem Flachwasser ebenfalls geeignet um Chronologien zu erstellen? (2) Kann der Aufbau einer Chronologie erleichtert, sowie das Inkrement-basierte Crossdating durch geochemische Methoden getestet werden? (3) Steuern Umweltfaktoren das Wachstum und die Spurenelemente-zu-Kalzium-Verhältnisse von *A. islandica* Schalen?

Im ersten Manuskript dieser Dissertation wurde gezeigt, dass die Wachstumsmuster von *A. islandica* Schalen aus flachem (ca. 9 – 23 m), nicht verunreinigtem Meerwasser nordöstlich vor Island (1) über bestimmte Zeitabschnitte synchron zueinander wuchsen und (2) dass das Wachstum von den lokalen ozeanographischen Bedingungen gesteuert wurde. (3) Das Ausmaß zu dem Umweltsignale in der Chronologie enthalten sind (d.h., der Grad zu welchem das Schalenwachstum zwischen Individuen synchronisiert ist) war hoch, wenn die inter-annuelle Variabilität von Umweltparametern ein bestimmtes Level erreicht, dessen Höhe in kommenden Studien bestimmt werden muss. Das zweite und dritte Manuskript befassten sich mit den Spurenelement-zu-Kalzium Verhältnissen von *A. islandica* Schalen, welche mittels Linien-Messungen der Laser ablation-inductively coupled plasma-mass spectrometry (LA-ICP-MS) bestimmt wurden. Der zweite Artikel behandelte die Barium-zu-Kalzium (Ba/Ca) Verhältnissen in den Schalen von Exemplaren, welche von vier unterschiedlichen Habitaten stammen (Island, den Färöer Inseln, der Insel Man und dem Golf von Maine). Die Studie zeigte, dass die (4) Ba/Ca Verhältnisse in den Schalen der Muscheln, welche zeitgleich und im selben Habitat lebten, hochgradig synchron verliefen und (5) eventuell mit

ausgeprägten Anstiegen der ozeanischen Primärproduktion in Zusammenhang stehen. (6) Die Synchronität zwischen den Ba/Ca Zeitreihen der Schalen wurde nicht durch Änderungen in den Inkrementbreiten beeinflusst (jedenfalls nicht, solange die räumliche Auflösung während der Messung angemessen war, also z.B. die Inkrementbreite nicht unterhalb der Breite eines Laser-Punktes lag). (7) Deshalb können die Ba/Ca Zeitreihen von Schalen verwendet werden, um zu testen, ob die zeitliche Anordnung von gleichzeitig lebenden Proben aus der gleichen Lokalität korrekt war. Der letzte Forschungsartikel ermittelte zusätzliche Methoden, um festzustellen, ob bestimmte Element-zu-Kalzium Verhältnisse der Muschelschalen, welche mittels Linien-Messungen der Laser ablation-inductively coupled plasma-mass spectrometry (LA-ICP-MS) bestimmt wurden, als Umweltanzeiger geeignet sind. Dafür wurde die Reproduzierbarkeit von Spurenelement-Zeitreihen innerhalb von Proben, sowie zwischen zeitgleich existierenden Schalen erforscht, welche von der gleichen Lokation stammten. (8) Die Na/Ca Zeitreihen dieser Spezies konnten größtenteils nicht reproduziert werden und enthalten daher wahrscheinlich keine Umwelt-Information. (9) Die Sr/Ca und Mg/Ca waren innerhalb jeder Probe gut reproduzierbar und verliefen synchron zwischen gleichzeitig lebenden *A. islandica*, solange deren Schalen ähnliche Wachstumsmuster aufwiesen. Demzufolge könnten die Sr/Ca und Mg/Ca Elementverhältnisse vorwiegend als Indikatoren für Wachstumslinien fungieren (wenn sie mit denselben Techniken ermittelt werden, die auch im Artikel verwendet worden sind). (10) Das Ausmaß zu welchem sich Mn/Ca Zeitreihen innerhalb von Proben reproduzieren ließen wurde wahrscheinlich dadurch verringert, dass die Mn/Ca Verhältnisse der Schalen nahe der Nachweisgrenze waren. Trotz dessen verliefen Mn/Ca Zeitreihen verschiedener Individuen derselben Population in bestimmten Zeitabschnitten synchron zueinander, was darauf hinweisen kann, dass die Mn/Ca Verhältnisse der Schalen durch Umweltparameter beeinflusst sein könnten. (11) Die Ba/Ca Zeitreihen der Schalen waren sowohl innerhalb als auch zwischen Proben exzellent reproduzierbar und spiegeln daher höchstwahrscheinlich Umweltsignale wieder.

Danksagung

Not displayed for reasons of data protection.

Table of contents

List of figures

Captions are shortened.

Manuscript I

Manuscript II

Manuscript III

List of tables

Titles are shortened.

Manuscript I

Manuscript II

Manuscript III

Chapter 1
Introduction

1.1 Climate change and the relevance of studying past environmental variability

As shown by numerous studies, climate[1] is not constant over time, but has considerably changed throughout Earth's history (e.g., Dansgaard et al., 1993; Bradley, 1999; Ruddiman, 2008). Climatic variability is induced by forcing factors such as solar radiation (e.g., Jiang et al., 2005) and influenced by manifold feedback mechanisms which can either amplify or reduce the effects of any forcing on the climate system (Hays et al., 1976; Ruddiman, 2008; Kappas, 2009). Recent observations revealed, however, that climate is not only driven by natural factors. Anthropogenic activity likewise has left a strong imprint on global climate (Barnett et al., 2001; IPCC, 2007, 2013, 2014). The increasing concentrations of greenhouse gases (e.g., methane, carbon dioxide, nitrous oxide, water vapor) in the atmosphere – 'fueled' by the combustion of fossil energy sources – has most probably contributed to the global rise in average air and water temperatures during the last decades (e.g., Arrhenius, 1896; Briffa and Jones, 1993; Houghton et al., 1996; Levitus et al., 2000; Barnett et al., 2001; Jones et al., 2001; Ruddiman, 2008; IPCC, 2013, 2014). The contemporaneous destruction of climate-regulating ecosystems (e.g., forest, peatland, permafrost) has likely further promoted this trend (IPCC, 2007, 2013, 2014). In turn, climate change severely affects aquatic and terrestrial ecosystems and – ultimately – human health and societies (IPCC, 2014). The assessment of future climate is therefore an essential cornerstone for developing adaptation strategies and means for mitigation against the effects of altered environmental conditions (Bradley, 1999; IPCC, 2013, 2014). Reasonable quantitative and/or qualitative estimates of future climate, however, require a holistic understanding of Earth's climate system, which is composed of the atmosphere, hydrosphere (including the world's oceans), cryosphere, lithosphere, and biosphere (e.g., Ruddiman, 2008; Kappas, 2009; IPCC, 2013).

Knowledge about the modern climate system is obtained from instrumental measurements and/or historical evidence of various kinds. The red-to-green ratio of sunsets in historic paintings, for instance, can be related to the increase of dust particles in the atmosphere after major volcanic eruptions (Zerefos et al., 2014). Quantitative and accurate instrumental data, however, are only available for the most recent past (e.g., Jones et al., 1999). Sea surface temperatures (SST), for example, have

[1] Climate is defined as the average weather of a specific time period and area and is quantified from the mean value and variance of significant environmental variables such as (air) temperature, wind speed or precipitation rate (Ruddiman, 2008). In theory, climate phenomena operate on various temporal and spatial scales (e.g., Hays et al., 1976; Fritts et al., 1980; Ruddiman, 2008; Kappas, 2009). For practical reasons, the World Meteorological Organization defined climate as the average weather condition prevailing over (at least) 30 years, whereas meteorological changes of shorter time scales (hours to weeks) are referred to as 'weather' (e.g. Claussen, 2007; Ruddiman, 2008; Kappas, 2009).

only been recorded since ca. 1850, whereas accurate measurements of subsurface water temperatures exist since 1950 (Houghton et al., 2001). Less recent measurements typically represent only 'snapshots' in space and time and have to be treated with caution (Hurrel and Trenberth, 1999), as they can be biased (Folland and Parker, 1995). Satellites are able to remotely sense several environmental parameters at a high spatiotemporal resolution, but are only employed the mid-20th century (e.g., Blondeau-Patissier et al., 2014; Gregg and Rousseaux, 2014). All these environmental records are obviously too limited in space and time to unambiguously identify (1) the natural and anthropogenic factors driving climate, (2) the complex, interactive processes operating within the climate system (i.e., the feedback mechanisms), (3) the amplitude and rapidity of environmental alterations, and (4) the climatic trends and oscillations, which may be predictable (e.g., Jones et al., 2001; Jones and Mann, 2004). Capturing the full range of climatic variability requires an array environmental records (e.g., Jones et al., 2001), which have a high temporal resolution, at best span multiple decades, centuries, or even millennia, and cover multiple areas and different realms (i.e., terrestrial, aquatic, marine settings; see Jones et al., 2001). Such records will further profoundly help refining boundary conditions and selecting proper input variables for numeric climate models, and thus, for estimating future environmental scenarios (Bradley and Eddy, 1991; Jones et al., 2001; Jones and Mann, 2004).

1.2 The influence of the marine realm on Earth's climate

The world's oceans are significant components of the climate system, as they contribute to the transport of heat and masses around the globe (e.g., Visbeck, 2002; Levitus et al., 2000) and to greater depths in areas of deep water formation (e.g., northeast off Iceland; Kuhlbrodt et al., 2007). One of the key players influencing climate and weather in the Northern Hemisphere is the extra-tropical North Atlantic (e.g., Broecker, 1997; Rodwell et al., 1999; Visbeck, 2002; Marshall et al., 2001a). Warm surface ocean currents such as the Gulf Stream and its prolongation – the North Atlantic Current – carry heat, moisture and nutrients from the southwestern to the northeastern Atlantic; cold surface currents (e.g., the East Greenland and East Icelandic Currents), by contrast, introduce low saline and nutrient-poor waters into the Atlantic (e.g., Dickson et al., 1998; Valdimarsson and Malmberg, 1999; Hansen and Østerhus, 2000). Because the surface ocean is interacting with both the overlying atmosphere and the deeper ocean, its physicochemical properties such as sea surface temperature (SST) influence atmospheric and oceanic circulation patterns and vice versa (e.g., Palmer and Zhaobo, 1985; Deser and Blackmon, 1993; Rodwell et al., 1999; Manabe and Stouffer, 2000; Marshall et al., 2001b; Wanner et al., 2001). For example, numerical climate models

indicate that SST patterns in the North Atlantic Ocean impact atmospheric phenomena such as local storm tracks (Woollings et al., 2010; Brayshaw et al., 2011) and wintertime North Atlantic Oscillation (NAO; e.g., Deser and Blackmon, 1993; Rodwell et al., 1999). The inflow of Atlantic surface water influences large scale oceanographic circulation patterns such as the Atlantic Meridional Overturning Circulation (Lund et al., 2006) or the amount of sea ice by heating the Arctic (Spielhagen et al., 2011). The upper 700 m of the oceans, however, have warmed over the past decades (Levitus, 2000; IPCC, 2013, 2014), and spatiotemporally well-resolved data of oceanic parameters such as SSTs (Keeley et al., 2012) are urgently needed to evaluate the consequences on climate arising from this change.

1.3 Means for extending environmental records through space and time – an introduction to archives and proxies

Long-term, quantitative and qualitative information about past and/or spatially remote environments can be reconstructed from proxies (i.e., 'substitutes' or 'approximations' for instrumental measurements; e.g., Fritts et al., 1980; Hillaire and de Vernal, 2007; Ruddiman, 2008). Proxy data are stored within biogenic or abiogenic materials, generally referred to as climate or environmental archives. The perfect archive (1) records environmental parameters at precisely datable time intervals, e.g., by displaying regularly formed layers, which can be used to place proxy data into a temporal context. Furthermore, it (2) offers a high temporal resolution (at best over long, uninterrupted time intervals), (3) has a relatively broad geographical range, and (4) is abundant through time. In practice, each environmental archive has its own characteristics in terms of spatiotemporal resolution and the type(s) of proxy data it contains. Common proxies are physical features (e.g., the width, density or hardness of periodically formed layers visible in a certain climate archive) or geochemical parameters of the archive (stable or radiogenic isotopes, trace elements etc.; see Fritts, 1976; Ruddiman, 2008). Ideally, one proxy is related to a single environmental driving factor or to a reasonable number of factors (e.g., seawater temperature; compare Freitas et al., 2006). The ratio of the heavy to the light isotope of oxygen (i.e., $^{18}O/^{16}O$, denoted as $\delta^{18}O$) of marine bivalve shells, for example, is directly related to both the temperature and the $\delta^{18}O$ value of the seawater from which the shell has been secreted, and thus, is a proxy for both parameters (e.g., Urey et al., 1951, Epstein et al., 1951, 1953; Epstein and Lowestam, 1953; Grossman and Ku, 1986; Dettman et al., 1999).

Tree-rings (e.g., Fritts, 1976; Briffa et al., 1986; Büntgen et al., 2011; Esper et al., 2002, 2016), speleothems (e.g., Treble et al., 2003; Fairchild et al., 2006; Drysdale et al., 2007; Scholz et al., 2014; Jamieson et al., 2015), ice cores (e.g., Dansgaard et al., 1982, 1993; Loulergue et al., 2008), terrestrial deposits (e.g., Hunt et al., 1995), as well as freshwater sediments containing plant or insect remains (Wooller et al., 2007) are important archives of the environmental variability in the terrestrial realm. Oceanic conditions are recorded, for example, by marine sediment cores (e.g., Martinson et al., 1987) and the microfossil assemblages within them (e.g., Eiríksson et al., 2006; Knudsen et al., 2012), photosynthetic corals (e.g., Beck et al., 1992; Mitsuguchi et al., 1996; Shen et al., 1996; Alpert et al., 2016) and their non-photosynthetic, cold-water counterparts (e.g., Montagna et al., 2007, 2014; McCulloch et al., 2010; López Correa et al., 2012; Marali et al., 2013), sclerosponges (e.g., Böhm et al., 2000), stromatolites (e.g., Rosenberg and Jones, 1975), coralline red algae (e.g., Kamenos et al., 2008; Hetzinger et al., 2013; Caragnano et al., 2014; Teichert and Freiwald, 2014), fish otoliths (e.g., Pannella, 1971; Bath et al., 2000; Black et al., 2008; Gillanders and Munro, 2012), and mollusks (e.g., Davenport, 1938; Schöne et al., 2002; Strom et al., 2005; Butler et al., 2010).

Among the marine proxy archives mentioned above, mollusk shells are particularly valuable environmental recorders, because they are common constituents of the benthic communities since the Cambrian era and are distributed worldwide. In fact, mollusks are not limited to the marine environment, but also occupy freshwater and terrestrial habitats (see Huber, 2010), and thus, archive the environmental variability in several realms. Most importantly, mollusk shells are accreted periodically and display well-defined shell growth patterns, subdivided into (a) relatively wide, rapidly accreted growth increments and (b) narrow, growth lines that are formed during slow growth and at regular – annual, seasonal, or even sub-daily – time periods (e.g., Rhoads and Lutz, 1980; Schöne et al., 2004, 2005a; Schöne, 2008). The environmental data encoded in the physicochemical properties of mollusk shells are deciphered with sclerochronological techniques which will be briefly introduced in the following section. Thereafter, the benefits of the bivalve mollusk *A. islandica* as an exceptional environmental recorder will be presented.

1.4 The bivalve mollusk *Arctica islandica*

The bivalve *A. islandica* (Linnaeus, 1767), commonly known as the 'ocean quahog', the 'Icelandic cyprine' or the 'mahogany clam', is an outstanding environmental archive for the extra-tropical North Atlantic. The ecology, growth and population dynamics of *A. islandica* have been intensively studied (e.g., Merril and Ropes, 1969; Murawski et al., 1982; Brey et al., 1990; Josefson et al., 1995; Thorarinsdóttir and Steingrímsson, 2000; Holmes et al., 2003), because this species is an important food source for benthic and pelagic fish populations (e.g., Brey et al., 1990) and has been exploited for human consumption (e.g., Merrill and Ropes, 1969). More recently, *A. islandica* shells have been recognized as archives of environmental variability (see Schöne, 2013 for a review).

1.4.1 Ecology

A. islandica is a shallow-borrowing bivalve that inhabits sandy, silty or muddy sediments (e.g., Thompson et al., 1980; Thorarinsdóttir and Jacobson, 2005; Huber, 2010), where it feeds on suspended particles (e.g., Josefson et al., 1995) and/or the organic-rich microlayer of the sediment surface (Morton, 2011). Due to its slow metabolism and its ability to respire anaerobically for several days, *A. islandica* is perfectly adapted to cold and temporally oxygen-deficient environments (e.g., Oeschger, 1990; Begum et al., 2009; Strahl et al., 2011a, b). It can even withstand anoxic conditions and increased hydrogen sulphide concentrations (Theede et al., 1969; Taylor, 1976; Oeschger, 1990; Oeschger and Storey, 1993). The condition and growth of invertebrates such as *A. islandica* depends on environmental factors, primarily the availability and quality of foodas well as ambient temperature. *Arctica islandica* prefers fresh phytodetritus over old, re-suspended organic matter (Erlenkeuser, 1976), and therefore, likely records changes in ocean primary productivity. Previous studies highlighted the dependence among shell growth and food supply (e.g., Witbaard et al., 1999; Butler et al., 2010, 2013; Schöne, 2013). An excess supply of food particles, however, has a negative influence on filtration rates (Winter, 1969) and probably hampers bivalve shell growth. Ambient water temperature affects the respiratory rates of *A. islandica* specimens (Begum et al., 2009) and ultimately the geographic distribution of the species (Merrill and Ropes, 1969; Mann, 1989). *A. islandica* tolerates water temperatures between 0 and 16 °C (Mann, 1982) and survives up to 20 °C for brief time periods (Winter, 1969), but prefers 6 °C to 10 °C (Mann, 1982). Icelandic specimens seem to prefer temperatures below 12 °C (Thorarinsdóttir and Jacobson, 2005). *A. islandica* bears salinities between 22 and 35 (Oeschger and Storey, 1993), but is stressed if low temperature and low salinity conditions prevail (Begum et al., 2010; Hiebenthal et al., 2012).

1.4.2 Reasons why A. islandica shells are unprecedented environmental archives

The aragonitic shell of *A. islandica* has been identified as a particularly well-suited environmental archive, because (1) it contains highly distinct, annual growth lines (e.g., Jones, 1980; Thompson et al., 1980; Turekian et al., 1982; Ropes et al., 1984; Witbaard et al., 1994). Even daily growth lines can be discerned in the relatively wide growth increments of the ontogenetically young, fast growing part of the shell (Schöne et al., 2004, 2005a). These annual (or daily) growth patterns provide an absolute dating control for assigning calendar years (or days) to each part of the shell. (2) Bivalve shell growth is controlled by biological parameters (e.g., bivalve health, metabolism) and environmental factors (see Thompson et al., 1980; Witbaard, 1996; Schöne, 2008, 2013). Therefore, information on ambient parameters can be inferred from the width of annual growth increments (e.g., Witbaard, 1996; Wanamaker et al., 2009; Butler et al., 2013; Lohmann and Schöne, 2013; Holland et al., 2014a; Mette et al., 2016). (3) The geochemical composition of *A. islandica* shells provides further information on environmental parameters (e.g., Weidman et al., 1994; Schöne et al., 2004, 2005b, c, 2010, 2013; Dunca et al., 2009; Wanamaker et al., 2011; Holland et al., 2014b). (4) *A. islandica* accretes its shell during both seasonal extremes, i.e., summer and winter conditions are recorded, for example, temperature by shell $\delta^{18}O$ (Schöne et al., 2005a, b, c).

(5) Due to their low metabolic rates, *A. islandica* specimens are extraordinarily long-lived (Ropes and Murawski, 1983; Thompson et al., 1980; see also Abele et al., 2008, 2010; Begum et al., 2009; Strahl et al., 2011a, b): Maximum ages of 375 to 507 years have been reported (Schöne et al., 2005c; Wanamaker et al., 2008; Butler et al., 2013), i.e., each single shell is a multi-decadal to multi-centennial archive of environmental conditions. Furthermore, (6) environmental drivers synchronize the shell growth patterns of different specimens from the same population (e.g., Jones, 1980; Thompson et al., 1980; Witbaard, 1996; Schöne, 2013) and even among populations living more than 80 km apart from each other (Witbaard et al., 1997; Butler et al., 2009; Holland et al., 2014a). Thus, the 'relative' shell growth of individuals with overlapping lifespans can be combined to form longer (master) chronologies (details on how 'relative' shell growth is determined are given in section 1.4.3; e.g., Thompson et al., 1980; Marchitto et al., 2000; Butler et al., 2010, 2013; Lohmann and Schöne, 2013; Holland et al., 2014a; Mette et al., 2016). The resulting chronologies can span several centuries (Lohmann and Schöne, 2013; Holland et al., 2014a; Mette et al., 2016) or more than one millennium (Butler et al., 2013) and include the growth histories and geochemical proxy records of several bivalve generations.

In addition, (7) *A. islandica* is widely distributed along the continental shelves and slopes of the North Atlantic Ocean. Modern populations occur along the eastern coast of North America from Cape Hatteras (North Carolina, USA) to southeastern Newfoundland, off Iceland, the Faroe Isles, the British Isles, and Spitzbergen, and inhabit the European waters from the Spain to Norway and the westernmost part of the Baltic Sea, the Barents Sea and the White Sea (Abbott, 1954; Merrill and Ropes, 1969; Nicol, 1951; Dahlgren et al., 2000). Subfossil populations had an even wider geographic range and stretched, for example, into the Mediterranean Sea and from northern Newfoundland to southwestern Greenland (see Dahlgren et al., 2000: Fig. 1 and references therein). (8) The bivalve species is suitable to study modern and deep time oceanographic change: Its fossil record reaches back into the early Cretaceous (Nicol, 1951) or even into the Jurassic (Casey, 1952). Finally, (9) *A. islandica* dwells from the first few meters of the ocean (Forbes and Hanley, 1853) down to 256 m (Merrill and Ropes, 1969) or even to 482 m water depth (Nicol, 1951), and thus, is an archive for both surface and deeper waters.

1.4.3 An introduction to bivalve scleorchronology

Sclerochronolgy is an analogue to dendrochronology (tree-ring research) and studies the growth patterns and the geochemistry of periodically accreted hard parts of organisms (Budenmeyer, 1974; Hudson et al., 1976; Oschmann, 2009) such as mollusk shells. The analysis of shell growth patterns and the construction of increment-width based chronologies is a prerequisite for dating the environmental record contained in the hard parts. In mollusk shells, precise calendar dates can be assigned to proxy data by counting back the number of growth increments accreted prior to the date of death (e.g., Schöne, 2008; Füllenbach et al., 2015). Since this dissertation focuses on the shells of the bivalve mollusk *A. islandica*, the techniques for growth pattern analysis in mollusk shells will be briefly outlined below.

Bivalve shell growth decreases throughout lifetime. *Arctica islandica* shells grow particularly fast during age three to seven (Thompson et al., 1980), but shell growth ceases markedly once the bivalve has reached sexual maturity after ca. ontogenetic age 10–13 (e.g., Thompson et al., 1980; Kennish et al., 1994; Thorarinsdóttir and Steingrímsson, 2000). Other authors also report an obvious decline in growth after the shell reached ca. 60 mm in height (which corresponds approximately to ontogenetic years 24 in males and 32 in female bivalves; Steingrímsson and Thórarinsdóttir, 1995). Superimposed on the ontogenetic trend in *A. islandica* shell growth is additional variability which is partly driven by environmental changes, but also caused by

biological factors (see chapter 1.4.2). In order to compare the shell growth patterns of different individuals from the same site with each other, the ontogenetic trend has to be estimated and eliminated mathematically. This methodology evolves from tree-ring research (e.g., Cook and Kairiukstis, 1990). The growth trend is removed by dividing or subtracting the measured increment width from the expected width; the latter is the value of the respective trend calculated for a shell (compare Schöne, 2013). By this, a new time-series of relative annual shell growth is created; the dimensionless values of this time-series (termed growth indices, GIs) provide information whether growth rate was higher or lower than the estimated rate in each single year of the time-series. The relative shell growth patterns of different individuals from the same population can be easily compared to each another, and growth patterns of shells with overlapping lifespans can be combined to a composite (sclero-) chronology. For ease of comparison with existing chronologies, the composite GI chronology can be 'standardized' by subtracting the mean of the whole chronology from each GI-value and then dividing the result by the standard deviation of the chronology to obtain a standardized growth index for each year (SGI; Schöne, 2005c; for details and equations see manuscript I). If a temporal variation in (relative) shell growth is shared by several specimens, the environmental signal within a chronology is particularly strong. The strength of this 'common signal' is statistically assessed with methods developed in dendrochronology (such as the expressed population signal, EPS; Wigley et al., 1984). A master chronology is considered statistically robust if the EPS value exceeds 0.85 (Wigley et al., 1984). The increment-width based chronologies are then the temporal frame for geochemical analysis.

1.5 Motivation and overview of research

As highlighted in the previous section, shells of *A. islandica* are precisely datable, annually to sub-annually resolved, multi-proxy archives that are eminently important for reconstructing the environmental variability in the northern North Atlantic and adjacent seas over long uninterrupted intervals of time. Various paleoclimate studies have been performed on *A. islandica* over the past decades (see Schöne, 2013, for a review). Nonetheless, there are still further research needs with respect to the proxies contained in the shells of this bivalve species. In the present thesis, two types of controversial proxies have been targeted: Shell growth rates and trace element-to-calcium ratios. Three studies were conducted for this purpose: The first one focuses on shell growth rates of shallow-dwelling *A. islandica* from the climate-sensitive North Icelandic Shelf. The second study explores shell Ba/Ca ratios of specimens from four different sites. The third one tests the reproducibility of element-to-calcium ratios (Na/Ca, Mg/Ca, Mn/Ca, Sr/Ca, Ba/Ca) derived from LA-ICP-MS analysis to assess the strength of an environmental signal within the geochemical time-series. The three manuscripts of this dissertation are already published or are in press in the international, peer-reviewed journal Palaeogeography, Palaeoclimatology, Palaeoecology.

1.5.1 Manuscript I: Shell growth

Manuscript I focuses on the growth of modern *A. islandica* collected from a relatively shallow water locality on the North Icelandic Shelf. This area is influenced by two surface ocean currents: The warm, saline Irminger Current (Atlantic water), which encircles Iceland clockwise, and the cold, fresher East Icelandic Current (Arctic and Polar water) approaching Iceland from the North. The boundary between these contrasting water masses is termed the oceanic Polar Front. The dominance of either surface current (i.e., the latitudinal position of the Polar Front) profoundly affects the oceanic and atmospheric circulation patterns, as well as local ecosystems. Understanding short-term and long-term environmental variability in this climate-sensitive area requires spatiotemporally well-resolved records of surface ocean parameters such as sea surface temperature.

Previous work on sediment cores revealed long-term paleoceanographic trends (e.g., Eiríksson et al., 2000, 2006; Knudsen et al., 2004; Jiang et al., 2005; Ran et al., 2011). However, the temporal resolution of these sedimentary archives varies among ca. 2 and 40 years, which is sufficient to study inter-decadal variability (e.g., Sicre et al., 2008a, b), but too low to resolve inter-annual or even seasonal environmental changes.

This resolution does also not permit the recognition of extreme events in SST or salinity. Annual shell growth patterns of *A. islandica* are synchronized among individuals from the same population (see chapter 1.3), and therefore, increment-width based chronologies probably likely information on the environmental cues controlling shell growth. However, the factors controlling and synchronizing relative shell growth patterns within a population are not fully understood, especially in the case of bivalves living in relatively shallow water. Knowledge about the driving factors is needed to interpret changes in relative shell growth patterns in terms of environmental change, and thus, to refine environmental reconstructions. According to Schöne et al., (2005c), *A. islandica* shell growth was also highly variable during times when climate varied strongly from year-to-year. Periods of low inter-annual climate variability, in turn, corresponded to reduced year-to-year variability in shell growth. Indeed, specimens which lived close to or below the thermocline display variations in shell growth at decadal and/or multi-decadal frequencies (e.g., Butler et al., 2010; Lohmann and Schöne, 2013; Holland et al., 2014a). Similar frequencies have been identified in environmental time-series (e.g., Holland et al., 2014a). For this reason, previous studies concluded that shell growth responds to relatively long-term changes in ambient conditions (e.g., food level and/or temperatures; see Witbaard et al., 1997), which are, in turn, related to (cyclic) variations of atmospheric parameters, e.g., sea level pressure (Lohmann and Schöne, 2013) and NAO (Schöne et al., 2004, 2005c), sea surface temperature (Butler et al., 2013; Lohmann and Schöne, 2013), oceanic circulation patterns (e.g., Atlantic Meridional Overturning Circulation, AMOC; Schöne et al., 2005c; Holland et al., 2014a), solar activity (Butler et al., 2010; Holland et al., 2014a) or volcanic cooling (Schöne et al., 2005c).

So far, two increment-width chronologies have been constructed for Iceland, both of which used *A. islandica* that lived well below or close to the thermocline (Butler et al., 2013; Lohmann and Schöne, 2013). Butler et al. (2013) constructed a 1357-year long chronology based on northern Icelandic specimens from 75 m water depth. The authors observed that shell growth was correlated to sea surface temperature on decadal time scales, but not on the year-to-year basis. Also, the strength of the decadal relationship was rather low and varied over time. Intriguingly, Butler et al. (2013) did not find any correlation between shell growth and bottom water temperature. Lohmann and Schöne (2013) examined *A. islandica* shells from ca. 30 m water depth and found relationships among shell growth and short-term atmospheric phenomena (i.e., sea level pressure patterns) or longer-term changes in North Atlantic oceanography. Shells from above the thermocline may record surface ocean conditions and (short-term) oscillations arising from ocean-atmosphere interactions in form of shell growth patterns and/or geochemical parameters (e.g., Dunca et al., 2009). However, previous studies reported that shells of shallow-dwelling specimens were not growing synchronously because of

(anthropogenic) disturbances. These shells did not contain a distinct environmental signal (Epplé et al., 2006), and were considered inappropriate for the construction of increment width-based chronologies (e.g., Turekian et al., 1982; Epplé et al., 2006; Stott et al., 2010). Consequently, the growth patterns of shallow-water specimens have not been used as environmental proxies, so far.

Manuscript I – Research questions

The first manuscript of this dissertation explores the potential of shallow-dwelling *A. islandica* as environmental recorders and addresses the following research questions:

- Is relative shell growth synchronized between *A. islandica* specimens from shallow and unpolluted waters off northeast Iceland? In other words, are the increment width time-series from shallow water specimens suitable to construct (statistically robust) composite chronologies?
- Which environmental factors control and synchronize relative shell growth of *A. islandica* specimens at the sampling locality? In particular, how strong is the relationship between shell growth and SST?
- Is the relationship between *A. islandica* shell growth and the environmental cues stable through time? And, if not, what are the potential reasons for temporal changes in the strength of the relationship?
- How do environmental conditions in the research area develop through time and what is the impact of changing oceanographic conditions on bivalve shell growth?
- And finally, is the relative shell growth rate of shallow water *A. islandica* a reliable and independent proxy for ambient sea surface temperature?

Manuscript I – Strategy

Living *A. islandica* and were sampled from ca. 9–23 m water depth. Additionally, subfossil shells were collected from two beaches. All specimens were stained with Mutvei's solution, to increase the distinguishability of annual growth lines and facilitate the measurement of annual growth increments. The increment width time-series of different (live-collected and subfossil) individuals were aligned in time with dendrochronological methods based on synchronous changes in relative annual shell growth and two versions of a composite chronology were constructed: The first version was constructed by using a stiff detrending technique (negative exponentials, NE) to

retain longer term variations in shell growth. The second chronology version used first differencing (FD) to increase year-to-year variability in relative increment widths. The spectral characteristics of both chronology versions (i.e., periodic changes in relative shell growth patterns) were investigated. Finally, it was tested, if relative shell growth patterns were correlated to ambient sea surface temperature or sea surface salinity, which were, in turn, driven by the strength of local surface ocean currents.

1.5.2 Manuscript II: Shell Ba/Ca ratios

The barium-to-calcium (Ba/Ca) ratios of bivalve shells are promising proxies for oceanic water chemistry. Typically, Ba/Ca time-series of bivalve shells consist of low and invariant 'background' values, which are interrupted by sharp, erratic maxima (Ba/Ca 'peaks'; see Stecher et al., 1996; Gillikin et al., 2006, 2008). The background Ba/Ca ratios of bivalve shells are strongly correlated to the Ba/Ca ratio of the water in which the bivalve lived (Gillikin et al., 2006; Poulain et al., 2015). In turn, the water Ba/Ca ratio is negatively correlated to ambient salinity and can be influenced by various oceanic processes (Goldberg and Arrhenius, 1958; Dehairs et al., 1980; Dymond et al., 1992) such as the release of dissolved barium from sedimentary barite particles (Dymond et al., 1999) or decaying phytoplankton associates (e.g., Dehairs et al., 1980) under oxygen-deficient conditions.

Previous studies suggested that the Ba/Ca peaks of bivalve shells could also be triggered by environmental factors (e.g. Stecher et al., 1996; Vander Putten et al., 2000; Gillikin et al., 2008; Barats et al., 2009), because different individuals from the same locality display Ba/Ca maxima of similar amplitudes at exactly the same time of the year(s) (Stecher et al., 1996; Vander Putten et al., 2000; Gillikin et al., 2008; Barrats et al., 2009). The inter-specimen synchrony of Ba/Ca maxima, however, has only been proven for short-lived bivalve species and/or young individuals of longer-lived species (Schöne et al., 2013). Moreover, despite intensive research, the environmental control which causes Ba/Ca shell maxima is unknown. If Ba/Ca maxima were unrelated to increment widths and synchronized even between specimens from the same locality which differ in ontogenetic age, Ba/Ca peaks may even help identifying genuine or false increments, and thus, improving the accuracy of crossdating.

Manuscript II –Research questions

The second manuscript examines the Ba/Ca ratios of mature and ontogenetically old *A. islandica* specimens tackling the following research questions:

- What are the characteristics of Ba/Ca shell time-series of mature and ontogenetically old shells?
- Is there any relationship between shell growth patterns and shell Ba/Ca maxima?
- Are there any trends in shell Ba/Ca background or maximum values through the lifetime of the bivalves? And, if so, are they related to shell aging and is there any technique for eliminating such trends?
- Are maximum Ba/Ca ratios synchronized among coeval mature *A. islandica* specimens of similar and different ontogenetic age living at the same locality? And are synchronous Ba/Ca maxima similar in terms of amplitude and shape?
- Do annually averaged Ba/Ca ratios of shells differ among different habitats (shallow/deeper water; nearshore/offshore)?
- Which environmental factors trigger Ba/Ca shell peaks? Is there any relationship to surface ocean primary productivity pulses (i.e., to chlorophyll a; Chl *a*)?
- Can Ba/Ca maxima serve as an additional means for crossdating different *A. islandica* specimens from the same locality?

Manuscript II – Strategy

Specimens were selected from four published composite increment-width based chronologies, corresponding to four distinct habitats: (1) The shallow (ca. 10 m), unpolluted waters off northeastern Iceland (i.e., the chronology established in the course of the first manuscript; see section 2.1), (2) shallow (ca. 30 m) marine waters within the Faroe Island fjords (Matras, 2011), (3) deeper waters off the Isle of Man (ca. 30–57 m; Butler et al., 2010) and (4) from the Gulf of Maine (ca. 80 m; Griffin, 2012). The specimens at each site differ by ontogenetic age and/or the degree to which shell growth is synchronized. Laser ablation-inductively coupled plasma -mass spectrometry (LA-ICP-MS) analysis was applied to determine Ba/Ca ratios in the hinge area of the shells. Annual averages of Ba/Ca ratios were compared to conspicuous annual Chl *a* maxima in the North Atlantic. Furthermore, the synchrony of non-averaged and annually averaged Ba/Ca time-series between specimens from the same habitat was assessed.

1.5.3 Manuscript III: Shell trace elements as proxies

In addition to Ba/Ca ratios, various other element-to-calcium ratios have been considered as potential paleo-environmental proxies. Therefore, trace elements were previously explored in *A. islandica* shells, as well as in other biogenic and non-biogenic calcium carbonates. Sr/Ca ratios of tropical, photosynthetic coral species, for example, are closely related to ambient sea surface temperature (e.g., Smith et al., 1979; Beck et al., 1992; Mitsuguchi et al., 1996), whereas in shells of the bivalve *Tridacna gigas* Sr/Ca ratios traced the daily light cycle (Sano et al., 2012; Warter and Müller, 2017). Mg/Ca ratios are paleo-temperature tracers in corals (e.g., Mitsuguchi et al., 1996) or foraminifera (Lea et al., 1999). However, in bivalve shells both the Sr/Ca and the Mg/Ca ratios are not considered fully reliable indicators of water temperature (e.g., Takesue and van Geen, 2004; Freitas et al., 2006). In fact, both Vander Putten et al. (2000) and Freitas et al. (2006) reported that the relationship between Mg/Ca and temperature changes within bivalve specimens. The Na/Ca ratio of foraminifera tests serves as a salinity proxy (Wit et al., 2013), whereas in the case of bivalve shells, the applicability of Na/Ca is yet uncertain (e.g., Rucker and Valentine, 1961; O'Neil and Gillikin, 2014). Other element-to-calcium ratios in bivalve shells (such as Ba/Ca and Mn/Ca) have apparently a greater potential as proxies for water geochemistry, which is in turn related to complex, interactive environmental processes (e.g., redox processes which can be associated with oxygen deficiency caused by increased primary productivity pulses; compare Vander Putten et al., 2000; Langlet et al., 2007 for Mn/Ca, Gillikin et al., 2006, 2008 for Ba/Ca). Despite promising results, element-to-calcium ratios of biogenic hard tissues are still considered 'equivocal' proxies, because they are not only driven by environmental controls, but also influenced by biological parameters (so-called 'vital effects'). Furthermore, analytical uncertainties cause 'noise' (i.e., random, non-reproducible temporal variations) to the trace element time-series. For this reason, it is inevitable to thoroughly test, if a measured trace element time-series contains an external environmental 'signal', biological information or merely reflects (analytical) noise.

Basically, three approaches allow for testing, if a genuine environmental (or biological) signal, is encoded within the temporal variation of a trace element of a biogenic carbonate (e.g., a bivalve shell): (1) In calibration studies, the trace element time-series are compared to changes in environmental factors and/or physiological parameters (e.g., bivalve shell growth rates; e.g., Carré et al., 2006; Füllenbach et al., 2015). (2) The biological controls on trace element transport and incorporation mechanisms into the shell provide the basis for determining whether any trace element could serve as an environmental proxy (e.g., Foster et al., 2008, 2009; Soldati et al., 2016). (3) The third, rather simple, but effective approach is to test, if a trace

element time-series – determined with a certain analytical technique – is reproducible within and/or between specimens (Sinclair et al., 2005, 2011; Anagnostou et al., 2011). Environmental and/or biological signals, contained in any trace element time-series should be consistent within a specimen, as well as between specimens from a common growth period and habitat (e.g. Sinclair et al., 1998; Vander Putten et al., 2000; DeLong et al., 2007). However, trace element time-series may also be synchronized between specimens which have similar shell growth patterns, if the concentration of the element under examination is somehow associated with skeletal growth (Gillikin et al., 2005).

Assessing element-to-calcium ratios in bivalve shells and other climate archives requires an appropriate analytical technique. LA-ICP-MS is a promising methodology for determining trace elements in situ. Holland et al. (2014a), for instance, applied LA-ICP-MS in the hinge region of long-lived *A. islandica* from the North Sea and revealed relations among shell Fe/Ca ratios and land-use in adjacent agricultural areas. At a higher temporal resolution, Füllenbach et al. (2015) revealed that Sr/Li ratios determined by LA-ICP-MS in shells of the short-lived bivalve Cerastoderma edule were highly correlated to ambient water temperature in the dynamic intertidal zone of the North Sea. In summary, the degree of reproducibility of trace element time-series within and between specimens is a measure for (a) the fidelity of LA-ICP-MS measurements and (b) the amount of environmental and/or biological signal comprised in shell element-to-calcium ratios. So far, however, only few studies assessed whether trace element time-series determined by LA-ICP-MS in line scan mode were reproducible and thus reliable environmental tracers.

Manuscript III – Research questions

The third manuscript of this thesis explores means for evaluating the potential of trace element-to-calcium ratios of *A. islandica* shells as environmental proxies by assessing intra- and inter-specimen reproducibility of Na/Ca, Mg/Ca, Mn/Ca, Sr/Ca, and Ba/Ca ratios determined by LA-ICP-MS line scans in the hinge area. The following main research questions were addressed:

- Which element-to-calcium ratios are associated with a certain shell microstructure (i.e., annual growth lines and/or increments)?
- Are element-to-calcium ratios related to the ontogenetic age of a specimen? If so, is this relationship resulting from the reduced spatial resolution with increasing age (i.e., decreasing annual increment widths)?
- How well can Na/Ca, Mg/Ca, Mn/Ca, Sr/Ca, and Ba/Ca ratios be reproduced within the hinge of each specimen?

- How synchronous run element-to-calcium ratios between specimens which lived at the same locality and time period?
- Is the synchrony of trace element time-series between coeval shells from the same habitat related to the specimens having similar shell growth patterns?

Manuscript III – strategy

The reproducibility of element-to-calcium time-series Na/Ca, Mg/Ca, Mn/Ca, Sr/Ca, and Ba/Ca, measured by LA-ICP-MS in line scan mode, was systematically tested within and between coeval specimens of *A. islandica* from the Isle of Man and the Gulf of Maine (using three specimens per site). The intra-specimen reproducibility of an additional specimen from Iceland, examined in former studies (Holland et al., 2014b; Marali et al., 2017, see manuscript II), were also assessed to strengthen the results. In order to determine intra-specimen reproducibility, one LA-ICP-MS line scan was measured per specimen in the hinge area of the shell following the axis of maximum growth. Then, all specimens were re-polished and a replicate line scan was performed in the same area of each shell. Data of replicate line scans were aligned with the aid of shell Ba/Ca ratios (which are always almost perfectly reproducible within bivalve shells or corals; e.g., Elliot et al., 2009; Sinclair et al., 2005, 2011). Then data sets were reduced so that replicate data sets consisted of an equal number of data points. The degree of reproducibility of (reduced) data sets was assessed from linear regression analysis. The synchrony of element-to-calcium time-series between specimens was gauged for the coeval individuals from the Isle of Man and the Gulf of Maine. Element time-series were smoothed by computing 31-data point running averages. Also, annual averages were calculated for element and specimen. The element time-series were visually inspected among non-averaged, smoothed and annually averaged datasets corresponding to coeval shells from the Gulf of Maine and the Isle of Man, respectively. Time periods during which several shells showed similar fluctuations (e.g., prominent peaks) in element-to-calcium ratios were determined. Annually averaged trace element data sets of different specimens were compared by linear regression analysis. Gillikin et al. (2005) assumed that Sr/Ca ratios were synchronized between coeval bivalves of *Saxidomus giganteus*, because this element was related to shell growth that was in turn synchronized between specimens. We accounted for this issue, by (a) assessing the degree to which shell growth was synchronized between individuals and (b) testing if annual trace element time-series co-varied with increment widths (in mm) or with relative shell growth rates (i.e., dimensionless SGI-values). Actually, two of the three specimens selected from each site have highly similar ontogenetic ages and shell growth patterns.

Chapter 2
Manuscripts

Manuscript I

Oceanographic control on shell growth of *Arctica islandica* (Bivalvia) in surface waters of Northeast Iceland – Implications for paleoclimate reconstructions

Published in
Palaeogeography, Palaeoclimatology, Palaeoecology

Soraya Marali and Bernd R. Schöne

Institute of Geosciences, University of Mainz, Johann-Joachim-Becher-Weg 21, 55128 Mainz, Germany

Authors' contributions
Concept: S. Marali, B. R. Schöne
Growth pattern analysis: S. Marali
Data interpretation: S. Marali
Writing: S. Marali, B. R. Schöne

Marali, S., Schöne, B.R., 2015. Oceanographic control on shell growth of *Arctica islandica* (Bivalvia) in surface waters of Northeast Iceland — Implications for paleoclimate reconstructions. Palaeogeogr. Palaeoclimatol. Palaeoecol. 420, 138–149. doi:10.1016/j.palaeo.2014.12.016.

Abstract

Absolutely dated, annually resolved sea surface temperature records from middle to higher latitudes covering long time intervals are crucial to better understand the climate system. Such data can potentially be obtained from variations in shell growth of long-lived bivalves such as *Arctica islandica*. This study presents the first statistically robust 178-yr long composite chronology (covering 1835–2012) based on sixteen live-collected and subfossil specimens of *A. islandica* from unpolluted, shallow waters of Northeast Iceland. Between 1875 and 1996, up to 43% of the variation in annual shell growth was explained by SST during February to September. Faster growth occurred when temperatures were warmer and food supply was elevated. However, the correlation was subject to strong temporal variations. Likewise, the inter-series correlation (synchrony among time series) was intermittently stronger and weaker. If more uniform environmental conditions prevailed over a longer time interval and the habitat was solely influenced by one of the major currents in this region – the warm, nutrient rich Irminger Current or the cold, nutrient poor East Iceland Current – the agreement between growth records of contemporaneous specimens broke down and the correlation between shell growth and SST was at minimum. However, when the habitat was under the alternating influence of both currents, the inter-annual variability of shell growth and synchrony in growth among the specimens were at maximum, and the correlation between SST and shell growth strengthened. As demonstrated here, the relationship between shell growth of *A. islandica* and environmental variables is highly complex and depends on oceanographic parameters. These findings should be taken into account in subsequent studies in order to reliably reconstruct SST and other environmental variables from shells of this species.

Keywords: Bivalve sclerochronology; *Arctica islandica*; Shell growth patterns; Cross-dating; Climate proxy

Highlights

- 178-yr stacked record based on *Arctica islandica* from surface waters (NE Iceland).
- Up to 43% of variations in common shell growth explained by SST.
- Correlation (growth vs. SST) and EPS vary through time, controlled by Polar Front.
- SST and shell growth fluctuate synchronously on quasi-decadal time-scales (2–6 yr).

1 Introduction

Shells of the bivalve mollusk *Arctica islandica* (Linnaeus, 1767) serve as a novel ultra high-resolution archive of paleoclimate dynamics in the upper 500 m of the boreal North Atlantic Ocean (Nicol, 1951; Jones, 1980; Schöne 2013). Like other mollusks, this species contains distinct growth patterns in its shell consisting of annual and daily growth lines and growth increments (Jones, 1980; Thompson et al., 1980; Schöne et al., 2005a). With these growth patterns, each increment can be placed in a temporal context. If the exact date of a particular growth increment is known, e.g., the date of death, it is also possible to assign precise calendar dates to the complete shell record. Changes of ambient environmental conditions (e.g., water temperature, food availability etc.) are recorded by the shells in the form of variable increment widths (e.g., Witbaard et al., 1997) and variable geochemical properties (e.g., Wanamaker et al., 2011; Schöne et al., 2011; Holland et al., 2014a). Since annual growth line formation, i.e., the period of retarded or halted growth, occurs during late summer/fall (Weidman et al., 1994; Witbaard et al., 1994; Schöne, 2013), shells of *A. islandica* record the full seasonal amplitude of environmental variables (Schöne et al., 2005a). What makes this species special among other sclerochronological paleoclimate archives is the extraordinary longevity of up to 500 years (Schöne et al., 2005b; Wanamaker et al., 2008; Butler et al., 2013). Individual shells can thus provide subseasonally resolved environmental information over a coherent time interval of several hundred years. Furthermore, based on synchronous changes in relative shell growth rates, it is also possible to combine increment width chronologies from specimens with overlapping life spans to build so-called composite or master chronologies covering centuries to millennia (e.g., Marchitto et al., 2000; Butler et al., 2010; Lohmann and Schöne, 2013; Holland et al., 2014b).

A number of studies successfully constructed such composite or master chronologies from specimens of *A. islandica* that lived near or below the thermocline (Marchitto et al., 2000; Schöne et al., 2003; Butler et al., 2010, 2013; Matras, 2011). For example, Marchitto et al. (2000) presented a 154-yr long chronology from Georges Bank (Gulf of Maine) using three live-collected and four dead, single shells from 57–79 m water depth. Specimens used in the 1357-yr long master chronology by Butler et al. (2013) came from slightly deeper settings (81–83 m) west of Grímsey Island, Northern Iceland. However, only a few studies targeted shells of *A. islandica* specimens that dwelled in the upper few meters of the ocean (Epplé et al., 2006; Stott et al., 2010; Turekian et al., 1982). These studies found only a poor agreement between increment width series of contemporaneous specimens which complicates the construction of composite chronologies. Furthermore, the correlation between shell growth and SST

(or other variables, such as the NAO as investigated by Epplé et al., 2006) was very weak or statistically non-significant. However, coherent, high-resolution and well-dated extratropical proxy SST reconstructions spanning centuries to millennia are crucial to better understand the forcings and feedbacks that operate in the climate system. This is because the uppermost ca. 20 m of the ocean are directly interacting with the overlaying atmosphere and as such control weather and climate phenomena (Wanner et al., 2001). Whereas shallow-water corals have provided coherent, seasonally and annually resolved SST proxy records for tropical settings, only a very limited number of potential SST archives with same temporal resolution are currently available for the extratropical oceans. Potential archives include coralline red algae (Kamenos, 2010; Halfar et al., 2007), cold-water corals (McCulloch et al., 2010) and shells of bivalve mollusks (Strom et al., 2005; Black et al., 2008; Brocas et al., 2013). Clearly, there is the need for additional paleoclimate archives offering extremely high temporal resolution and uninterrupted time series.

Here, we tested the hypothesis that *A. islandica* specimens from the upper, well-mixed portion of the water column (<23 m) of an unpolluted setting off Northeast Iceland can be used for high-resolution paleoclimate analyses. Specifically, we addressed the following questions: Are there synchronous changes in shell growth among specimens from surface waters permitting the construction of statistically robust composite chronologies? Which factors control changes in the coherency of shell growth among coeval specimens? How strongly are changes of annual shell growth related to sea surface temperature? Results of our study can help to better comprehend historical ocean-atmosphere interactions and past weather phenomena in the North Atlantic realm.

2 Material and methods

Eleven specimens of *Arctica islandica* were obtained by dredging near Lónafjörður, Langanes Peninsula, Northeast Iceland in August 2012 (Fig. 1; Tab. 1). The majority of samples came from 8.4 to 11.7 m water depth, and one specimen lived in 23.4 m depth (Tab. 1). Furthermore, two subfossil specimens were collected at a nearby beach, and three additional specimens came from another beach (Bakkafjörður) ca. 30 km east of Lónafjörður (Fig. 1; Tab. 1). All subfossil shells were extremely well preserved with the periostracum still intact. Some valves were still articulated (Tab. 1). This precludes extensive post-mortem transport and suggests that the shells lived in nearby shallow waters.

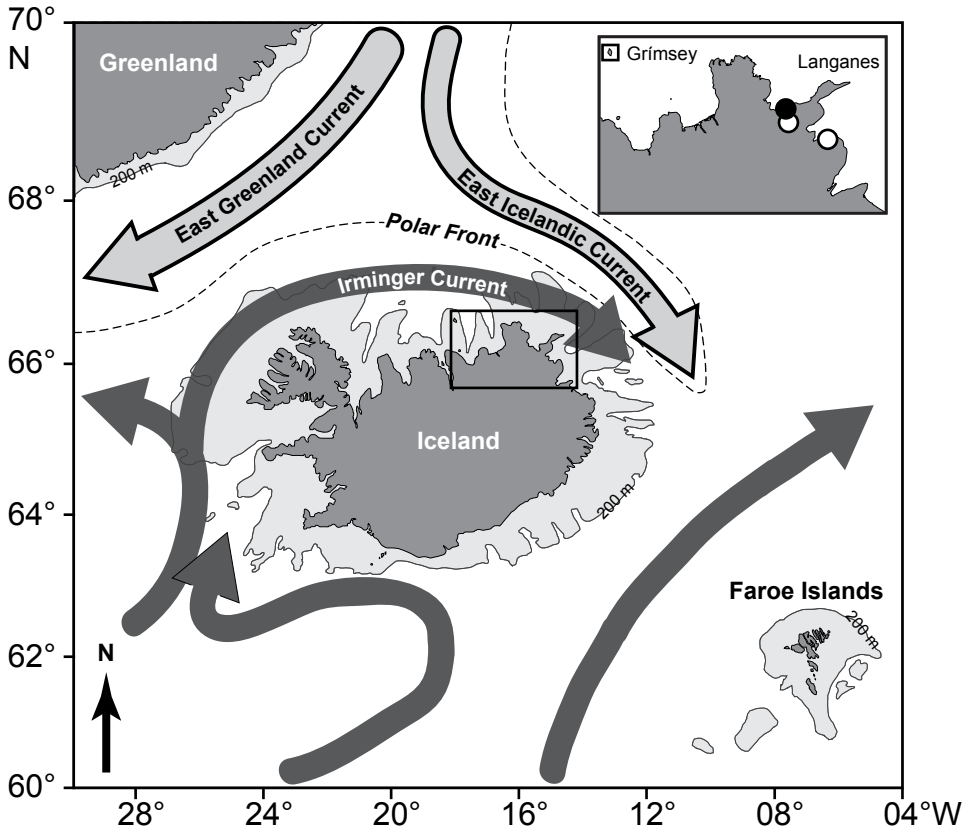

Fig. 1. Map showing oceanographic patterns in the boreal North Atlantic (based on Valdimarsson and Malmberg, 1999) and the sample localities of *Arctica islandica* shells in Northeast Iceland (filled circle: live-collected specimens at Lónafjörður, between 66°09‘58.9“N, 15°22‘58.9“W and 66°13‘5.3“N, 15°21‘54.8“W; open circles: subfossil shells from beaches near Lónafjörður, 66°09‘49.8“N, 15°21‘30.3“W, and Bakkafjörður, 66°00‘32.4“N, 14°50‘46.5“W). Also shown is the station near Grímsey Island (open square) where the SST data were recorded. Light grey: shelf 0–200 m water depth.

Both sample localities were strongly influenced by the nutrient-rich, warm Irminger Current that encircles Iceland clockwise. At times, the Polar Front shifts southward so that the Langanes Peninsula comes under the influence of the cold, nutrient-poor polar or arctic waters (Thórdardóttir, 1984; Stéfansson and Ólafsson, 1991). It should be noted that the freshwater runoff from land has only a negligible effect on the habitat in which the bivalves lived. According to Logemann et al. (2013), the area around Langanes receives much smaller amounts of freshwater than settings around the southern coasts of Iceland. However, even at these settings, the freshwater influx is barely recorded by the oxygen isotope signature of the water. Monthly water samples from the coast near Reykjavík, for example, exhibit very little seasonal $\delta^{18}O_{water}$ changes (unpublished data by one of us, BRS).

2.1 Radiocarbon dating ($^{14}C_{AMS}$)

To place the dead collected specimens in a rough temporal context and test whether they could have been alive during the same time interval as the live-collected specimens, we radiocarbon dated three of the subfossil shells (Tab. 1). For that purpose, the periostracum of the umbonal region was physically removed. Then, small carbonate chunks (~ 200 µg) were cut from the outer layer of the shells. Each sample represented several years' worth of growth. $^{14}C_{AMS}$ dating was performed at the ANU Radiocarbon Dating Laboratory (Fallon et al., 2010). Uncalibrated radiocarbon ages (Libby years) are given in Table 1. Calibrated ^{14}C ages and two sigma ranges were calculated using CALIB 6.1.0 (http://calib.qub.ac.uk/calib/) assuming a ΔR value (marine reservoir effect) of 58 ± 14 years (Reimer et al., 2009; Tab. 1).

2.2 Shell preparation and sclerochronological studies

Soft tissues were removed from the live-collected shells immediately after collection. All specimens were carefully cleaned with water to remove adherent sediment. Then, one valve of each specimen was mounted on a plexiglass cube with EpoFix. To avoid shell fracturing during the cutting process, a quick-drying metal epoxy resin (WIKO Flüssigmetall) was applied to the shells along the axis of maximum growth. Along that axis, a 3-mm-thick section was cut from each specimen using a low-speed precision saw (Buehler Isomet 1000) equipped with a 0.4-mm-thick diamond-coated wafering blade. Next, shell sections were mounted on glass slides with metal epoxy resin, ground (800 and 1200 grit SiC powder) and polished (1 µm Al_2O_3 powder) and subsequently immersed for ca. 20–40 min under constant stirring in Mutvei's solution (Schöne et al., 2005c). This treatment greatly facilitated the recognition of annual growth patterns (Figs. 2A+B). Stained shell cross-sections were digitized with a Canon EOS 550D digital camera attached to a Wild Heerbrugg M8 stereomicroscope equipped with sectoral dark field illumination (Schott VisiLED MC 1000). Furthermore, shell portions with very narrow growth patterns were digitized with a Canon EOS 600D digital camera mounted to a fluorescence light microscope (Zeiss AxioImager.A1m stereomicroscope, HBO 100 mercury lamp producing UV light, Zeiss filter set 38 with excitation and emission wavelengths of 450-500 nm and 500-550 nm, respectively, as well as filter set 18 with excitation and emission wavelengths of 400-800 nm and 450-800 nm, respectively) (Fig. 2C). Annual increment widths were measured in the hinge plate and the ventral margin of the shells using the image processing software Panopea (® Peinl & Schöne).

Table 1. Shells of *Arctica islandica* used in the present study. Sample numbers are the same as in Fig. 3A. Last two digits of Sample ID stand for A = collected alive, D = dead collected, R = right valve, L = left valve. Subfossil shells #12 and 13 were found articulated.

	Sample no.	Sample ID	Locality	Water depth [m]	Conventional $^{14}C_{AMS}$ age [yr]	95.4% (2σ) calibrated age ranges [cal yr AD]	Chronology coverage [yr AD]	Series length [yr]
Live-collected	1	ICE12-15-02AR		11.2–11.7			1955–2012	58
	2	ICE12-15-05AL		11.2–11.7			1948–2012	65
	3	ICE12-05-01AL		8.6			1947–2012	66
	4	ICE12-15-03AL		11.2–11.7			1947–2012	66
	5	ICE12-05-03AR		8.6			1941–2012	72
	6	ICE12-05-05AL	Lónafjorður	8.6			1935–2012	78
	7	ICE12-10-01AL		8.4			1934–2012	79
	8	ICE12-15-04AR		11.2–11.7			1898–2012	115
	9	ICE12-08-11AL		23.4			1888–2011	124
	10	ICE12-14-01AL		10.1–10.8			1840–2012	173
	11	ICE12-07-03AL		11.3–11.5			1835–2012	178
Dead-collected	12	ICE12-11-21DL	Lónafjörður		535±20	1725–1740; 1755–1798; 1801–1949	1948–2012	65
	13	ICE12-17-05DL	Bakkafjörður				1918–2011	94
	14	ICE12-11-05DL	Lónafjörður				1884–1997	114
	15	ICE12-17-01DR	Bakkafjörður		575±20	1700–1898; 1935–1949	1884–1972	89
	16	ICE12-17-07DL	Bakkafjörður		585±25	1692–1895; 1940–1949	1861–1948	88

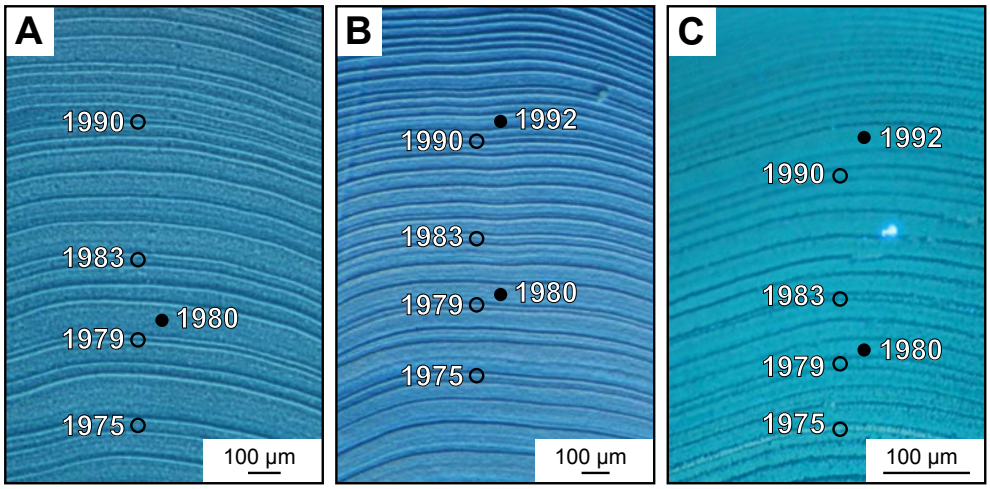

Fig. 2. Annual growth patterns (increments and lines) in the hinge portions of three Mutvei-stained specimens (A: ICE12-10-01AL, B: ICE12-11-21DL, C: ICE12-07-03AL) of *Arctica islandica*. A and B were viewed under sectoral dark field, C unter UV light with filter set 18. Some increments were particularly narrow (e.g., 1975, 1979, 1983, 1990) or wide (e.g., 1980, 1992) and stood out from the remaining growth record. These so-called 'pointer years' were used to visually cross-date the individual chronologies.

2.2.1 Cross-dating

Cross-dating describes a method that is used to temporally align the increment width chronologies of live-collected and subfossil specimens based on synchronous growth patterns (wiggle-matching) (Fig. 3). To do so, we firstly visually compared the sixteen time series by identifying common "pointer years" (Schweingruber et al., 1990), i.e., particularly narrow or wide increments that stood out significantly from the remainder of the growth patterns and were present in all specimens (Fig. 2). Secondly, we used the dendrochronological software COFECHA (Grissino-Mayer, 2001) to cross-date the growth curves semi-automatically using a 22-yr high-pass filter. First-order autoregressive modeling (Box and Jenkins, 1976) has been applied to remove the lag-1 autocorrelation. The robustness of the chronology was then assessed with the interseries correlation value, R_{bar}, the expressed population signal, EPS (Wigley et al., 1984), as well as with the running similarity test (Gleichläufigkeitstest) after Huber (1943). Further details are described in Schöne (2013). Both R_{bar} and EPS values were calculated in 31-year running windows, overlapping by 30 years (Fig. 3). For subsequent comparisons with environmental parameters, EPS values were also computed in 15-yr windows overlapping by 14 years. It is notable that to cross-date the time series it was not necessary to add missing years or remove superfluous ones (see Butler et al., 2009, for details about the identification of genuine growth lines). Instead, equivocal shell portions were carefully re-assessed and hinge and ventral margin records compared to each other to detect misidentifications.

2.2.2 Chronology construction

Once the chronologies were placed in an absolute temporal context, ontogenetic age trends were removed from the raw time series. These age trends not only include decreasing increment widths, I, with increasing ontogenetic age, t, but also a decrease of the year-to-year variance. In logarithmic space, the local mean

$$M = \frac{I_t + I_{t-1}}{2} \quad (1)$$

and local variance

$$V = \left| I_t - I_{t-1} \right| \quad (2)$$

are therefore often linearly correlated (b = slope, k = y-axis intercept),

$$\log V = b \cdot \log M + k\,, \quad (3)$$

indicating that the time series is heteroscedastic. Since traditional ratio-based indexing (GI_t = measured increment width, I_t, divided by predicted growth, P_t) does not fully remove the heteroscedasticity from the chronologies and can produce artificially inflated growth indices (GI_t), the APT (data-adaptive power transformation) method of Cook and Peters (1997) was applied here. With this method, the raw increment width data are transformed in real space into a power-transformed chronology:

$$I_t^* = I_t^p, \quad (4)$$

where $p = \left|1 - b\right|$. APT removes the high correlation between the local mean and local variance, i.e., makes the variance of older, slower growing shell portions comparable to those of faster growing, juvenile shell portions. Thus, APT produces a homoscedastic time series.

To normalize the I_t^* values and remove the remaining ontogenetic age related growth trend (i.e., decreasing increment widths through lifetime) from the chronologies, the APT-transformed time series were fitted with curves that estimate this declining growth trend and then indexed by computing residuals:

$$GI_t^* = I_t^* - P_t \quad , \quad (5)$$

where GI_t^* refers to growth index. For further details and caveats of the method, the reader is also referred to Schöne (2013). In the present study, we used negative

exponentials (NE) to estimate the growth trends. This method eliminates the majority of high-frequency oscillations and largely preserves environmental signals that fluctuate on longer time periods (Figs. 3C). In addition, a method known as 'first differencing' (FD) was applied (Fritts, 1976) which preserves the high frequencies and is particularly useful to explore the year-to-year variations:

$$GI_t^* = I_t^* - I_{t-1}^* \quad . \tag{6}$$

Subsequently, for each year, a bi-weight robust mean (Cook et al., 1990) $GIbw_t^*$ value was computed from all existing GI_t^* values. Mathematical transformations required to remove inherent age trends from the increment width chronologies and compute the bi-weight means were accomplished with the dendrochronological software package ARSTAN (Holmes et al., 1986; Cook and Krusic, 2007). Finally, standardized $GIbw_t^*$ values, SGI_t, were computed for better comparison with other existing sclerochronologies as follows:

$$SGI_t = \frac{GIbw_t^* - \mu}{SD} \quad , \tag{7}$$

where μ is the average and SD the standard deviation of all GI_t^* values (Schöne et al., 2005b). The standardized growth index (SGI) can be considered a dimensionless measure of how shell growth deviates from the estimated growth curve. Units are given in standard deviations (σ). In the following, the two composite chronologies are referred to as 'NE composite chronology' and 'FD composite chronology' (Fig. 3D).

To test whether the variance of the composite chronology may be biased due to the fluctuating sample depth, an additional variance stabilization of the SGI chronology after Osborne et al. (1997) was performed.

2.3 Instrumental data

Monthly sea surface temperature (SST; Fig. 4) data were obtained from the nearest station at Grímsey (obtained from KMNI Climate Explorer at http://climexp.knmi.nl/). One of the two data sets, Grim4065 (WMO station code 4065 GRIMSEY; 66.53°N, 18.02°W), remained untreated and contained a number of gaps in the record (Fig. 4A). In the second data set, Grim12FILL (Fig. 4B), taken from Hanna et al. (2006), these missing data were filled with other station data and air temperature data (available online in the data set NIceSST at http://www.shef.ac.uk/geography/staff/hanna_edward/seasurface). Therefore, the Grim12FILL time series is significantly less variable

than Grim4065. Since no station data were available directly from where the shells lived, we also used a gridded SST record (HadISST; also available from the KMNI website, see above) and computed a SST time series for 65-70°N, 14-16°W covering the Langanes Peninsula (compare Fig. 1; Fig. 4C). Although 120 km away from the sample localities, the Grímsey station data should reflect the temperatures at Langanes Peninsula much better than a gridded data set that averages SST over a much larger area. Like Langanes Peninsula, Grímsey station was largely influenced by the narrow, clockwise-flowing, warm Irminger Current (Fig. 1). The HadISST record, however, captured SST of both the warm Irminger Current and the cold East Iceland Current. To better evaluate how the SST data compare with the shell growth data with regard to variance, the low and middle frequencies were removed from the SST chronologies by applying the FD method (SST_{SI}; see section 2.2.2) and computing standardized SST indices, SST_{SI} (Fig. 4E), according to equations 6 and 7.

To evaluate a possible relationship between shell growth and salinity, gridded sea surface salinity data (SSS; UKMO EN3) were obtained from the KMNI Climate Explorer website (see above) and averages computed for 66-65°N, 14-16°W (Fig. 4D). Furthermore, partial correlation analysis was performed with the software PAST (version 2.17; Hammer et al., 2001) to test, weather salinity changes can affect the correlation between shell growth (NE) and SST (Grim12FILL $SST_{Feb–Sep}$).

2.4 Time series analyses

To identify the temporal dynamics of the composite chronologies and sea surface temperature records, continuous wavelet-transforms were computed from the time series (wave number 6, Morlet wavelet) using the Matlab algorithm by Torrence and Compo (1998) (Fig. 5). 95% confidence intervals were calculated by applying an univariate red-noise autoregressive model (lag-1).

3 Results

Cross-dated growth increment time series of eleven live-collected *Arctica islandica* specimens from surface waters (<23 m) of Lónafjörður, Northeast Iceland, covered the time interval from AD 1835 to 2012 (Fig. 3). Growth data of five subfossil shells did not extend the stacked record in length, but strengthened the composite chronology and increased the EPS and R_{bar} values, respectively. Support for the correct temporal alignment of subfossil specimens came from $^{14}C_{AMS}$ analyses. Calibrated radiocarbon age ranges for umbonal shell portions overlapped with the time interval covered by the composite chronology (Tab. 1). Since 1885, running EPS values (31-yr windows) largely remained well above the critical threshold of 0.85 (Wigley et al., 1984) (Fig. 3E). It seems appropriate to name this portion of the stacked record 'master chronology' (see also Butler et al., 2013), whereas the entire stacked record that also contains portions with EPS values below 0.85 (i.e., prior to 1885) is referred to as 'composite chronology'. A minimum of four to five increment width series were required to reach EPS values of at least 0.85 (Fig. 3). Between 1930 and 1960, EPS values exceeded the 0.85 level, but remained well below the values attained during the remainder of the master chronology (Fig. 3E). Concomitantly, the R_{bar} values reached minima of 0.33 to 0.37 (Fig. 3E). Interestingly, the observed EPS decline was unrelated to changes of the sample depth (Fig. 3).

Cross-dating was not only assessed with EPS and R_{bar} statistics, but also verified by the pointer-year approach and running similarity test (Tab. 2). Visual comparison of the age-detrended time series revealed highly synchronous growth patterns and a number of outstandingly narrow (e.g., 1975, 1979, 1983; Fig. 2) and broad increments that helped to place the chronologies in the proper temporal context. According to the Gleichläufikeitstest by Huber (1943), the degree of synchrony among the individual time series equaled, on average, 68.9±7% (1σ) (Tab. 2) and as such exceeded the critical threshold of 65% which Butler et al. (2009) regarded as highly significant.

The shortest and longest of the sixteen time series that were used to build the composite chronology comprised 58 and 178 years, respectively (Fig. 3A; Tab. 1). On average, the series length equaled 95.3±37.0 years. The sample depth (= number of series averaged per year) ranged between 11 and 15 after 1947 and decreased backward in time (Fig. 3B). The first sixteen years of the composite chronology (1835–1850) were only represented by a single specimen (Fig. 3). For further statistical data, the reader is referred to Figure 3B.

Table 2. Running similarities (Gleichläufigkeiten in %, running window length: 31 years) of raw increment width chronologies of the sixteen *Arctica islandica* shells. The average running similarity is 68.9±7.0%. Years of overlap are given in italicized number.

Sample ID	ICE12-05-01AL	ICE12-05-03AR	ICE12-05-05AL	ICE12-07-03AL	ICE12-08-11AL	ICE12-10-01AL	ICE12-14-01AL	ICE12-15-02AR	ICE12-15-03AL	ICE12-15-04AR	ICE12-15-05AL	ICE12-11-05DL	ICE12-11-21DL	ICE12-17-01DR	ICE12-17-05DL	ICE12-17-07DL
ICE12-05-01AL		*66*	*66*	*66*	*65*	*66*	*66*	*58*	*66*	*66*	*65*	*51*	*65*		*65*	
ICE12-05-03AR	81.8		*72*	*72*	*71*	*72*	*72*	*58*	*66*	*72*	*65*	*57*	*65*	*32*	*71*	
ICE12-05-05AL	66.7	73.6		*78*	*77*	*78*	*78*	*58*	*66*	*78*	*65*	*63*	*65*	*38*	*77*	
ICE12-07-03AL	62.1	66.7	67.9		*124*	*79*	*173*	*58*	*66*	*115*	*65*	*114*	*65*	*89*	*94*	*88*
ICE12-08-11AL	64.6	64.8	58.4	73.4		*78*	*124*	*57*	*65*	*114*	*64*	*110*	*64*	*85*	*94*	*61*
ICE12-10-01AL	75.8	76.4	69.2	68.4	66.7		*79*	*58*	*66*	*79*	*65*	*64*	*65*	*39*	*78*	
ICE12-14-01AL	63.6	72.2	73.1	70.5	62.1	73.4		*58*	*66*	*115*	*65*	*114*	*65*	*89*	*94*	*88*
ICE12-15-02AR	81.0	82.8	70.7	69.0	71.9	79.3	74.1		*58*	*58*	*58*	*43*	*58*		*57*	
ICE12-15-03AL	68.2	65.2	56.1	57.6	61.5	68.2	65.2	70.7		*66*	*65*	*51*	*65*		*65*	
ICE12-15-04AR	71.2	69.4	61.5	70.4	69.3	72.2	73.9	75.9	69.7		*65*	*100*	*65*	*75*	*94*	*51*
ICE12-15-05AL	78.5	75.4	66.2	64.6	62.5	80.0	75.4	84.5	70.8	73.8		*50*	*65*		*64*	
ICE12-11-05DL	72.5	78.9	71.4	69.3	77.3	73.4	64.0	88.4	74.5	69.0	76.0		*50*	*89*	*80*	*65*
ICE12-11-21DL	75.4	78.5	69.2	64.6	62.5	73.8	63.1	77.6	64.6	76.9	78.5	78.0			*64*	
ICE12-17-01DR		65.6	65.8	62.9	61.2	59.0	65.2			54.7		68.5			*66*	*76*
ICE12-17-05DL	64.6	69.0	59.7	64.9	66.0	66.7	55.3	63.2	64.6	59.6	60.9	70.0	54.7	56.1		*31*
ICE12-17-07DL				73.9	57.4		73.9			62.7		58.5		72.4	64.5	
Average	**71.2**	**72.2**	**65.8**	**67.5**	**65.3**	**71.8**	**67.8**	**76.7**	**68.8**	**66.1**	**71.8**	**68.8**	**49.3**	**64.2**	**64.5**	
SD	6.8	5.9	5.6	4.7	5.7	6.5	6.9	9.1	4.3	8.6	9.5	8.0	7.6	11.5		

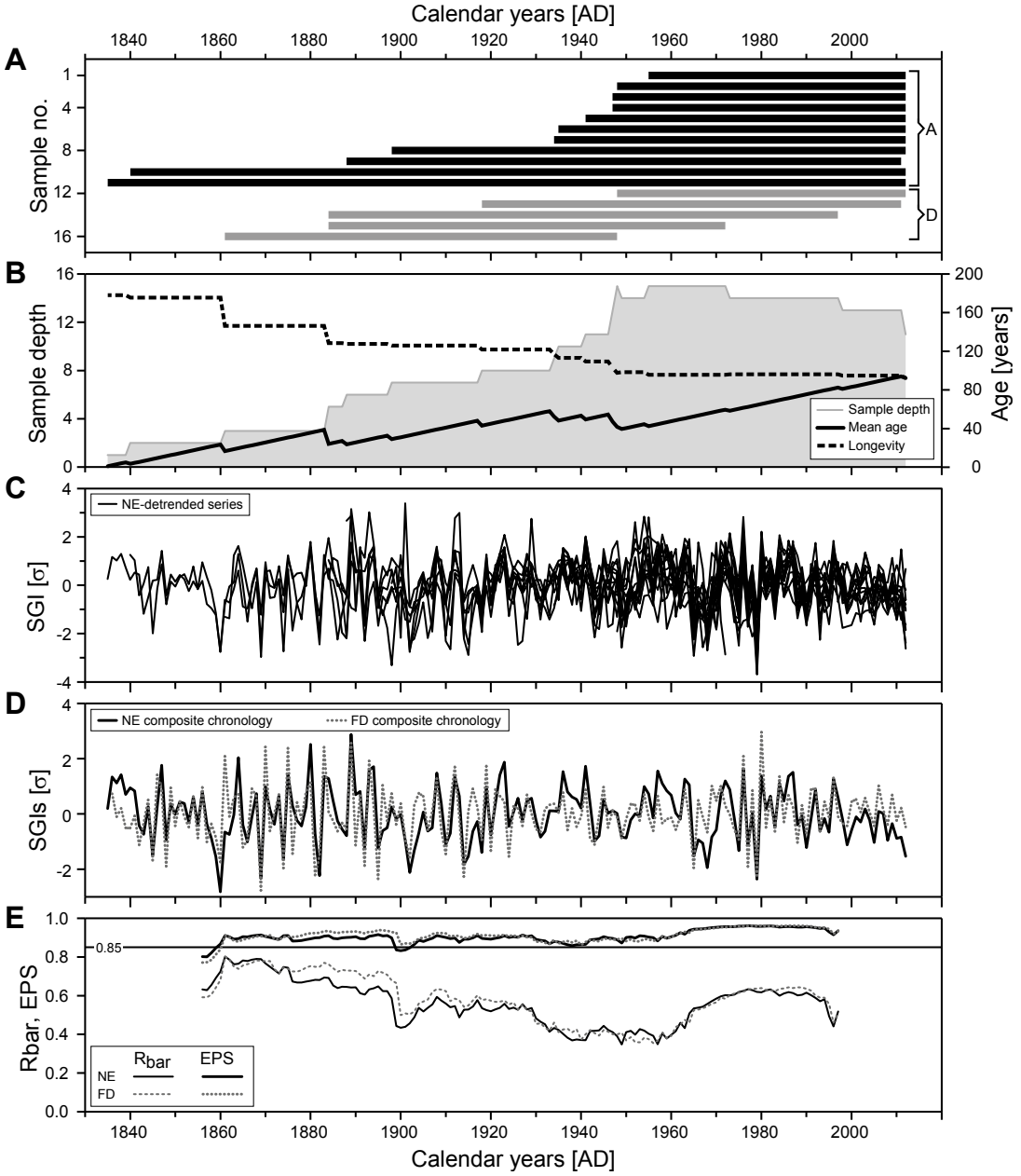

Fig. 3. Northeast Iceland composite chronology constructed from shells of *Arctica islandica*. (A) Lifespans of individual specimens, A = specimens collected alive, D = dead-collected specimens. Numbers refer to those listed in Table 1. (B) Further statistics of the chronology. Sample depth = number of individuals used per time slice; Mean age and mean longevity = average ontogenetic age and average longevity of all specimens at a given time. (C) Individual age-detrended (negative exponential) and standardized growth increment (SGI) time series. (D) Composite chronologies based on two different age-detrending methods: NE = negative exponential detrending (black solid curve), FD = first differencing (grey dotted curve). (E) EPS and R_{bar} values for the two composite chronologies of D computed in 31-yr running windows.

3.1 Assessment of age-detrended composite chronologies

The two age-detrending methods, NE and FD, were used for different purposes. Stiff, deterministic growth functions such as negative exponentials are typically employed to identify the longer-term variability of shell growth. However, highly flexible growth equations including the 'first differencing' method filter out the middle to low frequencies while emphasizing the year-to-year variability of growth (= high frequencies).

The NE composite chronology (Figs. 3D, 4A–D) revealed short-term and longer-term oscillations in common shell growth at frequencies corresponding to periods of 2–6 and 14–16 years, respectively (Fig. 5A). As shown by the continuous wavelet transformation of the time series, these periods were non-stationary signals that were intermittently strong and occasionally reached the 95% confidence level against a red noise background. We also noticed a transient development from higher to lower frequency regimes through time (Fig. 5A). For example, significant 2–6-yr oscillations occur between 1860 and 1920 with the most coherent portion between 1870 and 1890. 14–16-yr periods were particularly strong and significant between 1900 and 1980 (Fig. 5A).

The FD composite chronology (Figs. 3D, 4E) exhibited time intervals of increased SGI amplitudes during the 1870s-1890s, 1910s-1920s and 1960s-1990s (Fig. 5B). In contrast, the year-to-year variance of shell growth was remarkably attenuated between ca. 1930 and 1960 (Figs. 4E, 5B). During that time, the synchrony among the individual chronologies was notably reduced. An additional variance stabilization accounting for potential sample depth-related variance increases (Osborn et al., 1997) also did not change the observed trends (not depicted).

3.2 Shell growth and sea surface temperature

During the main growing season, shell growth was positively and highly significantly ($p<0.01$) correlated to sea surface temperature (Figs. 6A–C; Tab. 3). Specifically, this was the case for the time interval between February and September (Figs. 5+6), i.e., when the shells were growing at fastest rates (Schöne et al., 2005a). Therefore, we computed February-to-September SST averages from all three data sets (Grim4065, Grim12FILL and HadISST) and compared these data to the NE and FD composite chronologies (Fig. 5A–E). Only those years were considered for which SST measurements were available for each month of the growing season.

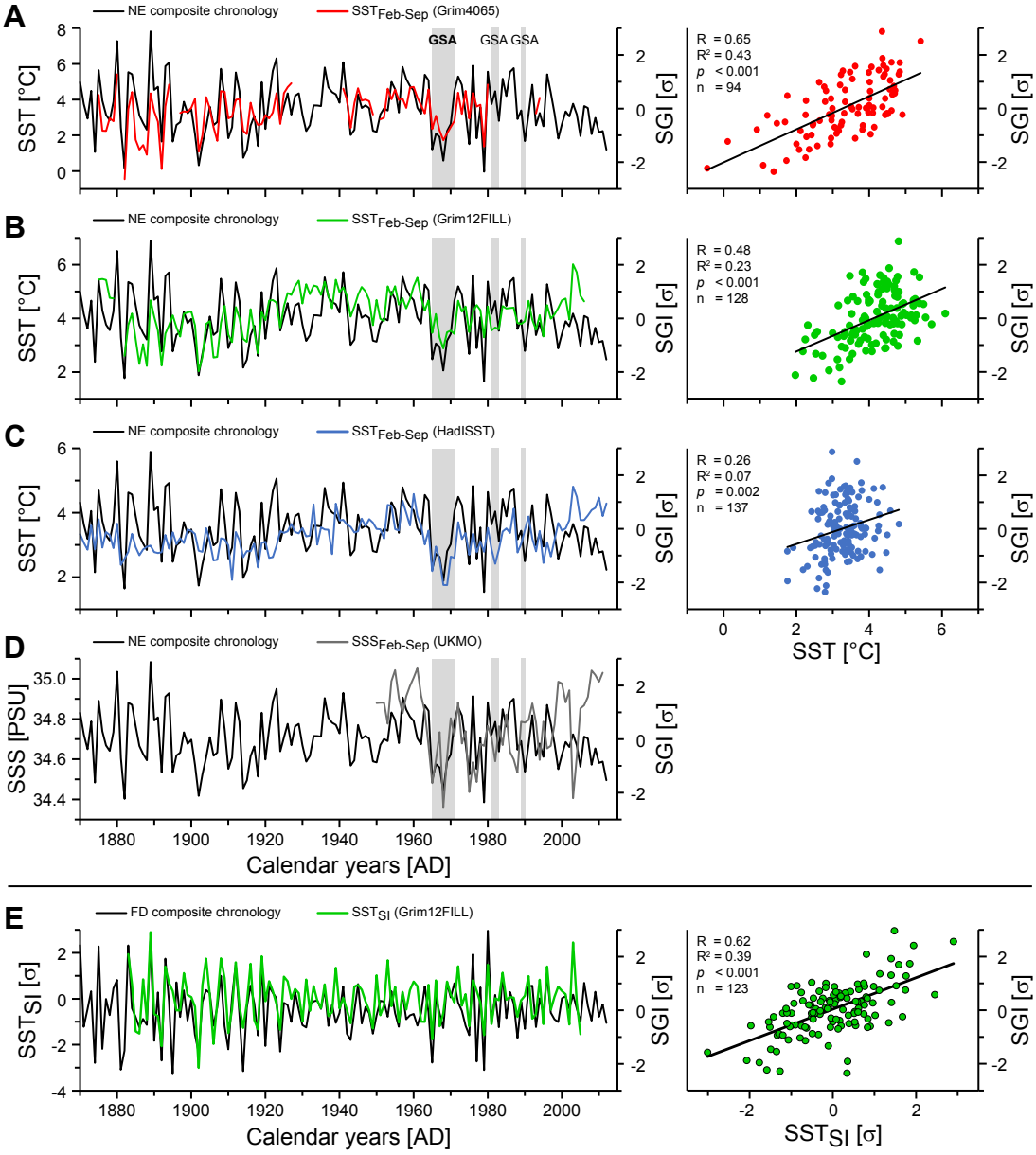

Fig. 4. Relationship between (age-detrended and standardized) common shell growth (SGI) of *Arctica islandica* and environmental data between February and September (= time interval of fastest shell growth). (A)–(C) Comparison of the NE composite chronology with three different SST datasets: station data near Grímsey Island (see Fig. 1), (A) Grim4065 = raw data, (B) Grim12FILL = modeled SST (from Hanna et al., 2006), gaps in the record filled with data from other stations and air temperature data; (C) HadISST = gridded SST data from Hadley Center averaged over 65–70°N and 14–16°W. Respective cross-plots and statistical values are depicted in the right panels. (D) NE composite chronology in comparison with sea surface salinity data, $SSS_{Feb\text{-}Sep}$ (gridded data set UKMO). Cross-plot between the SGI and the $SSS_{Feb\text{-}Sep}$ data is not shown, because the correlation is not significant (p>0.05). (E) High-frequency component of the composite chronology in relation to the high-frequency component of the Grim12FILL $SST_{Feb\text{-}Sep}$ record. Both data sets were age-detrended with first differencing (FD). SGI = standardized shell growth, SST_{ST} = first-differenced sea surface temperature, GSA = Great Salinity Anomaly (time intervals of the GSAs are indicated by horizontal grey bars).

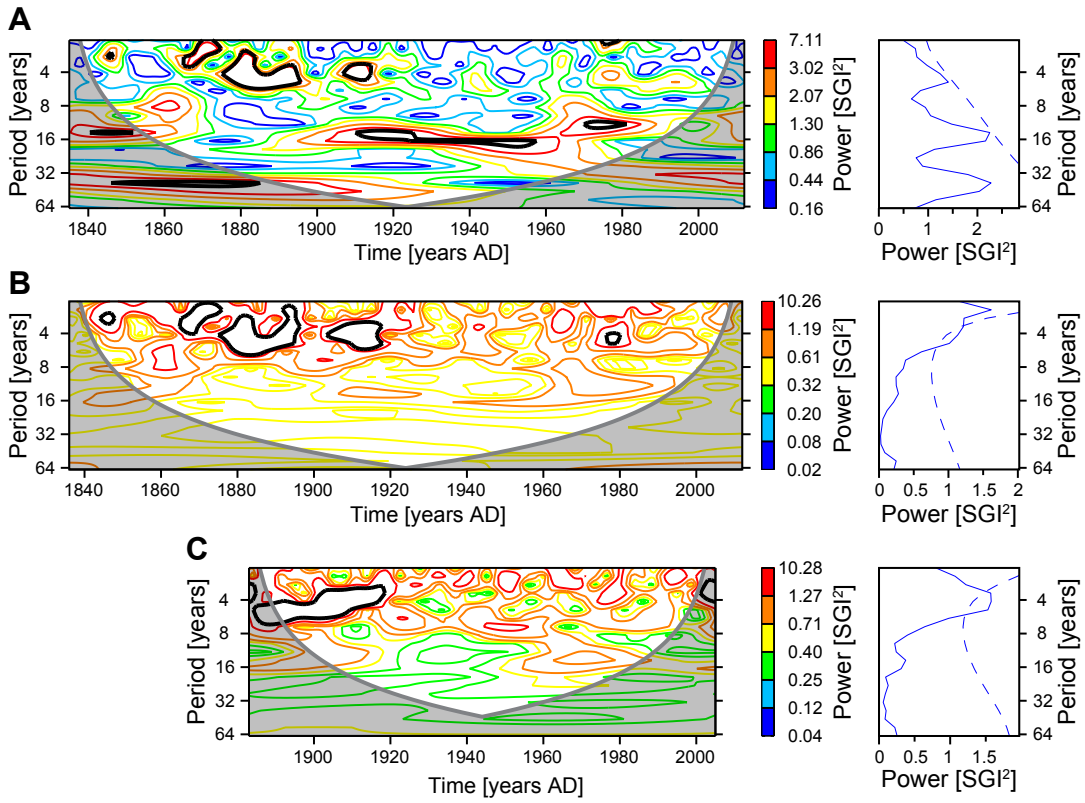

Fig. 5. Spectral analyses (continuous wavelet transformations, Morlet wavelet, wavenumber 6) of the composite chronologies of *Arctica islandica* (A: NE composite chronology, B: FD composite chronology, see Fig. 3 for abbreviations) and the first-differenced Grim12Fill $SST_{Feb-Sep}$ series (C). Grey portions in wavelet power spectra (left panels) refer to cone-of-influence, where zero padding has reduced the variance. Thick black contour lines indicate the 5% significance level, using a red-noise background spectrum. The dashed lines in the global wavelet power spectra (right panels) indicate the significance for the global wavelet spectrum, assuming the same significance level. Wavelet spectra were computed with the algorithm of Torrence and Compo (1998).

The NE composite chronology showed highest correlation values with the Grim4065 $SST_{Feb–Sep}$ (Figs. 4A, 6A) and lowest with the HadISST $SST_{Feb–Sep}$ (Figs. 4C, 6C; Tab. 3). How strong the correlation was on a year-to-year basis is best seen in a direct comparison of first-differenced $SST_{Feb–Sep}$ and shell growth data (Fig. 4E.).

As indicated by running regression analyses (15-yr windows), the correlation between shell growth and $SST_{Feb–Sep}$ was underlying strong temporal variations (Figs. 7A+B). At times, the correlation coefficients, R, and coefficients of determination, R^2, were as high as 0.6 and 0.4, respectively (e.g., 1975–1980), whereas the correlation coefficient decreased to less than 0.3 at other times (Fig. 7A). In the case of $HadISST_{Feb–Sep}$ vs. NE composite chronology, the correlation was even negative during ca. 1930 and 1940 (Fig. 7B).

Running correlations between shell growth and sea surface temperature also exhibited a strong positive agreement with running EPS and R_{bar} values (Fig. 7C). Lower synchrony among the individual chronologies was apparently linked to times when the agreement between water temperature and increment widths was reduced (Figs. 7A–C). At the same time, the year-to-year variability in both $SST_{Feb–Sep}$ and common shell growth was much lower (Fig. 4A+E).

Notably, continuous wavelet power spectra of the (FD detrended) Grim12FILL $SST_{Feb–Sep}$ time series and the FD composite chronology revealed remarkable similarities (Fig. 5). Shell growth and $SST_{Feb–Sep}$ shared strong spectral power in the 2–6-yr band, particularly during 1880–1920 (Fig. 5).

3.3 Shell growth and sea surface salinity

Although $SSS_{Feb–Sep}$ data were only available for a relatively short time interval of 62 years (Fig. 4D), it was still possible to identify important dependencies between salinity and shell growth. As shown in Figures 4D and 7C, the synchrony among individual series expressed by the EPS value was uncoupled from salinity changes. Between ca. 1962 and 1983 salinity and shell growth were positively correlated, but anti-correlated thereafter. As revealed by partial correlation analysis, the correlation between relative shell growth and $SST_{Feb–Sep}$ was still relatively high and significant ($R = 0.38$; $p = 0.003$; $n = 62$ years) after eliminating the effect of salinity. Likewise, salinity did not affect the rate at which the shells grow.

Table 3. Correlation statistics of common age-detrended and standardized shell growth (SGI) of *Arctica islandica* and sea surface temperature (three data sets). R = correlation coefficient (Pearson's R), R^2 = coefficient of determination, *p* = probability values (*p*) and n = number of years.

Grim4065	**R**	**R^2**	***p***	**n**
$SST_{Feb–Sep}$	0.65	0.43	<0.0001	94
Jan	0.31	0.10	0.0017	101
Feb	0.26	0.07	0.0093	103
Mar	0.48	0.23	<0.0001	102
Apr	0.55	0.31	<0.0001	103
May	0.46	0.21	<0.0001	102
Jun	0.39	0.15	<0.0001	103
Jul	0.47	0.22	<0.0001	99
Aug	0.36	0.13	0.0002	103
Sep	0.24	0.06	0.0157	102
Oct	0.03	0.00	0.7737	101
Nov	0.00	0.00	0.9945	102
Dec	-0.01	0.00	0.9065	101
Grim12FILL	**R**	**R^2**	***p***	**n**
$SST_{Feb–Sep}$	0.48	0.23	<0.0001	128
Jan	0.32	0.10	0.0002	130
Feb	0.39	0.15	<0.0001	130
Mar	0.45	0.20	<0.0001	130
Apr	0.47	0.23	<0.0001	129
May	0.49	0.24	<0.0001	129
Jun	0.49	0.24	<0.0001	129
Jul	0.49	0.24	<0.0001	128
Aug	0.48	0.23	<0.0001	128
Sep	0.47	0.22	<0.0001	128
Oct	0.44	0.19	<0.0001	128
Nov	0.37	0.14	<0.0001	129
Dec	0.31	0.10	0.0003	130
HadISST1	**R**	**R^2**	***p***	**n**
$SST_{Feb–Sep}$	0.26	0.07	0.0020	137
Jan	0.09	0.01	0.2617	143
Feb	0.13	0.02	0.1192	143
Mar	0.28	0.08	0.0008	143
Apr	0.32	0.10	0.0001	143
May	0.27	0.07	0.0011	143
Jun	0.20	0.04	0.0189	143
Jul	0.16	0.02	0.0624	143
Aug	0.13	0.02	0.1122	143
Sep	0.07	0.00	0.4289	143
Oct	0.01	0.00	0.9403	143
Nov	0.04	0.00	0.6209	143
Dec	0.12	0.02	0.1371	143

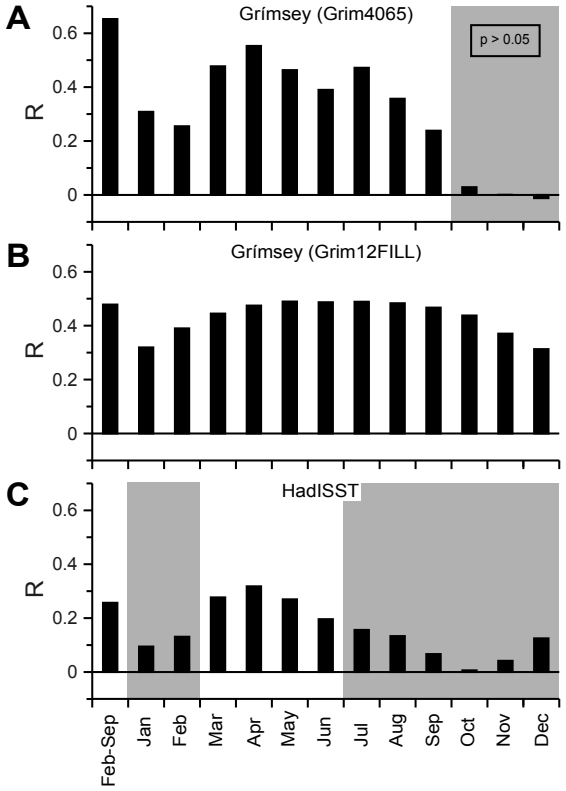

Fig. 6. Relationship (correlation coefficients) between instrumental monthly SST and age-detrended (with negative exponential functions), standardized shell growth (SGI) of *Arctica islandica*. SST datasets were introduced in Figure 4. (A) Grim4065, (B) Grim12FILL; (C) HadISST. Grey area denotes months during which correlation was not significant at the 95% level.

4 Discussion

As demonstrated by the results of this study, shell growth of contemporaneous specimens of *Arctica islandica* from surface waters off the coast of Northeast Iceland (ca. 9–23 m water depth) was highly synchronized. For the first time, this permitted the compilation of a statistically robust composite chronology based on ocean quahogs from shallow waters. The majority of existing *A. islandica* composite or master chronologies were constructed from specimens that lived near or below the thermocline (Butler et al., 2010; Lohmann and Schöne, 2013; Witbaard et al., 1997). For example Butler et al. (2010) presented a 489-yr long stacked record from the Irish Sea using specimens from 35–70 m water depth. Another master chronology by these authors was constructed from specimens collected at 81–83 m on the North Icelandic shelf and covered 1347 years (Butler et al. 2013). However, the few studies using specimens from shallow surface waters above the thermocline (Epplé et al., 2006; Stott et al., 2010; Turekian et al., 1982) noticed a poor interseries correlation and low EPS values. For example, Epplé et al. (2006) observed a very low synchrony among growth of eight specimens that lived in 15–20 m water depth at the inner

German Bight, southern North Sea. Epplé et al. (2006) related this finding to extreme variations in ambient salinity, temperature and turbidity. Likewise, Stott et al. (2010) reported a poor synchrony among nine specimens of *A. islandica* from ca. 11–17 m water depth at the west coast of Scotland. Between 1945 and 2005, the interseries correlation of first-differenced time series was as low as 0.09. Stott et al. (2010) related the low agreement among the specimens to anthropogenic disturbances of the habitat causing eutrophication and altered plankton dynamics. Furthermore, Turekian et al. (1982) noted the presence of non-periodic disturbance lines in *A. islandica* that lived in highly polluted surface waters of the New York Bight. These disturbance lines were difficult to distinguish from regular, periodic growth lines. Presumably, the overall excellent agreement in shell growth observed in the present study is attributed to the distinct annual growth patterns that formed under natural environmental conditions and under the absence of major non-periodic disturbances.

4.1 Shell growth and SST: contrasting findings

Synchronous changes in shell growth among contemporaneous specimens suggest the presence of common external drivers (Thompson et al., 1980; Witbaard and Duineveld, 1990; Marchitto et al., 2000). In the case of invertebrates, growth is predominantly governed by temperature, food quantity and food quality (Kennish and Olsson, 1975; Witbaard et al., 1997, 2001; Schöne et al., 2005a). Since long-term instrumental records of the latter two environmental variables are typically not available, the influence of food on shell growth is often difficult to evaluate (but see Witbaard et al., 2003, Wanamaker et al., 2009). In the present study, instrumental chlorophyll *a* data is only available for the last ten years or so which is too short for a meaningful statistical analysis. Furthermore, such large-scale satellite data are likely not representative for the food levels at the exact habitat of the bivalves. Therefore, most studies focused on shell growth and water temperature, and provided equivocal results in the case of *A. islandica*. Whereas some studies identified a statistically significant correlation (Holland et al., 2014b), others found the opposite (Witbaard, 1996; Marchitto et al., 2000; Epplé et al., 2006) or concluded that SST explained only a fraction of the variability of shell growth (Butler et al., 2010; Stott et al., 2010). Butler et al. (2013) detected some synchrony among shell growth and SST (HadISST) in the lower frequencies, but little agreement on the year-to-year basis, i.e., very little running similarity. This is in sharp contrast to the findings of the present study. As demonstrated here, up to 43% of the variations in annual shell growth were statistically highly significantly explained by changes of sea surface temperature during February to September (Fig. 4A). Furthermore, SST and shell growth exhibited a strong running similarity which is ideally examined in

the high-frequency domain (Fig. 4E). The discrepancy between previous findings and the ones presented here likely results from the following reasons. (1) The specimens used by Butler et al. (2013) lived in > 75 m water depth of the North Icelandic shelf. During summer, the water column in this region is stratified (e.g., Stéfansson, 1962; Stéfansson and Ólafsson, 1991; Malmberg et al., 1996; Knudsen et al., 2004) and waters below the thermocline are de-coupled from short-term changes in surface waters. This is particularly true for those years during which cold, low saline Arctic water masses reach the area via an intensified East Icelandic Current (Fig. 1). (2) Stacked records of *A. islandica* built from specimens with poorly synchronized growth patterns such as the composite chronologies presented by Epplé et al. (2006) and Stott et al. (2010) would not be expected to compare well to environmental data.

4.2 Shell growth as an independent temperature proxy?

Given the statistically robust correlation observed here, the question arises if variations in relative shell growth can serve as an independent proxy of water temperature. In fact, this is very challenging, because the correlation between shell growth and SST shows strong temporal variations (Fig. 7A+B). Highest R values coincided with time intervals during which the individual chronologies fitted particularly well to each other resulting in high EPS values (Fig. 7C). At the same time, year-to-year and quasi-decadal (2–6 year) changes of SST as well as SGI amplitudes were at maximum (Figs. 3–5). However, the strong correlation between temperature and shell growth vanished when only small inter-annual and quasi-decadal temperature fluctuations occurred over a longer time interval (e.g., 1920–1960; Figs. 3, 7A+B). During such time intervals, the synchrony in shell growth among contemporaneous specimens decreased (Fig. 7C) and the composite chronology showed a reduced higher-frequency variability of shell growth (Fig. 3D). This pattern could be an artifact caused by the incorporation of a larger number of SGI values from young individuals between the 1920s and 1960s (Fig. 3). During youth, the year-to-year variance is often significantly larger than during later stages of life (Butler et al. 2009), and age-detrending methods may not be capable of fully eliminating these ontogenetic differences in variance. Therefore, we computed a new composite chronology from individual growth curves that were lacking the first 30 years of growth, a technique also performed by Butler et al. (2010). As depicted in Figure 7C, there was no significant difference between the original stacked record and the one without considering the pre-mature portions of the shells. Accordingly, the period of low SGI variance between 1920 and 1960 reflected a true environmental signal. At least during these time intervals, it is barely possible to reliably reconstruct SST from SGI values.

4.3 Position of the Polar Front and synchrony of shell growth

Apparently, some inter-annual environmental variability – as long as it remains within the species-specific bounds of the ecological tolerance – is required to synchronize shell growth, whereas the agreement among shell growth of coeval specimens breaks down if uniform environmental conditions prevail. At the locality where the bivalves lived, the year-to-year and quasi-decadal variability of SST, SSS and food supply is strongly coupled to the position of the Polar Front (compare Knudsen et al., 2012; Stéfansson and Ólafsson, 1991). The Polar Front separates two very different water masses, namely the cold, less saline East Icelandic Current (EIC) that carries Arctic and Polar waters southward and the warm, more saline Irminger Current (IC) that transports Atlantic water northward (e.g. Valdimarsson and Malmberg, 1999; Hansen and Østerhus, 2000) (Fig. 1).

The IC has a vital influence on the primary productivity of the Icelandic Shelf (e.g., Stéfansson, 1962; Thórdardóttir, 1976, 1977, 1984; Stéfansson and Ólafsson, 1991; Asthorsson et al., 2007; Gudmundsson et al., 2009). It carries large amounts of nutrients (N and P) from the south towards the north, and thereby fuels primary productivity in shallow waters (e.g. Stéfansson and Ólafsson, 1991). Furthermore, the admixture of warm, more saline waters reduces the density difference between surface waters and (relatively saline) bottom waters, which leads to a reduced stratification in Northeast Iceland (e.g. Stéfansson, 1962; Stéfansson and Ólafsson, 1991). Wind-driven upwelling of deeper waters can then replenish the amount of nutrients in the surface waters and further enhance the primary productivity (e.g., Gudmundsson, 1998). In contrast, a greater influence of the EIC on the North and Northeast Icelandic shelf results in a decreased primary productivity, because the Arctic and Polar waters are poor in nutrients (Stéfansson and Ólafsson, 1991). In addition, the fresher waters carried by the EIC increase the stratification and prevent vertical admixture of nutrient-rich deeper water.

Regular latitudinal displacements of the Polar Front ensure that the bivalves experience inter-annual changes of temperature, salinity and, in particular, food supply. Under these conditions, growth patterns of coeval specimens are highly synchronized. However, if the Polar Front is shifted too far to the north or south, the habitat of the bivalves comes under the constant influence of either the IC or EIC and will no longer experience the alternating influence of one or the other water mass. As a consequence, the environmental conditions become much more uniform and shell growth is desynchronized. It should be added that *A. islandica* prefers fresh food particles over dead, re-suspended organic matter (Erlenkeuser, 1976). As such, this species is particularly sensitive to fluctuations of the primary productivity and reflects changes in food availability in its shell in the form of variable increment widths.

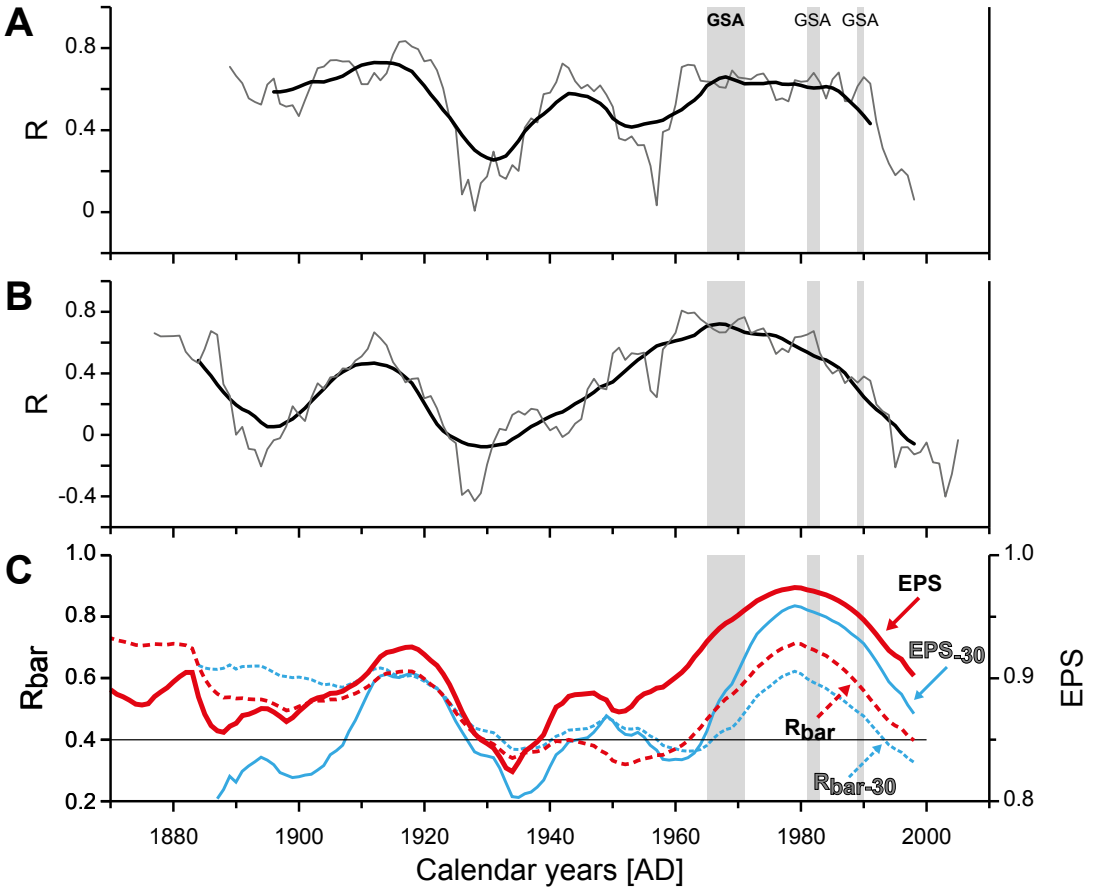

Fig. 7. Correlation of common shell growth of *Arctica islandica* (age-detrended and standardized) and sea surface temperature (A: Grim12FILL $SST_{Feb–Sep}$; B: $HadISST_{Feb–Sep}$) in comparison with running (15-yr windows) R_{bar} and EPS values (C). Horizontal line in C marks an R_{bar} of 0.4. GSA = Great Salinity Anomaly. Thin lines in A and B = correlation in 15-yr running windows, thick dark lines = smoothed running R. Note good agreement between EPS and R_{bar} in C and running correlations in A and B. Shell growth is more strongly correlated to SST when shell growth is more synchronized. Between 1920 and 1960, EPS and R_{bar} temporarily fell below critical thresholds of 0.85 and 0.40, respectively. At the same time, the agreement between shell growth and water temperature broke down. The patterns of running EPS and R_{bar} curves remain unchanged when the first thirty years of each growth increment width time series are omitted (EPS_{-30}, R_{bar-30} curves). Therefore, the low EPS and R_{bar} values between 1920 and 1960 are not an artifact caused by inclusion of a greater number of young individuals during this time interval, but likely reflect a true environmental signal.

Extended periods of uniform conditions and time intervals with strong environmental fluctuations on year-to-year and quasi-decadal time scales are well known. For example, during the so-called Great Salinity Anomaly (1965–1971; Dickson et al., 1988) extremely cold and low saline Polar waters were transported by the EIC to the North and Northeast Icelandic Shelf (Dickson et al., 1988; Belkin et al., 1998, Belkin, 2004). As a consequence, SST and SSS dropped, and the primary productivity in the stratified waters decreased (e.g., Thórdardóttir, 1977; Gudmundsson, 1998). During the same time interval, the common growth of *A. islandica* was strongly reduced (Fig. 4) and the correlation between shell growth and environmental variables (SST and SSS)

was highest. During the years following this dramatic event, i.e., during the 1970s, SST and SSS fluctuated strongly from year to year reflecting the alternating influence of Atlantic and Arctic/Polar waters, respectively (Gudmundsson, 1998; Stéfansson and Ólafsson, 1991). Cold years such as 1979 are characterized by a strong Polar influence with low SST, low SSS and low primary productivity, whereas the opposite characterized warm years such as 1980 (e.g., Thórdardóttir, 1984; Gudmundsson, 1998). These changes are well reflected by the composite chronology (Fig. 4). Other Great Salinity Anomalies reached Iceland in 1981–1983 and 1989–1990 (Belkin, 2004; Belkin et al., 1998), and may have triggered the decrease in shell growth in 1983 and 1990 (Fig. 4). During 1920–1960 as well as after 1990, however, Atlantic waters gained a stronger influence on the North and Northeast Icelandic Shelf (Gudmundsson, 1998; Hátún et al., 2005; Holliday et al., 2008). This resulted in weaker inter-annual and quasi-decadal fluctuations in temperature (Fig. 5) and food supply, and likely explains the strongly reduced variance in common shell growth of *A. islandica* (Fig. 7) described above.

During environmentally stable time intervals shell growth may be influenced by factors other than temperature and food, namely by diseases, predation pressure, individual tolerance levels etc. These influences only affect individual bivalves and therefore reduce the growth synchrony within an *A. islandica* population. Stronger variability in SST ad food supply, by contrast, may mask these ecological influences and result in well-synchronized shell growth.

5 Summary and conclusions

As demonstrated by the present study, shells of coeval specimens of *Arctica islandica* from unpolluted surface waters of Northeast Iceland shared common growth patterns permitting the construction of a robust composite chronology. This stacked record provides a reliable time frame to assign precise calendar dates to geochemical measurements taken from shells.

Variations in shell growth were explained by up to 43% by changes in SST during February to September. Faster growth typically occurred when temperatures were warmer and food supply was elevated. However, the link between SGI values and temperature was subject to strong temporal changes. It was weaker during time intervals of reduced inter-annual (year-to-year and quasi-decadal) variability in shell growth. Using SGI values as independent measures of SST may thus be extremely challenging and is likely confined to time intervals during which the interseries correlation and variance of the composite chronology is high.

Apparently, some environmental variability on inter-annual time scales was required to maintain the synchrony of shell growth among contemporaneous bivalves. At the locality where the bivalves lived, this variability was provided by the alternating influence of the warm, more saline, nutrient rich Irminger Current and the cold, fresher, nutrient poor East Iceland Current. If more uniform conditions prevailed over a longer time interval, the agreement between annual growth increment chronologies weakened. Such conditions occurred when the Polar Front was shifted too far north or south so that the habitat was solely controlled by the IC or EIC, respectively.

According to our study the relationship between shell growth of *A. islandica* and environmental variables is highly complex and depends on oceanographic parameters and a combination of several environmental variables. These findings should be taken into account in subsequent studies in order to reliably reconstruct paleoenvironmental conditions from shells of this species. Additional geochemical analysis of *A. islandica* shells (e.g. stable oxygen isotopes as temperature proxies) will be required to disentangle the effects of temperature, food supply and other factors on shell growth.

6 Acknowledgements

We are grateful to the editor, Thierry Corrège, Paul Butler and the second anonymous reviewer for their helpful and supportive comments. We gratefully acknowledge the help of Hilmar A. Holland during fieldwork in 2012 and his assistance with MATLAB. We deeply thank Gudrun Thórarinsdóttir, Siggeir Stefánsson, Erlendur Bogason and Sæmundur Einarsson for their help in sample collection in Iceland. We further acknowledge Johanna Boos and Katrin Böhm for their assistance with shell preparation. This study has been made possible by a German Research Foundation (DFG) grant to BRS (SCHO 793/10-1).

7 References

Astthorsson, O.S., Gislason, A., Jonsson, S., 2007. Climate variability and the Icelandic marine ecosystem. Deep Sea Res. Part II 54, 2456–2477.

Belkin, I.M., 2004. Propagation of the "Great Salinity Anomaly" of the 1990s around the northern North Atlantic. Geophys. Res. Lett., 31, L08306, 4 pp. doi:10.1029/2003GL019334.

Belkin, I.M., Levitus, S., Antonov, J., Malmberg, S.A., 1998. "Great Salinity Anomalies" in the North Atlantic. Prog. Oceanogr. 41, 1–68.

Black, B.A., Gillespie, D.C., MacLellan, S.E., Hand, C.M., 2008. Establishing highly accurate production-age data using the tree-ring technique of crossdating: a case study for Pacific geoduck (*Panopea abrupta*). Can. J. Fish. Aquat. Sci. 65, 2572–2578.

Box, G.E.P., Jenkins, G., 1976. Time series analysis, forecasting and control. Holden-Day, San Francisco, 575 pp.

Brocas, W.M., Reynolds, D.J., Butler, P.G., Richardson, C.A., Scourse, J.D., Ridgway, I.D., Ramsay, K., 2013. The dog cockle, *Glycymeris glycymeris* (L.), a new annually-resolved sclerochronological archive for the Irish Sea. Palaeogeogr. Palaeoclimatol. Palaeoecol. 373, 133–140.

Butler, P.G., Richardson, C., Scourse, J.D., Witbaard, R., Schöne, B.R., Fraser, N.M., Wanamaker Jr., A.D., Harris, I., Robertson, I., 2009. Accurate increment identification and the spatial extent of the common signal in five *Arctica islandica* chronologies from the Fladen Ground, northern North Sea. Paleoceanography 24, PA2210, 18 pp., doi:10.1029/2008PA001715.

Butler, P.G., Richardson, C.A., Scourse, J.D., Wanamaker Jr., A.D., Shammon, T.M., Bennell, J.D., 2010. Marine climate in the Irish Sea: analysis of a 489-year marine master chronology derived from growth increments in the shell of the clam *Arctica islandica*. Quat. Sci. Rev. 29, 1614–1632.

Butler, P.G., Wanamaker Jr., A.D., Scourse, J.D., Richardson C.A., Reynolds, D.J., 2013. Variability of marine climate on the North Icelandic Shelf in a 1357-year proxy archive based on growth increments in the bivalve *Arctica islandica*. Palaeogeogr. Palaeoclimatol. Palaeoecol. 373, 141–151.

Cook, E.R., Peters, K., 1997. Calculating unbiased tree-ring indices for the study of climatic and environmental change. Holocene 7, 361–370.

Cook, E.R., Krusic, P.J., 2007. Program ARSTAN – A tree-ring standardization program based on detrending and autoregressive time series modeling, with interactive graphics. Tree-Ring Laboratory, Lamont Doherty Earth Observatory of Columbia University, Palisade, NY, 14 pp.

Dickson, R.R., Meincke, J., Malmberg, S.-A., Lee, A.J., 1988. The „Great Salinity Anomaly" in the northern North Atlantic 1968–1982. Prog. Oceanogr. 20, 103–151.

Epplé, V.M., Brey, T., Witbaard, R., Kuhnert, K., Pätzold, J., 2006. Sclerochronological records of *Arctica islandica* from the inner German Bight. Holocene 16, 763–769.

Erlenkeuser, H., 1976. ^{14}C and ^{13}C isotope concentration in modern marine mussels from sedimentary habitats. Naturwissenschaften 63, 338.

Fallon, S.J., Fifield, L.K., Chappell, J.M., 2010. The next chapter in radiocarbon dating at the Australian National University: status report on single stage AMS. Nucl. Instruments Methods Phys. Res. B 268, 898–901.

Fritts, H.C., 1976. Tree rings and climate. Academic Press, London, 567 pp.

Grissino-Mayer, H.D., 2001. Evaluating crossdating accuracy: a manual and tutorial for the computer program COFECHA. Tree-ring Research 57, 205–221.

Gudmundsson, K., 1998. Long-term variability in phytoplankton productivity during spring in Icelandic waters. ICES J. Mar. Sci. 55, 635–643.

Gudmundsson, K., Heath, M.R., Clarke, E.D., 2009. Average seasonal changes in chlorophyll *a* in Icelandic waters. ICES J. Mar. Sci. 66, 2133–2140.

Hammer, Ø, Harper, D.A.T., Paul, D.R., 2001. Past: paleontological statistics software package for education and data analysis. Palaeontol. Electron. 4, 9 pp.

Hansen, B, Østerhus, S, 2000. North Atlantic-Nordic Seas exchanges. Prog. Oceanogr. 45, 109–208.

Hátún, H., Sandø, A.B., Drange, H., Hansen, B., Valdimarsson, H., 2005. Influence of the Atlantic subpolar gyre on the thermohaline circulation. Science 309, 1841–1844.

Halfar, J., Steneck, R., Schöne, B., Moore, G.W.K., Joachimski, M., Kronz, A., Fietzke, J., Estes, J., 2007. Coralline alga reveals first marine record of subarctic North Pacific climate change. Geophys. Res. Lett. 34, L07702, doi:10.1029/2006GL028811.

Holland, H.A., Schöne, B.R., Marali, S., Jochum, K.P., 2014a. History of bioavailable lead and iron in the Greater North Sea and Iceland during the last millennium a bivalve sclerochronological reconstruction. Mar. Pollut. Bull., in press, doi: 10.1177/0959683614530438.

Holland, H.A., Schöne, B.R., Lipowski, C., Esper, J., 2014b. Decadal climate variability of the North Sea during the last millennium reconstructed from bivalve shells (*Arctica islandica*). The Holocene 24, 771–786.

Holliday, N.P., Hughes, S.L., Bacon, S., Beszczynska-Möller, A., Hansen, B., Lavín, A., Loeng, H., Mork, K.A., Østerhus, S., Sherwin, T., Walczowski, W., 2008. Reversal of the 1960s to 1990s freshening trend in the northeast North Atlantic and Nordic Seas. Geophys. Res. Lett., 35, L03614, 5 pp., doi:10.1029/2007GL032675.

Holmes, R.L., Adams, R.K., Fritts, H.C., 1986. Tree-ring chronologies of western North America, California, eastern Oregon and northern Great Basin with procedures used in the chronology development work including user manuals for computer programs COFECHA and ARSTAN. Chronology series VI. 184 pp.

Huber, B., 1943. Über die Sicherheit jahrringchronologischer Datierung. Holz 6, 263–268.

Jones, D.S., 1980. Annual cycle of shell growth increment formation in two continental shelf bivalves and its paleoecologic significance. Paleobiology 6, 331–340.

Kamenos, N.A., 2010. North Atlantic summers have warmed more than winters since 1353, and the response of marine zooplankton. Proc. Natl. Acad. Sci. U. S. A. 107, 22442–22447.

Kennish, M.J., Olsson, R.K., 1975. Effects of thermal discharges on the microstructural growth of *Mercenaria mercenaria*. Environ. Geol. 1, 41–64.

Knudsen, K.L., Eiríksson, J., Jansen, E., Jiang, H., Rytter, F., Gudmundsdóttir, E.R., 2004. Palaeoceanographic changes off North Iceland through the last 1200 years: foraminifera, stable isotopes, diatoms and ice rafted debris. Quat. Sci. Rev. 23, 2231–2246.

Knudsen, K.L., Eiríksson, J., Bartels-Jónsdóttir, H.B., 2012. Oceanographic changes through the last millennium off North Iceland: temperature and salinity reconstructions based on foraminifera and stable isotopes. Mar. Micropaleontol. 84–85, 54–73.

Logemann, K., Ólafsson, J., Snorrason, Á, Valdimarsson, H., Marteinsdóttir, G., 2013. The circulation of Icelandic waters – a modelling study. Ocean Sci. 9, 931–955.

Lohmann, G., Schöne, B.R., 2013. Climate signatures on decadal to interdecadal time scales as obtained from mollusk shells (*Arctica islandica*) from Iceland. Palaeogeogr. Palaeoclimatol. Palaeoecol. 373, 152–162.

Malmberg, S.A., Valdimarsson, H., Mortensen, J., 1996. Long-time series in Icelandic waters in relation to physical variability in the northern North Atlantic. NAFO Scientific Council Studies 24, 69–80.

Marchitto Jr., T.M., Jones, G.A., Goodfriend, G.A., Weidman, C.R., 2000. Precise temporal correlation of holocene mollusk shells using sclerochronology. Quaternary Research 53, 236–246.

Matras, U., 2011. Annual variation in productivity on the Faroe Shelf during the 20th century. Havstovan 11–04, 1–19.

McCulloch, M, Taviani, M., Montagna, P., López Correa, M., Remia, A., Mortimer, G., 2010. Proliferation and demise of deep-sea corals in the Medterranean during the Younger Dryas. Earth Planet. Sci. Lett. 298, 143–152.

Nicol, D., 1951. Recent species of the veneroid pelecypod *Arctica*. J. Washingt. Acad. Sci. 41, 102–106.

Osborn, T.J., Briffa, K.R., Jones, P.D., 1997. Adjusting variance for sample-size in tree-ring chronologies and other regional mean timeseries. Dendrochronologia 15, 89–99.

Reimer, P.J., Baillie, M.G.L., Bard, E., Bayliss, A., Beck, J.W., Blackwell, P.G., Bronk Ramsey, C., Buck, C.E., Burr, G.S., Edwards, R.L., Friedrich, M., Grootes, P.M., Guilderson, T.P., Hajdas, I., Heaton, T.J., Hogg, A.G., Hughen, K.A., Kaiser, K.F., Kromer, B., McCormac, F.G., Manning, S.W., Reimer, R.W., Richards, D.A., Southon, J.R., Talamo, S., Turney, C.S.M., van der Plicht, J., Weyhenmeyer, C.E., 2009. INTCAL09 and MARINE09 radiocarbon age calibration curves, 0–50,000 years Cal BP. Radiocarbon 51, 1111–1150.

Schöne, B.R., 2013. *Arctica islandica* (Bivalvia): A unique paleoenvironmental archive of the northern North Atlantic Ocean. Glob. Planet. Change 111, 199–225.

Schöne, B.R., Oschmann, W., Rössler, J., Freyre Castro, A.D., Houk, S.D., Kröncke, I., Dreyer, W., Janssen, R., Rumohr, H., Dunca. E., 2003. North Atlantic Oscillation dynamics recorded in shells of a long-lived bivalve mollusk. Geology 31, 1037–1040.

Schöne, B.R., Houk, S.D., Freyre Castro, A.D., Fiebig, J., Kröncke, I., Dreyer, W., Oschmann, W., 2005a. Daily growth rates in shells of *Arctica islandica*: Assessing subseasonal environmental controls on a long-lived bivalve mollusk. Palaios 20, 78–92.

Schöne, B.R., Fiebig, J., Pfeiffer, M., Gleß, R., Hickson, J., Johnson, A.L.A., Dreyer, W., Oschmann, W., 2005b. Climate records from a bivalved Methuselah (*Arctica islandica*, Mollusca; Iceland). Palaeogeogr. Palaeoclimatol. Palaeoecol. 228, 130–148.

Schöne, B.R., Dunca, E., Fiebig, J., Pfeiffer, M., 2005c. Mutvei's solution: An ideal agent for resolving microgrowth structures of biogenic carbonates. Palaeogeogr. Palaeoclimatol. Palaeoecol. 228, 149–166.

Schöne, B.R., Zhang, Z., Radermacher, P., Thébault, J., Jacob, D., Nunn, E.V., Maurer, A.-F., 2011a. Sr/Ca and Mg/Ca ratios of ontogenetically old, long-lived bivalve shells (*Arctica islandica*) and their function as paleotemperature proxies. Palaeogeogr. Palaeoclimatol. Palaeoecol. 302, 52–64.

Schweingruber, F.H., Eckstein, D., Serre-Bachet, F., Bräker, O.U., 1990. Identification, presentation and interpretation of event years and pointer years in dendrochronology. Dendrochronologia 8, 9–38.

Stéfansson, U., 1962. North Icelandic Waters. Rit Fiskid. 3, 269 pp.

Stéfansson, U., Ólafsson, J., 1991. Nutrients and fertility of Icelandic waters. Rit Fiskid. 12, 1–56.

Stott, K.J., Austin W.E.N., Sayer, M.D.J., Weidman, C.R., Cage, A.G., Wilson, R.J.S., 2010. The potential of *Arctica islandica* growth records to reconstruct coastal climate in north west Scotland, UK. Quat. Sci. Rev. 29, 1602–1613.

Strom, A., Francis, R.C., Mantua, N.J., Miles, E.L., Peterson, D.L., 2005. Preserving low frequency climate signals in growth records of geoduck clams (*Panopea abrupta*). Palaeogeogr. Palaeoclimatol. Palaeoecol. 228, 167–178.

Thompson, I., Jones, D.S., Dreibelbis, D., 1980. Annual internal growth banding and life history of the ocean quahog *Arctica islandica* (Mollusca: Bivalvia). Mar. Biol. 57, 25–34.

Thórdardóttir, 1976. The spring primary production in Icelandic waters 1970–1975. ICES CM 1976/L:31, 37 pp.

Thórdardóttir, 1977. Primary production in North Icelandic waters in relation to recent climatic changes. In M.J. Dunbar (Ed.), Polar Oceans. Proceedings of the Polar Oceans Conference, McGill University, Montreal, 1974. Arctic Institute of America, Canada, 655–665.

Thórdardóttir, 1984. Primary production north of Iceland in relation to water masses in May–June 1970–1980. ICES 1984/L:20, 17 pp.

Torrence, C., Compo, G.P., 1998. A practical guide to wavelet analysis. Bull. Am. Meteorol. Soc. 79, 61–78.

Turekian, K.K., Cochran, J.K., Nozaki, Y., Thompson, I., Jones, D.S., 1982. Determination of shell deposition rates of *Arctica islandica* from the New York Bight using natural ^{228}Ra and ^{228}Th and bomb-produced 14C. Limnol. Oceanogr. 27, 737–741.

Valdimarsson, H., Malmberg, S.A., 1999. Near-surface circulation in Icelandic waters derived from satellite tracked drifters. Rit Fiskid. 16, 23–29.

Wanamaker Jr., A.D., Heinemeier, J., Scourse, J.D., Richardson, C.A., Butler, P.G., Eiríksson, J., Knudsen, K.L., 2008. Very long-lived mollusks confirm 17th century AD tephra-based radiocarbon reservoir ages for North Icelandic shelf waters. Radiocarbon 50, 399–412.

Wanamaker Jr., A.D., Kreutz, K.J., Schöne B.R., Maasch, K.A., Pershing, A.J., Borns, H.W., Introne, D.S., Feindel, S., 2009. A late Holocene paleo-productivity record in western Gulf of Maine, USA, inferred form growth histories of the long-lived ocean quahog (*Arctica islandica*). Int. J. Earth Sci. (Geologische Rundschau) 98, 19–29.

Wanamaker Jr., A.D., Kreutz, K.J., Schöne, B.R., Introne, D.S., 2011. Gulf of Maine shells reveal changes in seawater temperature seasonality during the Medieval Climate Anomaly and the Little Ice Age. Palaeogeogr. Palaeoclimatol. Palaeoecol. 302, 43–51.

Wanner, H., Brönnimann, S., Casty, C., Gyalistras, D., Luterbacher, J., Schmutz, C., Stephenson, D.B., Xoplaki, E., 2001. North Atlantic Oscillation – concepts and studies. Surv. Geophys. 22, 321–382.

Weidman, C.R., Jones, G.A., Lohmann, K.C., 1994. The long-lived mollusc *Arctica islandica*: A new paleoceanographic tool for the reconstruction of bottom temperatures for the continental shelves of the northern North Atlantic Ocean. J. Geophys. Res. 99, 18305–18314+22753.

Wigley, T.M.L., Briffa, K.R., Jones, P.D., 1984. On the average value of correlated time series, with applications in dendroclimatology and hydrometeorology. J. Clim. Appl. Meteorol. 23, 201–213.

Witbaard, R., 1996. Growth variations in *Arctica islandica* L. (Mollusca): a reflection of hydrography-related food supply. ICES J. Mar. Sci. 53, 981–987.

Witbaard, R., Duineveld, G.C.A., 1990. Shell-growth of the bivalve *Arctica islandica* (L.), and its possible use for evaluating the status of the benthos in the subtidal North Sea. Basteria 54, 63–74.

Witbaard, R., Jenness, M.I., van der Borg, K., Ganssen, G., 1994. Verification of annual growth increments in *Arctica islandica* L. from the North Sea by means of oxygen and carbon isotopes. Netherlands J. Sea Res. 33, 91–101.

Witbaard, R., Duineveld, G.C.A., de Wilde, P.A.W.J., 1997. A long-term growth record derived from *Arctica islandica* (Mollusca, Bivalvia) from the Fladen Ground (northern North Sea). J. Mar. Biol. Assoc. United Kingdom 77, 801–816.

Witbaard, R., Duineveld, G.C.A., Bergman, M., 2001. The effect of tidal resuspension on benthic food quality in the southern North Sea. Senck. Marit. 31, 225–234.

Witbaard, R., Jansma, E., Sass Klaassen, U., 2003. Copepods link quahog growth to climate J. Sea Res. 50, 77–83.

Manuscript II

Ba/Ca ratios in shells of *Arctica islandica* – Potential environmental proxy and crossdating tool

Published in
Palaeogeography, Palaeoclimatology, Palaeoecology

Soraya Marali[1], Bernd R. Schöne[1], Regina Mertz-Kraus[1], Shelly M. Griffin[2], Alan D. Wanamaker Jr.[2], Una Matras[3], Paul G. Butler[4]

[1] Institute of Geosciences, Johannes Gutenberg University,Johann-Joachim-Becher-Weg 21, 55128 Mainz, Germany
[2] Department of Geological and Atmospheric Sciences, Iowa State University, 253 Science I, Ames, IA 50011, USA
[3] Faroe Marine Research Institute, Nóatún 1, P.O. Box 3051, FO 110 Tórshavn, Faroe Islands
[4] School of Ocean Sciences, Bangor University, Menai Bridge, Anglesey, LL59 5AB, U.K.

Authors' contributions

Concept: S. Marali, B. R. Schöne
Growth pattern analysis: S. Marali, S. M. Griffin, P. G. Butler
LA-ICP-MS analysis: S. Marali, R. Mertz-Kraus
Data interpretation: S. Marali, B. R. Schöne
Writing: S. Marali, B. R. Schöne, R. Mertz-Kraus, S. M. Griffin, A. D. Wanamaker Jr., U. Matras, P. G. Butler

Marali, S., Schöne, B.R., Mertz-Kraus, R., Griffin, S.M., Wanamaker, A.D., Matras, U., Butler, P.G., 2017. Ba/Ca ratios in shells of *Arctica islandica* – Potential environmental proxy and crossdating tool. Palaeogeogr. Palaeoclimatol. Palaeoecol. 465, 347–361. doi:10.1016/j.palaeo.2015.12.018.

Abstract

Ba/Ca_{shell} time-series of marine bivalves typically show flat background levels which are interrupted by erratic sharp peaks. Evidence from the literature indicates that background Ba/Ca_{shell} ratios broadly reflect salinity conditions. However, the causes for the Ba/Ca_{shell} peaks are still controversial and widely debated although many researchers link these changes to primary productivity, freshwater input or spawning events. The most striking feature is that the Ba/Ca_{shell} peaks are highly synchronous in contemporaneous specimens from the same population. For the first time, we studied Ba/Ca_{shell} in mature and ontogenetically old (up to 251 year-old) specimens of the long-lived *Arctica islandica*. Also, we analyzed specimens from surface water and deeper water (below the thermocline). The typical pattern of low background and erratic peaks persisted throughout ontogeny. However, due to decreasing sampling resolution and greater time-averaging in older, slower growing shell portions, the background Ba/Ca_{shell} values appeared to gradually increase with ontogenetic age, whereas the peaks became attenuated and broader. Despite that, Ba/Ca_{shell} maxima were still highly synchronous among contemporaneous specimens from the same locality and habitat confirming previous reports from short-lived species. Computing of annual Ba/Ca_{shell} averages largely eliminated any bias introduced by time-averaging and sampling resolution. Strongly elevated annual Ba/Ca_{shell} peaks in specimens from surface waters (Iceland, Faroe Islands, Isle of Man) during the 1980s appear to coincide with an extreme primary productivity pulse recorded by remote sensing. However, due to the lack of in vivo experiments, we cannot ultimately test a causal link between annual Ba/Ca_{shell} excursions and primary productivity. We propose that Ba/Ca_{shell} time-series, specifically the highly synchronous Ba/Ca_{shell} peaks and annual Ba/Ca_{shell} values in contemporaneous specimens from the same locality can serve as a tool to verify crossdating and facilitate the construction of statistically robust growth increment width master chronologies. Long-term environmental reconstructions based on bivalve shell growth chronologies can likely greatly benefit from this new technique.

Keywords: Ba/Ca; Crossdating; Master chronology; Chlorophyll *a*; Time-averaging

Highlights

- Time-series of Ba/Ca_{shell} of *A. islandica* exhibit highly synchronous patterns.
- Ba/Ca_{shell} are likely uncoupled from ontogenetic age and shell growth rate.
- Strong primary productivity coincides with annual Ba/Ca_{shell} peaks.
- Ba/Ca_{shell} can verify crossdating, facilitate stacked chronology construction.

1 Introduction

In recent years, bivalve shells have attracted much attention as high-resolution recorders of past climate change (Wanamaker et al., 2011; Schöne and Gillikin, 2013). Information on environmental conditions that prevailed during growth such as seawater temperature, food availability etc. is preserved in the shells, for example, in the form of variable increment widths (faster growth at optimal temperatures and when more food is available) and $\delta^{18}O_{shell}$ values. These environmental proxy data can be placed in a precise temporal context by careful visual inspection, and counting annual and daily growth increments and lines. Based on similar growth patterns (wiggle-matching or crossdating, Douglass, 1941) it is also possible to combine annual growth increment width time-series of specimens with overlapping lifespans to form stacked chronologies or master chronologies[1]. This method was first established in dendrochronology (Douglass, 1914) and later applied to bivalve shells (Jones et al., 1989; Black et al., 2008, 2015). Master chronologies can cover many centuries to millennia and in combination with environmental proxies, provide information on the climate history over long time intervals (e.g., Marchitto et al., 2000; Schöne et al., 2004; Black et al., 2008; Butler et al., 2010, 2013; Wanamaker et al., 2012).

However, bivalve sclerochronology still entails challenges. For example, in stressful environments (fluctuating salinity, temporarily low oxygen levels, pollution), periodic growth patterns are often difficult to discern (e.g., Stott et al., 2010). Growth lines may be indistinct or disturbance lines present which can barely be distinguished from true annual growth lines. At times, anomalous growth patterns occur which reduce the synchronicity among increment series of contemporaneous specimens. In such cases, the construction of stacked chronologies (and master chronologies) based on wiggle-matching of growth patterns can be a very time-consuming task. Furthermore, in contrast to biogenic hard parts of other organisms, in particular foraminifera and corals, the element signatures of bivalve shells are often difficult to interpret, because the incorporation of trace and minor elements is under strong biological control (e.g., Lorens and Bender, 1980; Gillikin et al., 2005; Freitas et al., 2006; Schöne et al., 2011). A notable exception is the Ba/Ca_{shell} ratio which may serve as a proxy for salinity (Gillikin et al. 2006) and phytoplankton blooms (Stecher et al., 1996).

[1] We use the term 'master (stacked) chronology' for a statistically robust (EPS value > 0.85; Wigley et al., 1984) stacked record of crossdated growth increment width time-series. In contrast, a 'stacked chronology' or 'stacked record' (without 'master') is less well replicated and and/or has an EPS < 0.85. In previous works, the latter has also been referred to as 'composite chronology' (Schöne, 2013). Since the connotation of this term is different in the field of dendrochronology, we refrain from using it here again. The terms 'time-series' and 'chronology' are used synonymously and denote a sequence of increment width data arranged in time.

A typical Ba/Ca_{shell} time-series exhibits a low and relatively invariable background which is interspersed by numerous sharp, erratic or periodic peaks at levels many times the background (e.g., Stecher et al., 1996; Vander Putten et al., 2000; Gillikin et al. 2006, 2008; Barats et al., 2009; Goodwin et al., 2013; Hatch et al., 2013). As demonstrated for a number of species in lab and field experiments, the background Ba/Ca_{shell} values are closely tied to Ba/Cawater which, in turn, is strongly negatively correlated to ambient salinity (Gillikin et al. 2006, 2008; Poulain et al., 2015)[2]. On the contrary, the reasons for the Ba/Ca_{shell} peaks still remain enigmatic. The strong synchronicity of Ba/Ca_{shell} peaks in contemporaneous specimens from the same population strongly argues for an external forcing. However, no satisfactory explanation has yet been provided as to which environmental parameter this might be. Ba/Ca_{shell} peaks may reflect primary productivity pulses (Stecher et al., 1996, Vander Putten et al., 2000; Lazareth et al., 2003; Thébault et al., 2009a), freshwater discharge or synchronized spawning (Gillikin et al., 2006). For an in-depth discussion of the topic see Gillikin et al. (2006, 2008). The striking feature of Ba/Ca_{shell} peaks occurring synchronously in all specimens from the same habitat indicates great potential to validate crossdating (see also Delong et al., 2007) and enable the construction of more robust stacked and master chronologies. So far, this aspect has been largely overlooked in bivalve sclerochronology.

Existing studies of Ba/Ca in bivalve shells have been exclusively conducted on relatively short-lived species (< 20 years; e.g., Stecher et al., 1996; Vander Putten et al., 2000; Lazareth et al., 2003; Thébault et al., 2009a) or ontogenetically young specimens of very long-lived species (>100 years; Toland et al., 2000; Elliot et al., 2009; Schöne et al., 2011). It therefore remains unknown whether similar synchronous Ba/Ca_{shell} peaks can be observed in mature and long-lived specimens – such observations would be required for using Ba/Ca_{shell} peaks to validate crossdating. It is also unclear whether there are lifelong ontogenetic trends in the Ba/Ca_{shell} peaks and background values. Furthermore, only a few studies have compared Ba/Ca_{shell} chronologies of contemporaneous specimens from different localities (Gillikin et al., 2006). It is largely unclear if there are coherent multiregional Ba/Ca_{shell} signatures. Addressing such questions may contribute to a better understanding of the nature of the Ba/Ca_{shell} peaks and greatly improve the emerging field of stacked and master chronology construction using bivalve shells. For this purpose, the present study focuses on Ba/Ca_{shell} data in old-grown specimens of the long-lived ocean quahog, *A. islandica* from four different localities in the northern North Atlantic.

[2] Rivers transport barium-rich particulate phases (of terrigenous origin) to coastal environments; barium desorbs from the particulate phases at low salinities in the estuarine mixing zone due to ion-exchange processes (Coffey et al., 1997). After desorption, dissolved barium displays conservative behavior in seawater, i.e., its concentration is related to changes in salinity (see Roy-Chester and Jickells, 2012 and references therein; Fig. 10 in Knee and Paytan, 2011).

In order to contribute to the on-going research of Ba/Ca_{shell} signatures, this study will (1) determine Ba/Ca_{shell} coherence across a population and the broader North Atlantic region, (2) determine the effects of ontogenetic age on the incorporation of Ba/Ca_{shell}, (3) compare Ba/Ca_{shell} values to environmental variables, and (4) determine the usefulness of Ba/Ca_{shell} in aiding the construction of master growth chronologies.

2 Material and methods

A total of twelve specimens of *Arctica islandica* were obtained by dredging (Iceland, Isle of Man, Gulf of Maine) and SCUBA diving (Faroe Islands) from four different localities in the northern North Atlantic Ocean (Fig. 1; Tab. 1A). Four individuals came from Þistilfjördur in NE Iceland (8–12 m water depth; Fig. 1B), two from the Faroe Islands (20 m water depth; Fig. 1C), and three each from the Isle of Man (30–57 meter water depth; Fig. 1D) and the Gulf of Maine (82–84 m water depth; Fig. 1E). All except one specimen from the Isle of Man (well-preserved with periostracum still intact) were collected alive (Tab. 1). The habitats at Iceland, the Isle of Man and the Gulf of Maine were located offshore where probably fully marine conditions prevailed throughout lifetime of the bivalves. Specimens from the Faroe Islands were sampled within a fjord between the Faroese Islands Streymoy and Vágar (close to the city of Vestamanna). This locality is thus potentially more strongly influenced by freshwater runoff from land than the other studied sites (Fig. 1). Specimens from the Isle of Man, Iceland and the Gulf of Maine were used for the construction of statistically robust, absolutely dated master chronologies in previous studies of Butler et al. (2009, 2010), Marali and Schöne (2015) and Griffin (2012), respectively.

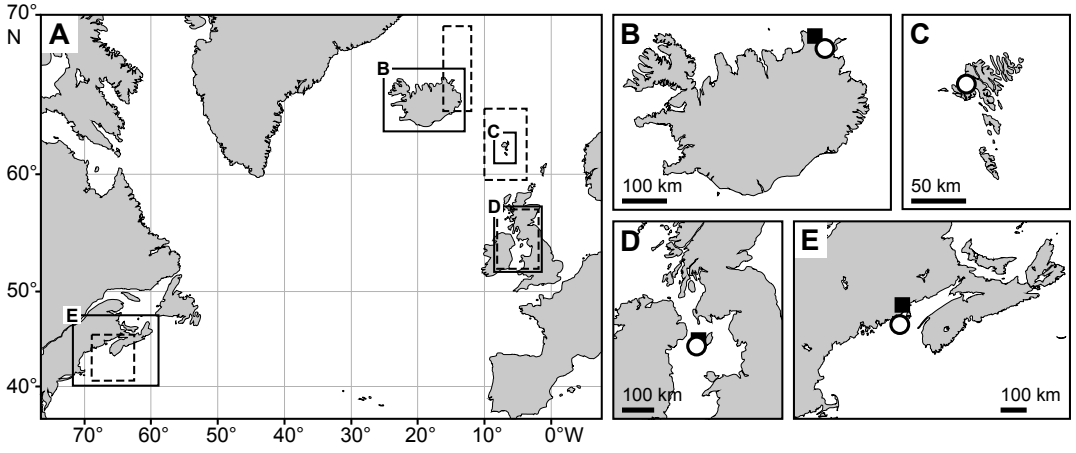

Fig. 1. Map showing sampling localities in the North Atlantic Ocean. (A) Overview map. Dashed rectangles denote regions for which average satellite-based chlorophyll *a* data was computed. (B–E) Detail maps: Iceland (B), Faroe Islands (C), Isle of Man (D) and Gulf of Maine (E). Open circles stand for sites where shells of *Arctica islandica* were collected, solid squares for environmental monitoring stations.

Table 1. Shell material (*Arctica islandica*) used in the present study. All specimens except one from the Isle of Man (ID 0525475) were collected alive.

Locality	Sample ID	Water depth [m]	Latitude	Longitude	Studied time interval	Number of studied annual increments
Iceland	ICE12-05-01 AL	9	66°9'58.92" N	15°22'58.92"W	1947–2010	64
	ICE12-05-05 AL	9	66°9'58.92" N	15°22'58.92"W	1936–2010	75
	ICE12-07-03 AL	11	66°11'13.68" N	15°20'48.3"W	1837–2008	172
	ICE12-14-01 AL	10	66°11'28.98" N	15°20'25.44"W	1840–2008	169
Faroe Islands	V6	20	62°9'15" N	7°10'25"W	1896–2007	112
	V12	20	62°9'15" N	7°10'25"W	1856–2006	151
Isle of Man	0505319	57	54°8'25.8" N	4°53'58.8"W	1924–2003	80
	0505327	30	54°18'34.8" N	4°43'14.4"W	1920–2003	84
	0525475	40	54°7'15.0"N	4°52'20.4"W	1758–2002	245
Gulf of Maine	090797	82–84	44°9.829'24.0"N	67°18.045'26.0"W	1964–2008	45
	090803	82–84	44°9.829'24.0"N	67°18.045'26.0"W	1953–2007	55
	090829	82–84	44°9.829'24.0"N	67°18.045'26.0"W	1952–2008	57

2.1 Preparation of the shells

Soft-tissues were removed from the live-collected specimens soon after collection. In the laboratory, shells were rinsed with deionized water and air-dried. One valve of each specimen was glued to a plexiglass cube with a plastic welder and wrapped in a protecting layer of a quick-drying epoxy resin (WIKO Flüssigmetall). Then, two ca. 3-mm-thick sections were cut from each specimen along the axis of maximum growth by using a low-speed precision saw (Buehler Isomet 1000) quipped with 0.4-mm-thick low-concentration diamond-coated saw blade. Shell slabs were mounted on glass slides with epoxy resin and surfaces ground (800 and 1200 grit SiC powder) and polished (1 µm Al_2O_3 powder). Shells from the Isle of Man were completely embedded in translucent epoxy (MetPrep Kleer-Set Type FF) prior to cutting sections from them at Bangor University. One section of each specimen was selected for sclerochronological analysis, the second section was used for LA-ICP-MS analysis (see below; Fig. 2).

2.2 Sclerochronological studies and construction of stacked chronologies

For growth pattern analysis of shells from Iceland and the Faroe Islands, Mutvei's immersion technique was applied (Schöne et al., 2005). Stained cross-sections were photographed with a Canon EOS 550D digital camera attached to a Wild Heerbrugg M8 stereomicroscope. Samples were illuminated with sectoral dark field (Schott VisiLED

MC 1000). Mature shell portions with very narrow increments were studied under a fluorescence light stereomicroscope (Zeiss AxioImager.A1m, HBO 100 mercury lamp for UV light, Zeiss filter set 18 with an excitation wavelength of 390–420 nm and an emission wavelength of > 450 nm). The combined use of Mutvei solution and UV light greatly facilitated the recognition of annual growth lines (Marali and Schöne, 2015). Previously, Wanamaker et al. (2009) noticed that annual growth lines in the hinge of unstained *A. islandica* shells fluoresce, which is eventually caused by larger amounts of organic components in these shell portions. Annual increment widths were determined in the hinge plate with the image processing software Panopea (available on request from BRS). Annual growth increment widths measurements of shells from the other two studied localities (Isle of Man, Gulf of Maine) were completed on acetate peel replicas. A detailed description of the method is provided in Butler et al. (2009). Annual increment width measurements of the specimens from the Isle of Man were previously reported by Butler et al. (2010), those from Iceland by Marali and Schöne (2015) and those from the Gulf of Maine by Griffin (2012). To temporally align the Ba/Ca_{shell} data it was necessary to measure the annual increment widths of all twelve specimens regardless of whether they were previously measured or not. New measurements generally agreed well with published data (Fig. 3).

For each locality, the annual increment width chronologies of all studied specimens (Tab. 1) were crossdated and a (new) stacked chronology computed (Fig. 4). A detailed description of the crossdating and chronology construction methods is provided in Marali and Schöne (2015). Briefly, (1) age trend removal was accomplished with a 32-year spline function, and variance adjustment with adaptive power transformation of the time-series. (2) Chronologies were also corrected for lag-1 autocorrelation. (3) A bi-weight robust mean was used to compute local stacked chronologies. (4) Relative growth rates are expressed as standardized growth indices (SGI; given in standard deviations) to facilitate the comparison between time-series from different specimens (Schöne, 2003, 2013; Schöne et al., 2005). (5) The robustness of the crossdating was assessed with the inter-series correlation value (R_{bar}) and the expressed population signal value (EPS) (Wigley et al., 1984). R_{bar} provides information on the degree of synchrony among the individual growth increment width chronologies and the EPS value quantifies the strength with which the common signal within the population is expressed in the stacked chronology. Steps 1–3 and 5 were performed with the dendrochronological software package ARSTAN (Holmes et al., 1986; Cook and Krusic, 2007).

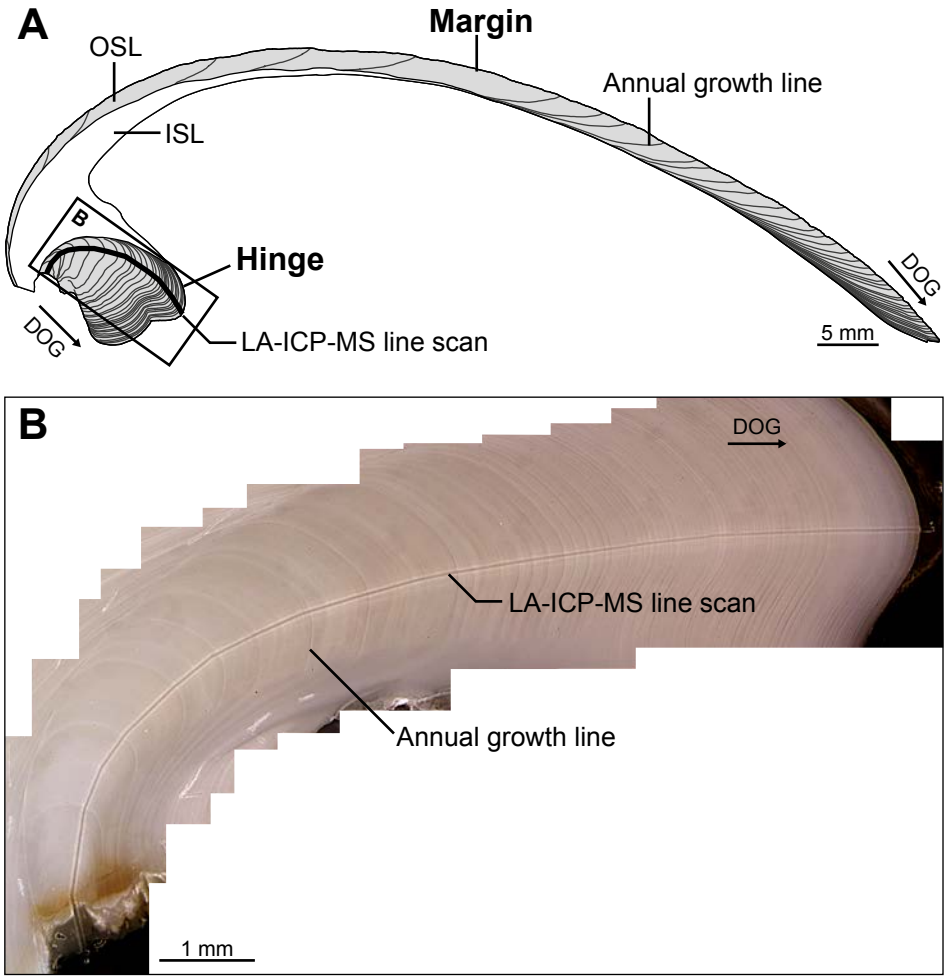

Fig. 2. Cross-sectioned shell of *Arctica islandica* highlighting shell layers, growth patterns and position of LA-ICP-MS line scan. (A) Annual growth lines are visible in the outer shell layer (OSL) of the margin and in the hinge area. The inner shell layer (ISL) is typically not used for sclerochronological analysis. A LA-ICP-MS line scan was placed in the hinge of each *A. islandica* specimen, following the axis of maximum growth (i.e., running perpendicular to annual growth lines). (B) Stitched image of the hinge of specimen 0505319 from the Isle of Man after laser ablation, depicting annual growth lines and the LA-ICP-MS line scan. DOG = direction of growth.

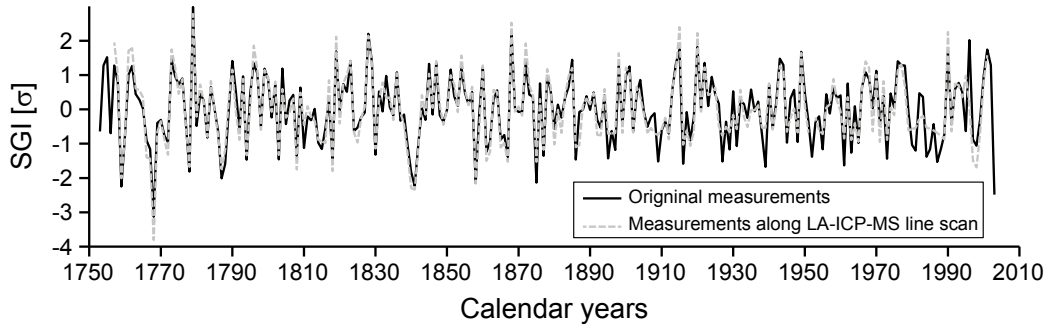

Fig. 3. Comparison of age-detrended (32-year spline) and standardized annual shell growth data (SGI) of an *Arctica islandica* specimen (ID 0525475) from the Isle of Man computed from original measurements used in Butler et al. (2009, 2010) (black line) with those measured in this study (dashed grey line). Note good agreement between both time-series.

2.3 LA-ICP-MS analysis

For barium analyses, the remaining polished slab of each shell was used. The hinge plate was cut from the rest of the shell, embedded in epoxy and polished with a Struers Tegramin-25 polishing machine using polishing discs with 9 µm, 3 µm and 1 µm grit. Barium (measured as ^{137}Ba) concentrations were determined by a quadrupole laser ablation – inductively coupled plasma – mass spectrometry (LA-ICP-MS) in line scan mode at the Institute of Geosciences, University of Mainz. Measurements were completed in the hinge plate of each specimen (Fig. 2). This portion of the shell has been used for several reasons. (1) The crystal fabrics are more homogenous in the hinge than in the ventral margin (Schöne, 2013). (2) This section of the shell is likely better preserved against diagenetic alteration because it is thicker than the central margin. (3) Growth patterns are more distinctly developed in this portion of the shell and, due to geometrical reasons, easier to measure.

Analyses were performed using an ArF Excimer laser system (193 nm wavelength, NWR193 by esi/NewWave) coupled to an Agilent 7500ce quadrupole ICP-MS. The laser was operated at a repetition rate of 10 Hz with laser energy at the sample site of ~7 J/cm2. Line scans were carried out after pre-ablation of the sample surface with a beam diameter of 55 µm, and a scan speed of 5 µm/s. Backgrounds were measured for 20 s prior to each line scan. NIST SRM 612 was used for calibration, applying the preferred values reported in the GeoReM database (http://georem.mpch-mainz.gwdg.de/, application version 18) (Jochum et al., 2005, Jochum et al., 2011) as the "true" concentrations to calculate the element concentrations in the samples. During each run, synthetic NIST SRM 610 (n = 24), basaltic USGS BCR-2G (n = 6) and synthetic carbonate USGS MACS-3 (n = 6) were analyzed as unknowns to monitor accuracy and reproducibility of the analyses (Tab. 2). Therefore, ca. 160 µm long line scans were completed on the reference materials. For all materials ^{43}Ca was used as

Table 2. LA ICP-MS quality control via reference materials NIST SRM 610, USGS BCR-2G and USGS MACS-3 (materials: synthetic glass, basaltic glass and synthetic carbonate, respectively). Average barium concentration ± one standard deviation (1 σ) is given in µg/g. Measured barium concentrations are given for two sequences. Sequence 1: samples from Iceland and Faroe Islands; Sequence 2: samples from Isle of Man and Gulf of Maine (for specimen IDs see Table 1). Reference values are taken from the sources stated below and can be found at the GeoReM database (http://georem.mpch-mainz.gwdg.de/).

Reference material	Measured values [µg/g]		Reference values [µg/g]	Source of reference values
	Sequence 1	Sequence 2		
NIST SRM 610	444.0 ± 14.0	450.0 ± 13.9	451.0 ± 22.0	GeoReM, Jochum et al. (2011)
BCR-2G	603.1 ± 12.8	649.9 ± 11.5	645.0 ± 26.0	GeoReM, Jochum et al. (2014)
MACS-3	66.0 ± 3.3	56.1 ± 1.6	58.7 ± 2.0	GeoReM, USGS

internal standard applying for the reference materials the calcium concentrations reported in the GeoReM database and for the samples a calcium concentration of 380,000 µg/g previously measured by ICP-OES, respectively (Marali, unpublished data). Data processing was performed using a Microsoft Excel spreadsheet following the methods of Longerich et al. (1996) and Jochum et al. (2007, 2011). Average detection limits (3σbackground; Jochum et al., 2012) for barium were 0.39 ± 0.10 µg/g. Values exceeding 5σ of 31-point running averages were regarded as outliers and therefore excluded from further analysis; this applied to < 0.001% of all values. Chemical data were placed in temporal context by means of growth pattern analysis.

The measured barium concentrations of the quality control materials NIST SRM 610 and USGS BCR-2G agree to within 0.4 to 11.7 % with published values and had relative standard deviations of 1.8 to 3.2 % (1 RSD; Tab. 2). The synthetic carbonate USGS MACS-3 is available as a pressed powder pellet. Due to the fine-grained structure of the pellet, particle sizes of MACS-3 can vary stronger during ablation than those of the silicate glass reference materials and the samples, causing potential differences in ionization in the plasma. Changes in ablation behavior of MACS-3 can occur in areas of the pellet that lie adjacent to the rim and/or previous ablation patterns where the original smooth and stable sample surface may be weakened. To account for resulting signal instabilities, barium measurements of the MACS-3 were filtered, i.e., values that deviated by more than 50 % from the median of the data set of each line scan are considered as outliers. After filtering, the barium concentrations of USGS MACS-3 deviated by 12.4 and 4.4 % from published values and had relative standard deviations of 5.0 and 2.8 % (1RSD; Tab. 2). All quality control materials measured during sequence 1 display slightly higher deviations from published values and RSDs than those measured during sequence 2. We cannot exclude potential instrumental variability as a cause. However, for both sequences the RSDs are within the repeatability range of LA-ICP-MS (Jochum et al. 2012; GeoReM database).

2.4 Mathematical treatment of Ba/Ca_{shell} chronologies and statistical analysis

To eliminate potential ontogenetic effects in Ba/Ca_{shell} data related to differences in sampling resolution (number of laser ablation spots per year) between ontogenetically younger and older shell portions, the Ba/Ca_{shell} data of each increment were arithmetically averaged and annually resolved time-series were computed (= re-sampling, down-sampling). Increments lying close to the epoxy coating (i.e., the first and few of the last formed increments) may be contaminated with barium coming from the epoxy. Therefore, Ba/Ca_{shell} data from these increments were not used to calculate annual Ba/Ca_{shell} averages. The averaged Ba/Ca_{shell} time-series thus contain fewer years than original increment width chronologies. In surface waters[3], *A. islandica* mainly grows its shell between February/March and August/September, although the growing season starts in October/November of the previous year (Weidman et al., 1994; Witbaard et al., 1994; Thébault et al., 2009b; Schöne, 2013; Marali and Schöne, 2015). Therefore, annual Ba/Ca_{shell} of the studied sample should largely represent the time interval of February/March to August/September. A pairwise Mann-Whitney U-test was applied (via the software PAST v. 2.17; Hammer et al., 2001) to test if the medians of the annual Ba/Ca_{shell} values of each specimen and locality were statistically different ($p < 0.05$).

2.5 Instrumental data

Annual Ba/Ca_{shell} data were compared to instrumental data during the main growing season, namely to sea surface temperature (SST), sea surface salinity (SSS) and chlorophyll *a* (Chl *a*). Chlorophyll *a* data (Fig. 1A) were extracted with the software SeaDAS 7.2 (available from NASA – National Aeronautics and Space Administration, http://seadas.gsfc.nasa.gov/) from three different data products available at NASA Goddard Space Flight Center (http://oceancolor.gsfc.nasa.gov/cgi/l3): CZCS – Coastal Zone Color Scanner (1979–1986), SeaWIFS – Sea-Viewing Wide Field-of-View Sensor (1987-2010) and Aqua MODIS – Moderate Resolution Imaging Spectroradiometer (2011+2012). No remotely sensed Chl *a* data are available for the time interval between 1987 and 1996 (Blondeau-Patissier et al., 2014). SST for the study site in Iceland was recorded during 1931–1999 by the station in Raufarhöfn (ca. 40 km NW of the sampling site; Fig. 1B; for suitability of this locality see Marali and Schöne, 2015). These data were provided by the Icelandic Meteorological Office (http://en.vedur.is/). SSS data for Iceland (65.5–67.5°N, 13.5–16.5°W) and the Faroe Islands (59.5–63.5°N, 3.5–9.5°W) were taken from the gridded dataset UKMO EN4 available at the Met Office Hadley

[3] It remains to be confirmed if the same applies to the specimens from the Gulf of Maine

Center from their website at http://www.metoffice.gov.uk/hadobs/en4/. Likewise, SST for the study site at Faroe Island were obtained from the Met Office Hadley Centre (HadISST1, 60–63°N, 4–9°W; 1901–2007; http://hadobs.metoffice.gov.uk/hadisst/). Representative SST and SSS data for the Isle of Man were recorded in 37 m water depth at Cypris Station during 1954–2003 (Fig., 1D; data were obtained from the British Oceanographic Data Centre from their website at http://www.bodc.ac.uk/). Temperature and salinity at 80 m water depth in the Gulf of Maine were recorded at Prince5 Station (Fig. 1E; data available at the website of the Bedford Institute of Oceanography; http://www.bio.gc.ca/index-en.php). All websites were last checked on 27 August 2015.

3 Results

3.1 Growth increment width chronologies

Regional stacked chronologies covered the time interval between AD 1755 and 2012 (Fig. 4; Tab. 1). The longest record came from a dead collected specimen from the Isle of Man (specimen ID: 0525475; 1755–2003; Tab. 1) which extended the length of the stacked record of this site and further strengthened the EPS and R_{bar} statistics (Fig. 4C). As indicated by 15-year running EPS values and concomitant high R_{bar} values, the most robust crossdated record was constructed from the four shells of NE Iceland (Fig. 4A). At this locality, EPS values were laying largely above the critical threshold of 0.85 (Wigley et al., 1984), even during times of sample depth as low as two shells (e.g., prior to 1920). However, at other localities, specifically the Faroe Islands, the critical threshold of 0.85 was only occasionally exceeded and sharp drops of the EPS and R_{bar} values occurred (Figs. 4B–D). Synchrony between growth patterns of the two specimens from the Faroe Islands was lower than that at other sites during the same time interval. Furthermore, disturbance lines aggravated annual increment counting in shell from this locality. Significantly more time was thus required to construct a stacked record. No statistically robust synchrony was observed between the three stacked chronologies from relatively shallow water (i.e., Iceland, the Faroe Islands and the Isle of Man; *p*-values of correlation analysis remained above 0.05; Fig. 4E).

It should be pointed out that EPS and R_{bar} statistics for published master chronologies from Iceland, the Isle of Man and the Gulf of Maine were generally higher than values reported here, because they were based on a much larger number of specimens.

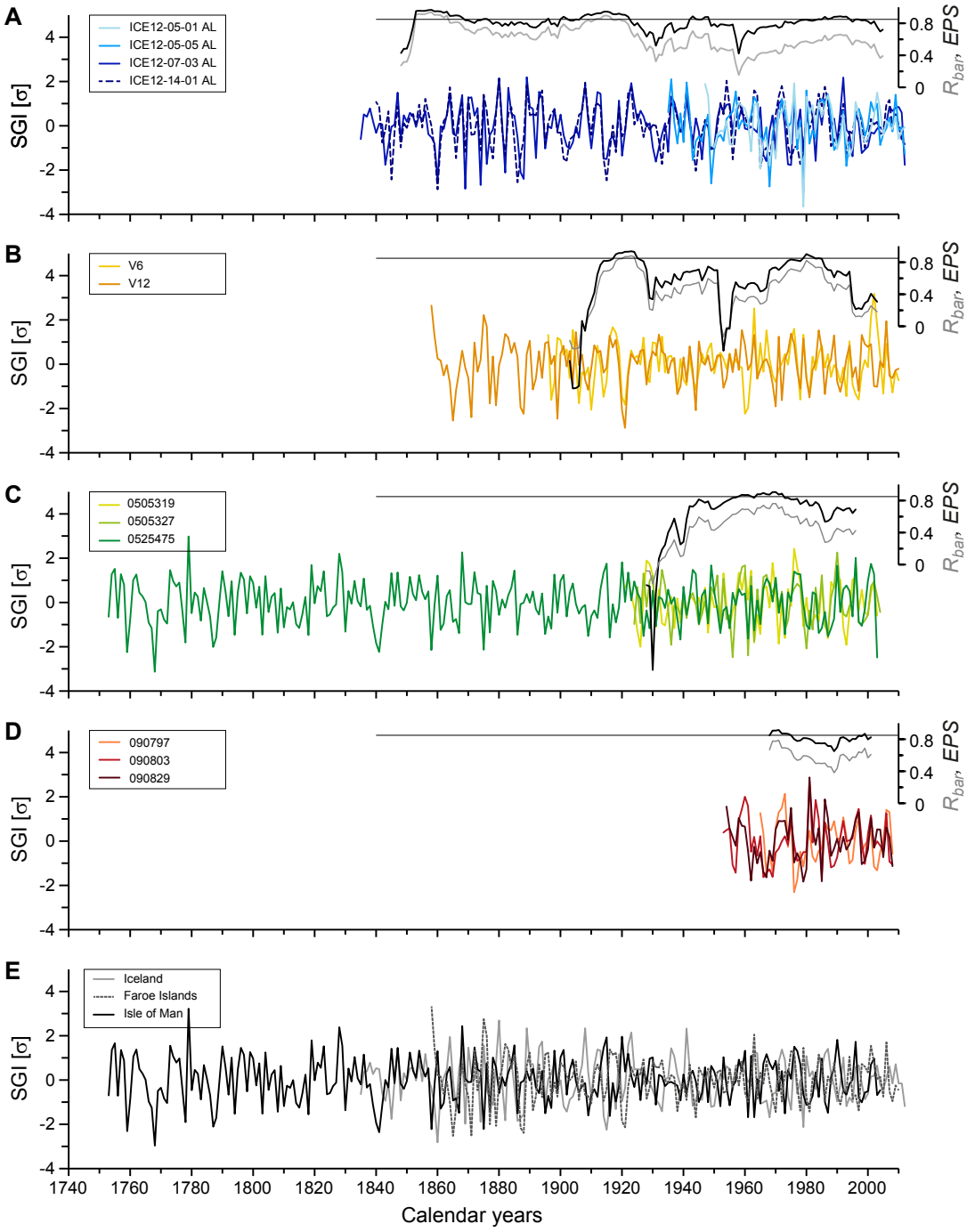

Fig. 4. Age-detrended (32-year spline) and standardized growth increment width (SGI) time-series of the specimens of *Arctica islandica* collected in NE Iceland (A), the Faroe Islands (B), the Isle of Man (C), and the Gulf of Maine (D). The inter-series correlation (R_{bar}) and expressed population signal (EPS) were calculated in 15-year running windows (overlapping by 14 years) for each locality. An EPS value of 0.85 is marked by a thin horizontal line. Numbers in boxes refer to specimen IDs. (E) Average SGI chronologies for the three relatively shallow water sites (i.e., Iceland, the Faroe Islands and the Isle of Man).

3.2 Ba/Ca_{shell} time-series

Ba/Ca_{shell} time-series of the studied shells were characterized by low background levels and episodic sharp peaks. Typically, Ba/Ca_{shell} peaks ranged between 22 and 84 µmol/mol. Values of 160 to 299 µmol/mol were recorded in shells from the Isle of Man (Fig. 5). In juvenile shell portions (age 1 to 12), background Ba/Ca_{shell} values ranged between 0.1 and 4 µmol/mol. High background values of ca. 0.2 to 6 µmol/mol occurred at the Isle of Man and smaller range of values of ca. 0.1 to 2 µmol/mol at the Gulf of Maine and Iceland. During lifetime, the Ba/Ca_{shell} background seemed to increase and peaks became smaller and broader (Figs. 5+6).

Ba/Ca_{shell} peaks were not associated with any particular growth pattern, e.g., growth lines or disturbance lines, but occurred during different times of the growing season. For example, specimens 0505327 and 0505319 from the Isle of Man showed peaks at the beginning of the growing season (e.g., 1924) as well as later during the year (e.g., 1920; Fig. 5C). At some localities, double peaks were present in some years, whereas in other years, Ba/Ca_{shell} peaks were completely absent (e.g., Gulf of Maine; Fig. 5D). Most importantly, irrespective of the ontogenetic age, *A. islandica* specimens from the same population showed generally highly synchronized Ba/Ca_{shell} peaks, i.e., the peaks occurred at the exact same time of the growing season (Figs. 5A, C, D). Only in some years, slight offsets were observed (e.g., Gulf of Maine in 1958; Figs. 5A, D). In contrast, specimens from the Faroe Islands generally showed a lower degree of synchrony among Ba/Ca_{shell} peaks than specimens from the other studied localities (Figs. 5+6).

The height and shape of contemporaneous Ba/Ca_{shell} maxima varied among specimens. In general, higher, more pronounced peaks were observed in juvenile specimens and lower, broader peaks in ontogenetically older shells (Figs. 5+6). For example, during the late 1930s, sharp Ba/Ca_{shell} excursions were measured in juvenile specimen ICE12-05-05 AL, but attenuated, broad peaks in the two ontogenetically older specimens, ICE12-07-03 AL and ICE12-14-01 AL (Figs. 5A, 6A). However, there is no general rule of decreasing peak heights through lifetime. Sharply elevated Ba/Ca_{shell} values also occurred later during ontogeny. For example, during the first three decades of life, Ba/Ca_{shell} peaks of the two oldest specimens from Iceland (ICE12-07-03 AL and ICE12-14-01 AL) remained below ca. 17 µmol/mol, but attained values of ca. 24 µmol/mol at age 64 and 61 (= year 1892), respectively (Fig. 6A).

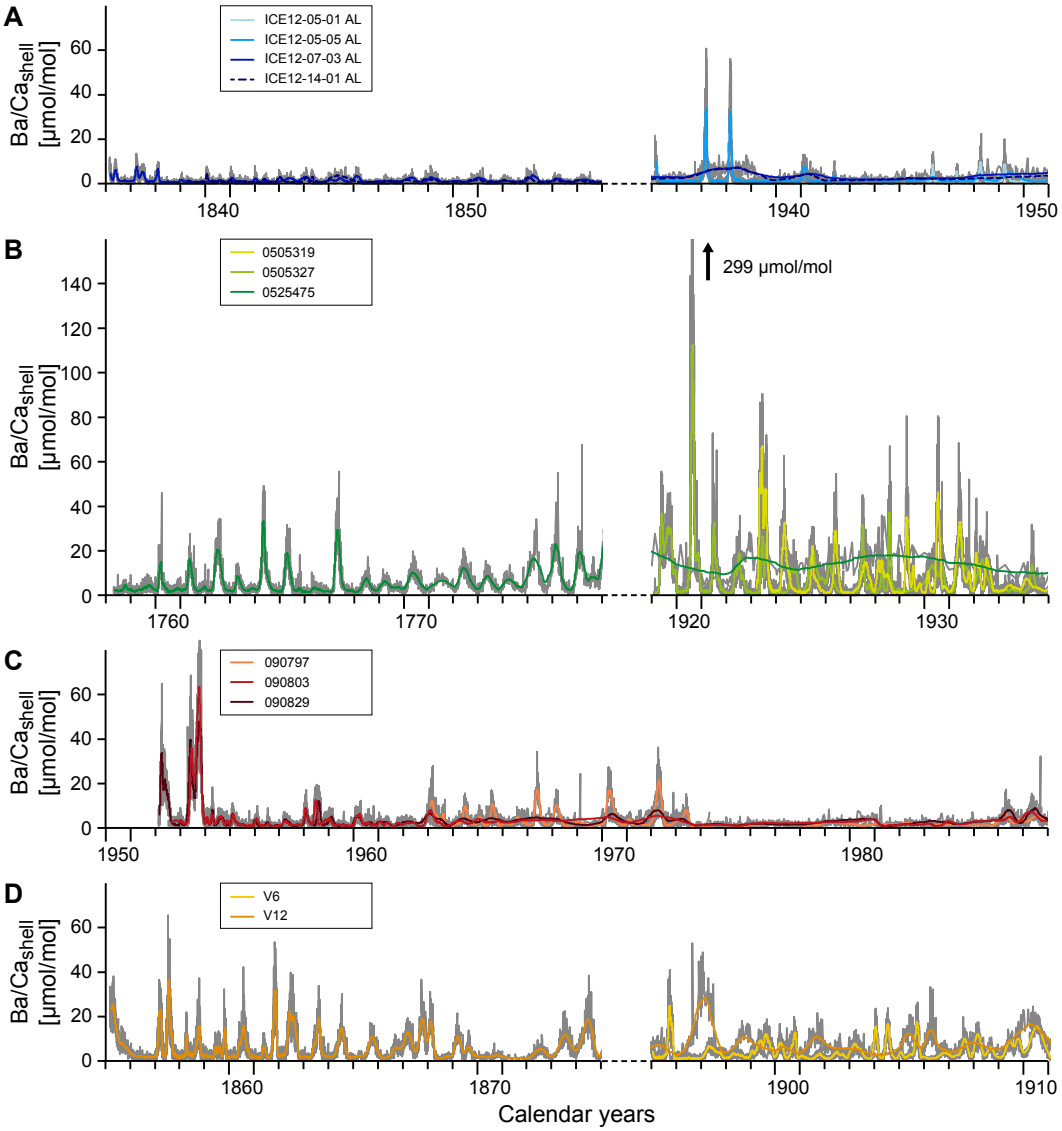

Fig. 5. Ba/Ca_{shell} data of *Arctica islandica* collected in NE Iceland (A), the Faroe Islands (B), the Isle of Man (C), and the Gulf of Maine (D). 31-pt running averages (colored curves) highlight the high degree of running similarity between individual Ba/Ca_{shell} time-series. Numbers in boxes refer to specimen IDs. Grey curves represent raw Ba/Ca_{shell} data of the studied specimens.

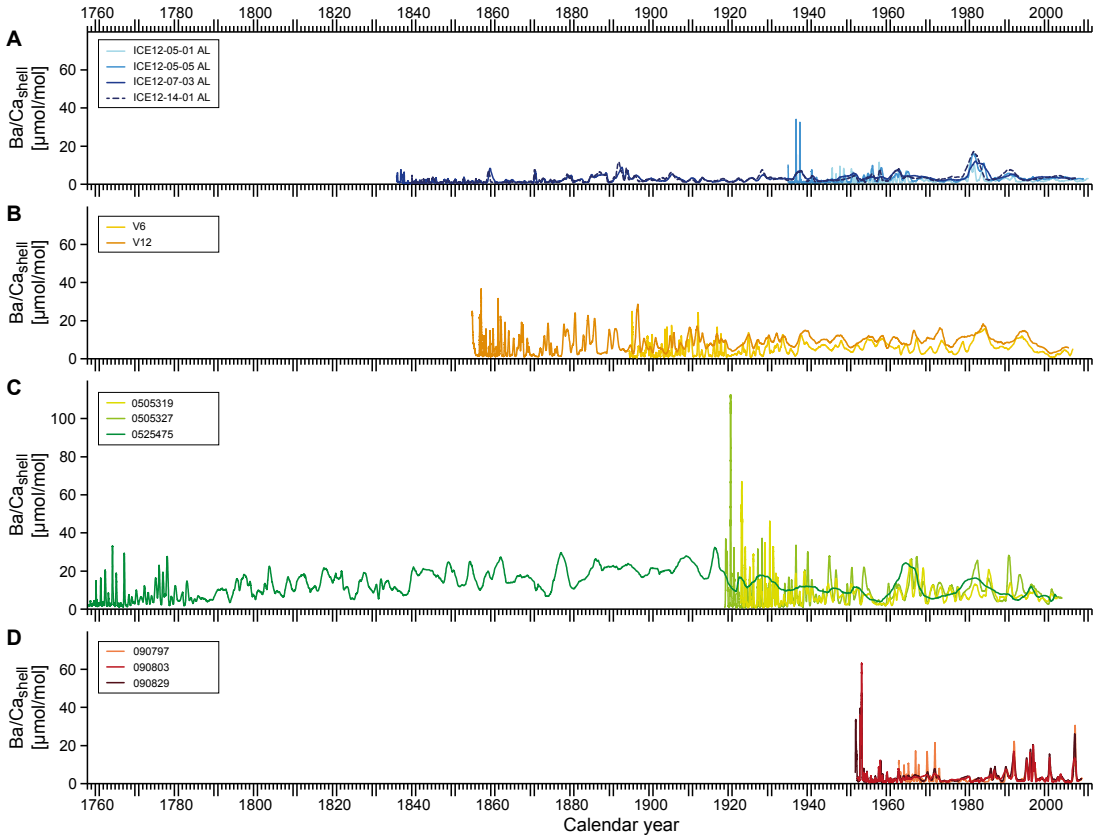

Fig. 6. Complete Ba/Ca_{shell} time-series of *Arctica islandica* from NE Iceland (A), the Faroe Islands (B), the Isle of Man (C), and the Gulf of Maine (D) displayed as 31-year running averages. Specimen IDs are displayed as numbers in boxes.

Annually resolved (= mathematically down-sampled to one data point per growing season) Ba/Ca_{shell} chronologies for each locality exhibited a remarkable degree of synchrony at all studied localities including Faroe Islands (Fig. 7). Even the peak heights in specimens of different age and the same calendar year were now much more similar than prior to this mathematical transformation (Figs. 3+4). Remarkably, EPS and R_{bar} values of Ba/Ca_{shell} chronologies were often larger than those for shell growth patterns (Figs. 2+4). For example, EPS values for the annual Ba/Ca_{shell} stacked chronologies from the Gulf of Maine and Iceland were above 0.85 over longer time intervals than those for the increment width (SGI) chronologies of these localities (Figs. 2A+D, 4A+D). Likewise, running EPS values for the Ba/Ca_{shell} stacked chronology from the Faroe Islands were closer to or exceeded the threshold of 0.85 more frequently than SGI-based EPS values (Figs. 2B, 4B).

Annual Ba/Ca_{shell} data were strongly site-specific (Fig. 8). Lowest median values of ca. 2.5 µmol/mol and the lowest variance among specimens were found in Iceland and the Gulf of Maine (Fig. 8). Ba/Ca_{shell} data of specimens from the same site having different ontogenetic ages were generally statistically indistinguishable (Fig. 8A; Mann-

Table 3. Linear regression analysis comparing annual increment widths (in mm) and annually averaged Ba/Ca_{shell} data for each specimen. n = number of compared years, r = Pearson's product moment correlation, r^2 = coefficient of determination. Significant correlations ($p < 0.05$) are indicated by bold letters.

Sample ID	*n*	*r*	r^2	*p*
ICE12-05-01 AL	64	-0.14	0.02	*0.255*
ICE12-05-05 AL	74	-0.16	0.03	*0.172*
ICE12-07-03 AL	172	-0.32	0.10	***< 0.001***
ICE12-14-01 AL	169	-0.27	0.07	***< 0.001***
V6	111	-0.22	0.05	***0.020***
V12	149	-0.24	0.06	***0.004***
0505319	80	-0.07	0.00	*0.554*
0505327	84	-0.10	0.01	*0.363*
0525475	244	-0.32	0.11	***< 0.001***
090797	44	0.21	0.04	*0.176*
090803	55	0.16	0.03	*0.238*
090829	57	0.42	0.18	***0.001***

Whitney U-test: $p > 0.05$). For example, the 75 and 172 year-old specimens at Iceland showed average medians of ca. 3 and 2.7 µmol/mol, respectively. On the contrary, the two specimens from the Faroe Islands as well as the three specimens from the Isle of Man were significantly different from each other with respect to Ba/Ca_{shell} (Fig. 8A) and medians differed considerably from those at the other two localities (ca. 6.5 and 10.5 µmol/mol, respectively; Fig. 8B).

Only in half of the studied shells, were annual Ba/Ca_{shell} data significantly ($p < 0.05$) correlated to increment widths in mm (negative in five specimens, positive in one), but corresponding coefficients of determination (r^2) were extremely low (ca. 0.10; Tab. 3). Visual inspection of the chronologies reveals the same result. For example, annual Ba/Ca_{shell} values of specimen 0525475 from the Isle of Man increased gradually from a local mean of ca. 5 µmol/mol to ca. 20 µmol/mol during the first 160 years of its life and then declined rapidly to values of ca. 8 µmol/mol at around 1940/1950 (Fig. 6C). However, no such corresponding change was observed in the annual increment chronology (Fig. 4C). After 1950, Ba/Ca_{shell} values of this specimen fluctuated greatly and reached maxima of more than 30 µmol/mol in 1965 (Fig. 6C). Again, such changes were unrelated to shell growth rate.

Table 4. Annual Ba/Ca_{shell} time-series for each locality (arithmetic average of all specimens per year and locality) were compared to environmental data (temperature, T; salinity, S; chlorophyll *a*, Chl *a*) during the growing season via linear regression analysis (Pearson's r). Significant correlations ($p < 0.05$) are given in bold letters.

Locality		Ba/Ca_{shell} vs. S (Mar-Aug)	Ba/Ca_{shell} vs. T (Mar-Aug)	Ba/Ca_{shell} vs. Chl a
Iceland	n	111	69	22
	r	< 0.01	-0.23	0.77
	r^2	< 0.01	0.05	0.59
	p	*0.983*	*0.061*	***< 0.001***
Faroe Islands	n	108	102	19
	r	0.12	-0.08	0.47
	r^2	0.01	0.01	0.22
	p	*0.230*	*0.386*	***0.044***
Isle of Man	n	42	39	15
	r	0.21	-0.42	0.52
	r^2	0.04	0.18	0.27
	p	*0.186*	***0.004***	***0.046***
Gulf of Maine	n	35	41	20
	r	-0.03	0.12	-0.21
	r^2	< 0.01	0.02	0.05
	p	*0.865*	*0.450*	0.365

3.3 Ba/Ca_{shell} chronologies and environmental data

As shown in Table 4, Ba/Ca_{shell} data were largely uncorrelated to SST and SSS, but compared relatively well with a strong Chl *a* event in the 1980s (Figs. 9+10). In the studied specimens from shallow water, Ba/Ca_{shell} values were significantly elevated during the early 1980s when strong phytoplankton blooms were recorded in large portions of the North Atlantic surface water by remote sensing (Figs. 9+10). This was particularly well expressed in shells from NE Iceland where elevated Chl *a* levels of more than 8 mg/m3 in 1981 were accompanied by annual Ba/Ca_{shell} maxima of 9 to 17 µmol/mol. At Faroe Islands and the Isle of Man, a marked Chl *a* increase occurred in 1982 and 1981, respectively. The annual Ba/Ca_{shell} maximum, however, corresponds to 1983 and 1984 in the Faroe Islands and to 1982 in the Isle of Man (Fig. 10), i.e. the annual Ba/Ca_{shell} peaks at these two sites lagged behind the local Chl *a* maximum by ca. two years. In contrast, the barium content of the shells from the Gulf of Maine showed no direct response to elevated primary productivity in surface waters (Fig. 10).

As in the case of SGI values, the agreement of the Ba/Ca_{shell} chronologies among sites was poor. Ba/Ca_{shell} data only compared reasonably well during times of strongly increased primary productivity in the early 1980s (Fig. 10).

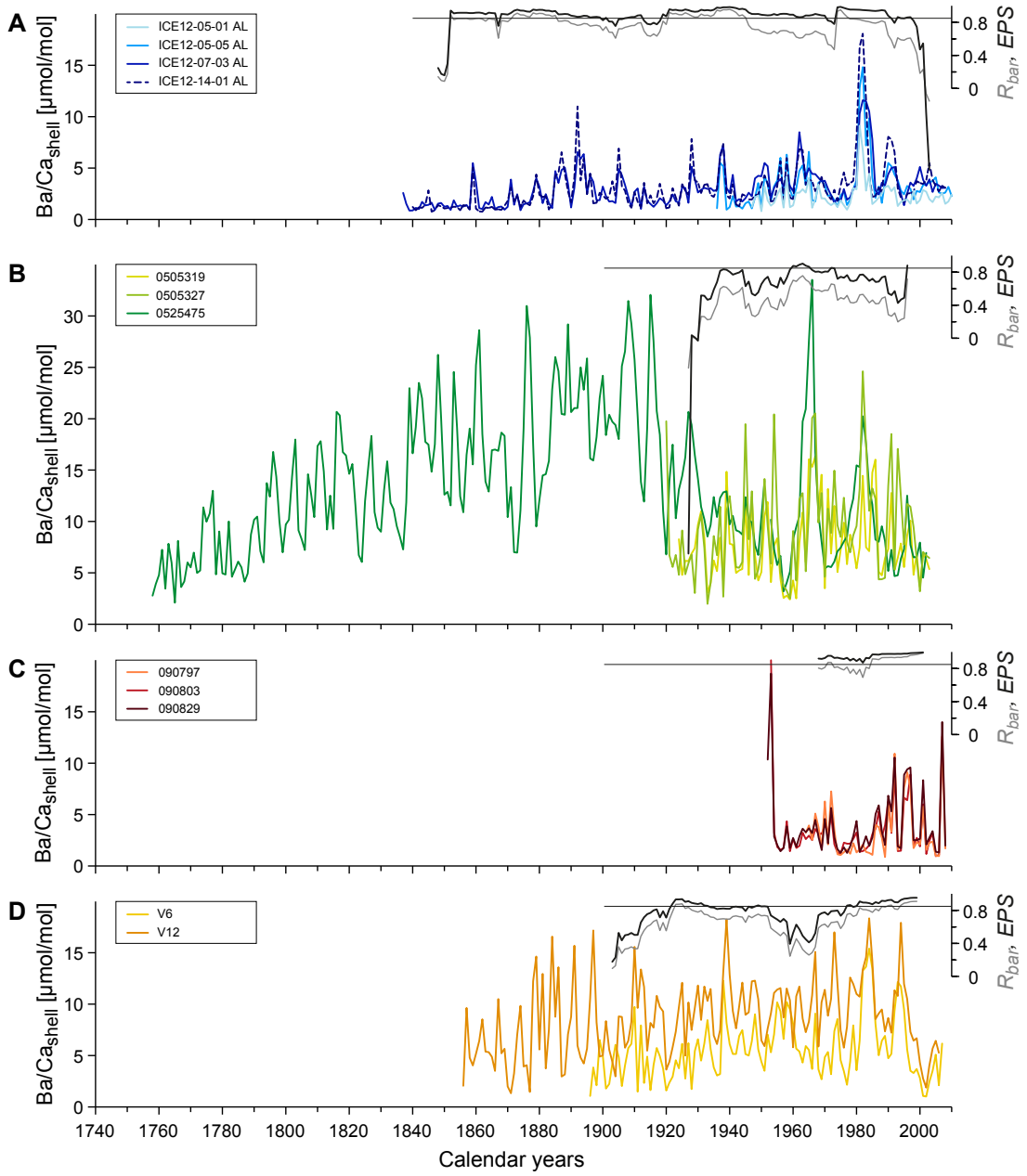

Fig. 7. Annually resolved Ba/Ca_{shell} data of *Arctica islandica* collected in NE Iceland (A), the Faroe Islands (B), the Isle of Man (C), and the Gulf of Maine (D). R_{bar} and EPS values were calculated in 15-year running windows (with 14 years of overlap). An EPS value of 0.85 is marked by a thin horizontal line. Numbers in boxes refer to specimen IDs.

4 Discussion

According to previous studies, high-resolution Ba/Ca_{shell} time-series of bivalve mollusks consistently show a flat, low background interrupted by sharp, erratic peaks which are highly synchronous in conspecific, contemporaneous specimens from the same locality. Without exception, these observations were based on short-lived species such as *Mercenaria mercenaria* (Stecher et al., 1996), *Saxidomus gigantea* and *Pecten maximus* (Gillikin et al., 2008), *Mesodesma donacium* and *Chione subrugosa* (Carré et al., 2006), *Mytilus edulis* (Vander Putten et al., 2000; Gillikin et al., 2006), *Comptopallium radula* (Thébault et al., 2009a) and *Isognomon ephippium* (Lazareth et al., 2003) or juvenile specimens of very long-lived bivalves such *Tridacna gigas* (Elliot et al., 2009) and *Arctica islandica* (Toland et al., 2000; Schöne et al., 2013). For the first time, the present study confirmed most of these findings for mature and ontogenetically old specimens of *A. islandica*, as well as for specimens coming from shallow and relatively deep waters (Tab. 1). Provided sufficient sampling resolution, prominent Ba/Ca_{shell} peaks were observed in old specimens (Figs. 3+4). Furthermore, irrespective of ontogenetic age, annual Ba/Ca_{shell} time-series were highly synchronous among specimens from the same population. As will be demonstrated below, Ba/Ca_{shell} has great potential to become a complementary tool in crossdating and the construction of stacked and master chronologies.

4.1 Ba/Ca_{shell} background level and peaks, annual Ba/Ca_{shell} values

In contrast to several existing studies, Ba/Ca_{shell} background levels did not always remain low and flat in *A. islandica*. For example, background levels in specimens from the Faroe Islands and the Isle of Man were up to three times as high as in shells from the other two studied localities (Figs. 5+6). This may suggest that the bioavailable barium in the water in which the shell lived differed among sites. In some specimens, background Ba/Ca_{shell} values seemed to gradually increase through lifetime (e.g., ICE-12-14-01 AL; Figs. 5A, 6A). This observation contrasts findings for S. gigantea by Gillikin et al. (2008), who measured higher background Ba/Ca_{shell} in younger (juvenile) parts in the ventral margin of the shell. The authors were able to preclude environmental causes (i.e., a change in salinity) for the observed trend in background Ba/Ca_{shell} and suggested an ontogenetic signal. In case of the present study, undertaken in the hinge area of *A. islandica*, we suggest that information on actual Ba/Ca_{shell} background values can only be obtained from ontogenetically young (therefore wide) shell increments where spatial resolution is sufficient to properly distinguish peaks from background levels within the same growing year. In slower-growing (ontogenetically older) parts of the

shell the sampling resolution is insufficient to resolve peaks from background. If the distance between adjacent Ba/Ca_{shell} peaks (including their tails) falls below the laser ablation spot size of 55 µm, genuine background values cannot be determined (signal smearing; compare Sanborn and Telmer, 2003). Similar arguments were brought forward by Gillikin et al. (2006). If physiological aging was causing ontogenetic trends of the Ba/Ca_{shell} background, one would expect the same trends to occur in all studied specimens. This is clearly not the case (Figs. 5+6). It seems more reasonable to assume that insufficient sampling resolution and time-averaging account for artificially raised background levels and apparent trends toward higher Ba/Ca_{shell} background values through ontogeny.

Likewise, the Ba/Ca_{shell} peak height (and shape) of *A. islandica* is unlikely to be controlled by physiology as hypothesized for other, much shorter-lived species (Vander Putten et al., 2000; Gillikin et al., 2006). More likely, attenuated peaks in ontogenetically older shell portions result from greater time-averaging and signal smearing. Directed trends of Ba/Ca_{shell} peak heights toward higher or lower values through lifetime were not observed in the present study (Figs. 5+6). In fact, specimens from Iceland and the Isle of Man occasionally showed higher peaks during adult life stages than during early ontogeny (Figs. 5A+C). This suggests that shell aging and ontogeny are at least not the main factors controlling the Ba/Ca_{shell} peak height in *A. islandica*. It is also possible that the observed changes of Ba/Ca_{shell} reflect spatial and temporal changes of the availability of barium. Further support for this hypothesis comes from mathematically down-sampled data (Fig. 7). This mathematical treatment largely removed potential time-averaging biases so that Ba/Ca_{shell} values from different specimens of the same locality and year could be directly compared. Annual Ba/Ca_{shell} data did also not reveal any ontogenetic trends toward lower or higher values, and they were presumably uncorrelated to annual increment width (Tab. 3). Furthermore, despite differences in the ontogenetic age of the studied specimens, the median Ba/Ca_{shell} from specimen ICE12-05-05 AL (75 years averaged) from Iceland was statistically indistinguishable (Kruskal-Wallis test $p > 0.05$) from that of specimen ICE12-07-03 AL (172 years averaged) from the same site (Fig. 8). However, Ba/Ca_{shell} averages of specimens from the Isle of Man and the Faroe Islands were substantially higher than those of the other two localities (Fig. 8). As argued above, this may be attributed to local differences of the bioavailable barium.

In existing studies, the most extreme Ba/Ca_{shell} peaks were observed in calcitic shell layers. Highest values occurred in *Mytilus edulis* (Vander Putten et al., 2000: 70 µmol/mol; Gillikin et al., 2006: ~ 44 µmol/mol), whereas the lowest values of less than 5 µmol/mol were observed in pectinids and oysters (*Pecten maximus*: Gillikin et al., 2008; Barats et al., 2009; *Comptopallium radula*: Thébault et al., 2009a; *Crassostrea gigas*:

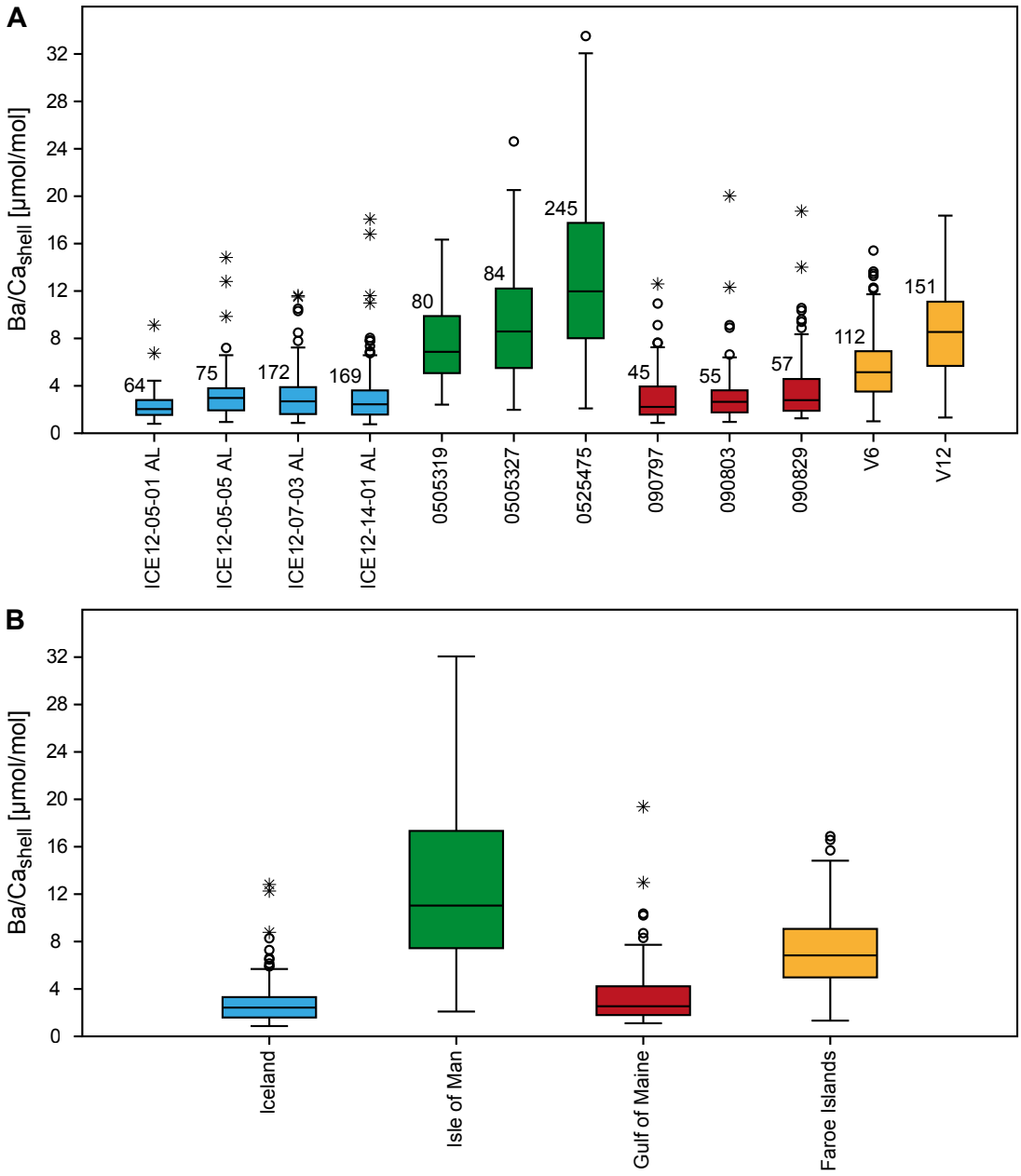

Fig. 8. Box plots of annual Ba/Ca_{shell} data of *Arctica islandica* collected in NE Iceland (blue), the Faroe Islands (yellow), the Isle of Man (green), and the Gulf of Maine (red). (A) Specimen-specific box-plots, (B) Site-specific box-plots. Numbers on x-axis in A denote specimen IDs. Numbers to the upper left of the box plots represent the number of averaged years. Open circles and asterisks stand for outliers (i.e., values deviating from the median by more than 1.5 and 3 times of the height of the boxes, respectively).

Goodwin et al., 2013). These findings somehow contradict the expectations, because shells of *Pecten maximus* yielded by far the highest temporal resolution. For example, in the study of Thébault et al. (2009a), the time represented by each laser ablation spot equaled only a few hours. Apparently, higher sampling resolution alone will not automatically result in higher Ba/Ca_{shell} peak values. It is possible that Ba/Ca_{shell} peak heights vary among species, but further research will be required to test this hypothesis. Although none of the previously studied aragonitic shells showed Ba/Ca_{shell} peaks as high as those observed in *M. edulis*, maximum values in (aragonitic) shells of *A. islandica* from the Isle of Man reported here were 299 µmol/mol, even though the time interval represented by each sample was longer than in the shorter-lived, fast-growing *M. edulis*. Clearly, the Ba/Ca_{shell} peak heights are not controlled by $CaCO_3$ polymorph. The same conclusion was drawn by Gillikin et al. (2008).

As in previous studies, Ba/Ca_{shell} peaks occurred at different times of the growing season and were not systematically associated with annual growth lines. This implies that the incorporation of barium into the shells is not controlled by biological factors, at least not the same as those that govern the incorporation of strontium and magnesium. The latter two elements are always strongly elevated near growth lines (e.g., Schöne et al., 2013). More likely, the Ba/Ca_{shell} peaks reflect an environmental signal. Support for this view comes from the highly synchronized Ba/Ca_{shell} signals, discussed in the following section. It should be noted that some Ba/Ca_{shell} peaks appear to be slightly offset from each other. Although we cannot preclude the possibility of asynchronous Ba/Ca_{shell} signals, an alternative explanation includes temporal misalignment of the Ba/Ca_{shell} data due to slight (unnoticed) differences in the timing of seasonal shell growth.

4.2 Potential links between Ba/Ca_{shell} and environmental changes

The synchronicity of Ba/Ca_{shell} peaks and annual Ba/Ca_{shell} values suggests an external forcing. Since intra-annual Ba/Ca_{shell} peaks were first described nearly two decades ago (Stecher et al., 1996), various hypothesis were brought forward, but no agreement was reached on the actual causes. Some authors suggested a relationship between Ba/Ca_{shell} peaks and primary productivity (Stecher et al., 1996, Vander Putten et al., 2000; Lazareth et al., 2003). It has been presumed that barium could be released from barium-rich phytoplankton[4] as it sinks to the seafloor and/or that barium-enriched phytoplankton flocs may be ingested by the bivalves (e.g., Stecher et al., 1996). In a detailed field study, Gillikin et al. (2008) demonstrated that Ba/Ca_{shell} peaks in *Saxidomus giganteа*n and *Pecten maximus* are temporally not well aligned with Chl *a* peaks and the peak heights do not correlate with Chl *a* intensity. Other authors observed a time lag of few days up to 3 months between seasonal Chl *a* peaks and seasonal Ba/Ca_{shell} maxima (e.g. Barats et al., 2009; Thébault et al., 2009; Hatch et al., 2013). The present study was not designed to examine the relationship between Chl *a* and Ba/Ca_{shell} maxima on a seasonal scale. A calibration study would require fast-growing, young specimens and highly resolved environmental data sets, i.e., similar to existing studies (e.g., Barats et al., 2009; Tabouret et al., 2012; Poulain et al., 2015). However, on an inter-annual scale, the extreme Chl *a* event in the 1980s (Gregg and Conkright, 2002) coincides with high annual Ba/Ca_{shell} values of all studied specimens at Iceland (Figs. 6+7). At the Isle of Man, the annual Ba/Ca_{shell} increase appears to occur with a lag of one year, and at the Faroe Islands with a lag of ca. two years relative to the local Chl *a* maximum (Fig. 10). We cannot preclude the possibility of errors in the stacked chronology at the latter site, because anomalous growth patterns occurred occasionally in one of the two specimens which made crossdating a very challenging task. Future studies with a longer Chl *a* data set are needed to test whether or not the observed lag represents a genuine signal (e.g., potentially explained by the environmental settings in which the shells lived, i.e., in a fjord in case of shells from the Faroe Islands).

At the Gulf of Maine, the increase of Chl *a* in surface waters was much less pronounced than at the other localities and none of the three studied specimens showed elevated annual Ba/Ca_{shell} values in the early 1980s. One possible explanation is that the primary productivity remained below a critical threshold that triggered Ba/Ca_{shell} peaks in the other shells (compare Toland et al., 2000,

[4] Barium is accumulated in the tests of certain phytoplankton species (Fisher et al., 1991; Bernstein and Byrne, 2004). Also, barite (barium sulfate) crystals can form in microenvironments provided by accumulations of decaying phytoplankton (i.e. phytoplankton flocs; barite precipitation probably occurring by bacterial activity; Dehairs et al., 1980; Torres-Crespo et al., 2015). Further, barium can adsorb to iron oxyhydroxides precipitating on the surface of diatom cells during phytoplankton growth (Sternberg et al., 2005).

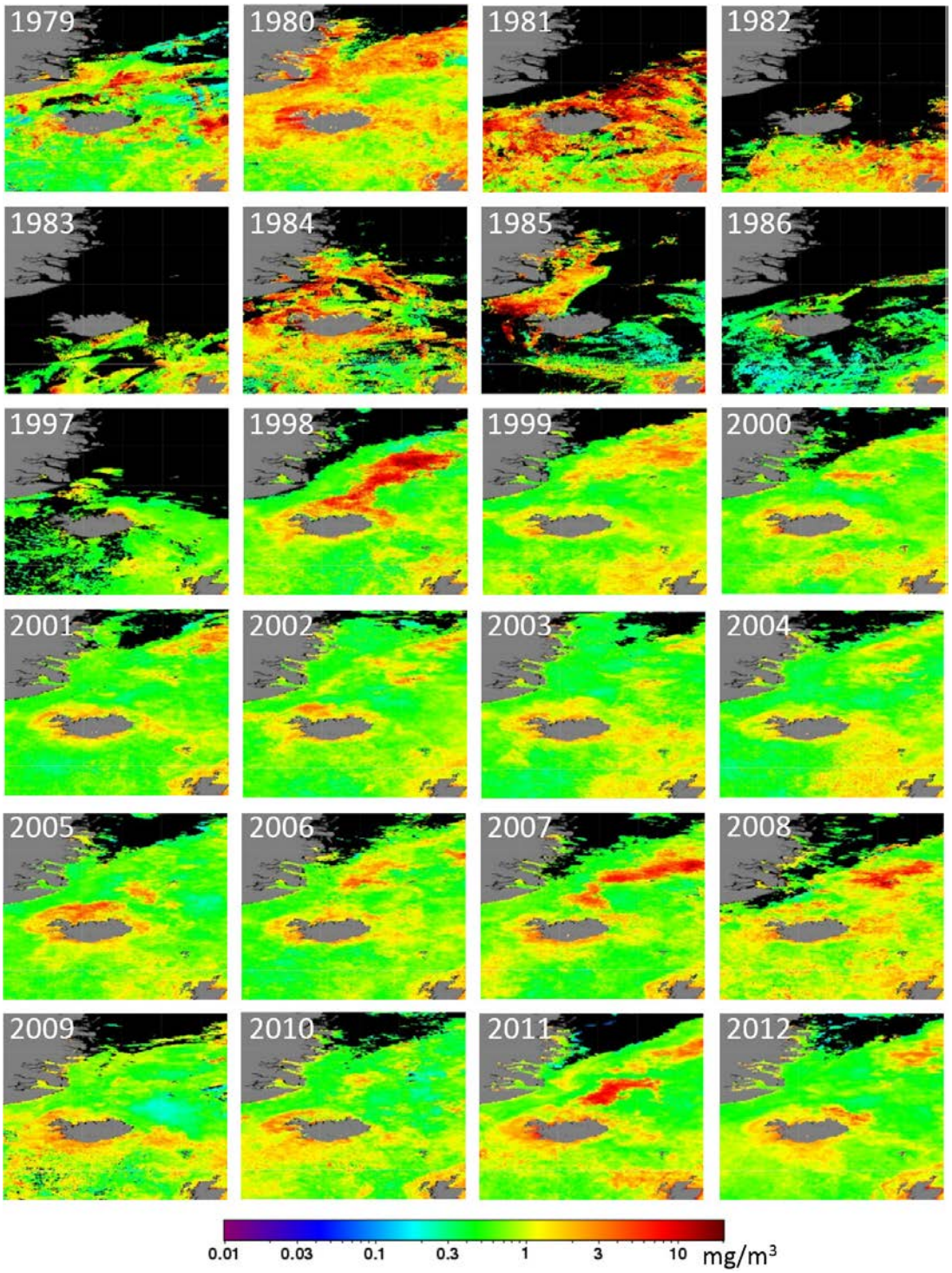

Fig. 9. Satellite-based chlorophyll *a* data (annual averages) between 1979 and 1986 as well as 1997 and 2012 around Iceland and the Faroe Islands.

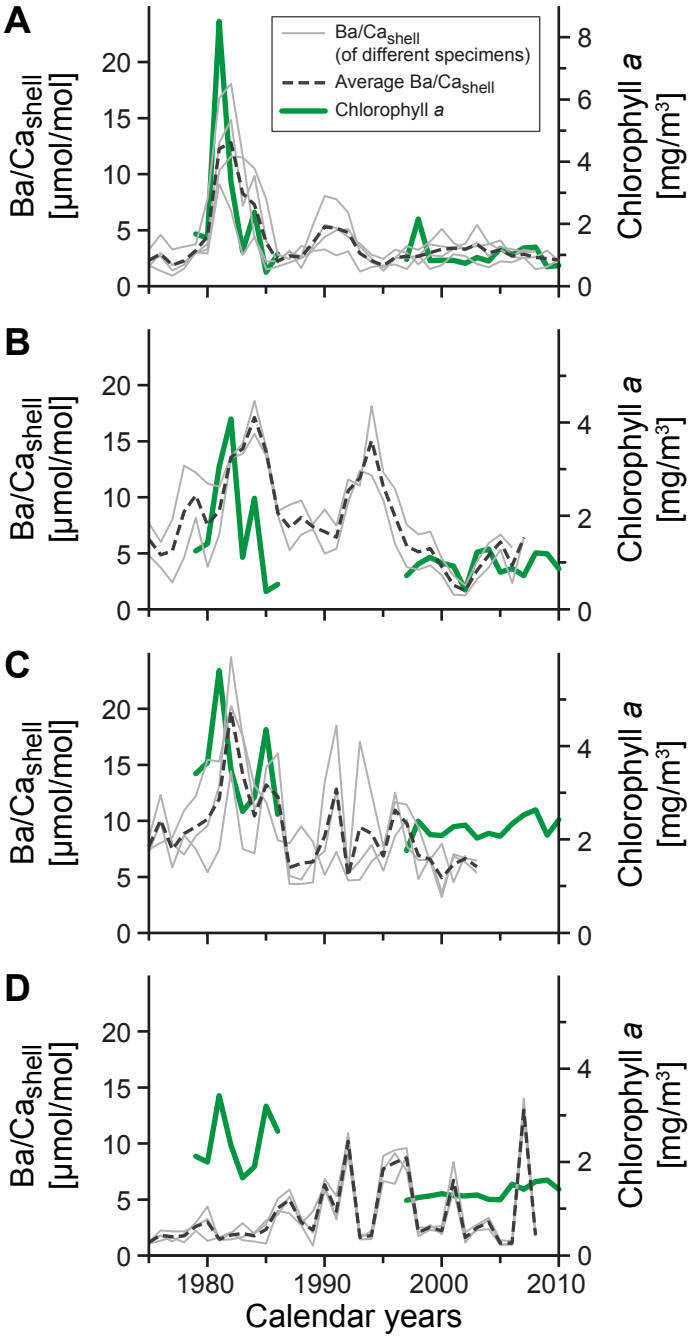

Fig. 10. Chlorophyll *a* data (solid green curve) extracted from satellite data (regional averages see Fig. 1A) in comparison to annual Ba/Ca$_{shell}$ data of *Arctica islandica* collected in NE Iceland (A), the Faroe Islands (B), the Isle of Man (C), and the Gulf of Maine (D). Please note that the Chl *a* scale has changed in B-D.

suggesting that extreme algal blooms may trigger Ba/Ca_{shell} excursions). Additionally, surface water Chl *a* remained relatively stable in the Gulf of Maine after 1997, while annual Ba/Ca_{shell} values displayed several excursions (Fig. 10D). This could indicate that shells in deeper water may be much less strongly linked to changes in surface waters, specifically if a seasonal thermocline is present.

In general, the concentration of dissolved and/or particulate barium in the habitat of the bivalves can be modulated by several factors: (1) Enhanced riverine influx (Coffey et al., 1997; see footnote 2), (2) processes related to primary productivity (e.g. Stecher et al., 1996; Barats et al., 2009; see footnote 4), also including diagenetic remobilization of dissolved barium in oxygen-deficient sediments under highly productive areas (Dymond et al., 1992; Gingele et al., 1999 and references therein; Henkel et al., 2012), potentially leading to barium-rich pore water, and/or (3) enrichment of dissolved barium in groundwater (due to desorption from aquifer solids; Shaw et al., 1998). Potentially, different barium sources may be responsible for the observed Ba/Ca_{shell} excursions in specimens from different habitats (i.e. surface or deeper water). Future experiments monitoring the concentration dissolved and particulate barium in surface and bottom water, as well as at the sediment-water interface will aid to trace the sources of barium for bivalves.

Changes in background Ba/Ca_{shell} data were previously interpreted as an indicator of salinity fluctuations (Gillikin et al. 2006, 2008; Poulain et al., 2015). We were unable to test if the same applies to *A. islandica*, because no appropriate salinity data were available for times when the studied shells were in their juvenile life stages and producing increments wide enough for a proper characterization of the Ba/Ca_{shell} background. Conversely, during times for which such environmental data are available, the specimens were already too old and grew too slowly, and the sampling resolution was thus insufficient to properly identify changes in the Ba/Ca_{shell} background (see further above: signal smearing).

4.3 Ba/Ca_{shell} peaks serve as a new crossdating tool

As demonstrated by the results of this study, annually resolved Ba/Ca_{shell} data can serve as a valuable and independent tool in crossdating and stacked or master chronology construction. If well-developed annual growth patterns are present in the hinge (as, for example, in the case of Iceland), annual Ba/Ca_{shell} time-series can be used to cross-validate increment-width based crossdating. Furthermore, annual Ba/Ca_{shell} time-series of two specimens can be used to check if their lifespans overlapped.

It can also be determined whether the growth increment time-series of a dead-collected specimen fits an existing stacked or master chronology. If this is the case, annual Ba/Ca_{shell} data could serve as a tool to preselect shells for radiocarbon dating or refine $^{14}C_{AMS}$ dates. In addition, where annual growth lines are difficult to discern, or numerous disturbance lines or anomalous growth patterns are present, annual Ba/Ca_{shell} time-series can be used to facilitate and verify crossdating based on growth pattern analysis (as in the case of the Faroe Islands). The new crossdating tool can be particularly useful when anomalous shell growth patterns are present, because they do not affect Ba/Ca_{shell} data. Common detrending techniques are typically not able to properly model growth anomalies, so that resulting SGI series do not crossdate well with those of other specimens.

Since the EPS and R_{bar} values of Ba/Ca_{shell}-based stacked chronologies appear in general to be stronger than those of chronologies based on shell growth patterns, a lower number of specimens may be sufficient to construct a statistically more robust stacked chronology. Typically, a minimum of four to five specimens is deemed sufficient to build a reliable stacked record from increment width chronologies of *A. islandica* (Stott et al., 2010; Marali and Schöne, 2015) as long as annual growth patterns are distinctly developed.

In the present study, high-resolution in-situ chemical analyses were exclusively performed in the hinge plate of *A. islandica* shells which contains a condensed growth record. Similar studies are also possible in the (outer) shell margin (compare Fig. 2), but would require significantly more time because the increments are broader. The use of a larger LA spot size or wet chemical analysis may be advised.

5 Summary and Conclusions

Mature and ontogenetically old specimens of the long-lived bivalve mollusk, *Arctica islandica*, showed Ba/Ca_{shell} patterns similar to those reported previously from short-lived bivalves, i.e., low background levels interrupted by sharp erratic peaks. However, due to increasingly lower sampling resolution and greater time-averaging, the background Ba/Ca_{shell} values appeared to increase toward higher values in some ontogenetically older shells, i.e., measurements represented averages of background and peak values. For similar reasons, the peaks became attenuated and broader in shell portions formed during later stages of life. Despite that, extreme Ba/Ca_{shell} values occurred nearly simultaneously in different, contemporaneous specimens from the same locality. Furthermore, the amplitude of Ba/Ca_{shell} values showed no clear relation

with growth rate and ontogenetic age. Time-averaging and sampling resolution biases were largely eliminated by mathematical transformation of the data, i.e., by computing annual Ba/Ca_{shell} averages. The annually averaged Ba/Ca_{shell} values of specimens from surface waters were strongly increased in the 1980s when an extreme primary productivity pulse was measured. Due to the lack of highly-resolved background data, however, this study cannot determine the exact cause of Ba/Ca_{shell} excursions. Despite that, we propose that Ba/Ca_{shell} time-series, specifically the highly synchronous Ba/Ca_{shell} peaks and annual Ba/Ca_{shell} values in contemporaneous specimens from the same locality can provide a tool to verify increment-based crossdating and facilitate chronology construction. The agreement between individual Ba/Ca_{shell} time-series expressed by the inter-series correlation (Rbar) and expressed population signal (EPS) values is even stronger than that based on annual increment width chronologies. Therefore, fewer shells are required to construct statistically more robust stacked bivalve sclerochronologies. Future studies are required to identify the environmental controls of Ba/Ca_{shell} values in *A. islandica*.

6 Acknowledgements

We deeply thank the editor, Thierry Corrège, Julien Thébault and the second anonymous reviewer for their supportive comments. We are grateful for discussions with Michael Maus, Michael Kersten and Thomas Tütken. We gratefully acknowledge the help of Hilmar A. Holland, Gudrun Thórarinsdóttir, Siggeir Stefánsson, Erlendur Bogason and Sæmundur Einarsson during fieldwork in Iceland and Ragnar við Streym (SP/F Streym Diving) for making divers available to collect shells near Faroe Islands. We thank the Captain and crew of the RV Prince Madog and of the scalloper Spaven Môr for assistance with the collection of shells from the Isle of Man. We further acknowledge Johanna Boos and Katrin Böhm for their assistance with shell preparation. This study has been made possible by a German Research Foundation (DFG) grant to BRS (SCHO 793/10-1).

7 References

Barats, A., Amouroux, D., Chauvaud, L., Pécheyran, C., Lorrain, a., Thébault, J., Church, T.M., Donard, O.F.X., 2008. High frequency Barium profiles in shells of the Great Scallop *Pecten maximus*: a methodical long-term and multi-site survey in Western Europe. Biogeosci. Discuss. 5, 3665–3698. doi:10.5194/bgd-5-3665–2008.

Bernstein, R.E., Byrne, R.H., 2004. Acantharians and marine barite. Mar. Chem. 86, 45–50. doi:10.1016/j.marchem.2003.12.003.

Black, B.A., Gillespie, D.C., MacLellan, S.E., Hand, C.M., 2008. Establishing highly accurate production-age data using the tree-ring technique of crossdating: a case study for Pacific geoduck (*Panopea abrupta*). Can. J. Fish. Aquat. Sci. 65, 2572–2578. doi:10.1139/F08-158.

Black, B.A., Dunham, J.B., Blundon, B.W., Brim-Box, J., Tepley, A.J., 2015. Long-term growth-increment chronologies reveal diverse influences of climate forcing on freshwater and forest biota in the Pacific Northwest. Global Change Biol. 21, 594–604. doi:10.1111/gcb.12756.

Blondeau-Patissier, D., Gower, J.F.R., Dekker, A.G., Phinn, S.R., Brando, V.E., 2014. A review of ocean color remote sensing methods and statistical techniques for the detection, mapping and analysis of phytoplankton blooms in coastal and open oceans. Prog. Oceanogr. 123, 123–144. doi:10.1016/j.pocean.2013.12.008.

Butler, P.G., Scourse, J.D., Richardson, C. a., Wanamaker, A.D., Bryant, C.L., Bennell, J.D., 2009. Continuous marine radiocarbon reservoir calibration and the ^{13}C Suess effect in the Irish Sea: Results from the first multi-centennial shell-based marine master chronology. Earth Planet. Sci. Lett. 279, 230–241. doi:10.1016/j.epsl.2008.12.043.

Butler, P.G., Richardson, C. a., Scourse, J.D., Wanamaker, A.D., Shammon, T.M., Bennell, J.D., 2010. Marine climate in the Irish Sea: analysis of a 489-year marine master chronology derived from growth increments in the shell of the clam *Arctica islandica*. Quat. Sci. Rev. 29, 1614–1632. doi:10.1016/j.quascirev.2009.07.010.

Butler, P.G., Wanamaker, A.D., Jr., Scourse, J.D., Richardson, C.A., and Reynolds, D.R., 2013. Variability of marine climate on the North Icelandic Shelf in a 1357-year proxy archive based on growth increments in the bivalve *Arctica islandica*. Palaeogeogr. Palaeclimatol. Palaeoecol. 373, 141–151. doi.10.1016/j.palaeo.2012.01.016.

Chester, R., Jickells, T.D., 2012. Marine Geochemistry, 3rd ed. Wiley-Blackwell, 420 pp.

Carré, M., Bentaleb, I., Bruguier, O., Ordinola, E., Barrett, N.T., Fontugne, M., 2006. Calcification rate influence on trace element concentrations in aragonitic bivalve shells: Evidences and mechanisms. Geochim. Cosmochim. Acta 70, 4906–4920. doi:10.1016/j.gca.2006.07.019.

Cook, E.R., Krusic, P.J., 2007. Program ARSTAN – A tree-ring standardization program based on detrending and autoregressive time-series modeling, with interactive graphics. Tree-Ring Laboratory, Lamont Doherty Earth Observatory of Columbia University, Palisade, NY, 14 pp.

Dehairs, F., Chesselet, R., Jedwab, J., 1980. Discrete suspended particles of barite and the barium cycle in the open ocean. Earth Planet. Sci. Lett. 49, 528–550. doi:10.1016/0012-821X(80)90094-1.

DeLong, K.L., Quinn, T.M., Taylor, F.W., 2007. Reconstructing twentieth-century sea surface temperature variability in the southwest Pacific: A replication study using multiple coral Sr/Ca records from New Caledonia. Paleoceanogr. 22, PA4212. doi:4210.1029/2007PA001444.

Douglass, A.E., 1914. A method of estimating rainfall by the growth of trees. Bull. Am. Geogr. Soc. 46, 321-335.

Douglass, A.E., 1941. Crossdating in Dendrochronology. J. For. 39, 825–831.

Dymond, J., Suess, E., Lyle, M., 1992. Barium in deep-sea sediment: A geochemical proxy for paleoproductivity. Paleoceanography 7, 163–181. doi:10.1029/92PA00181.

Elliot, M., Welsh, K., Chilcott, C., McCulloch, M., Chappell, J., Ayling, B., 2009. Profiles of trace elements and stable isotopes derived from giant long-lived *Tridacna gigas* bivalves: Potential applications in paleoclimate studies. Palaeogeogr. Palaeoclimatol. Palaeoecol. 280, 132–142. doi:10.1016/j.palaeo.2009.06.007.

Fisher, N.S., Guillard, R.R.L., Bankston, D.C., 1991. The accumulation of barium by marine phytoplankton grown in culture. J. Mar. Res. 49, 339–354. doi:10.1357/002224091784995882.

Freitas P.S., Clarke, L.J., Kennedy, H., Richardson, C.A., Abrantes, F. 2006. Environmental and biological controls on elemental (Mg/Ca, Sr/Ca and Mn/Ca) ratios in shells of the king scallop *Pecten maximus*. Geochim. Cosmochim. Acta 70, 5119–5133. doi:10.1016/j.gca.2006.07.029.

Gillikin, D.P., Lorrain, A., Navez, J., Taylor, J.W., André, L., Keppens, E., Baeyens, W., Dehairs, F., 2005. Strong biological controls on Sr/Ca ratios in aragonitic marine bivalve shells. Geochem. Geophys. Geosyst. 6, Q05009, doi:10.1029/2004GC000874.

Gillikin, D.P., Dehairs, F., Lorrain, A., Steenmans, D., Baeyens, W., André, L., 2006. Barium uptake into the shells of the common mussel (*Mytilus edulis*) and the potential for estuarine paleo-chemistry reconstruction. Geochim. Cosmochim. Acta 70, 395–407. doi:10.1016/j.gca.2005.09.015.

Gillikin, D.P., Lorrain, A., Paulet, Y.M., André, L., Dehairs, F., 2008. Synchronous barium peaks in high-resolution profiles of calcite and aragonite marine bivalve shells. Geo-Mar. Lett. 28, 351–358. doi:10.1007/s00367-008-0111-9.

Gingele, F.X., Zabel, M., Kasten, S., Bonn, W.J., Nürnberg, C.C., 1999. Biogenic barium as a proxy for paleoproductivity: methods and limitations of application, in: Fischer, G., Wefer, G. (Eds.), Use of Proxies in Paleoceanography. Examples from the South Atlantic. Springer, Berlin und Heidelberg, pp. 345–364. doi:10.1007/978-3-642-58646-0_13.

Goodwin, D.H., Gillikin, D.P., Roopnarine, P.D., 2013. Preliminary evaluation of potential stable isotope and trace element productivity proxies in the oyster *Crassostrea gigas*. Palaeogeogr. Palaeoclimatol. Palaeoecol. 373, 88–97. doi:10.1016/j.palaeo.2012.03.034.

Gregg, W.W., Conkright, M.E., 2002. Decadal changes in global ocean chlorophyll. Geophys. Res. Lett. 29, 1–4. doi:10.1029/2002GL014689.

Griffin, S.M., 2012. Applying dendrochronology visual crossdating techniques to the marine bivalve *Arctica islandica* and assessing the utility of master growth chronologies as proxies for temperature and secondary productivity in the Gulf of Maine. Unpublished Masters Thesis, Iowa State University, Ames, IA, 237 pp.

Hammer, Ø., Harper, D.A.T., Ryan, P.D., 2001. Paleontological statistics software package for education and data analysis. Palaeontol. Electron. 4, 9–18. doi:10.1016/j.bcp.2008.05.025.

Hatch, M.B.A., Schellenberg, S.A., Carter, M.L., 2013. Ba/Ca variations in the modern intertidal bean clam *Donax gouldii*: An upwelling proxy? Palaeogeogr. Palaeoclimatol. Palaeoecol. 373, 98–107. doi:10.1016/j.palaeo.2012.03.006.

Henkel, S., Mogollón, J.M., Nöthen, K., Franke, C., Bogus, K., Robin, E., Bahr, A., Blumenberg, M., Pape, T., Seifert, R., März, C., de Lange, G.J., Kasten, S., 2012. Diagenetic barium cycling in Black Sea sediments – A case study for anoxic marine environments. Geochim. Cosmochim. Acta 88, 88–105. doi:10.1016/j.gca.2012.04.021.

Holmes, R.L., Adams, R.K., Fritts, H.C., 1986. Tree-ring chronologies of Western North America, California, Eastern Oregon and Northern Great Basin with procedures used in the chronology development work including user manuals for computer programs COFECHA and ARSTAN. Chronology Series VI, 182 pp.

Jochum, K.P., Nohl, U., Herwig, K., Lammel, E., Stoll, B., Hofmann, A.W., 2005. GeoReM: A New Geochemical Database for Reference Materials and Isotopic Standards. Geostand. Geoanalytical Res. 29, 333–338. doi:10.1111/j.1751-908X.2005.tb00904.x.

Jochum, K.P., Stoll, B., Herwig, K., Willbold, M., 2007. Validation of LA-ICP-MS trace element analysis of geological glasses using a new solid-state 193 nm Nd:YAG laser and matrix-matched calibration. J. Anal. At. Spectrom. 22, 112. doi:10.1039/b609547j.

Jochum, K.P., Weis, U., Stoll, B., Kuzmin, D., Yang, Q., Raczek, I., Jacob, D.E., Stracke, A., Birbaum, K., Frick, D. a., Günther, D., Enzweiler, J., 2011. Determination of reference values for NIST SRM 610-617 glasses following ISO guidelines. Geostand. Geoanalytical Res. 35, 397–429. doi:10.1111/j.1751-908X.2011.00120.x.

Jochum, K.P., Scholz, D., Stoll, B., Weis, U., Wilson, S. a., Yang, Q., Schwalb, A., Börner, N., Jacob, D.E., Andreae, M.O., 2012. Accurate trace element analysis of speleothems and biogenic calcium carbonates by LA-ICP-MS. Chem. Geol. 318-319, 31–44. doi:10.1016/j.chemgeo.2012.05.009.

Jochum, K.P., Stoll, B., Weis, U., Jacob, D.E., Mertz-Kraus, R., Andreae, M.O., 2014. Non-Matrix-Matched Calibration for the Multi-Element Analysis of Geological and Environmental Samples Using 200 nm Femtosecond LA-ICP-MS: A Comparison with Nanosecond Lasers. Geostand. Geoanalytical Res. 38, 265–292. doi:10.1111/j.1751-908X.2014.12028.x.

Jones, D.S., Arthur, M.A., Allard, D.J., 1989. Sclerochronological records of temperature and growth from shells of *Mercenaria mercenaria* from Narragansett Bay, Rhode Island. Mar. Biol. 234, 225–234. doi:10.1007/BF00428284.

Lazareth, C.., Putten, E.V., André, L., Dehairs, F., 2003. High-resolution trace element profiles in shells of the mangrove bivalve *Isognomon ephippium*: a record of environmental spatio-temporal variations? Estuar. Coast. Shelf Sci. 57, 1103–1114. doi:10.1016/S0272-7714(03)00013-1.

Longerich, H.P., Jackson, S.E., Günther, D., 1996. Laser ablation inductively coupled plasma mass spectrometric transient signal data acquisition and analyte concentration calculation. J. Anal. At. Spectrom. 11, 899–904. doi:10.1039/JA9961100899

Lorens, R. B., Bender, M. L. 1977. Physiological exclusion of magnesium from *Mytilus edulis* calcite. Nature 269, 793–794. doi:10.1016/0016-7037(80)90087-3.

Marali, S., Schöne, B.R., 2015. Oceanographic control on shell growth of *Arctica islandica* (Bivalvia) in surface waters of Northeast Iceland — Implications for paleoclimate reconstructions. Palaeogeogr. Palaeoclimatol. Palaeoecol. 420, 138–149. doi:10.1016/j.palaeo.2014.12.016.

Marchitto, T.M., Jones, G.A., Goodfriend, G.A., Weidman, C.R., 2000. Precise temporal correlation of Holocene mollusk shells using sclerochronology. Quat. Res. 53, 236–246. doi:10.1006/qres.1999.2107.

Phung, A.T., Baeyens, W., Leermakers, M., Goderis, S., Vanhaecke, F., Gao, Y., 2013. Reproducibility of laser ablation-inductively coupled plasma-mass spectrometry (LA-ICP-MS) measurements in mussel shells and comparison with micro-drill sampling and solution ICP-MS. Talanta 115, 6–14. doi:10.1016/j.talanta.2013.04.019.

Poulain, C., Gillikin, D.P., Thébault, J., Munaron, J.M., Bohn, M., Robert, R., Paulet, Y.-M., Lorrain, A., 2015. An evaluation of Mg/Ca, Sr/Ca, and Ba/Ca ratios as environmental proxies in aragonite bivalve shells. Chem. Geol. 396, 42–50. doi:10.1016/j.chemgeo.2014.12.019.

Sanborn, M., Telmer, K., 2003. The spatial resolution of LA-ICP-MS line scans across heterogeneous materials such as fish otoliths and zoned minerals. J. Anal. At. Spectrom. 18, 1231–1237. doi:10.1039/b302513f.

Schöne, B.R., 2003. A "clam-ring" master-chronology constructed from a short-lived bivalve mollusc from the northern Gulf of California, USA. The Holocene 13, 39–49. doi:10.1191/0959683603hl593rp.

Schöne, B.R., 2013. *Arctica islandica* (Bivalvia): A unique paleoenvironmental archive of the northern North Atlantic Ocean. Global Planet. Change 111, 199–225. doi:10.1016/j.gloplacha.2013.09.013.

Schöne, B.R., Gillikin, D.P., 2013. Unraveling environmental histories from skeletal diaries – Advances in sclerochronology. Palaeogeogr. Palaeoclimatol. Palaeoecol. 373, 1–5. doi:10.1016/j.palaeo.2012.11.026.

Schöne, B.R., Freyre Castro, A.D., Fiebig, J., Houk, S.D., Oschmann, W., Kröncke, I., 2004. Sea surface water temperatures over the period 1884–1983 reconstructed from oxygen isotope ratios of a bivalve mollusk shell (*Arctica islandica*, southern North Sea). Palaeogeogr. Palaeoclimatol. Palaeoecol. 212, 215–232. doi:10.1016/j.palaeo.2004.05.024.

Schöne, B.R., Houk, S.D., Freyre Castro, A.D., Fiebig, J., Oschmann, W., 2005. Daily growth rates in shells of *Arctica islandica*: Assessing sub-seasonal environmental controls on a long-lived bivalve mollusk. Palaios 20, 78–92. doi:10.2110/palo.2003.p03-101.

Schöne, B.R., Zhang, Z., Jacob, D.E., Gillikin, D.P., Tütken, T., Garbe-Schönberg, D., McConnaughey, T., Soldati, A., 2010. Effect of organic matrices on the determination of the trace element chemistry (Mg, Sr, Mg/Ca, Sr/Ca) of aragonitic bivalve shells (*Arctica islandica*) – Comparison of ICP-OES and LA-ICP-MS data. Geochem. J. 44, 23–37.

Schöne, B.R., Zhang, Z., Radermacher, P., Thébault, J., Jacob, D., Nunn, E.V., Maurer, A.-F. 2011. Sr/Ca and Mg/Ca ratios of ontogenetically old, long-lived bivalve shells (*Arctica islandica*) and their function as paleotemperature proxies. Palaeogeogr. Palaeoclimatol. Palaeoecol. 302, 52–64. doi:10.1016/j.palaeo.2010.03.016.

Schöne, B.R., Radermacher, P., Zhang, Z., Jacob, D.E., 2013. Crystal fabrics and element impurities (Sr/Ca, Mg/Ca, and Ba/Ca) in shells of *Arctica islandica* - Implications for paleoclimate reconstructions. Palaeogeogr. Palaeoclimatol. Palaeoecol. 373, 50–59. doi:10.1016/j.palaeo.2011.05.013.

Stecher, H.A., Krantz, D.E., Lord, C.J., Luther, G.W., Bock, K.W., 1996. Profiles of strontium and barium in *Mercenaria mercenaria* and *Spisula solidissima* shells. Geochim. Cosmochim. Acta 60, 3445–3456. doi:10.1016/0016-7037(96)00179-2.

Sternberg, E., Tang, D., Ho, T.-Y., Jeandel, C., Morel, F.M.M., 2005. Barium uptake and adsorption in diatoms. Geochim. Cosmochim. Acta 69, 2745–2752. doi:10.1016/j.gca.2004.11.026.

Stott, K.J., Austin, W.E.N., Sayer, M.D.J., Weidman, C.R., Cage, A.G., Wilson, R.J.S., 2010. The potential of *Arctica islandica* growth records to reconstruct coastal climate in north west Scotland, UK. Quat. Sci. Rev. 29, 1602–1613. doi:10.1016/j.quascirev.2009.06.016.

Tabouret, H., Pomerleau, S., Jolivet, A., Pécheyran, C., Riso, R., Thébault, J., Chauvaud, L., Amouroux, D., 2012. Specific pathways for the incorporation of dissolved barium and molybdenum into the bivalve shell: An isotopic tracer approach in the juvenile Great Scallop (*Pecten maximus*). Mar. Environ. Res. 78, 15–25. doi:10.1016/j.marenvres.2012.03.006.

Thébault, J., Chauvaud, L., L'Helguen, S., Clavier, J., Barats, A., Jacquet, S., Pécheyran, C., Amouroux, D., 2009a. Barium and molybdenum records in bivalve shells: Geochemical proxies for phytoplankton dynamics in coastal environments? Limnol. Oceanogr. 54, 1002–1014. doi:10.4319/lo.2009.54.3.1002.

Thébault, J., Schöne, B.R., Hallmann, N., Barth, M., Nunn, E.V., 2009b. Investigation of Li/Ca variations in aragonitic shells of the ocean quahog *Arctica islandica*, northeast Iceland. Geochem. Geophys. Geosyst. 10. doi:10.1029/2009GC002789.

Toland, H., Perkins, B., Pearce, N., Keenan, F., Leng, M., 2000. Study of sclerochronology by laser ablation ICP-MS 15, 1143–1148. doi:10.1039/b002014l.

Torres-Crespo, N., Martínez-Ruiz, F., González-Muñoz, M.T., Bedmar, E.J., De Lange, G.J., Jroundi, F., 2015. Role of bacteria in marine barite precipitation: A case study using Mediterranean seawater. Sci. Total Environ. 512-513, 562–571. doi:10.1016/j.scitotenv.2015.01.044.

Vander Putten, E., Dehairs, F., Keppens, E., Baeyens, W., 2000. High resolution distribution of trace elements in the calcite shell layer of modern *Mytilus edulis*: Environmental and biological controls. Geochim. Cosmochim. Acta 64, 997–1011. doi:10.1016/S0016-7037(99)00380-4.

Wanamaker, A.D., Jr., Baker, A., Butler, P.G., Richardson, C.A., Scourse, J.D., Ridgway, I., Reynolds, D.J., 2009. A novel method for imaging internal growth patterns in marine mollusks: A fluorescence case study on the aragonitic shell of the marine bivalve *Arctica islandica* (Linnaeus). Limnol. Oceanogr. Meth. 7, 673–681. doi:10.4319/lom.2009.7.673.

Wanamaker, A.D., Jr., Hetzinger, S., Halfar, J., 2011. Reconstructing mid- to high-latitude marine climate and ocean variability using bivalves, coralline algae, and marine sediment cores from the Northern Hemisphere. Palaeogeogr. Palaeoclimatol. Palaeoecol. 302, 1–9. doi:10.1016/j.palaeo.2010.12.024.

Weidman, C.R., Jones, G.A., Lohmann, K.C., 1994. The long-lived mollusc *Arctica islandica*: a new paleoceanographic tool for the reconstruction of bottom temperatures for the continental shelves of the northern North Atlantic Ocean. J. Geophys. Res. 99, 18305–18314+22753. doi:10.1029/94JC01882.

Wigley, T.M.L., Briffa, K.R., Jones, P.D., 1984. On the Average Value of Correlated Time Series, with Applications in Dendroclimatology and Hydrometeorology. J. Clim. Appl. Meteorol. 23, 201–213. doi:10.1175/1520-0450(1984)023<0201:OTAVOC>2.0.CO;2.

Witbaard, R., Jenness, M.I., van der Borg, K., Ganssen, G., 1994. Verification of annual growth increments in *Arctica islandica* L. from the North Sea by means of oxygen and carbon isotopes. Neth. J. Sea Res. 33, 91–101. doi:10.1016/0077-7579(94)90054-X.

Manuscript III

Reproducibility of trace element variations (Na/Ca, Mg/Ca, Mn/Ca, Sr/Ca, and Ba/Ca) within and between specimens of the bivalve *Arctica islandica* – A LA-ICP-MS line scan study

Accepted for publication by
Palaeogeography, Palaeoclimatology, Palaeoecology

Soraya Marali[1], Bernd R. Schöne[1], Regina Mertz-Kraus[1], Shelly M. Griffin[2], Alan D. Wanamaker Jr.[2], Paul G. Butler[3], Hilmar A. Holland[1], Klaus P. Jochum[4]

[1] Institute of Geosciences, Johannes Gutenberg University, Johann-Joachim-Becher-Weg 21, 55128 Mainz, Germany
[2] Department of Geological and Atmospheric Sciences, Iowa State University, 253 Science I, Ames, IA 50011, USA
[3] School of Ocean Sciences, Bangor University, Menai Bridge, Anglesey, LL59 5AB, U.K.
[4] Climate Geochemistry Department, Max Planck Institute for Chemistry, P.O. Box 3060, 55020 Mainz, Germany

Authors' contributions

Concept: S. Marali
Growth pattern analysis: S. Marali, S. M. Griffin, P. G. Butler
LA-ICP-MS analysis: S. Marali, R. Mertz-Kraus
Data interpretation: S. Marali
Writing: S. Marali, B. R. Schöne, R. Mertz-Kraus, S. M. Griffin, A. D. Wanamaker Jr., P. G. Butler, H. A. Holland, K. P. Jochum

Marali, S., Schöne, B.R., Mertz-Kraus, R., Griffin, S.M., Wanamaker, A.D., Butler, P.G., Holland, H.A., Jochum, K.P., 2016 (*in press*). Reproducibility of trace element time-series (Na/Ca, Mg/Ca, Mn/Ca, Sr/Ca, and Ba/Ca) within and between specimens of the bivalve *Arctica islandica* – A LA-ICP-MS line scan study. Palaeogeogr. Palaeoclimatol. Palaeoecol. doi:10.1016/j.palaeo.2016.11.024.

Abstract

Trace element time-series in bivalve mollusk shells and other (biogenic) materials can potentially serve as environmental proxies. Yet, the applicability of element-to-calcium ratios is often challenging, because non-environmental factors such as vital effects distort or mask environmental signals. If a trace element time-series is driven by an environmental factor, it should be reproducible within and between coeval specimens of the same species. In the present study, we tested whether time-series of trace element-to-calcium ratios can be reproduced within and between coeval specimens of the bivalve *Arctica islandica* and thus whether an external signal is encoded in the temporal variations of trace elements along the shells. We determined the concentration of sodium, magnesium, manganese, strontium and barium by means of LA-ICP-MS in line scan mode in the hinge area of seven specimens from the Isle of Man, the Gulf of Maine and Iceland. In each specimen, the element composition was determined along two replicate line scans to gauge intra-specimen reproducibility. The degree to which trace element time-series can be reproduced was inferred from linear regression analysis and equaled on average 95 ± 4 % for Ba/Ca, 82 ± 27 % for Mg/Ca, 83 ± 18 % for Sr/Ca, 74 ± 23 % for Mn/Ca, and 22 ± 4 % for Na/Ca ratios (values correspond to coefficients of determination of the linear regression analysis expressed in percent).

The synchrony of Ba/Ca time-series between contemporaneous specimens from the same habitat has already been demonstrated in previous studies. Here, we observed common high-frequency variations (i.e., peaks) among coeval *A. islandica* from the same site for Mg/Ca, Sr/Ca, Mn/Ca and Na/Ca ratios, especially among specimens of similar ontogenetic age and with similar shell growth patterns. The results of the present study should be considered in interpretations of trace element time-series in bivalve shells as they can help to improve environmental and climate reconstructions.

Keywords: In-situ chemical analysis; Climate proxy; Environmental reconstructions; Biogenic calcium carbonate; Bivalve sclerochronology

Highlights

- Trace element signals should be reproducible within and between coeval specimens.
- Coeval *A. islandica* shells show reproducible (Ba, Mg, Mn, Sr)/Ca time-series.
- Na/Ca ratios are largely irreproducible within specimens.
- Na/Ca, Mg/Ca, Mn/Ca, Sr/Ca co-vary among specimens of similar ontogenetic age.

1 Introduction

The bivalve mollusk *Arctica islandica* is a powerful marine paleoclimate archive, being exceptionally long-lived (Butler et al., 2013) and widely distributed in the North Atlantic Ocean (Nicol, 1951; Merrill and Ropes, 1969; Dahlgren et al., 2000). Furthermore, shells of *A. islandica* contain precisely dated records of environmental change in the form of variable increment widths that are synchronous between individuals (Witbaard, 1996; Wanamaker et al., 2009a; Butler et al., 2013; Marali and Schöne, 2015), and geochemical properties such as isotopes and, potentially, trace and minor elements (Schöne et al., 2004; Wanamaker et al., 2008, 2012; Mette et al., 2016; Marali et al., 2017).

To determine the trace element record of bivalve shells, a precise analytical technique is required that offers a high spatial (and hence, for the proxy, temporal) resolution such as laser ablation – inductively coupled plasma – mass spectrometry (LA-ICP-MS). This technique has been successfully applied to bivalve shells (e.g., Gillikin et al., 2006; Schöne et al., 2010; Holland et al., 2014a; Füllenbach et al., 2015) and various biominerals (e.g., Sinclair et al., 1998; Jochum et al., 2012; Wit et al., 2013; Montagna et al., 2014), speleothems (e.g., Treble et al., 2003; Desmarchelier et al., 2006; Jochum et al., 2012) and sediments (e.g., Baker et al., 1999; Hennekam et al., 2015). When operated in line scan mode, i.e., in a succession of overlapping LA spots generated by moving the sample under the laser beam at a constant speed, LA-ICP-MS can provide uninterrupted trace element time-series (e.g., Montagna et al., 2006, 2007; Schöne et al., 2013; Holland et al., 2014a) that contain paleoenvironmental information on various temporal scales, ranging from multidecadal to sub-daily. Long-term, highly resolved environmental reconstructions, for instance of SST (e.g., Yan et al., 2015, based on ICP-OES analysis), expand our knowledge on past climate variability and can be used to test and verify numerical climate models (Mann et al., 2008, 2009).

However, the determination of the trace element concentrations of (non-) biogenic materials via LA-ICP-MS is a challenging task. Potential problems involve the calibration of the machine, interferences by molecules or multiply-charged ions, matrix effects and elemental fractionation (Harthorne et al., 2003; Jochum et al., 2012). Also, LA-ICP-MS line scan analysis can be complicated if the studied material is not homogenous, but composed of several layers or 'zones' (Sanborn and Telmer, 2003; Sinclair et al., 2005; Hennekam et al., 2015), and in particular, when these layers become narrower than the spot size of the laser (e.g. Marali et al., 2017). Because bivalve shells form by periodic accretion, a distinct layering or zonation is present consisting of growth lines (periods of relatively slow growth) and growth increments (periods of relatively fast growth). The mean widths of the growth increments generally decrease

as the bivalve grows older. Furthermore, the increment widths change in response to environmental conditions (e.g. Black et al., 2016). Favorable water temperature and higher food quality and availability have been shown in laboratory and field studies to result in faster shell growth and broader increments (e.g. Witbaard, 1996; Marali and Schöne, 2015; Mette et al., 2016). In contrast, the size of individual LA spots during one experiment typically remains invariant, so that the time represented by each geochemical data point changes during different ontogenetic stages of life and during different seasons of the year (see Schöne et al., 2011). In the case of bivalve shells, LA-ICP-MS analysis can be conducted along the ventral margin (e.g., Schöne et al., 2013) or in the hinge area (e.g., Schöne et al., 2011; Holland et al., 2014a; Marali et al., 2017), both of which contain the same growth history. The ventral margin contains broader increments than the hinge, but is also more heterogeneous with respect to microstructure and geochemistry (e.g., Schöne et al., 2013; Shirai et al., 2014). For this reason, the present study focuses on the hinge of *A. islandica* shells.

Instrumental uncertainties of the LA-ICP-MS system can lead to 'noise' in the measured trace element time-series. By definition, noise should be irreproducible within a sample. Additionally, the trace element content of a material can be linked to (micro-) structural variability (referred to as 'compositional noise' by Sinclair et al., 2011). In the case of biogenic materials, biological and/or mineralogical factors (such as crystal growth kinetics, metabolic rates and/or the activity of enzymes involved in the biomineralization process) affect the architecture and the incorporation of trace elements (e.g., Takesue and van Geen, 2004; Stephenson et al., 2008; Foster et al., 2009; Schöne et al., 2011). We will simply refer to these factors as 'vital effects' (Urey et al., 1951), mineralogical or biological 'signals'; these signals may be reproducible within and/or even between specimens to a certain extent.

A potential environmental signal, encoded in the trace element time-series of any material, should be reproducible within and between co-occurring samples (e.g. Sinclair et al., 1998, 2005). It is therefore crucial to establish that the measured trace element time-series of biogenic and non-biogenic carbonates are reproducible, i.e., that they largely reflect environmental signals and are not caused by noise and/or vital effects (Sinclair et al., 2005, 2011). The degree of reproducibility and fidelity of LA-ICP-MS line scan analysis can be assessed by re-measuring the same line partly or completely (e.g. Sinclair et al., 1998; Anagnostou et al., 2011) or by measuring an additional line scan parallel to the first one (Sinclair et al., 2005, 2011). Previous work has focused on testing the reproducibility of LA-ICP-MS line scans in coral skeletons (Sinclair et al., 1998, 2005, 2011; Anagnostou et al., 2011). Equivalent studies on bivalves, however, are scarce (Elliot et al., 2009) and/or only considered LA-ICP-MS measurements in spot mode (Fuge et al., 1993; Toland et al., 2000; Phung et al., 2013).

In this study we systematically examine the reproducibility of trace element time-series (Na/Ca, Mg/Ca, Mn/Ca, Sr/Ca, Ba/Ca) using LA-ICP-MS in line scan mode in the shells of *A. islandica*. First we tested whether trace element time-series were reproducible within individual *A. islandica* specimens. For this purpose two line scans were measured in each specimen. After the first scan, the surface was re-polished and a replicate scan was measured at the same position as the first one. The two analyses were compared by linear regression analysis. We performed this analysis for specimens from the Isle of Man and the Gulf of Maine. In addition, data of a single specimen from Iceland, which was previously studied by Holland et al. (2014a) and subsequently by Marali et al. (2017), was used to support our data set. Then we assessed the degree of synchrony of trace element time-series between different coeval specimens in the same population (from the Isle of Man and the Gulf of Maine, respectively). Inter-specimen synchrony of trace element time-series has been demonstrated for Ba/Ca ratios of bivalve shells (Gillikin et al., 2006, 2008; Schöne et al., 2013; Marali et al., 2017) and probably indicates that the Ba/Ca ratio in the shell is driven by an environmental control. Yet, trace element synchrony between specimens may also result from similarities among shell growth patterns (Gillikin et al., 2005). To account for this, we compared the trace element time-series, absolute shell growth rates and relative shell growth patterns of different coeval specimens at different ontogenetic stages but from the same locality. The confirmation (or otherwise) of reproducibility within and between specimens will inform future geochemical analyses of biogenic carbonates.

2 Material and methods

Specimens of *A. islandica* were collected by dredging from the Isle of Man, the Gulf of Maine and Iceland (at 30–57 m, 82–84 m, and 10 m water depth, respectively; Fig. 1; Table 1). Except for one specimen from the Isle of Man, which died two years prior to sampling (Butler et al., 2010; Marali et al., 2017), all specimens were collected alive (Table 1).

2.1 Shell preparation

Bivalve soft-tissues were removed shortly after collection. Prior to subsequent preparation, shells were cleaned with water and air-dried. The shells from the Gulf of Maine and Iceland were prepared according to the protocol at Johannes Gutenberg University (JGU), Mainz, Germany. One valve per specimen was mounted on a

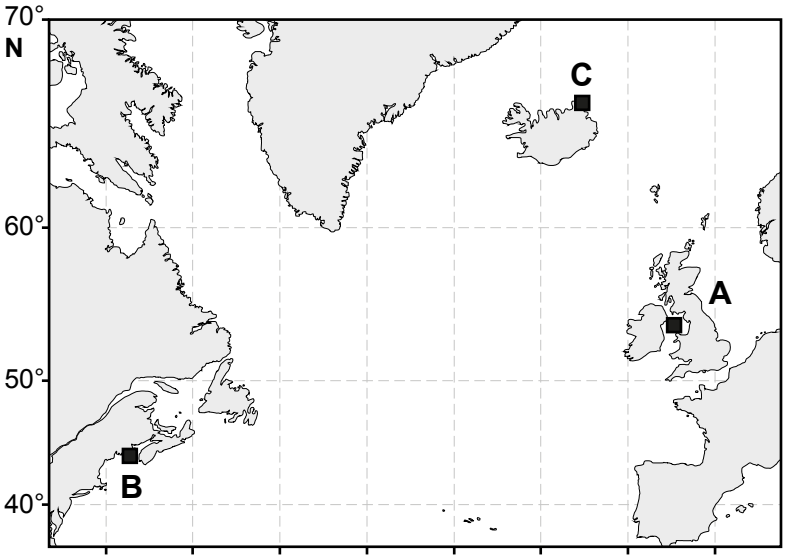

Fig. 1. Shell collection sites. Capital letters indicate (A) the Isle of Man, (B) the Gulf of Maine, (C) Iceland.

Plexiglas block using plastic welder. Then, a thin layer of quick drying metal epoxy resin (WIKO Flüssigmetall) was applied along the shell surfaces, to protect the shell during sectioning. From each valve, two ca. 3 mm-thick sections were cut along the axis of maximum growth with a low-speed precision saw (Buehler Isomet 1000) equipped with a 0.4-mm thick diamond-coated saw blade. These thick-sections were glued to glass slides, and then ground (800 and 1200 grit SiC powder) and polished (1 µm Al_2O_3 suspension). Shells from the Isle of Man were completely embedded in epoxy resin (MetPrep Kleer-Set Type FF) and cut at Bangor University. One section from each specimen was used for growth pattern analysis (sclerochronology), and the other section was analyzed by means of LA-ICP-MS. For LA-ICP-MS analysis, the hinge area of selected shell sections was separated from the margin, re-embedded into translucent epoxy (Araldite) and polished with a Struers Tegramin-25 polishing machine using grinding plates of a 9 µm, 3 µm and 1 µm grit, respectively.

2.2 Sclerochronology

To facilitate the recognition of growth patterns, shells from Iceland were immersed in Mutvei's solution (Schöne et al., 2005a) and studied under a Wild Heerbrugg M8 stereomicroscope using sectoral dark field illumination (Schott VsiLED MC 1000; reflective light). Digital images were taken with a Canon EOS 550D camera. Ontogenetically old parts of the shell, characterized by very narrow increments, were also photographed under a fluorescence light stereomicroscope (Zeiss AxioImager. A1m with a HBO 100 mercury lamp for UV light, using the Zeiss filter set 18 which

has an excitation wavelength of 390–420 nm and an emission wavelength of > 450 nm), because growth lines in *A. islandica* are fluorescent (Wanamaker et al., 2009b). Additional Mutvei staining prior to fluorescence microscopy can help to recognize faint growth lines (Marali and Schöne, 2015). The widths of annual growth increments were measured in the hinge area of the shells using the image processing software Panopea (© Peinl and Schöne). The shell growth patterns of the specimens from the Isle of Man and the Gulf of Maine were determined on acetate peel replicas (for a detailed description of the method see Butler et al., 2009).

Relative shell growth is highly synchronous among *A. islandica* specimens from the same population (i.e., the same habitat; e.g. Thompson et al., 1980). Therefore, shell growth patterns of specimens with overlapping lifespans can be combined to construct statistically robust stacked chronologies, so-called master chronologies (e.g., Butler et al., 2013; Holland et al., 2014b; Marali and Schöne, 2015). The specimens studied here have been successfully incorporated into such master chronologies. The shell growth patterns of specimens from the Isle of Man were described in Butler et al. (2010), while those from the Gulf of Maine and Iceland were analyzed by Griffin (2012) and Marali and Schöne (2015), respectively. The growth patterns of all specimens used in the current study are also shown in Marali et al. (2017). The increment width chronologies provide the temporal framework by which LA-ICP-MS data can be placed in a precise temporal context (see section 2.6).

2.3 LA-ICP-MS analysis

For LA-ICP-MS analysis, the hinge plate was analyzed. This part of the shell provides a condensed growth record. Long-term chemical time-series can be obtained relatively quickly, but at the expense of temporal resolution. In ontogenetically old parts of the shell, the width of annual increments can be narrower than the size of the laser spot. This leads to signal smearing (see discussion in Marali et al., 2017). However, the hinge of *A. islandica* is structurally and chemically much more uniform than the ventral margin (Foster et al., 2008, 2009; Schöne et al., 2013; Shirai et al., 2014; Stemmer and Nehrke, 2014) and has thus been preferred in the present study. The concentrations of sodium (measured as ^{23}Na), magnesium (^{25}Mg), manganese (^{55}Mn), iron (^{57}Fe), strontium (^{86}Sr at the Max Planck Institute for Chemistry (MPIC), Mainz, Germany; ^{88}Sr at JGU), and barium (^{137}Ba) were determined by means of LA-ICP-MS in the line scan mode. Each line scan was taken along the axis of maximum growth (Fig. 2; compare also Fig. 4 in Foster et al., 2009).

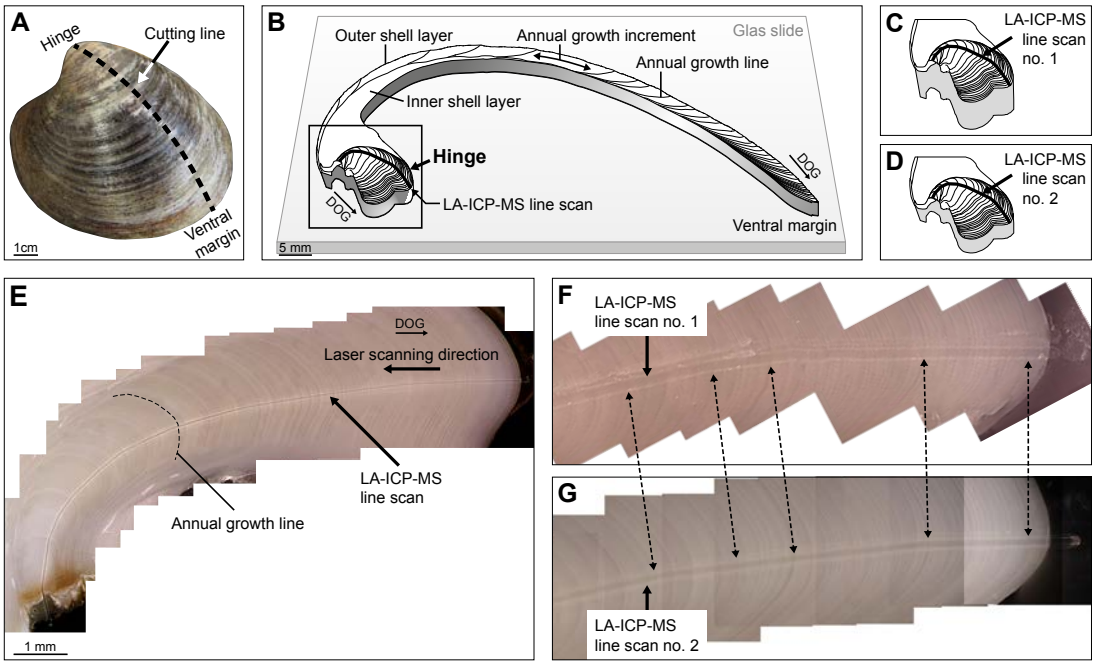

Fig. 2. The shell (A) of each *Arctica islandica* specimen was cut from the hinge towards the ventral shell margin along the axis of maximum growth. (B) Shell sections were mounted on glass slides, ground and polished. The same record of shell growth is comprised in both the outer shell layer of the margin and the hinge region in form of annual growth lines and increments; an arrow marks the direction of growth (DOG). The inner shell layer was not analyzed. LA-ICP-MS line scanning was performed in the hinge region along the direction of maximum hinge extension. (C, D) The hinge of all specimens was separated from the rest of the shell and prepared for trace element analysis. (C) A first LA-ICP-MS line scan was measured in each specimen. Then the samples were re-polished and (D) a second LA-ICP-MS line scan was measured in the same area of the shell as the first one. Note the loss of thickness of the shell section after re-polishing. (E) Stitched image of specimen 0505319 from the Isle of Man after LA-ICP-MS analysis. Annual growth lines and the laser line scan are visible. The laser scanning direction is opposite to the direction of growth. (F, G) Detail of the hinge of specimen 0505327 from the Isle of Man before and after re-polishing, displaying the first and second LA-ICP-MS line scan, respectively. Each line scan is ca. 55 µm wide. Annual growth lines can be distinguished on both images (dashed arrows mark some distinctive lines, visible before and after re-polishing). Differences in coloration of the shell between F and G are due to changing illumination during photographing.

2.3.1 Experimental setup

In order to assess the intra-specimen reproducibility, trace elements were measured along a LA-ICP-MS line scan of each specimen. Then, the shells were re-polished with a Struers Tegramin-25 (see above) and a second, replicate, LA-ICP-MS line scan was completed in the same area of each shell (Fig. 2). In total, four LA-ICP-MS sequences were performed (Table 1): Specimens from the Isle of Man and the Gulf of Maine were analyzed during sequence 0 and again during sequence 2 at JGU (sequence IDs refer to Marali et al., 2017). We further included the results from an additional specimen from Iceland to enlarge the data set. The first LA-ICP-MS analysis of the Icelandic specimen was conducted at MPIC, as part of a previous study, which dealt with the temporal distribution of pollutant metals iron and lead in *A. islandica* shells (Holland

et al., 2014a). The corresponding sequence is referred to as 'MPIC' (Table 1). The second LA-ICP-MS analysis of the Icelandic specimen was performed at JGU during sequence 1. The Ba/Ca measurements performed during sequences 1 and 2 were presented in Marali et al. (2017).

2.3.2 LA-ICP-MS instruments

LA-ICP-MS analysis at JGU (sequences 0, 1 and 2; Table 1) were conducted with an ArF Excimer laser system, operating at 193 nm wavelength (NWR193 from esi/NewWave), coupled to an Agilent 7500ce quadrupole ICP-MS. Laser repetition rate was 10 Hz. The laser energy on samples was about 7 J/cm2. Prior to each line scan, sample surfaces were pre-ablated to account for potential surface contamination. Background intensities were measured for 20 s. Line scans were carried out at a scan speed of 5 µm/s, using a beam diameter of 55 µm (Fig. 2). The LA-ICP-MS system applied at MPIC consists of a Nd:YAG laser with 213 nm wavelength (UP-213 from New Wave) coupled to a Thermo Element2 single collector sector-field ICP-MS (run in low-mass resolution mode). Laser energy density was ca.15.7 J/cm2. The laser beam size was 55 µm and measurements were performed with a scan speed of 5 µm/s. Background intensities were determined for ca. 12 s.

During each LA-ICP-MS sequence, the accuracy and precision of the LA-ICP-MS analysis was assessed by measuring ca. 160 µm long line scans on additional reference materials (USGS MACS-3, USGS BCR-2G, NIST SRM 610; Table 2). A detailed description of the LA-ICP-MS data quality control is given in the Supplementary Materials. The synthetic glass NIST SRM 612 (sequences 1, 2: n = 24; sequence 0: n = 21; sequence MPIC: n = 6) was used to calibrate element concentrations of *A. islandica* shell samples and the additional reference materials, applying the preferred values available from the GeoReM database (http://georem.mpch-mainz.gwdg.de/, application version 18; compare also Jochum et al., 2005, Jochum et al., 2011). ^{43}Ca was used as the internal standard for both *A. islandica* shells and reference materials. For *A. islandica* samples, a calcium concentration of 380,000 µg/g was used (ICP-OES analysis; Marali, unpublished data). Calcium concentrations of reference materials were taken from GeoReM database.

Table 1. List of *A. islandica* specimens, details on the shell collection sites and LA-ICP-MS analysis. All specimens, except 0525475 from the Isle of Man, were collected alive. Specimens from the Isle of Man and the Gulf of Maine were studied first via LA-ICP-MS during sequence 0; then the analysis was repeated during sequence 2. Both sequences were performed at Johannes Gutenberg University (JGU), Mainz, Germany, with an ArF Excimer laser with a wavelength of 193 nm. The specimen from Iceland was analyzed first at Max Planck Institute for Chemistry (MPIC) during sequence MPIC performed with a 213 nm Nd:YAG laser system. The analysis was repeated at JGU applying a 193 nm ArF Excimer laser (sequence 1).

Shell collection					LA-ICP-MS analysis				
Locality	**Specimen ID**	**Water depth [m]**	**Latitude**	**Longitude**	**Analyzed time interval**	**Number of studied annual increments**	**Laser type**	**Laser wavelength [nm]**	**LA-ICP-MS Sequence IDs**
Isle of Man	0505319	57	54°8'25.8" N	4°53'58.8"W	1924–2003	80	ArF Excimer	193	0, 2
	0505327	30	54°18'34.8" N	4°43'14.4"W	1920–2003	84	ArF Excimer	193	0, 2
	0525475	40	54°7'15.0"N	4°52'20.4"W	1758–2002	245	ArF Excimer	193	0, 2
Gulf of Maine	090797	82–84	44°9.829'24.0"N	67°18.045'26.0"W	1964–2008	45	ArF Excimer	193	0, 2
	090803	82–84	44°9.829'24.0"N	67°18.045'26.0"W	1953–2007	55	ArF Excimer	193	0, 2
	090829	82–84	44°9.829'24.0"N	67°18.045'26.0"W	1952–2008	57	ArF Excimer	193	0, 2
Iceland	ICE12-14-01 AL	10	66°11'28.98" N	15°20'25.44"W	1840–2008	169	Nd:YAG, ArF Excimer	213, 193	MPIC, 1

2.3.3 Data processing

LA-ICP-MS data from JGU and MPIC were processed after the methods described by Longerich et al. (1996) and Jochum et al. (2007, 2011) using a Microsoft Excel spreadsheet. Element concentrations of *A. islandica* samples which exceeded 31-point (31-pt) running averages by 5 σ were considered as outliers and excluded from further analysis (this threshold has been applied by Marali et al., 2017 as it effectively removed extreme outliers). Data from MPIC (Table 2) were collected at a lower effective spatial resolution than those from JGU (i.e., data is acquired every 1.4 s and 0.3 s at MPIC and JGU, respectively). For the ease of data visualization, elemental variations of samples measured at JGU were smoothed using symmetrical 31-pt running averages. For data from MPIC a symmetrical 5-pt running average was sufficient to smooth elemental data for specimen ICE12-14-01 AL (due to the lower effective spatial resolution).

2.4 Alignment of replicate LA-ICP-MS line scans

The replicate LA-ICP-MS line scans in each specimen slightly differed in total length (Fig. 2) and therefore needed to be scaled (i.e. aligned) to one another. As previously demonstrated for both coral skeletons and bivalve shells, time-series of Ba/Ca ratios are highly reproducible among parallel, contemporaneous LA-ICP-MS line scans performed in the same individual (Sinclair et al., 2005, 2011; Elliot et al. 2009). In the present study, Ba/Ca ratios of replicate line scans determined in each *A. islandica* specimen also display striking similarities, i.e. characteristic maxima and minima common to both line scans (Fig. 3). Replicate line scans were therefore aligned using the highly characteristic maxima and minima of the contemporaneous Ba/Ca signals (compare Elliot et al., 2009; Sinclair et al., 2011). To do so, characteristic maxima and minima were identified manually using the 'data picking' tool of the software Origin 7G. Then, one line scan was selected as a reference and the x-axis of the second line scan was interpolated, so that corresponding maxima or minima from both line scans overlapped (Fig. 3). In the case of specimens from the Isle of Man and the Gulf of Maine, we selected line scans performed during sequence 2 as the reference scans; for the Icelandic specimen the reference line scan was from sequence 1.

2.5 Assessing the intra-specimen reproducibility

The degree to which the time-series of a trace element-to-calcium ratio can be reproduced within a sample was evaluated by conducting linear regression analysis of mathematically resampled data sets. This was accomplished by averaging 100 consecutive data points to a new average value, referred to as '100-pt average'. Thereby, the spatial resolution of the data was reduced to ca. 150 µm (considering the effective spatial resolution of ca. 0.3 µm at 5 µm/s scan speed; section 2.3.3), which is the minimum spatial resolution recommended by Sinclair et al. (2005) for LA-ICP-MS analysis. Note that the x-axis (data points) of line scans performed during sequences 0 and MPIC were interpolated (see section 2.4). Also, some values were rejected from the trace element time-series as outliers (see section 2.3.3). Therefore, 100-pt average values corresponding to sequences determined at JGU comprise on average 85 ± 14 to 99 ± 2 data points (for Na/Ca and Mn/Ca, respectively). At MPIC, the effective spatial resolution of laser line scans was lower than at JGU (see section 2.3.3); 100-pt average values of sequence MPIC therefore comprise on average 20 ± 2 data points.

After resampling, the two 100-pt average data sets – corresponding to the two line scans per *A. islandica* specimen – comprise the same number of data points and can be readily compared via linear regression analysis. The resampling procedure also equals out small-scale differences between replicate line scans, arising from slight differences in the width of annual growth increments before and after re-polishing the sample surface (Fig. 2F, G). Finally, the intra-specimen reproducibility of trace element time-series measured by means of LA-ICP-MS was assessed by linear regression analysis using the software SPSS ver. 23. It should be emphasized that linear regression analysis can be used to test whether elemental data co-vary among two replicate line scans, even if the mean concentration of the corresponding element is slightly shifted between sequences (see Supplementary Materials). Although an outlier correction was performed before resampling (see section 2.3.3), Mg/Ca ratios of specimen 090797 determined during sequence 2 show three extremely high values. These three values exceed the mean of the data set by more than three standard deviations and we regard them as outliers. Deleting the three values significantly influenced the regression analysis performed for this specimen (see Table 3).

2.6 Temporal alignment and annual averaging of LA-ICP-MS data

To compare time-series of element-to-calcium ratios of different specimens from the same locality, n on-averaged trace element data were temporally aligned by

Table 2 (title is displayed on the following page).

Results for Na [µg/g]

Reference material	Measured values [µg/g]				Reference values [µg/g]	Source of reference values
	Sequence "MPIC"	Sequence 0	Sequence 1	Sequence 2		
MACS-3	5888.4 ± 1591.4	5125.5 ± 596.1	5776.1 ± 279.6	5408.3 ± 201.4	5900.0 ± 400.0	USGS, GeoReM*
BCR-2G		21405.7 ± 813.5	21189.2 ± 445.8	23258.6 ± 1198.1	23962.0 ± 519.3	GeoReM**
NIST SRM 610		95651.5 ± 2795.5	97302.8 ± 3451.5	102814.2 ± 3660.0	99408.9 ± 2225.6	Jochum et al. (2011); GeoReM**

Results for Mg [µg/g]

Reference material	Measured values [µg/g]				Reference values [µg/g]	Source of reference values
	Sequence "MPI"	Sequence 0	Sequence 1	Sequence 2		
MACS-3	1584.8 ± 231.1	1814.3 ± 135.0	1892.7 ± 104.7	1885.4 ± 61.9	1756.0 ± 136.0	USGS, GeoReM*
BCR-2G		23270.0 ± 802.8	21422.9 ± 367.0	23527.9 ± 505.4	21468.1 ± 542.7	GeoReM**
NIST SRM 610		538.6 ± 21.6	500.2 ± 13.2	533.8 ± 21.4	432.0 ± 29.0	Jochum et al. (2011); GeoReM**

Results for Mn [µg/g]

Reference material	Measured values [µg/g]				Reference values [µg/g]	Source of reference values
	Sequence "MPI"	Sequence 0	Sequence 1	Sequence 2		
MACS-3	516.4 ± 117.8	521.4 ± 14.6	524.9 ± 19.3	484.2 ± 15.0	536.0 ± 28.0	USGS, GeoReM*
BCR-2G		1574.2 ± 47.3	1404.6 ± 52.3	1558.5 ± 66.2	1471.5 ± 77.4	GeoReM**
NIST SRM 610		457.7 ± 15.9	429.3 ± 8.5	448.5 ± 13.9	444.0 ± 13.0	Jochum et al. (2011); GeoReM**

Results for Sr [µg/g]

Reference material	Measured values [µg/g]				Reference values [µg/g]	Source of reference values
	Sequence "MPI"	Sequence 0	Sequence 1	Sequence 2		
MACS-3	6162.0 ± 536.6	6421.2 ± 612.4	6689.5 ± 187.3	6862.1 ± 190.4	6760.0 ± 350.0	USGS, GeoReM*
BCR-2G		357.1 ± 12.9	315.8 ± 6.4	320.6 ± 5.2	342.0 ± 4.0	GeoReM**
NIST SRM 610		506.2 ± 24.1	504.7 ± 13.1	504.0 ± 16.3	515.5 ± 1.0	Jochum et al. (2011); GeoReM**

Results for Ba [µg/g]

Reference material	Measured values [µg/g]				Reference values [µg/g]	Source of reference values
	Sequence "MPI"	Sequence 0	Sequence 1	Sequence 2		
MACS-3	65.9 ± 7.6	60.0 ± 6.1	63.2 ± 4.1	55.3 ± 2.1	58.7 ± 2.0	USGS, GeoReM*
BCR-2G		725.2 ± 24.3	603.1 ± 12.8	649.9 ± 11.5	683.0 ± 7.0	GeoReM**
NIST SRM 610		451.6 ± 24.1	444.0 ± 14.0	450.0 ± 13.9	452.0 ± 9.0	Jochum et al. (2011); GeoReM**

Table 2 (see p. 100)**.** Average concentrations and standard deviations (± 1 σ) of sodium, magnesium, manganese, strontium, and barium in reference materials MACS-3, BCR-2G and NIST SRM 610 as determined during the four LA-ICP-MS sequences (sequence IDs = MPIC, 0, 1, 2; compare Table 1). Reference values (± 1 σ uncertainties) are available at GeoReM database (application version 20; published (*) or preferred compiled values (**)), from USGS (values for MACS-3 are shown in Jochum et al., 2012; Table 1; column: preliminary reference values (prel. RV), and/or Jochum et al. (2011; Table 8; column: overall mean (Ov. mean)). Reference values for sodium, magnesium, and manganese at GeoReM are given as oxide concentrations and were transferred into element concentrations using conversion factors from Küster and Thiel (2011).

using shell growth patterns as a calendar (details are given in Marali et al., 2017). Element-to-calcium ratios of different individuals can be directly compared with each other, because all specimens were analyzed during the same LA-ICP-MS sequence (i.e., differences in the resulting trace element concentrations between specimens are probably not caused by varying instrumental accuracy among different sequences; see Supplementary Materials). Temporal alignment was performed for the specimens from the Gulf of Maine and the Isle of Man. Briefly, the widths and number of annual increments in the hinge that were intersected by each LA-ICP-MS line scan (determined during sequence 2) were measured with the software Panopea. The growth increments were put into a temporal context by cross-matching them with the original increment width measurements of Griffin (2012; for specimens from the Gulf of Maine) and Butler et al. (2010; for specimens form the Isle of Man). Annual increment widths of all specimens used in the current study are also shown in Marali et al. (2017).

2.7 Inter-specimen synchrony of trace element time-series and shell growth patterns

Ba/Ca ratios are highly synchronous among coeval bivalve specimens from the same habitat (Stecher et al., 1996; Gillikin et al., 2006, 2008; Schöne et al., 2013; Marali et al., 2017). In addition, Gillikin et al., 2005 observed that Sr/Ca ratios also varied synchronously among different *Saxidomus gigantea* specimens, but assumed that the synchronous change in Sr/Ca resulted from the specimens having similar ontogenetic ages and shell growth rates. As shown in a previous LA-ICP-MS study, annually averaged Sr/Ca and Mg/Ca ratios in the hinge of *A. islandica* shells were related to ontogenetic age and the width of annual growth increments (Schöne et al., 2011).

In the present study, we tested the hypothesis that element-to-calcium ratios (Na/Ca, Mg/Ca, Mn/Ca, Sr/Ca, and Ba/Ca) were indeed varying synchronously among *A. islandica* with similar shell growth patterns or ontogenetic ages. The analysis was conducted in three specimens from the Isle of Man and three specimens from

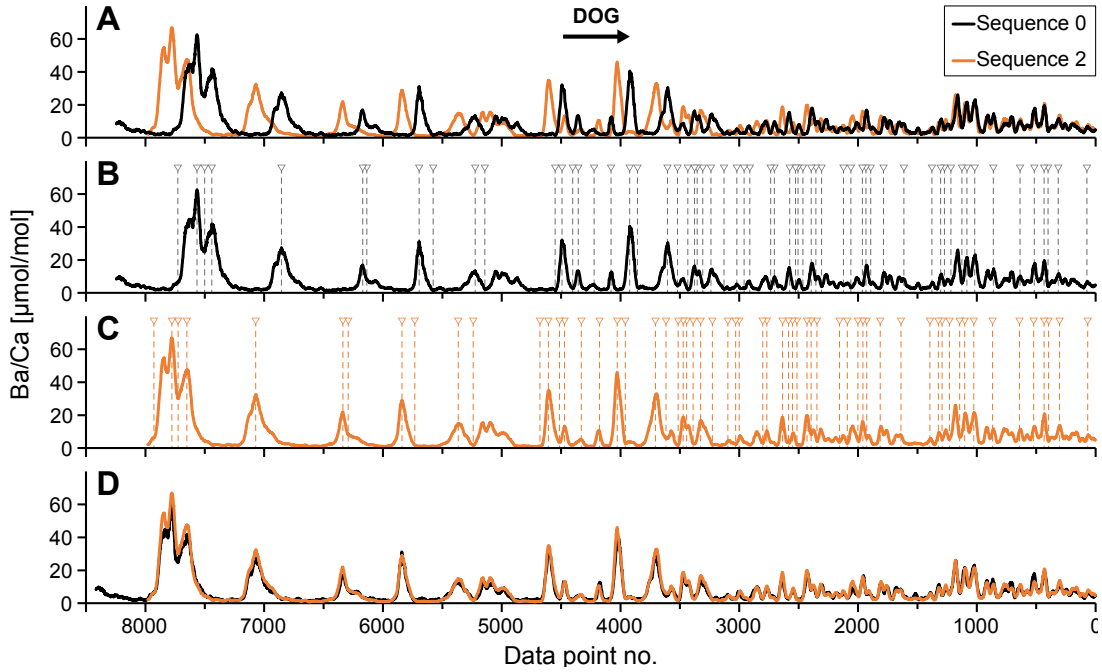

Fig. 3. Alignment of replicate LA-ICP-MS line scans performed on the same specimen by using Ba/Ca time-series (exemplified for specimen 0505319). Characteristic features in 31-pt running averages of shell Ba/Ca time-series (e.g. pronounced maxima and minima indicated by small arrows and dashed lines) were selected manually. The x-axis of the second line scan (corresponding to sequence 2 in the case of specimen 0505319) was interpolated, so that corresponding Ba/Ca maxima or minima from both line scans overlapped.

the Gulf of Maine. At each site, two specimens resembled each other with respect to ontogenetic age and shell growth patterns. Since the individuals were relatively old (between ca. 50 and 251 years), inter-specimen reproducibility could be studied over long time intervals. Future studies exploring short-lived species or ontogenetically young specimens should use a larger number of specimens per site. The similarity of shell growth patterns among coeval specimens from the same habitat was estimated from the strength of the correlation between standardized growth indices (SGIs[1]). This method is routinely applied in dendrochronology and bivalve sclerochronology to assess the strength of growth synchrony within populations of trees and bivalves, respectively (i.e., inter-series correlation; compare Wigley et al., 1984; Cook and Kairiukstis, 1990; Black et al., 2016). In a second step, element-to-calcium ratios were annually averaged to examine if trace element data co-varied with annual increment widths and corresponding SGI values, respectively. Annually averaged Ba/Ca ratios

[1] SGIs represent a dimensionless measure of how shell growth deviates from an estimated growth trend. Absolute increment width time-series were transformed into dimensionless SGIs by estimating and eliminating the growth trend (a technique also known as 'detrending') using the dendrochronological software package ARSTAN (Holmes et al., 1986; Cook and Krusic, 2007). For each specimen, a negative exponential trend curve was applied, and residuals from this trend (so called growth indices, GI) were calculated. Subsequently, GI values were standardized to obtain SGI values (for further details the reader is referred to Schöne, 2013).

were already compared to absolute increment widths in Marali et al. (2017). The authors used the annual increment widths determined by Butler et al. (2010) and Griffin (2012) on the shell section used for sclerochronological analysis, not the measurements along the LA-ICP-MS line scan. However, increment widths along the LA-ICP-MS line scan compared well to the original measurements (compare Marali et al., 2017). In the present study, we compared annually averaged Ba/Ca ratios of the *A. islandica* shells to annual increment widths measured along the laser line scan. Finally, we tested whether annually averaged element-to-calcium ratio of coeval *A. islandica* from the same site were significantly correlated with each other. Statistical analyses were performed using the software PAST (version 1.17; Hammer et al., 2001).

3 Results

The concentrations of sodium, magnesium, manganese, strontium and barium were determined via LA-ICP-MS in shells of the bivalve *A. islandica*. Results are given as element-to-calcium ratios (in mmol/mol or µmol/mol; Figs. 3–9) and average values are displayed with standard deviations (± 1 σ). For a detailed comparison of the Ba/Ca ratios between *A. islandica* specimens the reader is referred to Marali et al. (2017).

3.1 Characteristic trace element variations within *A. islandica* shells

Time-series of Na/Ca, Mg/Ca, Mn/Ca, Sr/Ca, and Ba/Ca ratios show characteristic temporal variations (Figs. 4, 5, 8, 9). Typically, high Na/Ca, Mn/Ca and Ba/Ca ratios were detected in the first years of growth during which annual increments were broad permitting a very high temporal resolution (Figs. 4, 5, 8; compare Marali et al., 2017, in the case of Ba/Ca). Whereas Na/Ca, Mn/Ca and Ba/Ca peaks occurred erratically and were not consistently associated with specific growth structures (see raw and smoothed time-series: Figs. 4, 8; Supplementary Materials, Fig. S1), Mg/Ca and Sr/Ca values, by contrast, attained maxima near annual growth lines. Particularly high Mg/Ca and Sr/Ca values were observed in shell portions in which annual increments are narrow and annual growth lines densely packed (Figs. 4, 8; Supplementary Materials, Fig. S1; compare also Schöne et al., 2011; Shirai et al., 2014). In specimens from the Isle of Man, which are ca. 40 to 200 years older than those from the Gulf of Maine, mean Mg/Ca and Sr/Ca ratios obviously increased throughout the lifetime of the speicmens (as visible in raw, smoothed and averaged data sets, Figs. 5, 8, 9; Supplementary Materials, Fig. S1).

3.2 Reproducibility of trace element time-series within each *A. islandica* specimen

The degree of reproducibility of Na/Ca, Mg/Ca, Mn/Ca, Sr/Ca, and Ba/Ca time-series between replicate LA-ICP-MS line scans was evaluated for each specimen (Figs. 4–7, Table 3). In the cases of Mg/Ca, Sr/Ca and Ba/Ca, the temporal changes (i.e., peaks and troughs) were very similar among replicate LA-ICP-MS line scans (Figs. 3–5), even before the alignment of the data based on Ba/Ca maxima and minima. In general, the degree of signal reproducibility within a specimen was poor for Na/Ca, high for Mn/Ca, Sr/Ca and Mg/Ca, and exceptionally high for Ba/Ca (Figs. 4–6; Table 3). As indicated by linear regression analysis, Ba/Ca, Mg/Ca and Sr/Ca time-series were highly reproducible within the same specimen (average r^2 values were 0.95 ± 0.04, 0.82 ± 0.27 and 0.83 ± 0.18, respectively; *p*-values < 0.05; Table 3, Fig. 7). This was expected for Ba/Ca, because the data of replicate LA-ICP-MS line scans were aligned by using the Ba/Ca time-series (see section 2.4). The average degree of reproducibility was lower for the Mn/Ca time-series (average r^2 = 0.74 ± 0.23). The reproducibility of the Mn/Ca time-series was lowest for specimen ICE12-14-01 AL (Table 4). By excluding the Mn/Ca data of this specimen, the average r^2 increased to values of 0.81 ± 0.15. In two specimens, the Na/Ca time-series of the replicate line scans were not significantly correlated (Table 3; *p*-values > 0.05). In the remaining five specimens, the reproducibility of Na/Ca time-series was markedly lower than that of the other elemental ratios (average r^2 = 0.22 ± 0.04).

The slopes of the linear regression lines were, on average, ca. 1 for Ba/Ca, Sr/Ca and Mn/Ca ratios, and ca. 0.9 for Mg/Ca (Table 3; Fig. 7). Slopes were positive for almost all element-to-calcium ratios, except Na/Ca (Table 3). The regression lines for the Na/Ca ratios were very shallow (average slope ca. 0.3, considering only significant correlations) and the slopes differed between individuals, being positive and steeper for specimens from the Gulf of Maine and the shell from Iceland, but negative and/or very shallow for shells from the Isle of Man (Table 3; Fig. 7).

3.3 Synchrony of trace elements between coeval specimens

For comparison, the results of Marali et al. (2017) for specimens from the Isle of Man and the Gulf of Maine are presented together with the data for Na/Ca, Mg/Ca, Mn/Ca, and Sr/Ca ratios as smoothed time-series (31-pt running averages; Fig. 8), as well as annual averages (Fig. 9; Tables 4, 5). Specimens of similar ontogenetic age from the same locality which display highly synchronous growth patterns also compare well to each

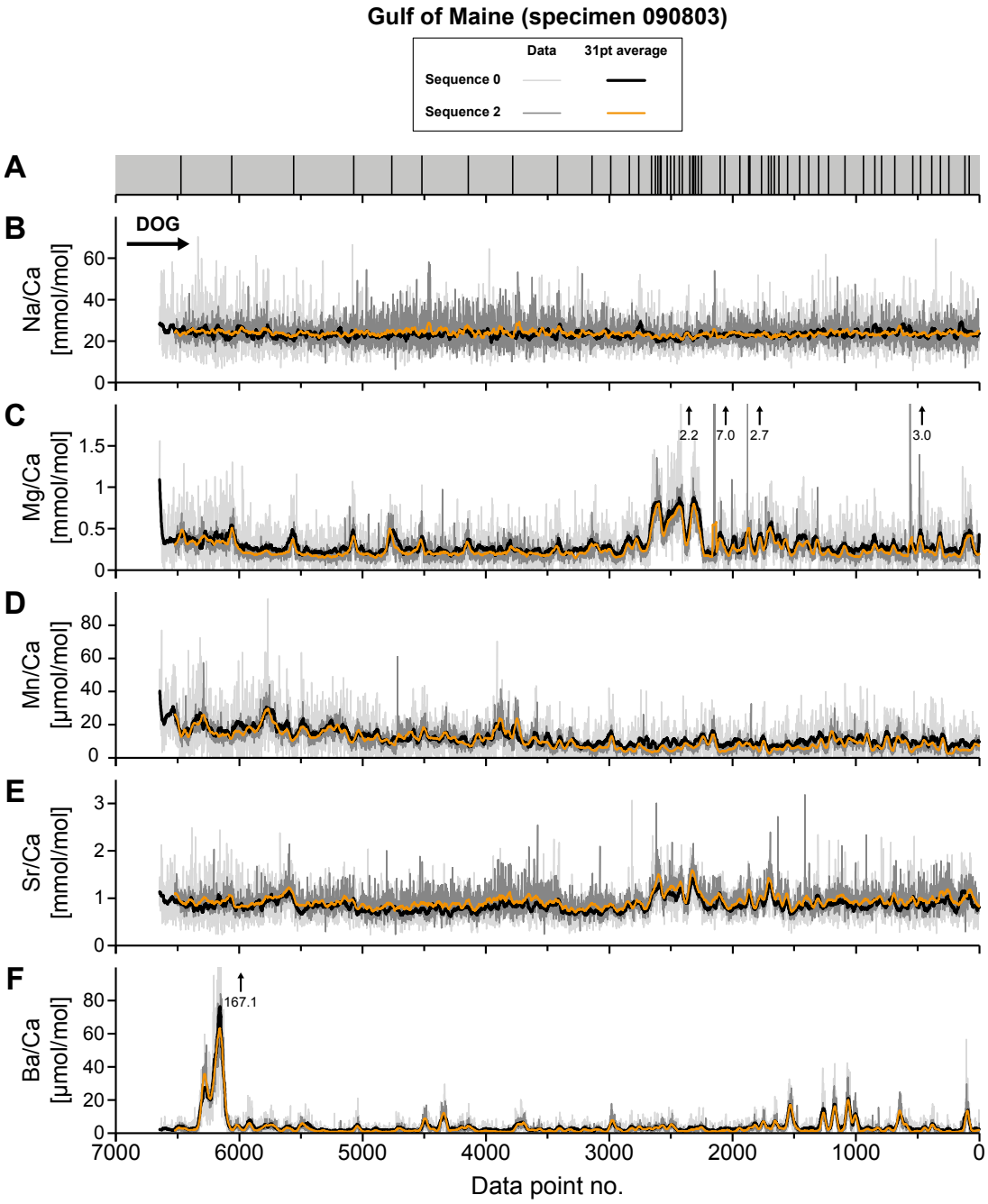

Fig. 4. (A) Shell growth pattern of specimen 090803 from the Gulf of Maine. Vertical black bars indicate the location of the annual growth lines which were intersected by the LA-ICP-MS line scan. (B-F) Reproducibility of trace element time-series within specimen 090803. (B) Na/Ca, (C) Mg/Ca, (D) Mn/Ca, (E) Sr/Ca, and (F) Ba/Ca time-series were determined along two replicate LA-ICP-MS line scans (corresponding to two different sequences; see Table 1). Data points are numbered in the laser scanning direction. Non-averaged data is depicted as light and dark grey lines for sequence 0 and 2, respectively, and as 31-pt running averages (sequence 0: thick black line; sequence 2: thick orange line). Note that Mg/Ca and Sr/Ca ratios generally increase close to annual growth lines and that both the Mg/Ca and Sr/Ca ratios are elevated where growth increments are relatively narrow (e.g., between data points no. 2500 and 2000).

other with respect to Mg/Ca, Sr/Ca, and Mn/Ca time-series (Figs. 8, 9). For example, specimens 0505319 and 0505327 from the Isle of Man – both around 80 years old – showed synchronous Mg/Ca peaks in the smoothed time-series between 1980 and 1995 (Fig. 8B). These specimens also share common temporal variations in smoothed Mn/Ca and Sr/Ca ratios (e.g. Mn/Ca: 1950-1980; Fig. 8C, D). However, the means and peak amplitudes of smoothed Mg/Ca and Mn/Ca differ among the two specimens (e.g. ca. 0.4 mmol/mol higher Mg/Ca between 1981 and 1983 in specimen 0505327; Fig. 8B). In general, higher Mg/Ca ratios and lower Mn/Ca ratios were measured in specimen 0505327 (Fig. 8B, C). Few common peaks were observed among smoothed Na/Ca ratios of specimens 0505319 and 0505327, and in some years, Na/Ca ratios of both specimens run in opposite directions (e.g. ca. 1973; Fig. 8A). The third specimen from the Isle of Man (0525475) was ca. 251 years old. The increments of this specimen were very narrow (minimum ca. 4 μm) in more recently formed portions of the hinge, i.e., the time interval during which the other specimens lived. Due to signal smearing, the trace element time-series from this specimen appear 'smoother' than those of the other coeval shells. Further, mean Na/Ca and Sr/Ca ratios from specimen 0525475 were offset from those of the two younger *A. islandica* shells (visible in both 31-pt running averages and annual averages; Figs. 8, 9). Despite the difference in ontogenetic age, some common variability in smoothed and annual Mg/Ca, Mn/Ca and Sr/Ca was observed among all three specimens from the Isle of Man (e.g., increased Sr/Ca ratios between 1980 and 1990; Figs. 8, 9).

The three specimens from the Gulf of Maine were younger than specimens from the other study locality (Table 1). Specimens 090803 and 090829 (both ca. 55 years old) showed common variations in smoothed Mg/Ca and Sr/Ca ratios (i.e., broad peaks between ca. 1965 and 1980; Fig. 8). These variations corresponded to parts of the hinge in which comparatively narrow growth increments were discerned (compare Fig. 4). During the same time interval, specimen 090797 from the same site showed broader annual growth bands and much narrower Mg/Ca and Sr/Ca peaks in smoothed data sets (Fig. 8). The annual Mn/Ca time-series of all three specimens are synchronous from ca. 1965 to 1972 and from ca. 1986 to 2000 (Fig. 9C). After ca. 2002, however, the annual Mn/Ca time-series of specimen 090797 was anticorrelated to that of the other two specimens from the Gulf of Maine (Fig. 9C). Overall, none of the element-to-calcium time-series are as synchronous between specimens as the Ba/Ca time-series at both sampling localities (compare Marali et al., 2017).

In most specimens, annual Na/Ca, Mg/Ca, Mn/Ca and Sr/Ca ratios co-varied significantly with the raw (undetrended) annual increment widths (Table 4a). In addition, significant negative correlations were observed between SGI values and annual time-series of Mg/Ca and Sr/Ca (Table 4b). In the case of annual Na/Ca and

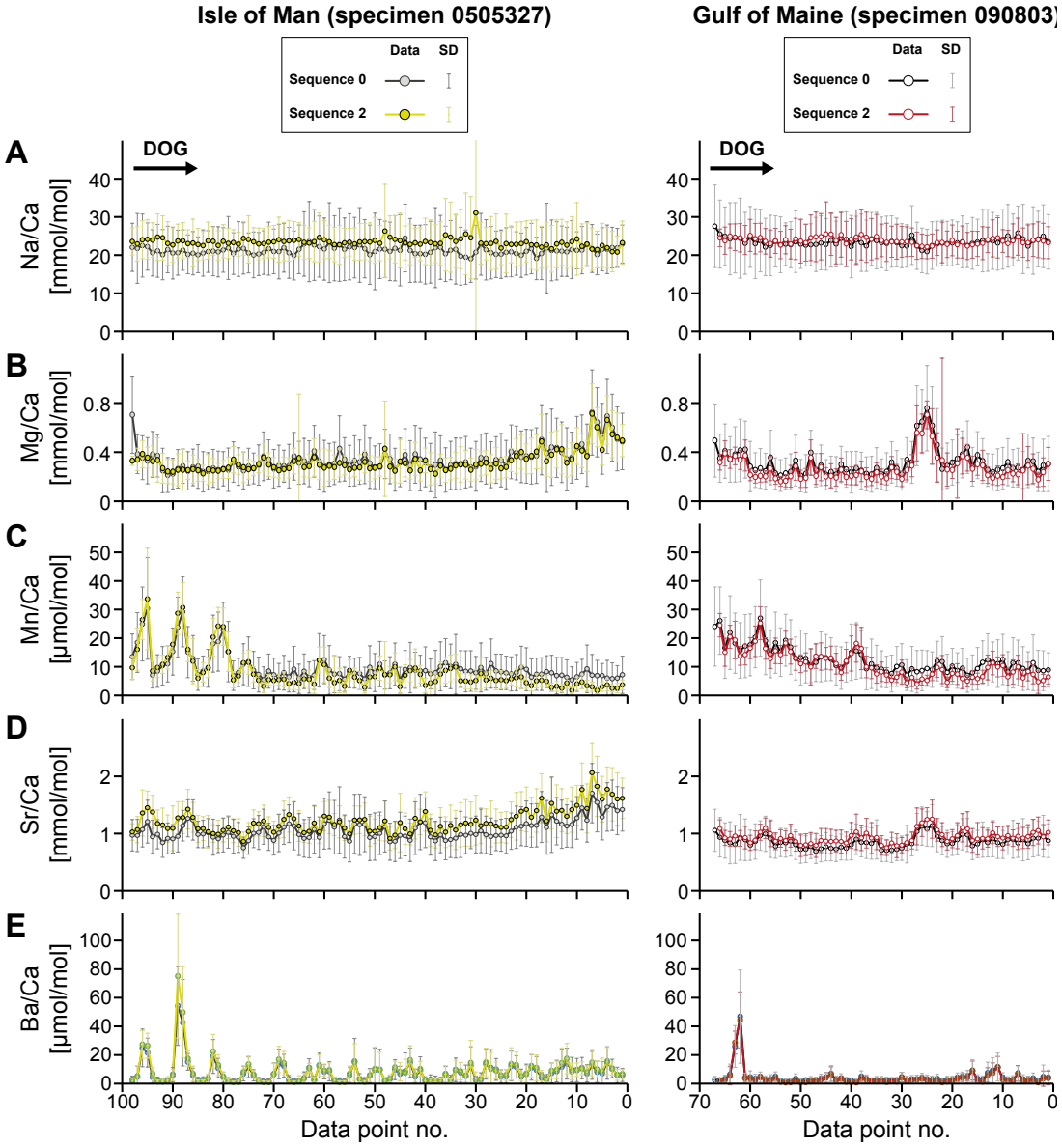

Fig. 5. Reproducibility of trace element time-series between replicate LA-ICP-MS line scans displayed as reduced data sets (100-pt averages) for (A) Na/Ca, (B) Mg/Ca, (C) Mn/Ca, (D) Fe/Ca, (E) Sr/Ca, and (F) Ba/Ca ratios. Data on the left panel is from specimen 0505327 (Isle of Man); data on the right panel corresponds to specimen 090803 (Gulf of Maine). DOG = direction of growth. Standard deviations (1 σ) for each data point are shown as vertical bars.

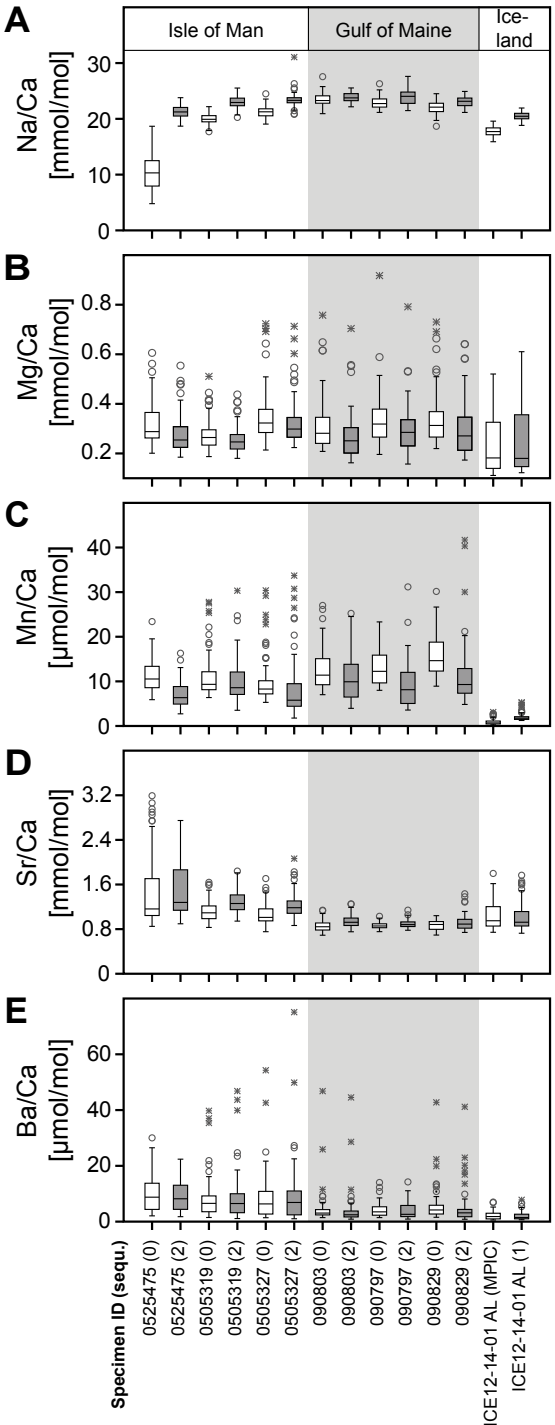

Fig. 6. Box plots of the decimated data sets (100-pt averages) corresponding to the (A) Na/Ca, (B) Mg/Ca, (C) Mn/Ca, (D) Fe/Ca, (E) Sr/Ca, and (F) Ba/Ca time-series of each specimen. Data corresponding to the first and second LA-ICP-MS line scans are displayed as white and grey boxes, respectively. All specimens from the Isle of Man and the Gulf of Maine (grey shaded area) were analyzed first during sequence 0, and a second time during sequence 2. The specimen from Iceland was examined first in sequence MPIC and then during sequence 1. Specimen IDs are displayed on the x-axis; corresponding sequence IDs are given in brackets. Median values are indicated by a horizontal line in each box. Circles and asterisks indicate outliers and extreme values, deviating ≥ 1.5 times and 3 times the box height from the box, respectively (outlier view of the software PAST v. 2.17).

Mn/Ca ratios, only half of the specimens showed a significant correlation to annual SGI values (Table 4b). Annual Ba/Ca ratios of most specimens were not significantly correlated to absolute or relative shell growth rates (Table 4a, b; compare also Marali et al., 2017).

To quantify the amount of trace element variability shared among coeval specimens from the same site, the significance and strength of correlations among annually averaged element-to-calcium ratios was studied (Table 5). Marali et al. (2017) showed that Ba/Ca time-series were significantly correlated among *A. islandica* specimens from the same site (all $p < 0.05$; average r = 0.94 and 0.46 for shells from the Gulf of Maine and the Isle of Man, respectively). In the present study, annual Na/Ca, Mg/Ca, Mn/Ca and Sr/Ca time-series were all significantly correlated among specimens which are of a similar ontogenetic age (i.e., excluding specimens 0525475 and 090797), and which have significantly correlated SGI time-series (Tables 4b, 5).

4 Discussion

Previous work suggested that trace element time-series of bivalve shells and other biogenic carbonates can potentially serve as proxies of environmental change (e.g. Dodd, 1965; Jochum et al., 2012; Füllenbach et al., 2015; Yan et al., 2015). Background Ba/Ca[2] ratios of bivalve shells, for example, are directly related to the Ba/Ca ratio of the ambient seawater (Gillikin et al., 2006; Poulain et al., 2015), which is in turn influenced by several oceanic processes (Goldberg and Arrhenius, 1958; Dehairs et al., 1980; Dymond et al., 1992). Likewise, peaks in shell Ba/Ca ratios are probably associated with environmental parameters (e.g. Stecher et al., 1996; Vander Putten et al., 2000; Gillikin et al., 2008; Barats et al., 2009; Marali et al., 2017). Mg/Ca and Sr/Ca ratios are used for temperature reconstructions in corals (Mitsuguchi et al., 1996; Beck et al., 1992; Cohen and Thorrold, 2007) and foraminifera tests (Lea et al., 1999), but their applicability as temperature proxies in bivalve shells is controversial (Takesue and van Geen, 2004; Klein et al., 1996a; Carré et al., 2006; Freitas et al., 2006, 2008, 2009; Wanamaker et al., 2008). In shells of the photosymbiotic *Tridacna gigas*, by contrast, highly resolved Sr/Ca time-series seem to trace the daily light cycle (Sano et al., 2012; Warter and Müller, 2016). Mn/Ca ratios of bivalve shells are potentially related to the dissolved manganese concentration of the ambient water (Freitas et al., 2006), which is driven by aquatic redox processes associated with other factors such as primary productivity

[2] The term 'background' refers here to the flat, relatively invariable part of a Ba/Ca shell time-series which is typically interrupted by sharp, erratic Ba/Ca maxima (e.g., Stecher et al., 1996; Gillikin et al., 2006, 2008).

(Vander Putten et al., 2000; Langlet et al., 2007). Na/Ca ratios serve as a salinity proxy in foraminifera (Wit et al., 2013). Rucker and Valentine (1961) reported that sodium, magnesium, manganese and strontium of *Crassostrea virginica* shells were significantly correlated with salinity, but correlation coefficients were relatively low (around ± 0.3). Dodd and Crisp (1982) found that Sr/Ca and Mg/Ca ratios of aragonitic bivalve shells co-varied with salinity, but the relationship was non-linear. More recently, O'Neil and Gillikin (2014) found that bulk Na/Ca of the freshwater bivalve Elliptio complanata increased during periods of intense road-salt pollution, but Na/Ca ratios displayed no clear intra-annual pattern and were not related to seasonal variations in riverine sodium concentrations. Furthermore, Zhao et al. (2016) observed that low ambient pH significantly affected the growth and Na/Ca ratio of *Mytilus edulis* shells.

Although many trace elements are discussed as climate proxies, the degree to which the trace element composition of a biogenic carbonate reflects environmental conditions varies between archives and from one (bivalve) species (or specimen) to another (Vander Putten et al., 2000; Freitas et al., 2006, 2008; Gillikin et al., 2005; Schöne et al., 2010; Yan et al., 2014). For example, the relationship of Mg/Ca to temperature changes even within specimens (Vander Putten et al., 2000; Freitas et al., 2006). Consequently, it is essential to test the extent to which the temporal variation of a certain trace element may be related to an external, potentially environmental factor.

4.1 Approaches to the identification of potential trace element climate proxies

There are a number of ways of determining the extent to which trace element time-series are driven by environmental parameters. A central approach is to unravel the processes and factors controlling the incorporation of trace elements into bivalve shells and other biogenic carbonates. Studies designed to accomplish this task focus on biomineralization (e.g., Foster et al., 2008; 2009; Zhao et al., 2015, 2016; Soldati et al., 2016) and/or calibrate the trace element time-series of biogenic carbonates against the presumed environmental controlling factor(s) (e.g. Poulain et al., 2015; Füllenbach et al., 2015). In the case of calibration studies, the trace element and the environmental time-series should ideally offer the same temporal resolution to assure an accurate proxy calibration and validation.

The other approach is to test if the trace element time-series can be reproduced within and/or among coeval specimens from the same habitat (e.g. Sinclair et al., 2005, 2011; DeLong et al., 2007, 2013; Elliot et al., 2009; Anagnostou et al., 2011; Yan et

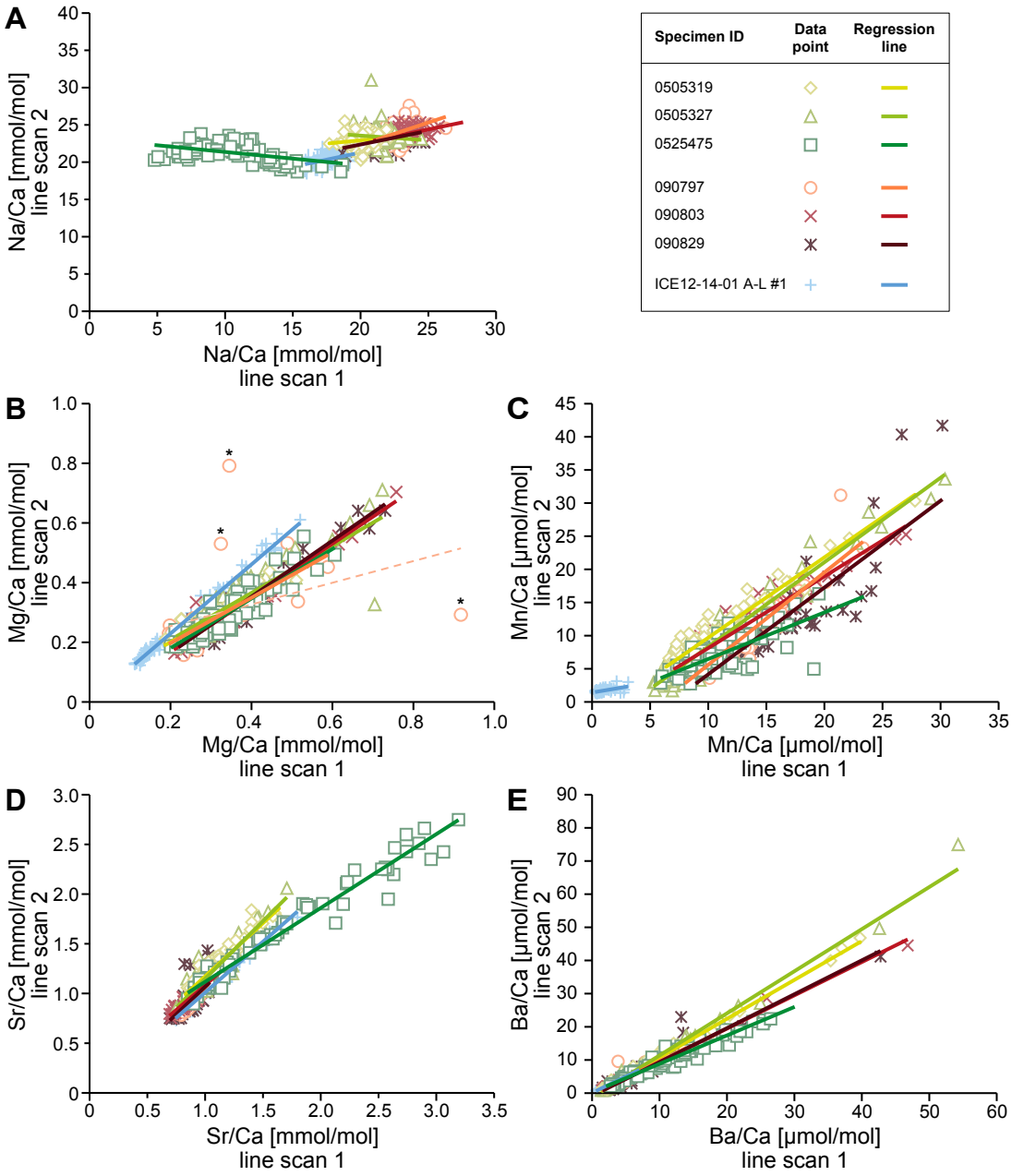

Fig. 7. Intra-specimen reproducibility inferred from decimated data sets of (A) Na/Ca, (B) Mg/Ca, (C) Mn/Ca, (D) Fe/Ca, (E) Sr/Ca, and (F) Ba/Ca ratios. Two replicate LA-ICP-MS line scans were measured in each *A. islandica* specimen. Trace element data sets were aligned by means of Ba/Ca ratios (see section 2.4) and then decimated (averaging of ca. 100 consecutive data points, resulting in a spatial resolution of ca. 150 µm) and then cross-plotted together with regression lines. Statistical parameters (r, r^2, *p*, slopes, intercepts) for each linear regression are listed in Table 3. In the case of specimens from the Isle of Man and the Gulf of Maine, data displayed to the x-axis and y-axis correspond to LA-ICP-MS sequences 0 and 2, respectively (Table 1). For the Icelandic specimen, data of sequences MPIC and 1 are given on the x-axis and y-axis, respectively (Table 1). Three Mg/Ca values of specimen 090797 were regarded as outliers (marked with an asterisk; B) and rejected from linear regression analysis. Without this additional outlier correction the regression line of this specimen (dashed orange) deviates strongly from that of the other specimens.

Table 3. Results of linear regression analysis of data from replicate line scans within each *A. islandica* specimen (using reduced data; 100-pt averages) for Na/Ca, Mg/Ca, Mn/Ca, Sr/Ca, and Ba/Ca ratios. Given statistics are the correlation coefficient (r), the coefficient of determination (r^2), the probability value (*p*), and the number of data (n). The slope and intercept of each linear regression line are added. Only r and r^2 values of significant correlations were averaged. In the case of Mg/Ca average r and r^2 values included values from sample 090797 after an additional outlier correction (*OC; see section 2.5; Fig. 7).

Na/Ca

Specimen ID	r	r^2	*p*	n	Slope	Intercept
0505319	0.16	0.02	0.081	80	0.18	19.40
0505327	-0.10	0.01	0.152	98	-0.13	26.14
0525475	-0.45	0.21	< 0.001	85	-0.18	23.16
090797	0.51	0.26	< 0.001	49	0.62	10.29
090803	0.42	0.17	< 0.001	66	0.38	15.06
090829	0.45	0.20	< 0.001	59	0.38	15.05
ICE12-14-01 A-L	0.51	0.26	< 0.001	69	0.38	13.63
Average	0.29 ± 0.42	0.22 ± 0.04			0.32 ± 0.30	

Mg/Ca

Specimen ID	r	r^2	*p*	n	Slope	Intercept
0505319	0.87	0.76	< 0.001	80	0.79	0.05
0505327	0.88	0.77	< 0.001	98	0.81	0.05
0525475	0.91	0.83	< 0.001	85	0.83	0.01
90797	0.40	0.16	0.002	49	0.37	0.18
090797 *OC	0.76	0.58	< 0.001	47	0.79	0.05
090803	0.97	0.94	< 0.001	66	0.93	-0.01
090829	0.95	0.91	< 0.001	59	0.97	-0.02
ICE12-14-01 A-L	0.99	0.99	< 0.001	69	1.16	0.00
Average	0.91 ± 0.08	0.82 ± 0.27			0.90 ± 0.14	

Mn/Ca

Specimen ID	r	r^2	*p*	n	Slope	Intercept
0505319	0.95	0.89	< 0.001	80	1.19	-2.44
0505327	0.96	0.93	< 0.001	98	1.25	-4.44
0525475	0.73	0.53	< 0.001	85	0.70	-0.55
090797	0.92	0.85	< 0.001	49	1.37	-8.34
090803	0.95	0.90	< 0.001	66	1.06	-2.70
090829	0.86	0.74	< 0.001	59	1.28	-8.94
ICE12-14-01 A-L	0.55	0.30	< 0.001	69	0.29	1.42
Average	0.85 ± 0.15	0.74 ± 0.23			1.02 ± 0.39	

Sr/Ca

Specimen ID	r	r^2	*p*	n	Slope	Intercept
0505319	0.94	0.88	< 0.001	80	1.01	0.10
0505327	0.93	0.87	< 0.001	98	1.10	-0.01
0525475	0.98	0.96	< 0.001	85	0.72	0.38
090797	0.91	0.83	< 0.001	49	1.11	-0.11
090803	0.92	0.85	< 0.001	66	0.95	0.09
090829	0.65	0.43	< 0.001	59	1.05	-0.04
ICE12-14-01 A-L	0.99	0.97	< 0.001	69	1.02	-0.01
Average	0.90 ± 0.11	0.83 ± 0.18			0.99 ± 0.13	

Ba/Ca

Specimen ID	r	r^2	*p*	n	Slope	Intercept
0505319	0.99	0.99	< 0.001	80	1.09	-1.00
0505327	0.99	0.98	< 0.001	98	1.18	-1.33
0525475	0.97	0.94	< 0.001	85	0.83	0.23
090797	0.94	0.88	< 0.001	49	0.94	-0.54
090803	1.00	0.99	< 0.001	66	0.93	-0.64
090829	0.96	0.93	< 0.001	59	0.95	-0.87
ICE12-14-01 A-L	0.99	0.98	< 0.001	69	0.99	0.08
Average	0.98 ± 0.02	0.95 ± 0.04			0.99 ± 0.12	

al., 2014; Alpert et al., 2016). It is assumed that a geochemical variation (recorded in a climate archive, e.g., a bivalve shell) which contains any information of interest (e.g., environmental information such as temperature), can be considered as a 'signal' (Sylvester, 2001; Sinclair et al., 1998). Any other geochemical variation can be regarded as 'noise' (Sylvester, 2001). In general, an environmental signal should be reproducible within a specimen and among different coeval specimens from the same site, whereas noise is defined as random and irreproducible variations (Sinclair et al., 2005; 2011). In addition, the geochemistry of a biogenic climate archive can be influenced by vital effects (e.g., Urey et al., 1951; Stephenson et al., 2008) and/or mineralogical controls (e.g., Foster et al., 2008, 2009) and the resulting biological or mineralogical signals can be reproducible within and/or between specimens (see sections below).

In total, three requirements have to be met before a trace element time-series measured in a biogenic carbonate can be considered to be a signal, and the element regarded as a (paleo-) environmental proxy: (1) Trace element analysis has to be accurate. (2) The time-series of the trace element have to be reproducible within a specimen (compare Sinclair et al., 2005, 2011; DeLong et al., 2007; Anagnostou et al., 2011). (3) If the concentration of the trace element is also varying synchronously between several coeval specimens, then it is most likely that the incorporation of this trace element into the biogenic carbonate is driven by an external (e.g. environmental) parameter (e.g., Stecher et al., 1996; Vander Putten et al., 2000; Gillikin et al., 2006, 2008; DeLong et al., 2007, 2013; Marali et al., 2017). Previous studies have already demonstrated that LA-ICP-MS is suitable to determine element-to-calcium ratios in biogenic carbonates (e.g. Sinclair et al., 1998), especially in the case of lithophile elements (Jochum et al., 2012) such as sodium, magnesium, manganese, strontium and barium (Goldschmidt, 1937; although manganese can also show siderophile behavior; Gessmann and Rubie, 2000). We suggest that the LA-ICP-MS data presented here is largely accurate within the limits of the analytical uncertainties (see Supplementary Materials). Improvement of LA-ICP-MS accuracy can be attained by correcting it with data obtained from wet-chemical analysis (Sinclair et al., 1998).

In this study, we have focussed on the reproducibility of trace element time-series determined by LA-ICP-MS line scans within and between shells of the bivalve *A. islandica*, taking account of potential instrumental uncertainties. It should be emphasized that this study presents a straightforward test of whether trace element time-series are reproducible within and between specimens and is applicable to other species. It does not include any calibration work with respect to environmental parameters. The determination of the controlling environmental or biological factors driving the geochemical variations will require more detailed research using highly resolved environmental data.

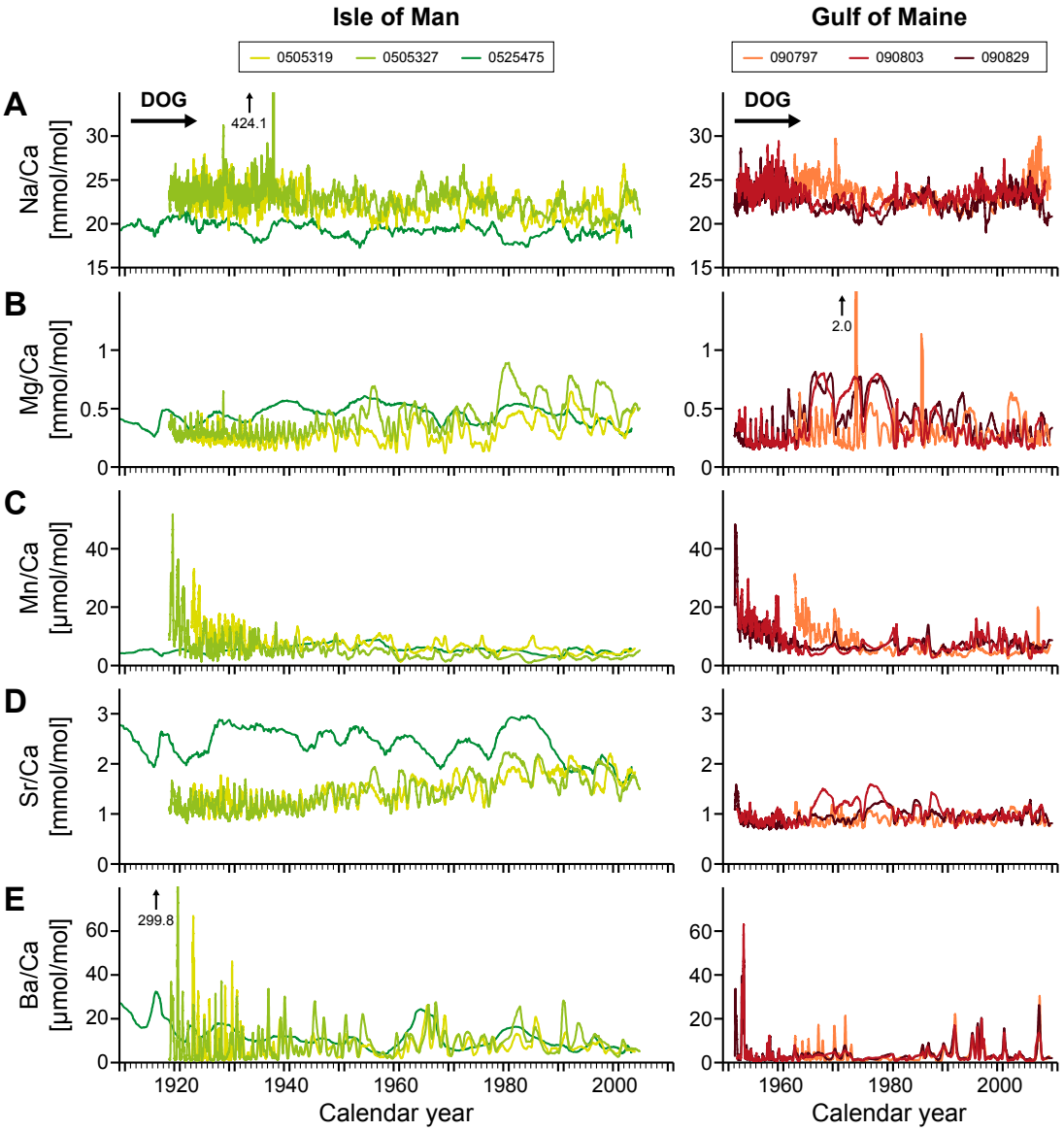

Fig. 8. Synchrony of trace element time-series between coeval specimens from the Isle of Man (left panel; time-period 1910 – 2003) and from the Gulf of Maine (right panel; data of years 1950 – 2009), respectively. 31-pt running averages are displayed for (A) Na/Ca, (B) Mg/Ca, (C) Mn/Ca, (D) Fe/Ca, (E) Sr/Ca ratios. Ba/Ca time-series of the corresponding specimens (F) were already depicted in Marali et al. (2017). DOG = direction of growth. Data values exceeding the y-scale are given next to black arrows.

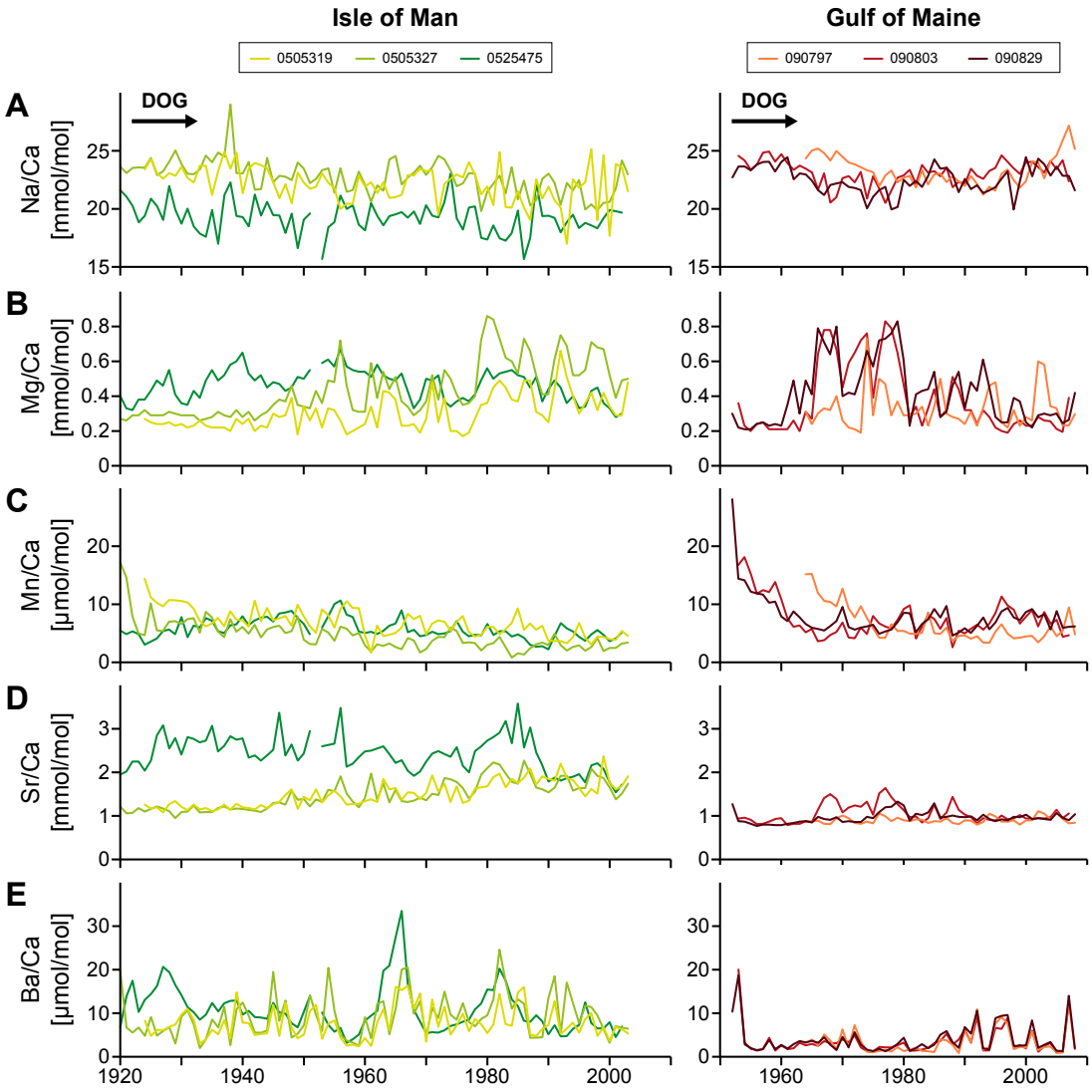

Fig. 9. Inter-specimen synchrony of annually averaged trace element time-series for (A) Na/Ca, (B) Mg/Ca, (C) Mn/Ca, (D) Sr/Ca and (E) Ba/Ca ratios (the latter were previously shown in Marali et al., 2017). DOG = direction of growth.

4.2 Factors determining the intra-specimen reproducibility of trace elements in *A. islandica* shells

Overall, the trace element time-series within each *A. islandica* shell were either non-reproducible (Na/Ca), generally well-reproducible with a degree of reproducibility that varies among specimens (Mg/Ca, Mn/Ca, Sr/Ca), or highly reproducible in the case of all examined specimens (Ba/Ca; Fig. 3; Fig. 7; Table 3). Non-reproducibility of trace element time-series could result from three factors: Firstly, the distribution of the trace element within the bivalve shell might be unrelated to any environmental factor and/or any quantifiable biological control. For instance, O'Neil and Gillikin (2014) found that intense road-salt pollution could lead to increased bulk Na/Ca ratios in the freshwater bivalve *E. complanata*, indicating that shell Na/Ca ratios in this species may contain environmental information. However, highly resolved Na/Ca ratios of *E. complanata* did not show clear seasonal patterns and were not related to shell growth patterns or to seasonal changes in the riverine salt content (O'Neil and Gillikin, 2014). As demonstrated here, highly resolved Na/Ca time-series, derived from LA-ICP-MS line scans, are largely irreproducible within *A. islandica* shells and are therefore likely unrelated to environmental factors such as salinity. Secondly, small-scale alterations of biological parameters (e.g., the composition of the extrapallial fluid from which the shell is potentially secreted) and/or changes of shell microstructure, organic content or the orientation of crystals may cause (sub-) micron-scale variations in the trace element composition of the shell (e.g., Carré et al., 2006; Takesue and van Geen, 2004; Foster et al., 2008; Schöne et al., 2013) that may not be reproducible with the resolution and/or technique employed in the present study (see below; compositional noise).

The third potential reason for non-reproducibility of trace element time-series within shells is that the applied methodology is not suitable to measure and quantify the variations of the studied trace element. In fact, sodium is prone to interference by doubly-charged 46Ca ions during LA-ICP-MS analysis (Jochum et al., 2012). However, the extent of the interference is thought to be comparatively small (Jochum et al., 2012). We suggest here that the Na/Ca ratios determined in the hinge of *A. islandica* by LA-ICP-MS line scans cannot be interpreted in terms of environmental or biological controlling factors. Instead, we recommend that the Na/Ca ratio is determined using an alternative methodology (electron microprobe analysis or solution ICP-MS / ICP-OES) and/or by measuring in another area of the shell (i.e., along ventral shell margin) and that the reproducibility of such results is tested. Mg/Ca, Mn/Ca and Sr/Ca ratios were well-reproducible within the hinge of most studied specimens (average r^2 values > 0.7; Fig. 7, Table 3). However, the degree of intra-specimen reproducibility varied between specimens (Table 3), which is probably an indicator of a certain amount of noise within the trace element time-series. Noise can result from two sources: Instrumental noise

introduced by instabilities of the LA-ICP-MS system (e.g., Sinclair et al., 2005; Jochum et al., 2012) and so-called compositional noise (Sinclair et al., 2005; p. 1050) associated with heterogeneities in the skeletal microstructure that cannot be reproduced between LA-ICP-MS line scans or lines of spots (see also Foster et al., 2008; Sinclair et al., 2011). Changes in the microstructure influence not only LA-ICP-MS analysis, but also other in situ techniques such as secondary ion mass spectrometry (SIMS; Allison and Finch, 2009; Freitas et al., 2009).

In the case of Mg/Ca ratios, some of the studied specimens showed randomly distributed extreme outliers (e.g., specimen 090797; Figs. 4C, 7B, 8B). Magnesium is probably not incorporated into the shell aragonite of *A. islandica*, but associated with organic shell compounds or inorganic nanoparticles (Foster et al., 2008; Schöne et al., 2010). The random Mg/Ca peaks may correspond to local organic or nanoparticulate impurities in the shell. More importantly for the present study such outliers were not reproducible within a specimen (Fig. 7B), therefore, they are probably not caused by an environmental control. Considering Mn/Ca ratios, the lowest intra-specimen reproducibility was found in the specimen from Iceland (Table 3). Mn/Ca ratios of this shell were also ca. 6 to 10 µmol/mol lower than Mn/Ca ratios of the specimens from the other two study localities (Figs. 6, 7) and close to or below detection limits for the LA-ICP-MS system at JGU (see Supplementary Materials, Table S1). This may lead to observed lowered intra-specimen reproducibility for Mn/Ca (Table 3). The Sr/Ca and Na/Ca ratios of all specimens, by contrast, were generally well above corresponding detection limits (Supplementary Materials, Table S1). Despite this, the intra-specimen reproducibility for Sr/Ca was reduced for specimen 090829 from the Gulf of Maine and Na/Ca ratios were typically non-reproducible within specimens (Table 3).

For specimen 0525475 from the Isle of Man, the reproducibility of Na/Ca, Mn/Ca and Mg/Ca was lower than for other specimens (Table 3). The first line scan performed for 0525475 during sequence 0 shows a peculiar decrease in Na/Ca, co-occurring with increased Mn/Ca and Mg/Ca ratios (Supplementary Materials, Fig. S1). These variations occurred over a time interval which is potentially too large to be explained by instabilities in the LA-ICP-MS system, and may therefore be related to structural heterogeneities of the sample surface. However, we did not observe obvious changes on the sample surface, which may have caused changes in Na/Ca, Mg/Ca or Mn/Ca ratios.

A high intra-specimen reproducibility, which is observed for the Ba/Ca ratios of all specimens (Fig. 3), and also for Mg/Ca, Sr/Ca and Mg/Ca in most studied specimens (Figs. 4, 5, 7; Table 3), may indicate a strong external control of trace element chemistry of the shell. However, a trace element time-series could also be highly reproducible

within a specimen when the concentration of this trace element is associated with a re-occurring skeletal feature such as the annual growth lines (Fig. 2). Sinclair et al. (2011), for example, performed LA-ICP-MS line scan analysis along the banded skeleton of a bamboo coral. According to their findings, some peaks of the lead concentration and also variations in uranium concentrations were highly reproducible between closely spaced parallel line scans, whereas the trace element time-series were unreproducible among line scans running along different growth radii of the same coral. In the case of lead, the peaks were associated with the occurrence of dark bands and/or detritus rich cracks, which crossed both of the closely spaced LA-ICP-MS line scans, whereas the bands or cracks did not run along the whole coral radius, and thus, did not influence line scans that were farther apart from each other. The uranium concentrations of the coral were, by contrast, only partly associated with clearly recognizable skeletal features such as cracks (Sinclair et al., 2011).

Here, Mg/Ca and Sr/Ca ratios of *A. islandica* were markedly elevated near annual growth lines of the hinge, Mg/Ca even more than Sr/Ca (Fig. 4). This observation is in line with most previous studies of these element-to-calcium ratios in the margin of bivalve shells (e.g. Foster et al., 2009; Schöne et al., 2013; Shirai et al., 2014). Some other studies, however, reported just the opposite: lowest Mg/Ca and Sr/Ca values near annual growth lines of the shell margin (e.g., Stecher et al., 1996; Toland et al., 2000; Takesue and van Geen, 2004). Irrespective of the direction of change in the trace element composition, however, according to the present study and previous reports, Sr/Ca and/or Mg/Ca ratios at growth lines can significantly differ from those within the growth increments. The growth lines in the hinge (and margin) of each *A. islandica* specimen are easily visible before and after re-polishing of the sample surface, even in the unstained sections (Fig. 2F, G). It is therefore not surprising that the spatial variations of Mg/Ca and Sr/Ca ratios, which are linked to annual shell growth lines, can be reproduced within each *A. islandica* shell as well (Figs. 4, 5, 7).

Ba/Ca ratios, by contrast, are apparently not associated with annual growth lines and/or increment widths (Marali et al., 2017). However, they are highly reproducible within all *A. islandica* specimens (Figs. 3, 4, 5, 7; Table 3). We would like to emphasize that Ba/Ca ratios were used to align replicate LA-ICP-MS line scans and therefore we expected that the correlation among Ba/Ca time-series is nearly 1 (deviations from 1 may result from misalignment or instrumental noise; Table 3). However, even before the alignment, Ba/Ca ratios of replicate line scans matched well (Fig. 3). Elliot et al. (2009) studied a specimen of *T. gigas* and observed that Ba/Ca time-series were even reproducible between different shell layers, which is remarkable because the shell layers of *T. gigas* differ in microstructure (Lin et al., 1993). Intriguingly, Ba/Ca ratios are not only highly reproducible in bivalve shells (Elliot et al., 2009; Marali et

Table 4a. Linear regression analysis was applied to test for any co-variation among annually averaged element-to-calcium ratios (Na/Ca, Mg/Ca, Mn/Ca, Sr/Ca, Ba/Ca) and absolute increment widths (in mm) along the LA-ICP-MS line scan for each A. islandica specimen from the Isle of Man and the Gulf of Maine. Given statistics are the correlation coefficient (r), the coefficient of determination (r^2), the probability value (p), and the number of data (n, in years). Significant correlations ($p < 0.05$) are shaded.

Na/Ca	**vs. increment widths [mm]**			
Specimen ID	**r**	**r^2**	***p***	**n**
0505319	0.30	0.09	0.008	80
0505327	0.30	0.09	0.005	84
0525475	0.13	0.02	0.257	82
090797	0.54	0.29	< 0.001	45
090803	0.64	0.40	< 0.001	55
090829	0.43	0.18	0.001	57
Mg/Ca	**vs. increment widths [mm]**			
Specimen ID	**r**	**r^2**	***p***	**n**
0505319	-0.32	0.10	0.003	80
0505327	-0.50	0.25	< 0.001	84
0525475	-0.47	0.22	< 0.001	82
090797	-0.36	0.13	0.015	45
090803	-0.53	0.29	< 0.001	55
090829	-0.53	0.28	< 0.001	57
Mn/Ca	**vs. increment widths [mm]**			
Specimen ID	**r**	**r^2**	***p***	**n**
0505319	0.68	0.46	< 0.001	80
0505327	0.73	0.54	< 0.001	84
0525475	-0.16	0.03	0.141	82
090797	0.80	0.64	< 0.001	45
090803	0.86	0.74	< 0.001	55
090829	0.85	0.72	< 0.001	57
Sr/Ca	**vs. increment widths [mm]**			
Specimen ID	**r**	**r^2**	***p***	**n**
0505319	-0.47	0.22	< 0.001	80
0505327	-0.54	0.29	< 0.001	84
0525475	-0.66	0.43	< 0.001	82
090797	-0.38	0.14	0.011	45
090803	-0.53	0.28	< 0.001	55
090829	-0.25	0.06	0.060	57
Ba/Ca	**vs. increment widths [mm]**			
Specimen ID	**r**	**r^2**	***p***	**n**
0505319	-0.07	0.00	0.554	80
0505327	-0.10	0.01	0.363	84
0525475	-0.29	0.08	0.009	82
090797	0.21	0.05	0.160	45
090803	0.16	0.03	0.238	55
090829	0.31	0.10	0.019	57

Table 4b. Linear regression analysis was further applied to statistically compare annually averaged trace element time-series to standardized growth indices (SGIs; i.e. relative annual shell growth).

Na/Ca	vs. SGIs [σ]			
Specimen ID	**r**	**r^2**	***p***	**n**
0505319	0.19	0.04	0.089	80
0505327	0.15	0.02	0.164	84
0525475	0.08	0.01	0.489	82
090797	0.36	0.13	0.017	44
090803	0.67	0.45	< 0.001	55
090829	0.42	0.18	0.001	57
Mg/Ca	**vs. SGIs [σ]**			
Specimen ID	**r**	**r^2**	***p***	**n**
0505319	-0.49	0.24	< 0.001	80
0505327	-0.47	0.22	< 0.001	84
0525475	-0.52	0.27	< 0.001	82
090797	-0.48	0.23	0.001	44
090803	-0.79	0.63	< 0.001	55
090829	-0.72	0.51	< 0.001	57
Mn/Ca	**vs. SGIs [σ]**			
Specimen ID	**r**	**r^2**	***p***	**n**
0505319	0.24	0.06	0.030	80
0505327	0.01	0.00	0.939	84
0525475	-0.26	0.07	0.017	82
090797	0.17	0.03	0.264	44
090803	0.36	0.13	0.007	55
090829	0.05	0.00	0.687	57
Sr/Ca	**vs. SGIs [σ]**			
Specimen ID	**r**	**r^2**	***p***	**n**
0505319	-0.29	0.08	0.010	80
0505327	-0.39	0.15	< 0.001	84
0525475	-0.58	0.34	< 0.001	82
090797	-0.43	0.19	0.003	44
090803	-0.69	0.48	< 0.001	55
090829	-0.56	0.31	< 0.001	57
Ba/Ca	**vs. SGIs [σ]**			
Specimen ID	**r**	**r^2**	***p***	**n**
0505319	0.03	0.00	0.825	80
0505327	0.02	0.00	0.831	84
0525475	-0.21	0.04	0.060	82
090797	0.37	0.14	0.013	44
090803	-0.12	0.01	0.392	55
090829	0.26	0.07	0.055	57

al., 2017), but also within coral skeletons (Sinclair et al., 2005, 2011; Anagnostou et al., 2011). Therefore, Ba/Ca ratios may function as an environmental proxy, unaffected by skeletal microstructure and potentially even unrelated to species. The latter hypothesis, however, needs to be tested in future studies. In order to fully quantify the degree to which Ba/Ca ratios can be reproduced, future work should use the shell growth patterns rather than the Ba/Ca time-series to align replicate LA-ICP-MS line scans.

In conclusion, a high intra-specimen reproducibility is not an a priori guarantee that the measured temporal changes in a trace element time-series are primarily linked to an external, environmental control. For example, the microstructure and/or growth pattern may have a strong influence on the geochemical composition of a bivalve shell, especially in the cases of Mg/Ca and Sr/Ca ratios (Schöne et al., 2010; Shirai et al., 2014; this study). Slight changes of the microstructure and/or increment widths between replicate or parallel LA-ICP-MS profiles may lower the degree to which trace element time-series can be reproduced within a specimen (e.g. Mg/Ca, Sr/Ca; compare also Sinclair et al., 2011; Foster et al., 2008). We therefore recommend testing the reproducibility of trace element time-series not only within specimens, but also between different coeval individuals from the same site.

4.3 Potential reasons for synchronous variations of trace element time-series among coeval *A. islandica* specimens

Compared to Ba/Ca ratios, variations in the Na/Ca, Mg/Ca, Mn/Ca and Sr/Ca ratios of the studied *A. islandica* shells are less synchronous between specimens from the same site and growth period (Figs., 8, 9; Table 5). Yet, there are clear synchronous changes in trace elements, especially in Mg/Ca and Sr/Ca, as well as Mn/Ca ratios between certain specimens during distinct time intervals (Figs., 8, 9). For example, peak Mg/Ca and Sr/Ca ratios are synchronized in specimens 090803 and 090829 from the Gulf of Maine, as well as in specimens 0505319 and 0505327 from the Isle of Man (Figs. 8, 9; Table 5). However, the trace element composition of a bivalve shell is not exclusively governed by environmental factors, but also by biological parameters (e.g., Lorens and Bender, 1977; Freitas et al., 2006). Gillikin et al. (2005), for example, reported that Sr/Ca ratios co-varied among different S. gigantea from the same habitat. However, the authors reasoned that the synchronous change of Sr/Ca among specimens was probably related to their similar ontogenetic age and growth rate, rather than to a direct environmental control on shell Sr/Ca. In *A. islandica*, both Sr/Ca and Mg/Ca increase near annual shell growth lines of the hinge and shell margin (Schöne et al., 2013; Shirai et al., 2014; this study) and where growth lines are close together. In

specimen 090803, for example, increment widths decrease after 1968 and smoothed Sr/Ca ratios increase by 1.5 mmol/mol. Considering a temperature sensitivity of ca. 0.02 mmol/mol/°C for Sr/Ca, as was determined for aragonitic (Füllenbach et al., 2015) and calcitic (Wanamaker et al., 2008) bivalve species, this change would translate to unreasonably large temperature fluctuations of ca. 35 °C between years. Furthermore, bivalve shell growth lines typically differ from adjacent growth increments in (a) microstructure (Schöne et al., 2010; Shirai et al., 2014), (b) organic content (Schöne et al., 2005a; Wanamaker et al., 2009b; Schöne et al., 2011; Karney et al., 2012), and (c) the rate at which they are precipitated (Rhoads and Lutz, 1980; Schöne et al., 2005c). Both shell microstructure and shell growth / precipitation / extension[3] rates are in turn influenced by the ambient environment (Füllenbach et al., 2014; Milano et al., 2015). In *A. islandica*, relative shell growth rates are synchronized by external controls such as food supply and temperature (Witbaard, 1996; Schöne et al., 2005c; Wanamaker et al., 2009a; Marali and Schöne, 2015). Thus, trace elements which are linked to shell growth patterns, such as strontium or magnesium (e.g. Schöne et al., 2013; Shirai et al., 2014; this study), are likely synchronized between *A. islandica* specimens that grow at similar rates.

Indeed, Mg/Ca and Sr/Ca shell ratios were significantly correlated to the absolute and relative annual increment widths of almost all specimens from the Isle of Man and the Gulf of Maine (only in specimen 090829 is Sr/Ca not significantly correlated to absolute annual increment width; Table 4a). Our results are in line with previous observations on Sr/Ca and Mg/Ca ratios of ontogenetically old *A. islandica* shells (Schöne et al., 2011) and strongly corroborate findings by Gillikin et al. (2005) in as much as Sr/Ca of different specimens with similar growth rates are synchronized; apparently, the same applies to the Mg/Ca ratios of *A. islandica* shells (Figs. 8, 9; Table 5). The more similar the growth patterns of *A. islandica* were, the higher the correlation among the annually averaged trace element time-series of Mg/Ca, Sr/Ca and Mn/Ca (Table 5). Mean and peak Mg/Ca and Sr/Ca ratios, however, differed between coeval specimens from the same site (see smoothed and annually averaged data; Figs. 8, 9), which indicates that these element-to-calcium ratios cannot be readily used as paleoenvironmental proxies when determined with the same spatial resolution and/or technique applied here.

Interestingly, Na/Ca ratios also significantly co-varied among specimens with similar shell growth patterns and ontogenetic ages (Figs., 8, 9; Table 5). This was

[3] Shell growth rate can be expressed as linear extension rate (Klein et al., 1996b; Gillikin et al., 2005; Carré et al., 2006). Calcification rate describes the amount of shell material accreted per unit area per unit time. Also crystal growth rate can be determined (Carpenter and Lohmann, 1992). In this study, we refer to growth rate as the extension rate of the hinge along the maximum axis of growth.

Table 5. Relative shell growth patterns (i.e., SGI-values) and annually averaged element-to-calcium ratios (Na/Ca, Mg/Ca, Mn/Ca, Sr/Ca, and Ba/Ca, respectively) of coeval specimens from the Isle of Man (left panel) and the Gulf of Maine (right panel) where statistically tested for co-variation. The Pearson's correlation coefficients (r) and *p*-values are displayed in the lower part and the upper part of each matrix, respectively. *p*-values < 0.05 (grey shades) indicate a significant correlation among time-series.

Correlation matrix (r-value \ p-value) for relative annual shell growth

Isle of Man				Gulf of Maine			
Specimen ID	**0505319**	**0505327**	**0525475**	**Specimen ID**	**090797**	**090803**	**090829**
0505319		0.026	0.797	**090797**		0.209	0.001
0505327	0.25		0.027	**090803**	0.19		< 0.001
0525475	0.03	0.24		**090829**	0.50	0.70	

Correlation matrix (r-value \ p-value) for annually averaged Na/Ca

Isle of Man				Gulf of Maine			
Specimen ID	**0505319**	**0505327**	**0525475**	**Specimen ID**	**090797**	**090803**	**090829**
0505319		0.006	0.185	**090797**		0.874	0.462
0505327	0.31		0.042	**090803**	-0.02		< 0.001
0525475	0.15	0.23		**090829**	0.11	0.56	

Correlation matrix (r-value \ p-value) for annually averaged Mg/Ca

Isle of Man				Gulf of Maine			
Specimen ID	**0505319**	**0505327**	**0525475**	**Specimen ID**	**090797**	**090803**	**090829**
0505319		< 0.001	0.799	**090797**		0.350	0.203
0505327	0.77		0.475	**090803**	0.14		< 0.001
0525475	-0.03	0.08		**090829**	0.19	0.82	

Correlation matrix (r-value \ p-value) for annually averaged Mn/Ca

Isle of Man				Gulf of Maine			
Specimen ID	**0505319**	**0505327**	**0525475**	**Specimen ID**	**090797**	**090803**	**090829**
0505319		< 0.001	0.084	**090797**		0.039	0.528
0505327	0.63		0.040	**090803**	-0.31		< 0.001
0525475	0.20	0.23		**090829**	-0.10	0.89	

Correlation matrix (r-value \ p-value) for annually averaged Sr/Ca

Isle of Man				Gulf of Maine			
Specimen ID	**0505319**	**0505327**	**0525475**	**Specimen ID**	**090797**	**090803**	**090829**
0505319		< 0.001	0.063	**090797**		0.935	0.344
0505327	0.75		0.822	**090803**	0.01		< 0.001
0525475	-0.21	0.03		**090829**	0.14	0.54	

Correlation matrix (r-value \ p-value) for annually averaged Ba/Ca

Isle of Man				Gulf of Maine			
Specimen ID	**0505319**	**0505327**	**0525475**	**Specimen ID**	**090797**	**090803**	**090829**
0505319		< 0.001	< 0.001	**090797**		< 0.001	< 0.001
0505327	0.71		0.025	**090803**	0.91		< 0.001
0525475	0.41	0.25		**090829**	0.94	0.96	

unexpected, because Na/Ca ratios were largely non-reproducible within each specimen (Fig. 7, Table 3), indicating the amount of an external signal contained in Na/Ca shell time-series should be comparatively small. Apparently, only low-frequency (ca. decadal) variations in Na/Ca were synchronous among *A. islandica* specimens (e.g., among 090803 and 090829; Fig. 9). Whether or not these oscillations in Na/Ca reflect a genuine environmental signal cannot be determined in the present study. However, since the reproducibility of Na/Ca ratios within shells was so low, we do not recommend interpretation of the observed Na/Ca time-series in terms of environmental signals. Since annually averaged Na/Ca ratios were significantly correlated to annual increment widths for almost all specimens (Table 4a), it is likely that the observed co-variation of Na/Ca among specimens is linked to the synchronous growth of the corresponding shells.

Based on the observations stated above, one could argue that Na/Ca, Mg/Ca, Sr/Ca ratios and Mn/Ca, in *A. islandica* shells are not related to environmental controls at all. However, it has to be stressed that the spatial resolution we applied in our study was not sufficient to track trace element variations within all annual growth increments, because increments become narrower than the laser spot size as a shell grows older and/or if growth occurs under environmental stress (Witbaard, 1996; Schöne et al., 2010). Furthermore, the laser spot we used for line scans had a circular shape, which, together with narrowness of increments, increases the potential of 'signal smearing' (compare discussion in Marali et al., 2017). The analysis of ontogenetically old *A. islandica* (or other long-lived species) can be particularly challenging for this reason (see Schöne et al., 2010). We therefore recommend improvement of the spatial resolution by the use of rectangular laser spots, as recently demonstrated by Warter and Müller (2016), or by applying other high-resolution techniques such as EPMA or nanoSIMS (Freitas et al., 2009; Shirai et al., 2014; Sano et al., 2012). Alternatively, LA-ICP-MS analysis can be performed in specimens and/or parts of the shell with broader growth increments, i.e., in ontogenetically younger specimens or along the ventral margin. In this way, the geochemical variations within annual increments can also be determined (see also discussion in Schöne et al., 2010; Marali et al., 2017). Future calibration and biomineralization studies are required to identify the environmental factors controlling trace element variations in bivalve shells.

5 Summary and conclusions

The current study presents a simple way to test whether or not an external (potentially environmental) or biological signal may be contained in trace element time-series measured in bivalve shells (and potentially, other archives). We determined the Na/Ca, Mg/Ca, Mn/Ca, Sr/Ca, and Ba/Ca ratios in the hinge area of *A. islandica* shells via LA-ICP-MS analysis in line scan mode. Assuming that any environmentally driven signal in a trace element time-series should be reproducible within a specimen (Sinclair et al., 2005, 2011) and between coeval specimens from the same locality (e.g. DeLong et al., 2007), we assessed the degree of reproducibility of trace element time-series within and between shells of the bivalve *A. islandica*. This simple test can also be performed with other species and prior to any time-consuming calibration work, for which high-resolution environmental data is needed.

- Na/Ca ratios are largely irreproducible among replicate line scans in *A. islandica* specimens (average $r^2 = 0.22 \pm 0.04$; Table 4), although the ratios are well above detection limits.

- Mg/Ca and Sr/Ca ratios are highly reproducible within each specimen (average $r^2 = 0.82 \pm 0.27$ and 0.83 ± 0.18, respectively; $p < 0.002$), because they are directly related to shell growth patterns, increasing at annual growth lines (compare Schöne et al., 2011). The parts of the shell in which growth lines lie closely together display elevated Mg/Ca and Sr/Ca ratios, because the laser-spot size exceeds the width of the annual increments. At the applied spatial resolution, Mg/Ca and Sr/Ca function predominantly as growth line indicators.

- Mn/Ca ratios were close to detection limits during LA-ICP-MS sequences 1 and 0 (Supplementary Materials, Table S1), reducing the average intra-specimen reproducibility (average $r^2 = 0.74 \pm 0.23$; $p < 0.001$).

- Ba/Ca ratios are highly reproducible within shells of *A. islandica* (Fig. 3; r^2 on average 0.95 ± 0.04; $p < 0.001$), corroborating the earlier finding that this elemental ratio can be reliably determined via LA-ICP-MS and that 'compositional' (e.g., microstructural) heterogeneity of the shell does not distort the underlying Ba/Ca signal. Yet, future studies should align replicate analysis by using (shell) growth patterns to quantify the degree of reproducibility for Ba/Ca ratios. As in the case of Mn/Ca, decreasing spatial resolution with ontogenetic age leads to reduced Ba/Ca peak heights (see discussion in Marali et al., 2017). Previous studies have already demonstrated the strong synchrony of Ba/Ca ratios between different

individuals from the same habitat, supporting the potential of Ba/Ca ratios as an environmental proxy (Stecher et al., 1996; Gillikin et al., 2006, 2008; Marali et al., 2017).

- Na/Ca, Mg/Ca, Mn/Ca, and Sr/Ca ratios were significantly correlated to annual increment widths (Tables 4, 5). Na/Ca, Mg/Ca and Sr/Ca, in contrast with Ba/Ca, varied most synchronously among those coeval specimens from the same site which showed similar ontogenetic ages and shell growth patterns (compare Gillikin et al., 2005 for Sr/Ca), i.e., which offered a similar spatial resolution for LA-ICP-MS analysis.

- Future studies, testing the applicability of Na/Ca, Mg/Ca, Mn/Ca, and Sr/Ca of *A. islandica* shells or other archives as environmental proxies, should make use of techniques for enhancing the spatial resolution of the analysis, e.g., by using rectangular LA-ICP-MS spots (Warter and Müller, 2016) or other high-resolution techniques and/or by analyzing areas of the shell where annual increments are broader (i.e., in ontogenetically young parts of the hinge or along the shell margin). Considering the equivocal findings in previous studies, which aim to relate Mg/Ca or Sr/Ca ratios of ontogenetically young or short-lived bivalve species to temperature (e.g. Takesue and van Geen, 2004; Gillikin et al., 2005; Schöne et al., 2010; Füllenbach et al., 2015), and the low intra-shell reproducibility of Na/Ca and Mn/Ca ratios in *A. islandica*, we further recommend testing of an alternative analytical technique to LA-ICP-MS to determine trace element ratios within bivalve shells.

- Finally, we strongly recommend testing the reproducibility of trace element time-series, measured by LA-ICP-MS line scans or other techniques, within and between coeval specimens of bivalves (or other species) before interpreting them in terms of environmental and/or climatic change.

6 Acknowledgements

We are grateful for comments raised by two anonymous reviewers. We thank the captain and crew of the RV Prince Madog and of the scalloper Spaven Môr for their help during shell collection off the Isle of Man and Hilmar A. Holland, Gudrun Thórarinsdóttir, Siggeir Stefánsson, Erlendur Bogason and Sæmundur Einarsson for their assistance during shell collection in Iceland. Michael Maus, Stephan Buhre, Johanna Boos, Kathrin Böhm are gratefully acknowledged for their help with shell preparation. We thank Brigitte Stoll and Ulrike Weis for performing LA-ICP-MS measurements at the Max Planck Institute for Chemistry, Mainz, and Marina Veter for assisting with LA-ICP-MS analysis at Johannes Gutenberg University, Mainz. Further, we are thankful to Christoph S. Füllenbach and Liqiang Zhao for discussion about trace elements in bivalve shells. This study was made possible by a German Research Foundation (DFG) grant to BRS (SCHO 793/10-1).

7 References

Allison, N., Finch, A.A., 2009. Reproducibility of minor and trace element determinations in *Porites* coral skeletons by secondary ion mass spectrometry. Geochemistry, Geophys. Geosystems 10. doi:10.1029/2008GC002239.

Alpert, A.E., Cohen, A.L., Oppo, D.W., Decarlo, T.M., Jamison, M., Young, C.W., 2016. Comparison of equatorial Pacific sea surface variability and trends with Sr/Ca records from multiple corals 1–14. doi:10.1002/2015PA002897.

Anagnostou, E., Sherrell, R.M., Gagnon, A., LaVigne, M., Field, M.P., McDonough, W.F., 2011. Seawater nutrient and carbonate ion concentrations recorded as P/Ca, Ba/Ca , and U/Ca in the deep-sea coral Desmophyllum dianthus. Geochim. Cosmochim. Acta 75, 2529–2543. doi:10.1016/j.gca.2011.02.019.

Baker, S.A., Bi, M., Aucelio, R.Q., Smith, B.W., Winefordner, J.D., 1999. Analysis of soil and sediment samples by laser ablation inductively coupled plasma mass spectrometry. J. Anal. At. Spectrom. 14, 19–26. doi:10.1039/A804060E.

Barats, A., Amouroux, D., Chauvaud, L., Pécheyran, C., Lorrain, A., Thébault, J., Church, T.M., Donard, O.F.X., 2009. High frequency Barium profiles in shells of the Great Scallop *Pecten maximus*: a methodical long-term and multi-site survey in Western Europe. Biogeosciences 6, 157 – 170. doi:10.5194/bgd–5–3665–2008.

Beck, J.W., Edwards, R.L., Ito, E., Taylor, F.W., Recy, J., Rougerie, F., Joannot, P., Henin, C., 1992. Sea-surface temperature from coral skeletal strontium/calcium ratios. Science 257, 644–647.

Black, B.A., Griffin, D., van der Sleen, P., Wanamaker, A.D., Speer, J.H., Frank, D.C., Stahle, D.W., Pederson, N., Copenheaver, C.A., Trouet, V., Griffin, S., Gillanders, B.M., 2016. The value of crossdating to retain high-frequency variability, climate signals, and extreme events in environmental proxies. Glob. Change Biol. 22, 2582–2595.

Butler, P.G., Scourse, J.D., Richardson, C. a., Wanamaker, A.D., Bryant, C.L., Bennell, J.D., 2009. Continuous marine radiocarbon reservoir calibration and the ^{13}C Suess effect in the Irish Sea: Results from the first multi-centennial shell-based marine master chronology. Earth Planet. Sci. Lett. 279, 230–241. doi:10.1016/j.epsl.2008.12.043.

Butler, P.G., Richardson, C. a., Scourse, J.D., Wanamaker, A.D., Shammon, T.M., Bennell, J.D., 2010. Marine climate in the Irish Sea: analysis of a 489-year marine master chronology derived from growth increments in the shell of the clam *Arctica islandica*. Quat. Sci. Rev. 29, 1614–1632. doi:10.1016/j.quascirev.2009.07.010.

Butler, P.G., Wanamaker, A.D., Scourse, J.D., Richardson, C. a., Reynolds, D.J., 2013. Variability of marine climate on the North Icelandic Shelf in a 1357-year proxy archive based on growth increments in the bivalve *Arctica islandica*. Palaeogeogr. Palaeoclimatol. Palaeoecol. 373, 141–151. doi:10.1016/j.palaeo.2012.01.016.

Carpenter, S.J., Lohmann, K.C., 1992. Sr/Mg ratios of modern marine calcite: Empirical indicators of ocean chemistry and precipitation rate. Geochim. Cosmochim. Acta 56, 1837–1849. doi:10.1016/0016–7037(92)90314–9.

Carré, M., Bentaleb, I., Bruguier, O., Ordinola, E., Barrett, N.T., Fontugne, M., 2006. Calcification rate influence on trace element concentrations in aragonitic bivalve shells: Evidences and mechanisms. Geochim. Cosmochim. Acta 70, 4906–4920. doi:10.1016/j.gca.2006.07.019.

Cohen, A.L., Thorrold, S.R., 2007. Recovery of temperature records from slow-growing corals by fine scale sampling of skeletons. Geophys. Res. Lett. 34, L17706. doi:10.1029/2007GL030967.

Cook, E.R., Kairiukstis, L.A. (Eds.), 1990. Methods of dendrochronology – Applications in the environmental sciences. Kluwer Academic Publishers, Dordrecht, Boston, London.

Cook, E.R., Krusic, P.J., 2007. Program ARSTAN – A tree-ring standardization program based on detrending and autoregressive time-series modeling, with interactive graphics. Tree-Ring Laboratory, Lamont Doherty Earth Observatory of Columbia University, Palisade, NY, 14 pp.

Dahlgren, T. G., J. R. Weinberg, and K. M. Halanych, 2000. Phylogeography of the ocean quahog (*Arctica islandica*): Influences of paleoclimate on genetic diversity and species range. Mar. Biol. 137, 487–495.

Dehairs, F., Chesselet, R., Jedwab, J., 1980. Discrete suspended particles of barite and the barium cycle in the open ocean. Earth Planet. Sci. Lett. 49, 528–550. doi:10.1016/0012–821X(80)90094–1.

DeLong, K.L., Quinn, T.M., Taylor, F.W., 2007. Reconstructing twentieth-century sea surface temperature variability in the southwest Pacific: A replication study using multiple coral Sr/Ca records from New Caledonia. Paleoceanography 22, 1–18. doi:10.1029/2007PA001444.

DeLong, K.L., Quinn, T.M., Taylor, F.W., Shen, C., Lin, K., 2013. Improving coral-base paleoclimate reconstructions by replicating 350 years of coral Sr/Ca variations. Palaeogeogr. Palaeoclimatol. Palaeoecol. 373, 6 – 24. doi:10.1016/j.palaeo.2012.08.019.

Desmarchelier, J.M., Hellstrom, J.C., McCulloch, M.T., 2006. Rapid trace element analysis of speleothems by ELA-ICP-MS. Chem. Geol. 231, 102–117. doi:10.1016/j.chemgeo.2006.01.002.

Dodd, J.R., 1965. Environmental control of strontium and magnesium in *Mytilus*. Geochim. Cosmochim. Acta 29, 385–398. doi:10.1016/0016–7037(65)90035–9

Dodd, J.R., Crisp, E.L., 1982. Non-linear variation with salinity of Sr/Ca and Mg/Ca ratios in water and aragonitic bivalve shells and implications for paleosalinity studies. Palaeogeogr. Palaeoclimatol. Palaeoecol. 38, 45–56. doi:10.1016/0031–0182(82)90063–3.

Dymond, J., Suess, E., Lyle, M., 1992. Barium in deep-sea sediment: A geochemical proxy for paleoproductivity. Paleoceanography 7, 163–181. doi:10.1029/92PA00181

Elliot, M., Welsh, K., Chilcott, C., McCulloch, M., Chappell, J., Ayling, B., 2009. Profiles of trace elements and stable isotopes derived from giant long-lived *Tridacna gigas* bivalves: Potential applications in paleoclimate studies. Palaeogeogr. Palaeoclimatol. Palaeoecol. 280, 132–142. doi:10.1016/j.palaeo.2009.06.007.

Foster, L.C., Finch, a. a., Allison, N., Andersson, C., Clarke, L.J., 2008. Mg in aragonitic bivalve shells: Seasonal variations and mode of incorporation in *Arctica islandica*. Chem. Geol. 254, 113–119. doi:10.1016/j.chemgeo.2008.06.007.

Foster, L.C., Allison, N., Finch, A.A., Andersson, C., 2009. Strontium distribution in the shell of the aragonite bivalve *Arctica islandica*. Geochemistry, Geophys. Geosystems 10. doi:10.1029/2007GC001915.

Freitas, P.S., Clarke, L.J., Kennedy, H., Richardson, C. a., Abrantes, F., 2006. Environmental and biological controls on elemental (Mg/Ca, Sr/Ca and Mn/Ca) ratios in shells of the king scallop *Pecten maximus*. Geochim. Cosmochim. Acta 70, 5119–5133. doi:10.1016/j.gca.2006.07.029.

Freitas, P.S., Clarke, L.J., Kennedy, H. a., Richardson, C. a., 2008. Inter- and intra-specimen variability masks reliable temperature control on shell Mg/Ca ratios in laboratory– and field–cultured *Mytilus edulis* and *Pecten maximus* (bivalvia). Biogeosciences 5, 1245–1258. doi:10.5194/bg–5–1245–2008.

Freitas, P.S., Clarke, L.J., Kennedy, H.A., Richardson, C.A., 2009. Ion microprobe assessment of the heterogeneity of Mg/Ca, Sr/Ca and Mn/Ca ratios in *Pecten maximus* and *Mytilus edulis* (bivalvia) shell calcite precipitated at constant temperature. Biogeosciences 6, 1209–1227. doi:10.5194/bg–6–1209–2009.

Fuge, R., Palmer, T.J., Pearce, N.J.G., Perkins, W.T., 1993. Minor and trace element chemistry of modern shells: a laser ablation inductively coupled plasma mass spectrometry study. Appl. Geochemistry 8, 111–116. doi:10.1016/S0883-2927(09)80020-6.

Füllenbach, C.S., Schöne, B.R., Branscheid, R., 2014. Microstructures in shells of the freshwater gastropod *Viviparus viviparus*: A potential sensor for temperature change? Acta Biomater. 10, 3911–3921. doi:10.1016/j.actbio.2014.03.030.

Füllenbach, C.S., Schöne, B.R., Mertz-Kraus, R., 2015. Strontium/lithium ratio in aragonitic shells of *Cerastoderma edule* (Bivalvia) – A new potential temperature proxy for brackish environments. Chem. Geol. 417, 341–355. doi:10.1016/j.chemgeo.2015.10.030.

Gessmann, C.K., Rubie, D.C., 2000. The origin of the depletions of V, Cr and Mn in the mantles of the Earth and Moon. Earth Planet. Sci. Lett. 184, 95–107. doi:10.1016/S0012–821X(00)00323–X.

Gillikin, D.P., Lorrain, A., Navez, J., Taylor, J.W., André, L., Keppens, E., Baeyens, W., Dehairs, F., 2005. Strong biological controls on Sr/Ca ratios in aragonitic marine bivalve shells. Geochemistry, Geophys. Geosystems 6. doi:10.1029/2004GC000874.

Gillikin, D.P., Dehairs, F., Lorrain, A., Steenmans, D., Baeyens, W., André, L., 2006. Barium uptake into the shells of the common mussel (*Mytilus edulis*) and the potential for estuarine paleo-chemistry reconstruction. Geochim. Cosmochim. Acta 70, 395–407. doi:10.1016/j.gca.2005.09.015.

Gillikin, D.P., Lorrain, A., Paulet, Y.M., André, L., Dehairs, F., 2008. Synchronous barium peaks in high-resolution profiles of calcite and aragonite marine bivalve shells. Geo-Marine Lett. 28, 351–358. doi:10.1007/s00367–008–0111–9.

Goldberg, E.D., Arrhenius, G.O.S., 1958. Chemistry of Pacific pelagic sediments. Geochim. Cosmochim. Acta 13, 153–212. doi:10.1016/0016–7037(58)90046–2.

Goldschmidt, V.M., 1937. The principles of distribution of chemical elements in minerals and rocks. J. Chem. Socienty 655–673. doi:10.1039/JR9370000655.

Griffin, S.M., 2012. Applying dendrochronology visual crossdating techniques to the marine bivalve *Arctica islandica* and assessing the utility of master growth chronologies as proxies for temperature and secondary productivity in the Gulf of Maine. Unpublished Masters Thesis, Iowa State University, Ames, IA, 237 pp.

Hammer, Ø., Harper, D. A. T., Ryan, P.D., 2001. Paleontological statistics software package for education and data analysis. Palaeontol. Electron. 4, 9–18. doi:10.1016/j.bcp.2008.05.025.

Hathorne, E.C., Alard, O., James, R.H., Rogers, N.W., 2003. Determination of intratest variability of trace elements in foraminifera by laser ablation inductively coupled plasma-mass spectrometry. Geochemistry, Geophys. Geosystems 4. doi:10.1029/2003GC000539.

Hennekam, R., Jilbert, T., Mason, P.R.D., de Lange, G.J., Reichart, G.-J., 2015. High-resolution line-scan analysis of resin-embedded sediments using laser ablation-inductively coupled plasma-mass spectrometry (LA-ICP-MS). Chem. Geol. 403, 42–51. doi:10.1016/j.chemgeo.2015.03.004.

Holland, H. A., Schöne, B.R., Marali, S., Jochum, K.P., 2014a. History of bioavailable lead and iron in the Greater North Sea and Iceland during the last millennium – A bivalve sclerochronological reconstruction. Mar. Pollut. Bull. 87, 104–116. doi:10.1016/j.marpolbul.2014.08.005.

Holland, H. A., Schöne, B.R., Lipowsky, C., Esper, J., 2014b. Decadal climate variability of the North Sea during the last millennium reconstructed from bivalve shells (*Arctica islandica*). The Holocene 24, 771–786. doi:10.1177/0959683614530438.

Holmes, R.L., Adams, R.K., Fritts, H.C., 1986. Tree-ring chronologies of Western North America, California, Eastern Oregon and Northern Great Basin with procedures used in the chronology development work including user manuals for computer programs COFECHA and ARSTAN. Chronology Series VI, 182 pp.

Jochum, K.P., Nohl, U., Herwig, K., Lammel, E., Stoll, B., Hofmann, A.W., 2005. GeoReM: A New Geochemical Database for Reference Materials and Isotopic Standards. Geostand. Geoanalytical Res. 29, 333–338. doi:10.1111/j.1751–908X.2005.tb00904.x.

Jochum, K.P., Stoll, B., Herwig, K., Willbold, M., 2007. Validation of LA-ICP-MS trace element analysis of geological glasses using a new solid–state 193 nm Nd:YAG laser and matrix–matched calibration. J. Anal. At. Spectrom. 22, 112. doi:10.1039/b609547j.

Jochum, K.P., Weis, U., Stoll, B., Kuzmin, D., Yang, Q., Raczek, I., Jacob, D.E., Stracke, A., Birbaum, K., Frick, D.A., Günther, D., Enzweiler, J., 2011. Determination of reference values for NIST SRM 610–617 glasses following ISO guidelines. Geostand. Geoanalytical Res. 35, 397–429. doi:10.1111/j.1751–908X.2011.00120.x.

Jochum, K.P., Scholz, D., Stoll, B., Weis, U., Wilson, S. a., Yang, Q., Schwalb, A., Börner, N., Jacob, D.E., Andreae, M.O., 2012. Accurate trace element analysis of speleothems and biogenic calcium carbonates by LA-ICP-MS. Chem. Geol. 318–319, 31–44. doi:10.1016/j.chemgeo.2012.05.009.

Karney, G.B., Butler, P.G., Speller, S., Scourse, J.D., Richardson, C.A., Schrder, M., Hughes, G.M., Czernuszka, J.T., Grovenor, C.R.M., 2012. Characterizing the microstructure of *Arctica islandica* shells using NanoSIMS and EBSD. Geochemistry, Geophys. Geosystems 13. doi:10.1029/2011GC003961.

Klein, R.T., Lohmann, K.C., Thayer, C.W., 1996a. Bivalve skeletons record sea–surface temperature and $\delta^{18}O$ via Mg/Ca and $^{18}O/^{16}O$ ratios. Geology 24, 415–418. doi:10.1130/0091–7613(1996)024<0415.

Klein, R.T., Lohmann, K.C., Thayer, C.W., 1996b. Sr/Ca and 13C/12C ratios in skeletal calcite of Mytilus trossulus: Covariation with metabolic rate, salinity, and carbon isotopic composition of seawater. Geochim 60, 4207–4221.

Küster, W.K., Thiel, A., 2011. Rechentafeln für die chemische Analytik: Basiswissen für die analytische Chemie. 107. Auflage. De Gruyter, Berlin/ New York.

Langlet, D., Alleman, L.Y., Plisnier, P.-D., Hughes, H., André, L., 2007. Manganese content records seasonal upwelling in Lake Tanganyika mussels. Biogeosciences 4, 195–203. doi:10.5194/bg–4–195–2007.

Lea, D.W., Mashiotta, T.A., Spero, H.J., 1999. Controls on magnesium and strontium uptake in planktonic foraminifera determined by live culturing. Geochim. Cosmochim. Acta 63, 2369–2379. doi:10.1016/S0016–7037(99)00197–0.

Lin, A.Y.M., Meyers, M.A., Vecchio, K.S., 2006. Mechanical properties and structure of Strombus gigas, *Tridacna gigas*, and Haliotis rufescens sea shells: A comparative study. Mater. Sci. Eng. C 26, 1380–1389. doi:10.1016/j.msec.2005.08.016.

Longerich, H.P., Jackson, S.E., Günther, D., 1996. Laser ablation inductively coupled plasma mass spectrometric transient signal data acquisition and analyte concentration calculation. J. Anal. At. Spectrom. 11, 899–904.

Lorens, R.B., Bender, M.L., 1977. Physiological exclusion of magnesium from *Mytilus edulis* calcite. Nature 269, 793–794.

Mann, M.E., Zhang, Z., Hughes, M.K., Bradley, R.S., Miller, S.K., Rutherford, S., Ni, F., 2008. Proxy-based reconstructions of hemispheric and global surface temperature variations over the past two millennia. Proc. Natl. Acad. Sci. U. S. A. 105, 13252–13257. doi:10.1073/pnas.0805721105.

Mann, M.E., Zhang, Z., Rutherford, S., Bradley, R.S., Hughes, M.K., Shindell, D., Ammann, C., Faluvegi, G., Ni, F., 2009. Global signatures and dynamical origins of the Little Ice Age and Medieval Climate Anomaly. Science 326, 1256–1260. doi:10.1126/science.1166349.

Marali, S., Schöne, B.R., 2015. Oceanographic control on shell growth of *Arctica islandica* (Bivalvia) in surface waters of Northeast Iceland – Implications for paleoclimate reconstructions. Palaeogeogr. Palaeoclimatol. Palaeoecol. 420, 138–149. doi:10.1016/j.palaeo.2014.12.016.

Marali, S., Schöne, B.R., Mertz-Kraus, R., Griffin, S.M., Wanamaker, A.D., Matras, U., Butler, P.G., 2017. Ba/Ca ratios in shells of *Arctica islandica* – Potential environmental proxy and crossdating tool. Palaeogeogr. Palaeoclimatol. Palaeoecol. doi:10.1016/j.palaeo.2015.12.018.

Merrill, A.S., Ropes, J.W., 1969. The general distribution of the surf clam and the ocean quahog. Proc. Natl. Shellfish. Assoc. 59, 40–45.

Mertz-Kraus, R., Brachert, T.C., Jochum, K.P., Reuter, M., Stoll, B., 2009. LA-ICP-MS analyses on coral growth increments reveal heavy winter rain in the Eastern Mediterranean at 9 Ma. Palaeogeogr. Palaeoclimatol. Palaeoecol. 273, 25–40. doi:10.1016/j.palaeo.2008.11.015.

Mette, M. J., Wanamaker, A. D., M. L. Carroll, W. G. Ambrose, and M. J. Retelle, 2016. Linking large-scale climate variability with *Arctica islandica* shell growth and geochemistry in northern Norway, Limnol. Oceanogr. 61, 748–764, doi: 10.1002/lno.10252.

Milano, S., Schöne, B.R., Witbaard, R., 2015. Changes of shell microstructural characteristics of *Cerastoderma edule* (Bivalvia) – A novel proxy for water temperature. Palaeogeogr. Palaeoclimatol. Palaeoecol. doi:10.1016/j.palaeo.2015.09.051.

Mitsuguchi, T., Matsumoto, E., Abe, O., Uchida, T., Isdale, P.J., 1996. Mg/Ca Thermometry in Coral Skeletons. Science. 274, 961–963. doi:10.1126/science.274.5289.961.

Montagna, P., McCulloch, M., Taviani, M., Mazzoli, C., Vendrell, B., 2006. Phosphorus in cold-water corals as a proxy for seawater nutrient chemistry. Science 312, 1788–1791. doi:10.1126/science.1125781.

Montagna, P., McCulloch, M., Mazzoli, C., Silenzi, S., Odorico, R., 2007. The non-tropical coral *Cladocora caespitosa* as the new climate archive for the Mediterranean: high-resolution (~weekly) trace element systematics. Quat. Sci. Rev. 26, 441–462. doi:10.1016/j.quascirev.2006.09.008.

Montagna, P., McCulloch, M., Douville, E., López Correa, M., Trotter, J., Rodolfo-Metalpa, R., Dissard, D., Ferrier-Pagès, C., Frank, N., Freiwald, A., Goldstein, S., Mazzoli, C., Reynaud, S., Rüggeberg, A., Russo, S., Taviani, M., 2014. Li/Mg systematics in scleractinian corals: Calibration of the thermometer. Geochim. Cosmochim. Acta 132, 288–310. doi:10.1016/j.gca.2014.02.005.

Nicol, D., 1951. Recent species of the veneroid pelecypod Arctica. J. Washingt. Acad. Sci. 41, 102–106.

O'Neil, D.D., Gillikin, D.P., 2014. Do freshwater mussel shells record road-salt pollution? Sci. Rep. 4, 6. doi:10.1038/srep07168.

Phung, A.T., Baeyens, W., Leermakers, M., Goderis, S., Vanhaecke, F., Gao, Y., 2013. Reproducibility of laser ablation-inductively coupled plasma-mass spectrometry (LA-ICP-MS) measurements in mussel shells and comparison with micro-drill sampling and solution ICP-MS. Talanta 115, 6–14. doi:10.1016/j.talanta.2013.04.019

Poulain, C., Gillikin, D.P., Thébault, J., Munaron, J.M., Bohn, M., Robert, R., Paulet, Y.-M., Lorrain, A., 2015. An evaluation of Mg/Ca, Sr/Ca, and Ba/Ca ratios as environmental proxies in aragonite bivalve shells. Chem. Geol. 396, 42–50. doi:10.1016/j.chemgeo.2014.12.019.

Rhoads, D.C., Lutz, R.A. (Eds.), 1980. Skeletal growth of aquatic organisms, Topics in Geobiology, 750 p.

Rucker, J.B., Valentine, J.W., 1961. Salinity response of trace element concentration in *Crassostrea virginica*. Nature 190, 1099–1100.

Sanborn, M., Telmer, K., 2003. The spatial resolution of LA-ICP-MS line scans across heterogeneous materials such as fish otoliths and zoned minerals. J. Anal. At. Spectrom. 18, 1231–1237. doi:10.1039/b302513f.

Sano, Y., Kobayashi, S., Shirai, K., Takahata, N., Matsumoto, K., Watanabe, T., Sowa, K., Iwai, K., 2012. Past daily light cycle recorded in the strontium/calcium ratios of giant clam shells. Nat. Commun. 3, 761. doi:10.1038/ncomms1763.

Schöne, B.R., 2013. *Arctica islandica* (Bivalvia): A unique paleoenvironmental archive of the northern North Atlantic Ocean. Global Planet. Change 111, 199–225. doi:10.1016/j.gloplacha.2013.09.013.

Schöne, B.R., Freyre Castro, A.D., Fiebig, J., Houk, S.D., Oschmann, W., Kröncke, I., 2004. Sea surface water temperatures over the period 1884 – 1983 reconstructed from oxygen isotope ratios of a bivalve mollusk shell (*Arctica islandica*, southern North Sea). Palaeogeogr. Palaeoclimatol. Palaeoecol. 212, 215–232. doi:10.1016/j.palaeo.2004.05.024.

Schöne, B.R., Dunca, E., Fiebig, J., Pfeiffer, M., 2005a. Mutvei's solution: An ideal agent for resolving microgrowth structures of biogenic carbonates. Palaeogeogr. Palaeoclimatol. Palaeoecol. 228, 149–166. doi:10.1016/j.palaeo.2005.03.054.

Schöne, B.R., Fiebig, J., Pfeiffer, M., Gleß, R., Hickson, J., Johnson, A.L.A., Dreyer, W., Oschmann, W., 2005b. Climate records from a bivalved Methuselah (*Arctica islandica*, Mollusca; Iceland). Palaeogeogr. Palaeoclimatol. Palaeoecol. 228, 130–148. doi:10.1016/j.palaeo.2005.03.049.

Schöne, B.R., Houk, S.D., Freyre Castro, A.D., Fiebig, J., Oschmann, W., 2005c. Daily Growth Rates in Shells of *Arctica islandica*: Assessing Sub-seasonal Environmental Controls on a Long-lived Bivalve Mollusk. Palaios 20, 78–92. doi:10.2110/palo.2003.p03–101.

Schöne, B.R., Zhang, Z., Jacob, D.E., Gillikin, D.P., Tütken, T., Garbe-Schönberg, D., McConnaughey, T., Soldati, A., 2010. Effect of organic matrices on the determination of the trace element chemistry (Mg, Sr, Mg/Ca, Sr/Ca) of aragonitic bivalve shells (*Arctica islandica*) – Comparison of ICP-OES and LA-ICP-MS data. Geochem. J. 44, 23–37.

Schöne, B.R., Zhang, Z., Radermacher, P., Thébault, J., Jacob, D.E., Nunn, E. V., Maurer, A.-F., 2011. Sr/Ca and Mg/Ca ratios of ontogenetically old, long-lived bivalve shells (*Arctica islandica*) and their function as paleotemperature proxies. Palaeogeogr. Palaeoclimatol. Palaeoecol. 302, 52–64. doi:10.1016/j.palaeo.2010.03.016.

Schöne, B.R., Radermacher, P., Zhang, Z., Jacob, D.E., 2013. Crystal fabrics and element impurities (Sr/Ca, Mg/Ca, and Ba/Ca) in shells of *Arctica islandica* – Implications for paleoclimate reconstructions. Palaeogeogr. Palaeoclimatol. Palaeoecol. 373, 50–59. doi:10.1016/j.palaeo.2011.05.013.

Shirai, K., Schöne, B.R., Miyaji, T., Radarmacher, P., Krause, R.A., Tanabe, K., 2014. Assessment of the mechanism of elemental incorporation into bivalve shells (*Arctica islandica*) based on elemental distribution at the microstructural scale. Geochim. Cosmochim. Acta 126, 307–320. doi:10.1016/j.gca.2013.10.050.

Sinclair, D.J., Kinsley, L.P.J., McCulloch, M.T., 1998. High resolution analysis of trace elements in corals by laser ablation ICP-MS. Geochim. Cosmochim. Acta 62, 1889–1901.

Sinclair, D., Sherwood, O., Risk, M., Hillaire-Marcel, C., Tubrett, M., Sylvester, P., McCulloch, M., Kinsley, L., 2005. Testing the reproducibility of Mg/Ca profiles in the deep-water coral *Primnoa resedaeformis:* putting the proxy through its paces. Cold-Water Corals Ecosyst. 1039–1060. doi:10.1007/3–540–27673–4_52.

Sinclair, D.J., Williams, B., Allard, G., Ghaleb, B., Fallon, S., Ross, S.W., Risk, M., 2011. Reproducibility of trace element profiles in a specimen of the deep-water bamboo coral *Keratoisis* sp. Geochim. Cosmochim. Acta 75, 5101–5121. doi:10.1016/j.gca.2011.05.012.

Soldati, A.L., Jacob, D.E., Glatzel, P., Swarbrick, J.C., Geck, J., 2016. Element substitution by living organisms: the case of manganese in mollusc shell aragonite. Sci. Rep. 6, 1–9. doi:10.1038/srep22514.

Stecher, H. a., Krantz, D.E., Lord, C.J., Luther, G.W., Bock, K.W., 1996. Profiles of strontium and barium in *Mercenaria mercenaria* and *Spisula solidissima* shells. Geochim. Cosmochim. Acta 60, 3445–3456. doi:10.1016/0016–7037(96)00179–2.

Stemmer, K., Nehrke, G., 2014. The distribution of polyenes in the shell of *Arctica islandica* from North Atlantic localities: A confocal Raman microscopy study. J. Molluscan Stud. 80, 365–370. doi:10.1093/mollus/eyu033.

Stephenson, A.E., DeYoreo, J.J., Wu, L., Wu, K.J., Hoyer, J., Dove, P.M., 2008. Peptides enhance magnesium signature in calcite: Insights into origins of vital effects. Science 322, 724–727. doi:10.1126/science.1159417.

Sylvester, P. (Ed.), 2001. Laser-Ablation-ICPMS in the Earth Sciences. Principles and Applications. Short Course Series 29. Mineralogical Association of Canada. 243 pp.

Takesue, R.K., van Geen, A., 2004. Mg/Ca, Sr/Ca, and stable isotopes in modern and Holocene *Protothaca staminea* shells from a northern California coastal upwelling region. Geochim. Cosmochim. Acta 68, 3845–3861. doi:10.1016/j.gca.2004.03.021.

Thomas, R., 2013. Practical Guide to ICP-MS. A tutorial for beginners. Third edition. CRC Press. 441 pp.

Thompson, I., Jones, D.S., Dreibelbis, D., 1980. Annual internal growth banding and life-history of the ocean quahog *Arctica islandica* (Mollusca, Bivalvia). Mar. Biol. 57, 25 – 34.

Toland, H., Perkins, B., Pearce, N., Keenan, F., Leng, M., 2000. Study of sclerochronology by laser ablation ICP-MS 15, 1143–1148. doi:10.1039/b002014l.

Treble, P., Shelley, J.M.G., Chappell, J., 2003. Comparison of high resolution sub-annual records of trace elements in a modern (1911-1992) speleothem with instrumental climate data from southwest Australia. Earth Planet. Sci. Lett. 216, 141–153. doi:10.1016/S0012-821X(03)00504-1.

Vander Putten, E., Dehairs, F., Keppens, E., Baeyens, W., 2000. High resolution distribution of trace elements in the calcite shell layer of modern *Mytilus edulis*: Environmental and biological controls. Geochim. Cosmochim. Acta 64, 997–1011.

Wanamaker, A.D., Kreutz, K.J., Wilson, T., Borns, H.W., Introne, D.S., Feindel, S., 2008. Experimentally determined Mg/Ca and Sr/Ca ratios in juvenile bivalve calcite for *Mytilus edulis*: Implications for paleotemperature reconstructions. Geo-Marine Lett. 28, 359 – 368. doi:10.1007/s00367–008–0112–8.

Wanamaker, A.D., Kreutz, K.J., Schöne, B.R., Maasch, K. a., Pershing, A.J., Borns, H.W., Introne, D.S., Feindel, S., 2009a. A late Holocene paleo-productivity record in the western Gulf of Maine, USA, inferred from growth histories of the long-lived ocean quahog (*Arctica islandica*). Int. J. Earth Sci. 98, 19–29. doi:10.1007/s00531–008–0318–z.

Wanamaker Jr, A.D., Baker, A., Butler, P.G., Richardson, C.A., Scourse, J.D., Ridgway, I., Reynolds, D.J., 2009b. A novel method for imaging internal growth patterns in marine mollusks : A fluorescence case study on the aragonitic shell of the marine bivalve *Arctica islandica* (Linnaeus). Limnol. Oceanogr. Methods 7, 673–681.

Wanamaker Jr, A.D., Butler, P.G., Scourse, J.D., Heinemeier, J., Eiríksson, J., Knudsen, K.L., Richardson, C.A., 2012. Surface changes in the North Atlantic meridional overturning circulation during the last millennium. Nat. Commun. 3, 237 – 252. doi:10.1038/ncomms1901.

Warter, V., Müller, W., 2016. Daily growth and tidal rhythms in Miocene and modern giant clams revealed via ultra-high resolution LA-ICPMS analysis – A novel methodological approach towards improved sclerochemistry. Palaeogeogr. Palaeoclimatol. Palaeoecol. doi:10.1016/j.palaeo.2016.03.019.

Wigley, T.M.L., Briffa, K.R., Jones, P.D., 1984. On the Average Value of Correlated Time-series, with Applications in Dendroclimatology and Hydrometeorology. J. Clim. Appl. Meteorol. 23, 201 – 213. doi:10.1175/1520–0450(1984)023<0201:OTAVOC>2.0.CO;2.

Wit, J.C., De Nooijer, L.J., Wolthers, M., Reichart, G.J., 2013. A novel salinity proxy based on na incorporation into foraminiferal calcite. Biogeosciences 10, 6375 – 6387. doi:10.5194/bg–10–6375–2013.

Witbaard, R., 1996. Growth variations in *Arctica islandica* L. (Mollusca): a reflection of hydrography-related food supply. ICES J. Mar. Sci. 53, 981–987.

Yan, H., Shao, D., Wang, Y., Sun, L., 2014. Sr/Ca differences within and among three Tridacnidae species from the South China Sea: Implication for paleoclimate reconstruction. Chem. Geol. 390, 22–31. doi:10.1016/j.chemgeo.2014.10.011.

Yan, H., Sun, L., Shao, D., Wang, Y., 2015. Seawater temperature seasonality in the South China Sea during the late Holocene derived from high–resolution Sr/Ca ratios of *Tridacna gigas*. Quat. Res. (United States) 83, 298–306. doi:10.1016/j.yqres.2014.12.001.

Zhao, L., Schöne, B.R., Mertz-Kraus, R., 2015. Controls on strontium and barium incorporation into freshwater bivalve shells (*Corbicula fluminea*). Palaeogeogr. Palaeoclimatol. Palaeoecol. 9. doi:10.1017/CBO9781107415324.004.

Zhao L., Schöne B.R., Mertz-Kraus, R., 2016. Delineating the role of calcium in shell formation and elemental composition of *Corbicula fluminea* (Bivalvia). Hydrobiologia, doi:10.1007/s10750-016-3037-7.

Zhao, L., Schöne, B.R., Mertz-Kraus, R., Yang, F., 2017. Insights from sodium into the impacts of elevated pCO_2 and temperature on bivalve shell formation. J. Exp. Mar. Bio. Ecol. 486, 148–154. doi:10.1016/j.jembe.2016.10.009.

Supplementary materials – manuscript III

Data quality control

At both MPIC and JGU, the synthetic carbonate reference material USGS MACS-3 (a pressed powder pellet; n = 6 per sequence) was analyzed to assess measurement accuracy of a carbonate matrix. During sequences 0 and 1, analyses of MACS-3 were performed at the rim of the carbonate pellet and close to previous ablation patterns, which can result in an uneven distribution of particle sizes during ablation, leading to signal instabilities. To account for this, we filtered MACS-3 results from JGU, rejecting all background corrected element intensities set relative to the internal standard ^{43}Ca (see below) which deviated by more than 50% from the median value of each data set (see Marali et al., 2017). At JGU, the synthetic glass NIST SRM 610 (n = 24 per sequence) and the basaltic glass USGS BCR-2G (n = 6 per sequence) were analyzed in addition to USGS MACS-3 to monitor reproducibility of the measurements by analyzing homogeneous materials.

LA-ICP-MS accuracy was tested by comparing the measured mean element concentrations of reference materials (USGS MACS-3, USGS BCR-2G, NIST SRM 610; see section 2.3.2) with the corresponding reference values (Table 2). On average, differences between measured and reference element values range from 4 to 7 % for USGS MACS-3 and from 6 to 8 % for USGS BCR-2G (Table 2). In the case of NIST SRM 610, average differences lie between 1 % and 3 % for all elements, except magnesium, for which measured values were on average 21 % higher than the reference value. Measuring a larger quantity of magnesium in NIST SRM 610 than is actually within the reference material could be due to surface contamination or interferences with other multiply-charged ions or molecules having the same mass-to-charge ratio as $^{25}Mg^{+}$, such as $^{50}Ti^{2+}$, $^{50}Cr^{2+}$ or $^{50}V^{2+}$. In general, the degree to which an interfering ion (or molecule) affects the analysis of the element of interest (i.e., the analyte) is influenced by (1) the ratio of the interfering ion (or molecule) and the analyte (Jochum et al., 2012) and (2) the mass resolution of the ICP-MS, which corresponds to its ability to separate the spectral peaks of the analyte and the interfering ion (or molecule), respectively (Thomas, 2013). Quadrupole instruments, as applied at JGU, offer a relatively low mass resolution (Thomas, 2013) and are therefore less effective in separating the masses of the interfering ions from that of $^{25}Mg^{+}$ than sector field instruments. Moreover, the interfering ion(s) / magnesium ratio is relatively high for NIST SRM 610, compared to those of NIST SRM 612, USGS MACS-3 and USGS BCR-2G (ratios calculated from element concentrations taken from GeoReM database, application version 20). The titanium/magnesium ratio, for example, equals 1.05 for

NIST SRM 610, but only 0.65, 0.66 and 0.03 for NIST SRM 612, USGS BCR-2B and USGS MACS-3, respectively. In both USGS MACS-3 and USGS BCR-2G magnesium concentrations agree well with reference values (average difference is 8 % and 2 %, respectively). *Arctica islandica* shells have a relatively low magnesium concentration, compared to the reference materials (overall average for all LA-ICP-MS line scans: 66 ± 10 µg/g), but their titanium, vanadium and chromium content is even lower (BRS, unpublished data based on whole shell analysis via ICP-OES). Correspondingly, the interfering ion / magnesium ratio is low (e.g. titanium-to-magnesium ratio = 0.35). We therefore suggest that the magnesium concentrations of the analyzed shells were unaffected by interference. Surface contamination of NIST SRM 610 with magnesium should have been avoided by the pre-ablation we performed before each line scan on the reference material. However, we recommend further testing magnesium analysis of NIST SRM 610 performed via quadrupole instruments.

LA-ICP-MS precision is evaluated from the relative standard deviations (RSDs) determined for the quality control materials. Average RSDs for USGS MACS-3 range from 6 to 12 %, from 2 to 4 % for USGS BCR-2G, and from 3 to 4 % for NIST SRM 610 (the corresponding standard deviations are given in Table 2). For USGS MACS-3, RSDs were lower at JGU than at MPIC (Table 2), which is probably associated with the use of a lower laser wavelength JGU (193 nm at JGU, 213 nm at MPIC; see Jochum et al., 2007, 2012).

For most trace elements the mean intensities of shell samples analysed in sequences 1, 2 and MPIC are generally well above the background intensities and detection limits (= three times the standard deviation of the background; Sinclair et al., 1998); as an exception, the mean manganese concentration of specimen ICE12-14-01 AL, analyzed during sequence 1, was below the detection limit (Supplementary Materials, Tables S1a and S1b). Sequence 0 was performed directly after a ca. 2 week period of instrumental non-use and background intensities for all line scans attained during this sequence were on average 8-times higher compared to sequence 2. Correspondingly, detection limits were relatively high during sequence 0, and exceeded the mean sample concentration in the cases of magnesium and manganese (Supplementary Materials, Tables S1a and S1b). Also, we observed a drift in the relative sensitivity factors (RSFs) of sodium and barium for the NIST SRM 612 analyzed during sequence 0 (the first three NIST SRM 612 were 9 % lower and ca. 25 % higher, respectively, with respect to the mean of the remaining eighteen NIST SRM 612). To account for this, we performed a batch-wise calibration, using the mean RSF of the twenty-one NIST SRM 612 for the first *A. islandica* sample (specimen 0525475) measured in the sequence and the first three measurements on quality control materials; the remaining *A. islandica* samples and quality control materials were calibrated with

the mean RSF of the remaining eighteen NIST SRM 612 (Supplementary Materials, Tables S1a and S1b). Despite varying instrumental conditions among sequences, the results for reference materials, excluding magnesium of NIST SRM 610 (see above), agree with those reported in previous studies (e.g. Mertz-Kraus, 2009; Jochum et al., 2012). We therefore conclude that element concentrations of *A. islandica* samples are accurate considering instrumental uncertainties.

Due to instrumental variability, however, mean element concentrations of line scan no. 1 of each specimen are typically offset from those of line scan no. 2, because each line scan was performed during a different sequence, i.e., on a different measurement day (see Table 1; Figs. 3-7). LA-ICP-MS accuracy and precision can change from one day of measurement to another (compare Sinclair et al., 2011). The present study does not compare absolute concentrations among different line scans. Instead, it was tested whether variations in trace element time-series (i.e., characteristic peaks and troughs) can be reproduced from one line scan to another, despite any instrumental variability, assuming that the reproducible part of each trace element time-series may result from an external (potentially environmental) control.

References for supplementary materials

Jochum, K.P., Stoll, B., Herwig, K. and Willbold, M., Validation of LA-ICP-MS trace element analysis of geological glasses using a new solid-state 193 nm Nd:YAG laser and matrix-matched calibration, J. Anal. At. Spectrom. 22, 2007, 112, doi:10.1039/b609547j.

Jochum, K.P., Scholz, D., Stoll, B., Weis, U., Wilson, S. A., Yang, Q., Schwalb, A., Börner, N., Jacob, D.E. and Andreae, M.O., Accurate trace element analysis of speleothems and biogenic calcium carbonates by LA-ICP-MS, Chem. Geol. 318–319, 2012, 31–44, doi:10.1016/j.chemgeo.2012.05.009.

Mertz-Kraus, R., Brachert, T.C., Jochum, K.P., Reuter, M. and Stoll, B., LA-ICP-MS analyses on coral growth increments reveal heavy winter rain in the Eastern Mediterranean at 9 Ma, Palaeogeogr. Palaeoclimatol. Palaeoecol. 273, 2009, 25–40, doi:10.1016/j.palaeo.2008.11.015.

Sinclair, D.J., Kinsley, L.P.J. and McCulloch, M.T., High resolution analysis of trace elements in corals by laser ablation ICP-MS, Geochim. Cosmochim. Acta 62, 1998, 1889–1901.

Sinclair, D.J., Williams, B., Allard, G., Ghaleb, B., Fallon, S., Ross, S.W. and Risk, M., Reproducibility of trace element profiles in a specimen of the deep-water bamboo coral Keratoisis sp., Geochim. Cosmochim. Acta 75, 2011, 5101–5121. doi:10.1016/j.gca.2011.05.012.

Thomas, R., Practical Guide to ICP-MS, In: A Tutorial for Beginners, third ed., 2013, CRC Press, (441 pp).

Table S1a. Table S1a. Supplementary data. For each LA-ICP-MS line scan average values and standard deviations (± 1 σ) of following variables were determined for the trace elements sodium, magnesium, manganese, strontium and barium: (1) Background signal intensities (in counts per second, CPS); (2) signal intensities (in CPS) of bivalve shells were converted into (3) trace element concentrations (in µg/g; details given in the text, section 2.3.3). (4) Limits of detection (in µg/g) are presented for each specimen. Table S1a presents data corresponding to the first LA-ICP-MS line scan performed during sequence 0 in cases of specimens from the Isle of Man and the Gulf of Maine, and during sequence 1 in the case of the Icelandic shell. Data of the second (replicate) line scan performed in each shell are displayed in Table S1b.

Line scan no. 1

(1) Background signal intensities [CPS]

Locality	Sample ID	Na	Mg	Mn	Sr	Ba
Isle of Man	0505319	1621967.0 ± 29806.0	636.8 ± 223.2	4658.4 ± 714.6	69.1 ± 81.5	75.0 ± 93.6
	0505327	1437530.3 ± 24075.2	569.1 ± 228.7	5429.4 ± 870.8	161.8 ± 132.7	94.1 ± 103.5
	0525475	1994425.8 ± 33303.5	567.7 ± 271.8	3597.7 ± 638.8	98.5 ± 101.5	64.7 ± 100.4
Gulf of Maine	090797	1336189.7 ± 24922.9	542.7 ± 276.1	6219.5 ± 851.5	100.0 ± 113.3	95.6 ± 102.8
	090803	1369066.1 ± 24300.7	529.4 ± 266.0	5672.1 ± 771.0	89.7 ± 105.3	80.9 ± 104.0
	090829	1308546.1 ± 24384.2	544.1 ± 270.1	6441.7 ± 848.0	100.0 ± 105.1	88.2 ± 104.4
Iceland	ICE12-14-01 AL	289515.3 ± 6677.6	310.3 ± 114.2	2372.7 ± 331.4	5781.6 ± 375.7	98.4 ± 80.4

Line scan no. 1

(2) Signal intensities of bivalve shells [CPS]

Locality	Sample ID	Na	Mg	Mn	Sr	Ba
Isle of Man	0505319	2301423.1 ± 229064.4	1342.3 ± 516.6	5583.3 ± 1217.6	244224.7 ± 78786.0	532.8 ± 650.5
	0505327	2059203.6 ± 204270.3	1415.0 ± 689.9	5604.2 ± 956.6	207611.4 ± 68575.8	432.3 ± 433.2
	0525475	2257080.6 ± 143692.4	1163.9 ± 453.0	4267.0 ± 854.3	231669.1 ± 97002.5	462.2 ± 430.0
Gulf of Maine	090797	1907707.3 ± 297445.3	1211.9 ± 3426.8	6835.9 ± 1195.7	140791.1 ± 54831.5	234.9 ± 342.3
	090803	2138962.1 ± 185121.9	1333.2 ± 547.6	6755.2 ± 1141.1	181436.9 ± 47862.2	301.2 ± 434.9
	090829	1866598.8 ± 210859.8	1324.8 ± 1356.7	8154.8 ± 7812.2	146134.9 ± 62283.3	333.0 ± 718.1
Iceland	ICE12-14-01 AL	23767019.8 ± 3339207.7	24398.3 ± 12670.4	5699.3 ± 7416.1	1090098.7 ± 267096.6	5215.9 ± 4591.6

Table S1a continued.

Line scan no. 1

(3) Trace element concentrations of bivalve shells [µg/g]

Locality	Sample ID	Na	Mg	Mn	Sr	Ba
Isle of Man	0505319	4244.3 ± 1716.6	58.0 ± 46.5	4.3 ± 6.1	979.8 ± 416.4	10.6 ± 14.9
	0505327	4512.4 ± 1582.5	76.8 ± 73.8	2.4 ± 6.2	940.3 ± 358.6	10.4 ± 15.9
	0525475	2237.6 ± 1333.1	69.5 ± 58.4	4.1 ± 5.8	1277.4 ± 735.3	13.2 ± 15.0
Gulf of Maine	090797	4851.7 ± 1795.5	69.8 ± 136.4	4.1 ± 7.9	761.8 ± 320.9	4.5 ± 10.8
	090803	4977.3 ± 1542.9	68.3 ± 49.9	5.4 ± 6.0	749.1 ± 258.4	5.6 ± 12.6
	090829	4694.7 ± 1882.2	81.1 ± 119.7	9.4 ± 33.6	770.4 ± 294.2	7.4 ± 17.4
Iceland	ICE12-14-01 AL	3850.2 ± 536.9	62.5 ± 101.0	0.6 ± 1.6	864.5 ± 254.6	3.0 ± 2.8

Line scan no. 1

(4) Limits of detection [µg/g]

Locality	Sample ID	Na	Mg	Mn	Sr	Ba
Isle of Man	0505319	535.0	52.4	9.6	0.9	5.7
	0505327	511.2	63.5	13.8	1.7	7.5
	0525475	819.2	87.4	11.7	1.5	8.4
Gulf of Maine	090797	619.3	89.7	15.8	1.7	8.7
	090803	460.9	66.0	10.9	1.2	6.7
	090829	595.2	86.2	15.4	1.5	8.7
Iceland	ICE12-14-01 AL	3.3	0.8	0.2	0.9	0.1

Table S1b. Average data (± 1 σ) of replicate line scans performed in each shell during the LA-ICP-MS sequence 2 (specimens from the Isle of Man and the Gulf of Maine) and during sequence 'MPIC' (Icelandic specimen). The (1) background signal intensities (in counts per second, CPS), (2) signal intensities (in CPS) of bivalve shells, (3) trace element concentrations of shells (in µg/g), and (4) limits of detection (in µg/g) are given for five trace elements (Na, Mg, Mn, Sr, and Ba).

Line scan no. 2

(1) Background signal intensities [CPS]

Locality	Sample ID	Na	Mg	Mn	Sr	Ba
Isle of Man	0505319	290559.9 ± 7343.7	80.9 ± 85.1	1413.3 ± 419.0	16.2 ± 37.1	2.9 ± 17.0
	0505327	267844.6 ± 6492.0	51.5 ± 68.0	1819.3 ± 442.3	14.7 ± 43.2	7.4 ± 31.5
	0525475	274935.5 ± 8449.6	42.6 ± 65.4	1558.9 ± 375.9	266.3 ± 1395.7	4.4 ± 20.7
Gulf of Maine	090797	254476.6 ± 7603.9	64.7 ± 70.7	1984.0 ± 507.0	4.4 ± 20.7	8.8 ± 28.6
	090803	264499.5 ± 8370.5	66.2 ± 70.4	1962.0 ± 476.7	10.3 ± 30.6	7.4 ± 26.3
	090829	252042.9 ± 6579.8	72.1 ± 78.9	2122.3 ± 510.3	35.3 ± 174.3	4.4 ± 27.0
Iceland	ICE12-14-01 AL	204184.5 ± 5701.1	64.7 ± 72.8	1909.0 ± 469.0	11.8 ± 36.8	4.4 ± 20.7

Line scan no. 2

(2) Element signal intensity of bivalve shells [CPS]

Locality	Sample ID	Na	Mg	Mn	Sr	Ba
Isle of Man	0505319	6202832.4 ± 1590136.6	5534.2 ± 44082.3	7088.3 ± 12698.7	1257497.7 ± 336353.9	2579.7 ± 3356.6
	0505327	5844854.8 ± 3059371.7	5878.7 ± 13906.2	5904.1 ± 5947.1	1099019.6 ± 367834.9	2490.7 ± 3981.7
	0525475	5465015.6 ± 1621521.6	5024.0 ± 6009.0	5298.2 ± 11589.0	1385408.9 ± 548444.0	2515.1 ± 2555.5
Gulf of Maine	090797	5544645.1 ± 23540130.0	4978.5 ± 22724.7	6668.6 ± 34314.3	682285.4 ± 194326.9	981.0 ± 4906.8
	090803	5694745.9 ± 1771055.2	5397.7 ± 41293.5	7063.5 ± 4806.0	803810.3 ± 196442.0	1085.5 ± 2358.8
	090829	5546312.6 ± 2666847.5	5946.1 ± 17947.9	7890.5 ± 14675.5	768804.7 ± 278585.6	1349.9 ± 3010.0
Iceland	ICE12-14-01 AL	3277258.2 ± 594300.8	2587.4 ± 1548.7	2256.1 ± 684.8	612598.4 ± 162024.1	386.6 ± 473.0

Table S1b continued.

Line scan no. 2

(3) Trace element concentrations of bivalve shells [µg/g]

Locality	Sample ID	Na	Mg	Mn	Sr	Ba
Isle of Man	0505319	5014.5 ± 1544.5	68.9 ± 558.2	5.4 ± 9.1	1078.7 ± 337.2	11.2 ± 14.1
	0505327	5143.9 ± 2337.8	80.0 ± 179.0	4.3 ± 6.5	1023.7 ± 325.5	11.6 ± 17.9
	0525475	4651.8 ± 1658.7	66.2 ± 73.5	3.9 ± 12.5	1254.2 ± 518.5	11.8 ± 11.9
Gulf of Maine	090797	5652.0 ± 22737.9	78.3 ± 389.3	5.6 ± 40.0	743.4 ± 205.3	5.2 ± 20.7
	090803	5228.0 ± 1739.5	76.1 ± 622.7	5.6 ± 5.0	779.9 ± 200.1	5.3 ± 11.1
	090829	5093.5 ± 2087.2	74.9 ± 227.2	6.2 ± 7.9	761.1 ± 220.8	6.8 ± 14.8
Iceland	ICE12-14-01 AL	4463.8 ± 1007.4	57.2 ± 39.0	0.6 ± 1.2	842.7 ± 284.9	2.4 ± 3.1

Line scan no. 2

(4) Limit of detection Corrected concentration [µg/g]

Locality	Sample ID	Na	Mg	Mn	Sr	Ba
Isle of Man	0505319	18.2	3.1	1.2	0.1	0.2
	0505327	17.7	2.8	1.4	0.1	0.4
	0525475	22.3	2.6	1.1	3.7	0.3
Gulf of Maine	090797	24.2	3.4	1.9	0.1	0.5
	090803	23.8	3.0	1.6	0.1	0.4
	090829	19.0	3.4	1.7	0.5	0.4
Iceland	ICE12-14-01 AL	24.4	4.7	2.3	0.1	0.4

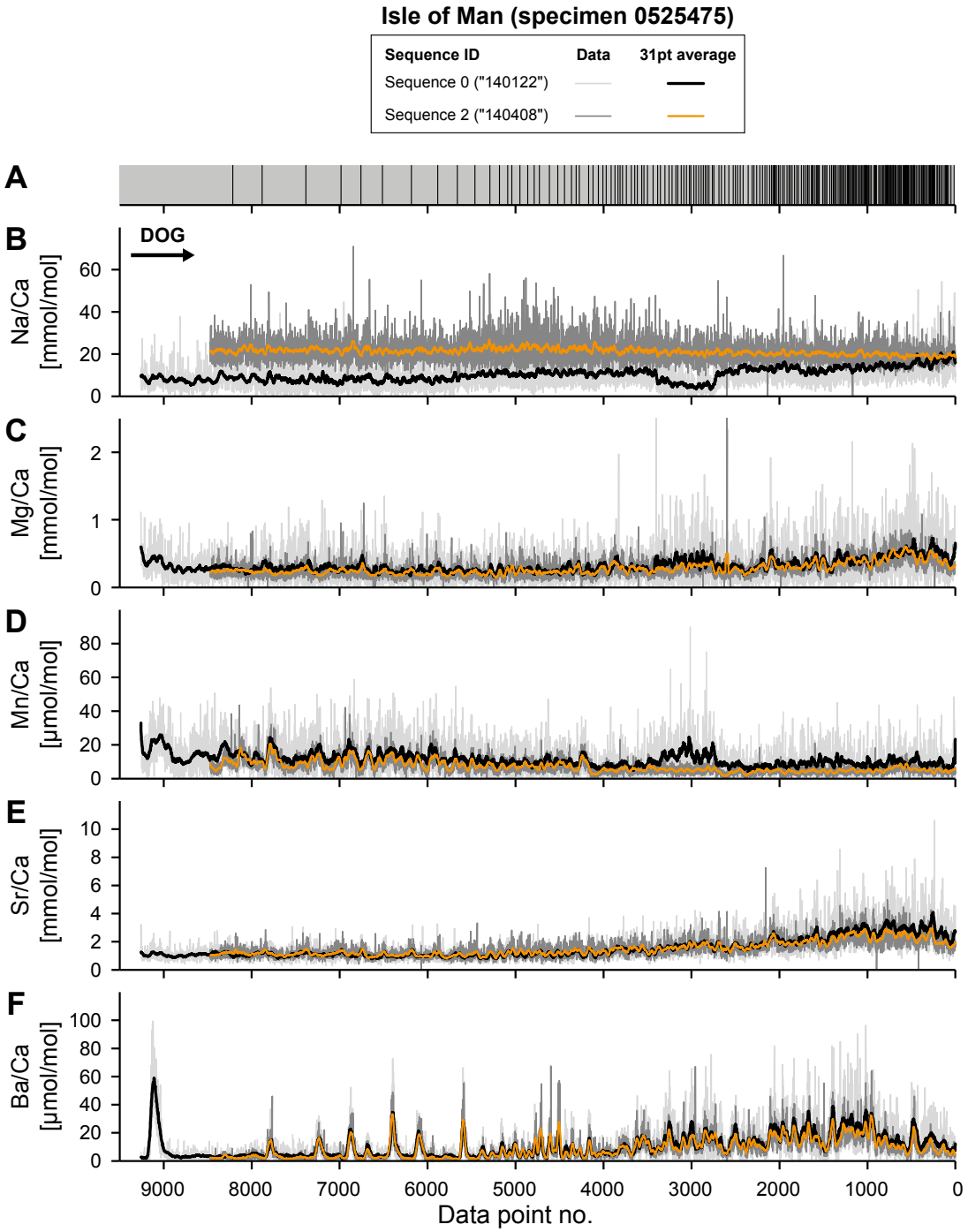

Fig. S1. Shell growth pattern and trace element time-series of specimen 0525475 from the Isle of Man. (A) Annual growth lines intersected by the LA-ICP-MS line scan are displayed as vertical black bars. Time-series of (B) Na/Ca, (C) Mg/Ca, (D) Mn/Ca, (E) Sr/Ca, and (F) Ba/Ca ratios were determined for two replicate LA-ICP-MS line scans running opposite to the direction of growth (DOG). Non-averaged trace element time-series are displayed as light grey and dark grey lines (sequences 0 and 2, respectively), and 31-pt running data averages are shown in black and orange (sequences 0 and 2, respectively). Please note that ca. between data points no. 2500 and 3500, Na/Ca ratios markedly decrease, while Mg/Ca and Mn/Ca ratios increase and that lower Na/Ca ratios were determined during sequence 0.

Chapter 3
Synthesis

3.1 Executive summary of manuscript I

The first study demonstrated (1) that shell growth is synchronized among *A. islandica* specimens from shallow (ca. 9–23 m), non-polluted waters off northeastern Iceland. Relative shell growth patterns of 16 individuals were combined to a master chronology which covered the time interval from 1835 to 2012. The chronology was statistically robust when the sample depth was ≥ 4. Accordingly, the expressed population signal, EPS, was ≥ 0.85 between 1885 and 2012. (2) Up to 43% of the variation in relative shell growth was explained by changes in sea surface temperature (SST) during parts of the growing season (February to September). Generally, shell growth was not related to sea surface salinity, but during the so-called Great Salinity Anomaly (ca. 1965 – 1975), SSS, SST and relative shell growth were reduced. (3) The coherency of growth among individuals as well as the strength of the correlation between shell growth and SST varied over time. Prior to ca. 1920 and after ca. 1960, environmental conditions varied strongly from one year to the next. Concomitantly, (a) relative annual shell growth differed markedly between years and (b) was highly synchronized among coeval specimens. Furthermore, (c) shell growth patterns (i.e., the composite chronology indices) displayed a high running similarity with SST. Between ca. 1920 and 1960 as well as after ca. 1990, by contrast, environmental conditions were rather stable and (d) shell growth was less synchronized among individual shells (the inter-series correlation fell below 0.4) and consequently (e) the composite chronology contained merely a weak common (environmental) signal and was only weakly correlated to ambient SST.

(4) Actually, the factors which likely govern bivalve shell growth, i.e., food availability and quality as well as seawater temperature and/or salinity, are positively related to each other on the North Icelandic Shelf, because they are controlled by two surface water masses. The warm, saline and nutrient-rich Atlantic water mass, the Irminger Current (IC), promotes primary productivity at the study site – directly by introducing nutrients, and indirectly by decreasing the density difference between bottom and surface waters, which in turn, reduces stratification and allows for wind-driven replenishment of nutrients to surface waters. The cooler, fresher and nutrient-deficient Polar or Arctic water mass carried towards Iceland by the East Icelandic Current (EIC), by contrast, has a negative influence on the local primary productivity because it also supports stratification. Alternating dominance of the IC and the EIC potentially synchronizes annual shell growth, because conditions change from favorable (warm and nutrient-rich) to 'hostile' (cold and nutrient-poor) between years. Probably, a certain amount of inter-annual environmental variability is required to increase the coherence of shell growth within a population (compare also Butler et al., 2013).

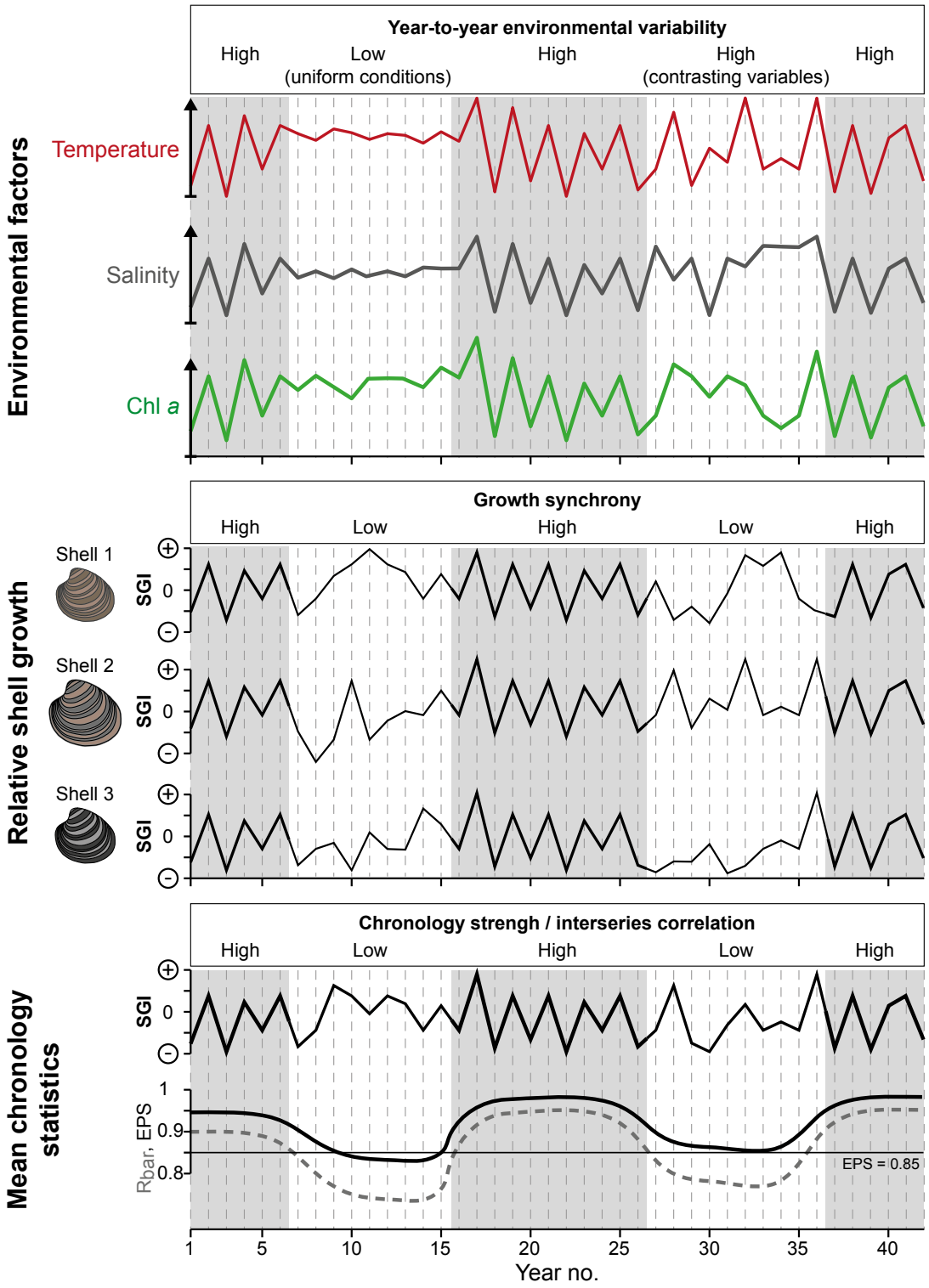

Fig. 1. Synthesis figure for manuscript I. When environmental factors, which may influence bivalve shell growth (i.e., seawater temperature, salinity and food quantity (inferred from the chlorophyll *a* concentration of the seawater), strongly vary from year-to-year, shell growth of individuals is synchronized and the chronology shows a high inter-series correlation (R_{bar}), and a strong common signal (i.e., a high expressed population signal, EPS). Time periods during which environmental conditions are rather uniform, by contrast, (i.e., the amplitude of environmental change is comparatively low from one year to the other), shell growth is less synchronized between individuals from the same habitat. Probably, shell growth is also de-synchronized when different environmental drivers of shell growth run into opposite directions and/or reach values beyond the tolerance levels of the studied bivalve species (e.g., temperature is too high, food levels too low etc.).

When only one current dominates the study locality over a relatively long, coherent time interval (i.e., the IC: 1920-1960, after 1990), bivalve shell growth is less synchronized by environmental cues. Instead, biological factors (e.g., fitness, predation stress) probably exert a stronger influence on shell growth. (5) Consequently, the composite chronology contains less common signal when environmental conditions are rather uniform. Therefore, variations in relative shell growth of *A. islandica* cannot serve as an independent proxy for seawater temperature (or other environmental factors). Further geochemical analysis may help to extract environmental information from *A. islandica* shells and can potentially provide information on the drivers of shell growth.

3.2 Executive summary of manuscript II

As shown by the second manuscript, (1) mature and ontogenetically old (ca. 50 to 251 years) specimens of *A. islandica* display similar characteristics in Ba/Ca shell time-series as short-lived bivalve species or ontogenetically young specimens of long-lived species, i.e., flat and low background values and sharp, erratic Ba/Ca maxima. (2) Ba/Ca peaks occurred at different times of the growing season and were detected in specimens from different habitats, e.g., deeper (ca. 80 m, Gulf of Maine) and shallow waters (shallowest: ca. 10 m, Iceland) or fjord-sites (Faroe Islands). Yet, (3) shells from different sites varied in terms of average Ba/Ca ratios, which may indicate that the amount of bioavailable barium differed between habitats (with higher shell Ba/Ca ratios in specimens from the Isle of Man and the Faroe Islands, and lower ratios from shells from the Gulf of Maine and Iceland).

LA-ICP-MS sampling resolution decreased as growth increments became narrower with increasing age. Therefore, (4) some ontogenetically older specimens displayed more elevated background Ba/Ca ratios and/or attenuated or broader Ba/Ca maxima with age. (5) The Ba/Ca maxima displayed no clear relationship with shell growth rates or certain growth patterns and shell microstructures (e.g., growth lines), and therefore, (6) Ba/Ca ratios were synchronized between coeval specimens from the same locality, even if shells differed in terms of ontogenetic age and/or shell growth pattern (see also section 6.3). (7) Annual Ba/Ca ratios were even more synchronous among specimens of a population than subseasonally resolved Ba/Ca time-series. (8) The correlation between annual Ba/Ca time-series and the strength of the common signal (R_{bar} and EPS, respectively) were higher and more stable through time than corresponding statistics of increment-width time-series. Therefore, annually averaged (and subseasonally resolved) Ba/Ca ratios may help to double-check if shells with overlapping lifespans were correctly crossdated, especially if shell growth patterns

were difficult to identify (e.g., if disturbance lines were present; see also manuscript I, section 6.1). Furthermore, (9) annual Ba/Ca ratios of Icelandic specimens were elevated contemporaneously with remotely sensed Chl *a* levels (in the 1980s). At the other studied localities, the increase of Ba/Ca in shells either lagged behind the Chl *a* maximum of the 1980s (Faroe Islands, Isle of Man), or were unrelated to surface water Chl *a* (Gulf of Maine). Future calibration studies should use long, coherent, highly-resolved environmental and geochemical data sets. Especially, the barium content of the ambient water and at the sediment-water-interface should be observed over long time intervals to fully unravel the reasons for Ba/Ca peaks in marine bivalve shells.

3.3 Executive summary of manuscript III

Long-term, highly resolved environmental data sets are mandatory for studies aiming to calibrate a geochemical or physical proxy. As shown in manuscripts I and II, environmental data are not always readily available for certain localities and/or time periods. The third study presents an alternative approach – other than calibration work – for assessing whether any environmental and/or biological information is encoded in the element-to-calcium ratios of *A. islandica* shells. This test is not only confided to the studied bivalve species, but applicable to other (biogenic or non-biogenic) climate archives. The main assumption of the third manuscript is that any external signal within the time-series should be reproducible within and between co-occurring specimens from the same population, while noise should be random and irreproducible (compare Sinclair et al., 1998, 2005, 2011). The study used LA-ICP-MS analysis in line scan mode to explore Na/Ca, Mg/Ca, Mn/Ca, Sr/Ca, and Ba/Ca ratios in *A. islandica* shells from different sites, which displayed varying shell growth patterns and ontogenetic ages.

Apparently, (1) element-to-calcium ratios displayed 'ontogenetic' trends, which were probably caused by changes in the sampling resolution. Shell growth increments became narrower with increasing ontogenetic age and/or in time intervals during which unfavorable environmental conditions made shell growth difficult. The spot size of the laser, by contrast, is invariant. This had two effects. (a) Mg/Ca and Sr/Ca ratios, which typically reached maxima at or close to annual growth lines, increased at shell portions with narrow increments (e.g., in ontogenetically older parts of the shells of specimens from the Isle of Man). (b) Maximum Na/Ca and Mn/Ca ratios, by contrast, were usually detected in the broadest increments (= during youth), which offered the highest sampling resolution (i.e., for these elements the measured signal is 'smeared' in parts of the shell which displayed narrow increments). The same finding was reported for Ba/Ca in manuscript II (see above). 'Signal smearing' probably reduces maximum

peak heights in Na/Ca, Mn/Ca and Ba/Ca time-series in ontogenetically older parts of the hinge or where shell growth is reduced due to adverse environmental conditions. In addition, Mn/Ca ratios declined exponentially through the first years of growth. Whether or not this trend is a genuine ontogenetic effect (i.e., caused by changes in the bivalve metabolism) has to be tested in further studies.

Moreover, the third study demonstrated that the degree to which element time-series were reproducible within and among coeval shells varied for different element-to-calcium ratios. (2) Ba/Ca time-series were almost perfectly reproducible within each specimen (only a small amount of noise was found, i.e., r^2-values deviated only slightly from 1; average r^2 for Ba/Ca was 0.95 ± 0.04; $p < 0.001$), as well as between shells (see manuscript II), which strongly implies that Ba/Ca ratios of bivalve shells contain a strong environmental signal. (3) Mg/Ca and Sr/Ca time-series were well-reproducible within specimens, because these element-to-calcium ratios are strongly associated with shell growth patterns (average $r^2 = 0.82 \pm 0.27$ and 0.83 ± 0.18, respectively; $p < 0.002$). Therefore, maxima of Mg/Ca and Sr/Ca time-series were also synchronized between coeval *A. islandica* from the same habitat which resembled each other in terms of (a) ontogenetic age and (b) shell growth pattern, i.e., which offered a similar spatial (and hence temporal) resolution for LA-ICP-MS analysis. The means and amplitudes of the Mg/Ca and Sr/Ca time-series, however, differed between coeval specimens from the same locality, which indicates that these element-to-calcium ratios cannot be readily used as environmental proxies, at least when studied via LA-ICP-MS and in the hinge area of the shell of ontogenetically older specimens. Instead, the Mg/Ca and Sr/Ca ratios are indicators of shell growth patterns, when following the methodology and spatial resolution employed in the third manuscript.

(4) The Mn/Ca ratios of *A. islandica* shells were close to the LA-ICP-MS detection limits, which may explain that the intra-specimen reproducibility is lower than that for Mg/Ca and Sr/Ca time-series (average r^2 for Mn/Ca = 0.74 ± 0.23; $p < 0.001$). Although this element may be an environmental tracer in other bivalve species, there was no temporally consistent synchrony in Mn/Ca time-series among coeval shells. (5) Na/Ca time-series were mainly irreproducible within *A. islandica* specimens (average $r^2 = 0.22 \pm 0.04$; $p < 0.001$). The synchrony of Na/Ca time-series between coeval shells from the same habitat was low. Over certain time intervals, Na/Ca time-series of different individuals appeared to be synchronous. However, this was most probably related to Na/Ca being related to similar shell growth patterns between specimens.

The results of the third manuscript should be considered for improving the interpretation of element-to-calcium time-series in biogenic (or non-biogenic) climate archives such as bivalve shells. When trace elements (or other potential geochemical proxies) are determined via LA-ICP-MS (or other techniques), the reproducibility of the geochemical time-series should be tested within and between coeval samples from the same locality. The spatial sampling resolution should be improved (e.g., by analyzing the margin of the shell in the case of bivalve specimens and/or by using rectangular shaped laser spots; see Warter and Müller, 2017). Further studies on biomineralization and calibration work will provide further insights on the environmental (and biological) controls dictating the trace element geochemistry of (biogenic) climate recorders.

Chapter 4
Conclusions

4.1 Conclusions on trace elements drawn from other proxy archives

Each (new or established) geochemical proxy measured in a biogenic material (e.g., a bivalve shell) has to be thoroughly tested. It has to be clear, if any relationship between the proxy and an environmental parameter is direct (e.g., thermodynamically controlled) or indirect (i.e., the environment controls biological factor(s) which then dictate the geochemistry of the hard part; Fig. 2). Although scleractinian corals and bivalves likely differ in terms of biomineralization mechanisms with which they accrete their skeletal material (Weiner and Dove, 2003), this section will outline some critical findings on trace elements from coral skeletons and bivalve shells. It is known from shallow-water corals (such as *Porites* sp.) or the bivalve *Tridacna* sp. – organisms living in photosymbiosis with algae – that trace element signals in coral skeletons and bivalve shells, respectively, vary in accord with ambient temperature or the daily light cycle (*Tridacna*: e.g. Elliot et al., 2009; Sano et al., 2012). In cold-water corals (living without photosymbionts) or bivalve species other than Tridacna sp., the relationship between the trace element concentration of skeletal materials and environmental parameters is usually not that clear. Studies comparing the element-to-calcium ratios in both corals and bivalves to environmental parameters report controversial results (see section 2; manuscripts II and III), whereas certain element-to-element ratios (e.g. Mg/Li, Li/Mg, Sr/Li) determined in corals or bivalve shells hold some promising data (Case et al., 2010; Montagna et al., 2014; Füllenbach et al., 2015).

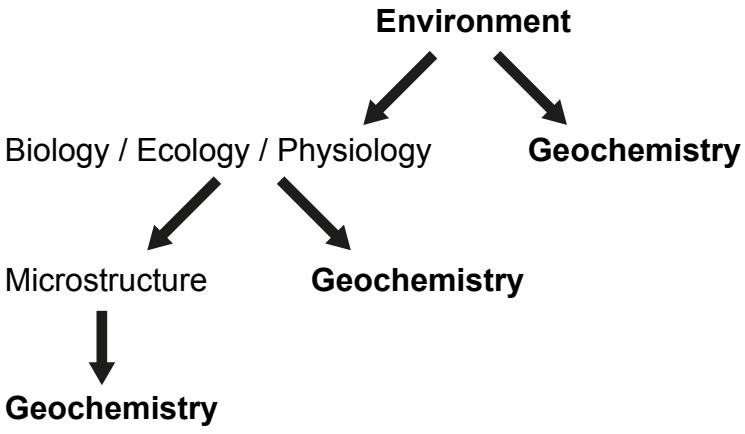

Fig. 1. In summary the geochemistry of a climate archive (e.g., a bivalve shell) is influenced (a) directly by one/many environmental driving factor(s), (b) by biological / metabolic processes that are, in turn, controlled by the environment, (c) by measurable changes in the microstructure of the material which again is determined by biological factors that can be related to environmental changes.

Al-Horani et al. (2003) demonstrated that the Ca^{2+} ion transport within photosynthetic corals was related to the daily light-cycle. Allison and Finch (2009) studied the skeleton of Porites corals and found relatively large changes in trace element concentrations on a sub-daily scale. Relating this to Al-Horani's findings, Allison and Finch (2009) supposed that not only the transport rates of Ca^{2+}, but also that of other ions (e.g. Sr^{2+} or Mg^{2+}) could change during the course of a day. Putting together the lines of evidence, it is possible that the variations of trace elements within a coral skeleton and/or bivalve shell may vary along with (1) ion transport rates which, in turn, control and/or co-vary with (2) metabolic activity and/or (3) skeletal expansion (i.e. skeletal growth) rates or other biologic parameters. Assuming that changes in ion transport run parallel to both the daily light and the daily temperature cycles, then it appears plausible that the concentrations of trace elements within the skeleton of photosymbiotic corals or photosymbiotic bivalves is correlated to the ambient temperature and/or light signal. In fact, even $\delta^{18}O$ is not easily to interpret in case of cold-water corals which usually dwell in habitats which are stable / uniform with respect to environmental conditions (e.g. low temperature variability throughout the year; Smith et al., 2000; Adkins et al., 2003; Marali et al., 2013).

However, for different localities different calibration equations exist which relate, for example, photosynthetic coral Sr/Ca ratios to ambient seawater temperature. Even within the same reef Sr/Ca vs. temperature calibrations can change (Alpert et al., 2016). Furthermore, Mg/Ca ratios of Porites corals are not always correlated to ambient sea surface temperature (Fallon et al., 2003). It thus appears that the relationship between (1) trace element content, (2) biological factors (ion transport rates / skeletal expansion rates etc.), and (3) environmental parameters can also vary between coral specimens and/or locality. This implies that relationship between trace element variations and environmental variables is indirect. Trace element incorporation likely depends on biological processes, which are influenced by both environmental and physiological parameters.

4.2 Future research needs

For the above mentioned reasons, future studies should (re-) evaluate if a proxy can be used as an environmental tracer under both highly variable and low-variable environmental conditions, e.g. testing the sensitivity of the proxy, potentially during the course of any calibration study. The latter could be performed with the same or different (bivalve) species to check if environmental signals are coherent between species. For example, shells (of the same species) could be examined along

depth and/or latitudinal gradients to test the spatial coherency of environmental signals encoded in shell growth rates or geochemical proxies (such as major and trace elements). Sampling shells of the same species along a depth gradient, along which also the degree of environmental variability changes, may help to detect 'threshold conditions' below which certain proxies are not tracing environmental changes, but reflect biological factors (i.e., vital effects). Further, geochemical analysis will benefit from an improved sampling resolution in order to overcome "the curse of physiology" in bivalve shells (Schöne, 2008), i.e., a decreasing sampling resolution when increments become narrower with increasing ontogenetic age. During LA-ICP-MS analysis, for example, new methodologies such as rectangular spots (Warter and Müller, 2017) can be used or ontogenetically younger (parts of) shells can be analyzed (compare also Schöne et al., 2004). Finally, "To be able to use the environmental information provided by proxy elements to their full potential it is critical to understand the mechanisms behind the uptake and storage in the biomineral" (Soldati et al., 2016, p. 6).

Chapter 5
References

Abbott, R.T., 1954. American Seashells. New York, Van Nostrand. doi:10.1017/CBO9781107415324.004.

Abele, D., Kruppe, M., Philipp, E.E.R., Brey, T., 2010. Mantle cavity water oxygen partial pressure (PO2) in marine molluscs aligns with lifestyle. Can. J. Fish. Aquat. Sci. 67, 977–986. doi:10.1139/F10-035.

Abele, D., Strahl, J., Brey, T., Philipp, E.E.R., 2008. Imperceptible senescence: ageing in the ocean quahog *Arctica islandica*. Free Radic. Res. 42, 474–480. doi:10.1080/10715760802108849.

Adkins, J., Boyle, E.A., Curry, W.B., Lutringer, A., 2003. Stable isotopes in deep-sea corals and a new mechanism for "vital effects." Geochim. Cosmochim. Acta 67, 1129–1143. doi:10.1016/S0016-7037(00)01203-6.

Al-Horani, F.A., Al-Moghrabi, S.M., de Beer, D., 2003. The mechanism of calcification and its relation to photosynthesis and respiration in the scleractinian coral *Galaxea fascicularis*. Mar. Biol. 142, 419–426. doi:10.1007/s00227-002-0981-8.

Allison, N., Finch, A.A., 2009. Reproducibility of minor and trace element determinations in Porites coral skeletons by secondary ion mass spectrometry. Geochemistry, Geophys. Geosystems 10. doi:10.1029/2008GC002239.

Alpert, A.E., Cohen, A.L., Oppo, D.W., Decarlo, T.M., Jamison, M., Young, C.W., 2016. Comparison of equatorial Pacific sea surface variability and trends with Sr/Ca records from multiple corals. Paleoceanography 31, 1–14. doi:10.1002/2015PA002897.

Anagnostou, E., Sherrell, R.M., Gagnon, A., LaVigne, M., Field, M.P., McDonough, W.F., 2011. Seawater nutrient and carbonate ion concentrations recorded as P/Ca , Ba/Ca, and U/Ca in the deep-sea coral Desmophyllum dianthus. Geochim. Cosmochim. Acta 75, 2529–2543. doi:10.1016/j.gca.2011.02.019.

Arrhenius, S., 1896. On the influence of carbonic acid in the air upon the temperature of the ground. Philos. Mag. J. Sci. 41, 237–279.

Barats, A., Amouroux, D., Chauvaud, L., Pécheyran, C., Lorrain, A., Thébault, J., Church, T.M., Donard, O.F.X., 2009. High frequency barium profiles in shells of the Great Scallop *Pecten maximus*: A methodical long-term and multi-site survey in Western Europe. Biogeosciences 6, 157–170. doi:10.5194/bgd-5-3665-2008.

Barnett, T.P., Pierce, D.W., Schnur, R., 2001. Detection of anthropogenic climate change in the World's Oceans. Science 292, 270–274. doi:10.1126/science.1058304.

Bath, G.E., Thorrold, S.R., Jones, C.M., Campana, S.E., McLaren, J.W., Lam, J.W.H., 2000. Strontium and barium uptake in aragonitic otoliths of marine fish. Geochim. Cosmochim. Acta 64, 1705–1714. doi:10.1016/S0016-7037(99)00419-6.

Beck, J.W., Edwards, R.L., Ito, E., Taylor, F.W., Recy, J., Rougerie, F., Joannot, P., Henin, C., 1992. Sea-surface temperature from coral skeletal strontium/calcium ratios. Science 257, 644–647.

Begum, S., Basova, L., Strahl, J., Sukhotin, A., Heilmayer, O., Philipp, E., Brey, T., Abele, D., 2009. A metabolic model for the ocean quahog *Arctica islandica*–effects of animal mass and age, temperature, salinity, and geography on respiration rate. J. Shellfish Res. 28, 533–539. doi:10.2983/035.028.0315.

Begum, S., Basova, L., Heilmayer, O., Philipp, E.E.R., Abele, D., Brey, T., Wegener, A., Box, P.O., Petersburg, S., Nab, U., Centre, G.A., 2010. Growth and energy budget models of the bivalve *Arctica islandica* at six different sites in the northeast Atlantic realm. J. Shellfish Res. 29, 107–115.

Black, B. A., Boehlert, G.W., Yoklavich, M.M., 2008. Establishing climate-growth relationships for yelloweye rockfish (*Sebastes ruberrimus*) in the northeast Pacific using a dendrochronological approach. Fish. Oceanogr. 17, 368–379. doi:10.1111/j.1365-2419.2008.00484.x.

Blondeau-Patissier, D., Gower, J.F.R., Dekker, A.G., Phinn, S.R., Brando, V.E., 2014. A review of ocean color remote sensing methods and statistical techniques for the detection, mapping and analysis of phytoplankton blooms in coastal and open oceans. Prog. Oceanogr. 123, 123–144. doi:10.1016/j.pocean.2013.12.008.

Böhm, F., Joachimski, M, M., Lehnert, H., Retiner, J., 2002. Evidence for preindustrial variations in the marine surface water carbonate system from coralline sponges. Geochemistry Geophys. Geosystems 3, 1–13. doi:10.1029/2001GC000264.

Böhm, F., Joachimski, M.M., Dullo, W.-C., Eisenhauer, A., Lehnert, H., Reitner, J., Wörheide, G., 2000. Oxygen isotope fractionation in marine aragonite of coralline sponges. Geochim. Cosmochim. Acta 64, 1695–1703.

Bradley, R.S., 1999. Paleoclimatology. Reconstructing climates of the Quaternary, 2nd ed. Elsevier, Academic Press, International Geophysics Series, 68.

Bradley, R.S., Eddy, J.A., 1991. Records of past global changes. *In:* Global Changes of the Past (R.S. Bradley, ed.). Boulder: University Corporation for Atmospheric Research, 5-9.

Brayshaw, D.J., Hoskins, B.J., Blackburn, M., 2011. The basic ingredients of the North Atlantic storm track. Part II: Sea surface temperatures. J. Atmos. Sci. 68, 1784–1805. doi:10.1175/2011JAS3674.1.

Brey, T., Arntz, W., Pauly, D., Rumohr, H., 1990. *Arctica islandica* in Kiel Bay: Growth, production and ecological significance. J. Exp. Mar. Bio. Ecol. 136, 217–235.

Briffa, K.R., Jones, P.D., 1993. Global surface air temperature variations during the twentieth century: Part 2, implications for large-scale high-frequency paleoclimatic studies. The Holocene 3, 77–88.

Briffa, K.., Jones, P.D., Wigley, T.M.L., 1986. Climate reconstruction from tree rings: Part 2, spatial reconstruction of summer mean sea-level pressure patterns over Great Britain. J. Climatol. 6, 1–15.

Broecker, W.S., 1997. Thermohaline circulation, the Achilles heel of our climate system: Will man-made CO2 upset the climate balance? Science 278, 1582–1588.

Buddemeier, R.W., Maragos, J.E., Knutson, D.W., 1974. Radiographic studies of reef coral exoskeletons: Rates and patterns of coral growth. J. Exp. Mar. Bio. Ecol. 14, 179–200.

Büntgen, U., Tegel, W., Nicolussi, K., McCormick, M., Frank, D., Trouet, V., Kaplan, J.O., Herzig, F., Heussner, K.U., Wanner, H., Luterbacher, J., Esper, J., 2011. 2500 Years of European climate variability and human susceptibility. Science 331, 578–582. doi:10.1126/science.1197175.

Butler, P.G., Richardson, C. A., Scourse, J.D., Wanamaker, A.D., Shammon, T.M., Bennell, J.D., 2010. Marine climate in the Irish Sea: analysis of a 489-year marine master chronology derived from growth increments in the shell of the clam *Arctica islandica*. Quat. Sci. Rev. 29, 1614–1632. doi:10.1016/j.quascirev.2009.07.010.

Butler, P.G., Scourse, J.D., Richardson, C. A., Wanamaker, A.D., Bryant, C.L., Bennell, J.D., 2009. Continuous marine radiocarbon reservoir calibration and the 13C Suess effect in the Irish Sea: Results from the first multi-centennial shell-based marine master chronology. Earth Planet. Sci. Lett. 279, 230–241. doi:10.1016/j.epsl.2008.12.043.

Butler, P.G., Wanamaker, A.D., Scourse, J.D., Richardson, C. A., Reynolds, D.J., 2013. Variability of marine climate on the North Icelandic Shelf in a 1357-year proxy archive based on growth increments in the bivalve *Arctica islandica*. Palaeogeogr. Palaeoclimatol. Palaeoecol. 373, 141–151. doi:10.1016/j.palaeo.2012.01.016.

Caragnano, A., Basso, D., Jacob, D.E., Storz, D., Rodondi, G., Benzoni, F., Dutrieux, E., 2014. The coralline red alga Lithophyllum kotschyanum f. affine as proxy of climate variability in the Yemen coast, Gulf of Aden (NW Indian Ocean). Geochim. Cosmochim. Acta 124, 1–17. doi:10.1016/j.gca.2013.09.021.

Carré, M., Bentaleb, I., Bruguier, O., Ordinola, E., Barrett, N.T., Fontugne, M., 2006. Calcification rate influence on trace element concentrations in aragonitic bivalve shells: Evidences and mechanisms. Geochim. Cosmochim. Acta 70, 4906–4920. doi:10.1016/j.gca.2006.07.019.

Case, D.H., Robinson, L.F., Auro, M.E., Gagnon, A.C., 2010. Environmental and biological controls on Mg and Li in deep-sea scleractinian corals. Earth Planet. Sci. Lett. 300, 215–225. doi:10.1016/j.epsl.2010.09.029.

Casey, R., 1952. Some genera and subgenera, mainly new, of Mesozoic heterodont lamellibranchs. Proc. Malacol. Soc. London 29, 121.

Claussen, M., 2007. Introduction to climate forcing and climate feedbacks. *In:* Sirocko, F., Claussen, M., Goñi, M.F.S., Litt, T. (Eds.). The climate of past interglacials. Developments in Quaternary Sciences 7, 3–11. Doi:10.1016/S1571-0866(07)80026-1.

Cook, E.R., Kairiukstis, L.A. (Eds.), 1990. Methods of dendrochronology – Applications in the environmental sciences. Kluwer Academic Publishers, Dordrecht, Boston, London.

Dahlgren, T.G., Weinberg, J.R., Halanych, K.M., 2000. Phylogeography of the ocean quahog (*Arctica islandica*): influences of paleoclimate on genetic diversity and species range 137, 487–495.

Dansgaard, W., Clausen, H.B., Gundestrup, N., Hammer, C.U., Johnsen, S.F., Kristinsdottir, P.M., Reeh, N., 1982. A new Greenland deep ice core. Science 218, 1273–1277.

Dansgaard, W., Johnsen, S.J., Clausen, H.B., Gundestrup, D.D.N.S., Hammer, C.U., Hvidberg, C.S., Steffensen, J.P., Sveinbjërnsdottir, A.E., Jouzel, J.-, Bond, G., 1993. Evidence for general instability of past climate from a 250-kyr ice-core record. Nature 364, 218–220.

Davenport, C.B., 1938. Growth lines in fossil Pectens as indicators of past climates. J. Paleontol. 12, 514–515.

Dehairs, F., Chesselet, R., Jedwab, J., 1980. Discrete suspended particles of barite and the barium cycle in the open ocean. Earth Planet. Sci. Lett. 49, 528–550. doi:10.1016/0012-821X(80)90094-1.

DeLong, K.L., Quinn, T.M., Taylor, F.W., 2007. Reconstructing twentieth-century sea surface temperature variability in the southwest Pacific: A replication study using multiple coral Sr/Ca records from New Caledonia. Paleoceanography 22, 1–18. doi:10.1029/2007PA001444.

Deser, C., Blackmon, M.L., 1993. Surface Climate Variations over the North Atlantic Ocean during Winter: 1900–1989. J. Clim. 6, 1743–1753. doi:10.1175/1520-0442(1993)006<1743:SCVOTN>2.0.CO;2.

Dettman, D.L., Reische, A.K., Lohmann, K.C., 1999. Controls on the stable isotope composition of seasonal growth bands in aragonitic fresh-water bivalves (unionidae). Geochim. Cosmochim. Acta 63, 1049–1057. doi:10.1016/S0016-7037(99)00020-4.

Dickson, R., 2000. The "Great Salinity Anomaly" in the northern North Atlantic 1968-1982 20, 103–151.

Drysdale, R.N., Zanchetta, G., Hellstrom, J.C., Fallick, A.E., McDonald, J., Cartwright, I., 2007. Stalagmite evidence for the precise timing of North Atlantic cold events during the early last glacial. Geology 35, 77–80. doi:10.1130/G23161A.1.

Dunca, E., Mutvei, H., Göransson, P., Mörth, C.M., Schöne, B.R., Whitehouse, M.J., Elfman, M., Baden, S.P., 2009. Using ocean quahog (*Arctica islandica*) shells to reconstruct palaeoenvironment in Öresund, Kattegat and Skagerrak, Sweden. Int. J. Earth Sci. 98, 3–17. doi:10.1007/s00531-008-0348-6.

Dymond, J., Suess, E., Lyle, M., 1992. Barium in deep-sea sediment: A geochemical proxy for paleoproductivity. Paleoceanography 7, 163–181. doi:10.1029/92PA00181.

Eiríksson, J., Bartels-Jónsdóttir, H.B., Cage, A.G., Gudmundsdóttir, E.R., Klitgaard-Kristensen, D., Marret, F., Rodrigues, T., Abrantes, F., Austin, W.E.N., Jiang, H., Knudsen, K.-L., Sejrup, H.-P., 2006. Variability of the North Atlantic Current during the last 2000 years based on shelf bottom water and sea surface temperatures along an open ocean/shallow marine transect in western Europe. The Holocene 16, 1017–1029. doi:10.1177/0959683606hl991rp.

Eiríksson, J., Knudsen, K.L., Haflidason, H., Henriksen, P., 2000. Late-glacial and Holocene palaeoceanography of the North Icelandic shelf. J. Quat. Sci. 15, 23–42. doi:10.1002/(SICI)1099-1417(200001)15:1<23::AID-JQS476>3.0.CO;2-8.

Elliot, M., Welsh, K., Chilcott, C., McCulloch, M., Chappell, J., Ayling, B., 2009. Profiles of trace elements and stable isotopes derived from giant long-lived *Tridacna gigas* bivalves: Potential applications in paleoclimate studies. Palaeogeogr. Palaeoclimatol. Palaeoecol. 280, 132–142. doi:10.1016/j.palaeo.2009.06.007.

Epplé, V.M., Brey, T., Witbaard, R., Kuhnert, H., Pätzold, J., 2006. Sclerochronological records of *Arctica islandica* from the inner German Bight. The Holocene 16, 763–769. doi:10.1191/0959683606hl970rr.

Epstein, S., Buchsbaum, R., Lowestam, H.A., Urey, H.C., 1953. Revised carbonate-water isotopic temperature scale. Bull. Geol. Soc. Am. 64, 1315–1326.

Epstein, S., Lowenstam, H.A., 1953. Temperature-shell-growth relations of recent and interglacial Pleistocene shoal-water biota from Bermuda. J. Geol. 61, 424–438. doi:10.1086/626110.

Epstein, S., Buchsbaum, R., Lowenstam, H., Urey, H.C., 1951. Carbonate-water isotopic temperature scale. Bull. Geol. Soc. Am. 62, 417–426. doi:10.1130/0016-7606(1951)62[417:CITS]2.0.CO;2.

Erlenkeuser, H., 1976. 14C and 13C isotope concentration in modern marine mussels from sedimentary habitats. Naturwissenschaften 63, 338. doi:10.1007/BF01166971.

Esper, J., Cook, E.R., Schweingruber, F.H., 2002. Low-frequency signals tree-ring chronologies for past reconstructing temperature variability. Science 295, 2250–2253. doi:10.1126/science.1066208.

Esper, J., Krusic, P.J., Ljungqvist, F.C., Luterbacher, J., Carrer, M., Cook, E., Davi, N.K., Hartl-Meier, C., Kirdyanov, A., Konter, O., Myglan, V., Timonen, M., Treydte, K., Trouet, V., Villalba, R., Yang, B., Büntgen, U., 2016. Ranking of tree-ring based temperature reconstructions of the past millennium. Quat. Sci. Rev. 145, 134–151. doi:10.1016/j.quascirev.2016.05.009.

Fairchild, I.J., Smith, C.L., Baker, A., Fuller, L., Spötl, C., Mattey, D., McDermott, F., 2006. Modification and preservation of environmental signals in speleothems. Earth-Science Rev. 75, 105–153. doi:10.1016/j.earscirev.2005.08.003.

Fallon, S.J., McCulloch, M.T., Alibert, C., 2003. Examining water temperature proxies in Porites corals from the Great Barrier Reef: A cross-shelf comparison. Coral Reefs 22, 389–404. doi:10.1007/s00338-003-0322-5.

Folland, C.K., Parker, D.E., 1995. Correction of instrumental biases in historical sea surface temperature data. Q. J. R. Meteorol. Soc. 121, 319–367. doi:10.1256/smsqj.52205

Forbes, E., Hanley, S., 1853. A history of British mollusca and their shells. London. doi:http://dx.doi.org/10.5962/bhl.title.12672.

Foster, L.C., Finch, a. a., Allison, N., Andersson, C., Clarke, L.J., 2008. Mg in aragonitic bivalve shells: Seasonal variations and mode of incorporation in *Arctica islandica*. Chem. Geol. 254, 113–119. doi:10.1016/j.chemgeo.2008.06.007.

Foster, L.C., Allison, N., Finch, A.A., Andersson, C., 2009. Strontium distribution in the shell of the aragonite bivalve *Arctica islandica*. Geochemistry, Geophys. Geosystems 10. doi:10.1029/2007GC001915.

Freitas, P.S., Clarke, L.J., Kennedy, H., Richardson, C. A., Abrantes, F., 2006. Environmental and biological controls on elemental (Mg/Ca, Sr/Ca and Mn/Ca) ratios in shells of the king scallop *Pecten maximus*. Geochim. Cosmochim. Acta 70, 5119–5133. doi:10.1016/j.gca.2006.07.029.

Fritts, H.C., 1976. Tree rings and climate. Academic Press, London, 567 pp.

Fritts, H.C., Lofgren, G.R., Gordon, G.A., 1980. Past climate reconstructed from tree rings. J. Interdiscip. Hist. 10, 773–793.

Füllenbach, C.S., Schöne, B.R., Mertz-Kraus, R., 2015. Strontium/lithium ratio in aragonitic shells of *Cerastoderma edule* (Bivalvia) – A new potential temperature proxy for brackish environments. Chem. Geol. 417, 341–355. doi:10.1016/j.chemgeo.2015.10.030.

Gillanders, B.M., Munro, A.R., 2012. Hypersaline waters pose new challenges for reconstructing environmental histories of fish based on otolith chemistry. Limnol. Oceanogr. 57, 1136–1148. doi:10.4319/lo.2012.57.4.1136.

Gillikin, D.P., Dehairs, F., Lorrain, A., Steenmans, D., Baeyens, W., André, L., 2006. Barium uptake into the shells of the common mussel (*Mytilus edulis*) and the potential for estuarine paleo-chemistry reconstruction. Geochim. Cosmochim. Acta 70, 395–407. doi:10.1016/j.gca.2005.09.015.

Gillikin, D.P., Lorrain, A., Navez, J., Taylor, J.W., André, L., Keppens, E., Baeyens, W., Dehairs, F., 2005. Strong biological controls on Sr/Ca ratios in aragonitic marine bivalve shells. Geochemistry, Geophys. Geosystems 6. doi:10.1029/2004GC000874.

Gillikin, D.P., Lorrain, A., Paulet, Y.M., André, L., Dehairs, F., 2008. Synchronous barium peaks in high-resolution profiles of calcite and aragonite marine bivalve shells. Geo-Marine Lett. 28, 351–358. doi:10.1007/s00367-008-0111-9.

Goldberg, E.D., Arrhenius, G.O.S., 1958. Chemistry of Pacific pelagic sediments. Geochim. Cosmochim. Acta 13, 153–212. doi:10.1016/0016-7037(58)90046-2.

Gregg, W.W., Rousseaux, C.S., 2014. Decadal trends in global pelagic ocean chlorophyll: A new assessment integrating multiple satellites, in situ data, and models. J. Geophys. Res. C Ocean. 119, 5921–5933. doi:10.1002/2014JC010158.

Griffin, S.M., 2012. Applying dendrochronology visual crossdating techniques to the marine bivalve *Arctica islandica* and assessing the utility of master growth chronologies as proxies for temperature and secondary productivity in the Gulf of Maine. Unpublished Masters Thesis, Iowa State University, Ames, IA, 237 pp.

Grossman, E.L., Ku, T.-L., 1986. Oxygen and carbon isotope fractionation in biogenic aragonite: Temperature effects. Chem. Geol. Isot. Geosci. Sect. 59, 59–74. doi:10.1016/0168-9622(86)90057-6.

Hansen, B., Østerhus, S., 2000. North Atlantic–Nordic Seas exchanges. Prog. Oceanogr. 45, 109–208. doi:10.1016/S0079-6611(99)00052-X.

Hays, J.D., Imbrie, J., Shackleton, N.J.J., 1976. Variations in the Earth's orbit : Pacemaker of the Ice Ages. Science 194, 1121–1132. doi:10.1126/science.194.4270.1121.

Hetzinger, S., Halfar, J., Zack, T., Mecking, J. V., Kunz, B.E., Jacob, D.E., Adey, W.H., 2013. Coralline algal barium as indicator for 20th century northwestern North Atlantic surface ocean freshwater variability. Sci. Rep. 3, 1–8. doi:10.1038/srep01761.

Hiebenthal, C., Philipp, E.E.R., Eisenhauer, A., Wahl, M., 2012. Interactive effects of temperature and salinity on shell formation and general condition in Baltic Sea *Mytilus edulis* and *Arctica islandica*. Aquat. Biol. 14, 289–298. doi:10.3354/ab00405.

Holland, H.A., Schöne, B.R., Lipowsky, C., Esper, J., 2014. Decadal climate variability of the North Sea during the last millennium reconstructed from bivalve shells (*Arctica islandica*). The Holocene 24, 771–786. doi:10.1177/0959683614530438.

Holland, H.A., Schöne, B.R., Marali, S., Jochum, K.P., 2014. History of bioavailable lead and iron in the Greater North Sea and Iceland during the last millennium – A bivalve sclerochronological reconstruction. Mar. Pollut. Bull. 87, 104–116. doi:10.1016/j.marpolbul.2014.08.005.

Holmes, S.P., Witbaard, R., van der Meer, J., 2003. Phenotypic and genotypic population differentiation in the bivalve mollusc *Arctica islandica*: results from RAPD analysis. Mar. Ecol. Prog. Ser. 254, 163–176. doi:10.3354/meps254163.

Houghton, J.T., Meira Filho, L.G., Callander, B.A., Harris, N., Kattenberg, A., Maskell, K. (Eds.), 1996: Climate change 1995, the science of climate change; Contribution to assessment report of IPCC.

Houghton, J., Ding, Y., Griggs, D., Noguer, M., van der Linden, P., Dai, X., Maskell, K., Johnson, C.A. (Eds.), 2001. Climate change 2001: The scientific basis. Cambridge University Press. doi:10.1256/004316502320517344.

Huber, M., 2010. Compendium of Bivalves. ConchBooks, Hackenheim (901 pp).

Hudson, J.H., Shinn, E.A., Halley, R.B., Lidz, B., 1976. Sclerochronology: A tool for interpreting past environments. Geology 4, 361–364. doi:10.1130/0091-7613(1976)4<361:SATFIP>2.0.CO;2.

Hunt, C.P., Banerjee, S.K., Han, J., Solheid, P.A., Oches, E., Sun, W., Liu, T., 1995. Rock-magnetic proxies of climate change in the loess-paleosol sequences of the western Loess Plateau of China. Geophys. J. Int. 123, 232–244.

Hurrell, J.W., Trenberth, K.E., 1999. Global sea surface temperature analyses: Multiple problems and their implications for climate analysis, modeling, and reanalysis. Bull. Am. Meteorol. Soc. 80, 2661–2678. doi:10.1175/1520-0477(1999)080<2661:GSSTAM>2.0.CO;2.

IPCC, 2007. Summary for policymakers. *In:* Solomon, S., Qin, D., Manning, M., Chen, Z., Marquis, M., Averyt, K.B., Tignor, M., Miller, H.L. (Eds.), Climate change 2007: The physical science basis. Contribution of working group I to the fourth assessment report of the Intergovernmental Panel on Climate Change. Cambridge University Press, Cambridge, United Kingdom and New York, NY, USA, 18 pp.

IPCC, 2013. *In:* Stocker, T.F., Qin, D., Plattner, G.-K. , Tignor, M., Allen, S.K., Boschung, J., Nauels, A., Xia, Y., Bex V., Midgley, P.M. (Eds.), Climate Change 2013. The physical science basis. Contribution of working group I to the fifth assessment report of the Intergovernmental Panel on Climate Change. Cambridge University Press, Cambridge, United Kingdom and New York, NY, USA, 1535 pp.

IPCC, 2014. *In:* Core Writing Team, Pachauri, R.K., Meyer, L.A. (Eds.), Climate change 2014: Synthesis report. Contribution of working groups I, II and III to the fifth assessment Report of the Intergovernmental Panel on Climate Change. IPCC, Geneva, Switzerland, 151 pp.

Jamieson, R. A., Baldini, J.U.L., Frappier, A.B., Müller, W., 2015. Volcanic ash fall events identified using principal component analysis of a high-resolution speleothem trace element dataset. Earth Planet. Sci. Lett. 426, 36–45. doi:10.1016/j.epsl.2015.06.014.

Jiang, H., Eiríksson, J., Schulz, M., Knudsen, K.L., Seidenkrantz, M.S., 2005. Evidence for solar forcing of sea-surface temperature on the North Icelandic Shelf during the late Holocene. Geology 33, 73–76. doi:10.1130/G21130.1.

Jones, D.S., 1980. Annual cycle of shell growth increment formation in two continental shelf bivalves and its paleoecologic significance. Paleobiology 6, 331–340. doi:10.1017/S0094837300006837.

Jones, P.D., Mann, M.E., 2004. Climate over past millennia. Rev. Geophys. 42, 1–42. doi:10.1029/2003RG000143.CONTENTS.

Jones, P.D., Osborn, T.J., Briffa, K.R., 2001. The evolution of climate over the last millennium. Science 292, 662–667. doi:10.1126/science.1059126.

Jones, P.D., New, M., Parker, D.E., Martin, S., Rigor, I.G., 1999. Surface air temperature and its changes over the past 150 years. Rev. Geophys. 37, 173–199. doi:10.1029/1999RG900002.

Josefson, A.B., Jensen, J.N., Nielsen, T.G., Rasmussen, B., 1995. Growth parameters of a benthic suspension feeder along a depth gradient across the pycnocline in the southern Kattegat, Denmark. Mar. Ecol. Prog. Ser. 125, 107–115. doi:10.3354/meps125107.

Kamenos, N.A., Cusack, M., Moore, P.G., 2008. Coralline algae are global palaeothermometers with bi-weekly resolution. Geochim. Cosmochim. Acta 72, 771–779. doi:10.1016/j.gca.2007.11.019.

Keeley, S.P.E., Sutton, R.T., Shaffrey, L.C., 2012. The impact of North Atlantic sea surface temperature errors on the simulation of North Atlantic European region climate. Q. J. R. Meteorol. Soc. 138, 1774–1783. doi:10.1002/qj.1912.

Kennish, M.J., Lutz, R.A., Dobarro, J.A., Fritz, L.W., 1994. In situ growth rates of the ocean quahog, *Arctica islandica* (Linnaeus, 1767), in the Middle Atlantic Bight. J. Shellfish Res. 13, 473–478.

Kappas, M., 2009. Klimatologie. Klimaforschung im 21. Jahrhundert – Herausforderung für Natur- und Sozialwissenschaften, Springer Spektrum, 358 pp.

Knudsen, K.L., Eiríksson, J., Bartels-Jónsdóttir, H.B., 2012. Oceanographic changes through the last millennium off North Iceland: Temperature and salinity reconstructions based on foraminifera and stable isotopes. Mar. Micropaleontol. 84–85, 54–73. doi:10.1016/j.marmicro.2011.11.002.

Knudsen, K.L., Eiríksson, J., Jansen, E., Jiang, H., Rytter, F., Ruth Gudmundsdóttir, E., 2004. Palaeoceanographic changes off North Iceland through the last 1200 years: Foraminifera, stable isotopes, diatoms and ice rafted debris. Quat. Sci. Rev. 23, 2231–2246. doi:10.1016/j.quascirev.2004.08.012.

Langlet, D., Alleman, L.Y., Plisnier, P.-D., Hughes, H., André, L., 2007. Manganese content records seasonal upwelling in Lake Tanganyika mussels. Biogeosciences 4, 195–203. doi:10.5194/bg-4-195-2007.

Lea, D.W., Mashiotta, T.A., Spero, H.J., 1999. Controls on magnesium and strontium uptake in planktonic foraminifera determined by live culturing. Geochim. Cosmochim. Acta 63, 2369–2379. doi:10.1016/S0016-7037(99)00197-0.

Levitus, S., Antonov, J.I., Boyer, T.P., Stephens, C., 2000. Warming of the world ocean. Science 287, 2225–2229. doi:10.1126/science.287.5461.2225.

Lohmann, G., Schöne, B.R., 2013. Climate signatures on decadal to interdecadal time scales as obtained from mollusk shells (*Arctica islandica*) from Iceland. Palaeogeogr. Palaeoclimatol. Palaeoecol. 373, 152–162. doi:10.1016/j.palaeo.2012.08.006.

López Correa, M., Montagna, P., Joseph, N., Rüggeberg, A., Fietzke, J., Flögel, S., Dorschel, B., Goldstein, S.L., Wheeler, A., Freiwald, A., 2012. Preboreal onset of cold-water coral growth beyond the Arctic Circle revealed by coupled radiocarbon and U-series dating and neodymium isotopes. Quat. Sci. Rev. 34, 24–43. doi:10.1016/j.quascirev.2011.12.005.

Loulergue, L., Schilt, A., Spahni, R., Masson-Delmotte, V., Blunier, T., Lemieux, B., Barnola, J.-M., Raynaud, D., Stocker, T.F., Chappellaz, J., 2008. Orbital and millennial-scale features of atmospheric CH_4 over the past 800,000 years. Nature 453, 383–386. doi:10.1038/nature06950.

Lund, D.C., Lynch-Stieglitz, J., Curry, W.B., 2006. Gulf Stream density structure and transport during the past millennium. Nature 444, 601–604. doi:10.1038/nature05277.

Manabe, S., Stouffer, R., 2000. Study of abrupt climate change by a coupled ocean atmosphere model. Quat. Sci. Rev. 19, 285–299.

Mann, M.E., Zhang, Z., Hughes, M.K., Bradley, R.S., Miller, S.K., Rutherford, S., Ni, F., 2008. Proxy-based reconstructions of hemispheric and global surface temperature variations over the past two millennia. Proc. Natl. Acad. Sci. U. S. A. 105, 13252–13257. doi:10.1073/pnas.0805721105.

Mann, M.E., Zhang, Z., Rutherford, S., Bradley, R.S., Hughes, M.K., Shindell, D., Ammann, C., Faluvegi, G., Ni, F., 2009. Global signatures and dynamical origins of the Little Ice Age and Medieval Climate Anomaly. Science 326, 1256–1260. doi:10.1126/science.1166349.

Mann, R., 1982. The seasonal cycle of gonadal development in *Arctica islandica* from the Southern New England Shelf. Fish. Bull. 80, 315–326.

Mann, R., 1989. Larval ecology of *Arctica islandica* on the inner continental shelf of the eastern United States. *In:* Journal of Shellfish Research. p. 464. doi:10.2983/035.029.0302.

Marali, S., Schöne, B.R., Mertz-Kraus, R., Griffin, S.M., Wanamaker, A.D., Matras, U., Butler, P.G., 2017. Ba/Ca ratios in shells of *Arctica islandica* – Potential environmental proxy and crossdating tool. Palaeogeogr. Palaeoclimatol. Palaeoecol. 465, 347–361. doi:10.1016/j.palaeo.2015.12.018.

Marali, S., Wisshak, M., López Correa, M., Freiwald, A., 2013. Skeletal microstructure and stable isotope signature of three bathyal solitary cold-water corals from the Azores. Palaeogeogr. Palaeoclimatol. Palaeoecol. 373, 25–38. doi:10.1016/j.palaeo.2012.06.017.

Marchitto, T.M., Jones, G. A, Goodfriend, G. A, Weidman, C.R., 2000. Precise temporal correlation of Holocene mollusk shells using sclerochronology. Quat. Res. 53, 236–246. doi:10.1006/qres.1999.2107.

Marshall, J., Kushnir, Y., Battisti, D., Chang, P., Czaja, A., Dickson, R., Hurrell, J., McCartney, M., Saravanan, R., Visbeck, M., 2001a. Review North Atlantic climate variability: Phenomena, impacts and mechanisms. Int. J. Climatol. 21, 1863–1898. doi:10.1002/joc.693.

Marshall, J., Johnson, H., Goodman, J., 2001b. A study of the interaction of the North Atlantic Oscillation with ocean circulation. J. Clim. 14, 1399–1421. doi:10.1175/1520-0442(2001)014<1399:ASOTIO>2.0.CO;2.

Martinson, D.G., Pisias, N.G., Hays, J.D., Imbrie, J., Moore, T.C., Shackleton, N.J., 1987. Age dating and the orbital theory of the ice ages: Development of a high resolution 0 to 300,000 year chronostratigraphy. Quat. Res. 27, 1–29.

Matras, U., 2011. Annual variation in productivity on the Faroe Shelf during the 20th century. Havstovan 11-04, 1-19.

McCulloch, M., Taviani, M., Montagna, P., López Correa, M., Remia, A., Mortimer, G., 2010. Proliferation and demise of deep-sea corals in the Mediterranean during the Younger Dryas. Earth Planet. Sci. Lett. 298, 143–152. doi:10.1016/j.epsl.2010.07.036.

Merrill, A.S., Ropes, J.W., 1969. The general distribution of the surf clam and the ocean quahog. Proc. Natl. Shellfish. Assoc. 59, 40–45.

Mette, M.J., Wanamaker, A.D., Carroll, M.L., Ambrose, W.G., Retelle, M.J., 2016. Linking large-scale climate variability with *Arctica islandica* shell growth and geochemistry in northern Norway. Limnol. Oceanogr. 61, 748–764. doi:10.1002/lno.10252

Mitsuguchi, T., Matsumoto, E., Abe, O., Uchida, T., Isdale, P.J., 1996. Mg/Ca thermometry in coral skeletons. Science 274, 961–963. doi:10.1126/science.274.5289.961.

Montagna, P., McCulloch, M., Douville, E., López Correa, M., Trotter, J., Rodolfo-Metalpa, R., Dissard, D., Ferrier-Pagès, C., Frank, N., Freiwald, A., Goldstein, S., Mazzoli, C., Reynaud, S., Rüggeberg, A., Russo, S., Taviani, M., 2014. Li/Mg systematics in scleractinian corals: Calibration of the thermometer. Geochim. Cosmochim. Acta 132, 288–310. doi:10.1016/j.gca.2014.02.005.

Montagna, P., McCulloch, M., Mazzoli, C., Silenzi, S., Odorico, R., 2007. The non-tropical coral Cladocora caespitosa as the new climate archive for the Mediterranean: High-resolution (~weekly) trace element systematics. Quat. Sci. Rev. 26, 441–462. doi:10.1016/j.quascirev.2006.09.008.

Morton, B., 2011. The biology and functional morphology of *Arctica islandica* (Bivalvia: Arcticidae) – A gerontophilic living fossil. Mar. Biol. Res. 7, 540–553. doi:10.1080/17451000.2010.535833.

Murawski, S.A., Ropes, J.W., Serchuk, F.M., 1982. Growth of the ocean quahog, *Arctica islandica*, in the Middle Atlantic Bight. Fish. Bull. 80, 21–34.

Nicol, D., 1951. Recent species of the veneroid pelecypod *Arctica*. J. Washingt. Acad. Sci. 41, 102–106.

Oeschger, R., 1990. Long-term anaerobiosis in sublittoral marine invertebrates from the Western Baltic Sea: *Halicryptus spinulosus* (Priapulida), *Astarte borealis* and *Arctica islandica* (Bivalvia). Mar. Ecol. Prog. Ser. 59, 133–143. doi:10.3354/meps059133.

Oeschger, R., Storey, K.B., 1993. Impact of anoxia and hydrogen sulphide on the metabolism of *Arctica islandica* L. (Bivalvia). J. Exp. Mar. Bio. Ecol. 170, 213–226. doi:10.1016/0022-0981(93)90153-F.

O'Neil, D.D., Gillikin, D.P., 2014. Do freshwater mussel shells record road-salt pollution? Sci. Rep. 4, 6. doi:10.1038/srep07168.

Oschmann, W., 2009. Sclerochronology: Editorial. Int. J. Earth Sci. 98, 1–2. doi:10.1007/s00531-008-0403-3.

Palmer, T.N., Zhaobo, S., 2007. A modelling and observational study of the relationship between sea surface temperature in the North-West Atlantic and the atmospheric general circulation. Q. J. R. Meteorol. Soc. 111, 947–975. doi:10.1002/qj.49711147003.

Pannella, G., 1971. Fish otoliths: Daily growth layers and periodical patterns. Science 173, 1124–1127.

Poulain, C., Gillikin, D.P., Thébault, J., Munaron, J.M., Bohn, M., Robert, R., Paulet, Y.-M., Lorrain, A., 2015. An evaluation of Mg/Ca, Sr/Ca, and Ba/Ca ratios as environmental proxies in aragonite bivalve shells. Chem. Geol. 396, 42–50. doi:10.1016/j.chemgeo.2014.12.019.

Ran, L., Jiang, H., Knudsen, K.L., Eiríksson, J., 2011. Diatom-based reconstruction of palaeoceanographic changes on the North Icelandic shelf during the last millennium. Palaeogeogr. Palaeoclimatol. Palaeoecol. 302, 109–119. doi:10.1016/j.palaeo.2010.02.001.

Rhoads, D.C., Lutz, R.A. (Eds.), 1980. Skeletal growth of aquatic organisms. Biological records of environmental change. Plenum Press, New York and London, 750 pp.

Rodwell, M.J., Rowell, D.P., Folland, C.K., 1999. Oceanic forcing of the wintertime North Atlantic Oscillation and European climate. Nature 398, 320–323. doi:10.1038/18648.

Ropes, J.W., Jones, D.S., Murawski, S.A., Serchuk, F.M., Jearld, A., 1984. Documentation of annual growth lines in ocean quahogs, *Artica islandica* Linné. Fish. Bull. 82, 1–19.

Rosenberg, G.D., Jones, C.B., 1975. Approaches to chemical periodicities in molluscs and stromatolites. *In*: Rosenberg, G.D., Runcorn, S.K. (Eds.), Growth rhythms and the history of the Earth's rotation. London: Wiley, pp. 223–242.

Rucker, J.B., Valentine, J.W., 1961. Salinity response of trace element concentration in *Crassostrea virginica*. Nature 190, 1099–1100.

Ruddiman, W.F., 2008. Earth's Climate: Past and Future. 2nd ed., New York: H.H. Freeman, 388 pp.

Sano, Y., Kobayashi, S., Shirai, K., Takahata, N., Matsumoto, K., Watanabe, T., Sowa, K., Iwai, K., 2012. Past daily light cycle recorded in the strontium/calcium ratios of giant clam shells. Nat. Commun. 3. doi:10.1038/ncomms1763.

Scholz, D., Tolzmann, J., Hoffmann, D.L., Jochum, K.P., Spötl, C., Riechelmann, D.F.C., 2014. Diagenesis of speleothems and its effect on the accuracy of ^{230}Th/U-ages. Chem. Geol. 387, 74–86. doi:10.1016/j.chemgeo.2014.08.005.

Schöne, B.R., 2008. The curse of physiology—challenges and opportunities in the interpretation of geochemical data from mollusk shells. Geo-Marine Lett. 28, 269–285. doi:10.1007/s00367-008-0114-6.

Schöne, B.R., 2013. *Arctica islandica* (Bivalvia): A unique paleoenvironmental archive of the northern North Atlantic Ocean. Glob. Planet. Change 111, 199–225. doi:10.1016/j.gloplacha.2013.09.013.

Schöne, B.R., Lega, J., Flessa, K.W., Goodwin, D.H., Dettman, D.L., 2002. Reconstructing daily temperatures from growth rates of the intertidal bivalve mollusk *Chione cortezi* (northern Gulf of California, Mexico). Palaeogeogr. Palaeoclimatol. Palaeoecol. 184, 131–146.

Schöne, B.R., Freyre Castro, A.D., Fiebig, J., Houk, S.D., Oschmann, W., Kröncke, I., 2004. Sea surface water temperatures over the period 1884–1983 reconstructed from oxygen isotope ratios of a bivalve mollusk shell (*Arctica islandica*, southern North Sea). Palaeogeogr. Palaeoclimatol. Palaeoecol. 212, 215–232. doi:10.1016/j.palaeo.2004.05.024.

Schöne, B.R., Houk, S.D., Freyre Castro, A.D., Fiebig, J., Oschmann, W., 2005a. Daily growth rates in shells of *Arctica islandica*: Assessing sub-seasonal environmental controls on a long-lived bivalve mollusk. Palaios 20, 78–92. doi:10.2110/palo.2003.p03-101.

Schöne, B.R., Pfeiffer, M., Pohlmann, T., Siegismund, F., 2005b. A seasonally resolved bottom-water temperature record for the period AD 1866–2002 based on shells of *Arctica islandica* (Mollusca, North Sea). Int. J. Climatol. 25, 947–962. doi:10.1002/joc.1174.

Schöne, B.R., Fiebig, J., Pfeiffer, M., Gleß, R., Hickson, J., Johnson, A.L.A., Dreyer, W., Oschmann, W., 2005c. Climate records from a bivalved Methuselah (*Arctica islandica*, Mollusca; Iceland). Palaeogeogr. Palaeoclimatol. Palaeoecol. 228, 130–148. doi:10.1016/j.palaeo.2005.03.049.

Schöne, B.R., Zhang, Z., Jacob, D.E., Gillikin, D.P., Tütken, T., Garbe-Schönberg, D., McConnaughey, T., Soldati, A., 2010. Effect of organic matrices on the determination of the trace element chemistry (Mg, Sr, Mg/Ca, Sr/Ca) of aragonitic bivalve shells (*Arctica islandica*) — Comparison of ICP-OES and LA-ICP-MS data. Geochem. J. 44, 23–37.

Schöne, B.R., Radermacher, P., Zhang, Z., Jacob, D.E., 2013. Crystal fabrics and element impurities (Sr/Ca, Mg/Ca, and Ba/Ca) in shells of *Arctica islandica*–Implications for paleoclimate reconstructions. Palaeogeogr. Palaeoclimatol. Palaeoecol. 373, 50–59. doi:10.1016/j.palaeo.2011.05.013.

Shen, C.-C., Lee, T., Chen, C.-Y., Wang, C.-H., Dai, C.-F., Li, L.-A., 1996. The calibration of D[Sr/Ca] versus sea surface temperature relationship for *Porites* corals. Geochim. Cosmochim. Acta 60, 3849–3858.

Sicre, M.A., Jacob, J., Ezat, U., Rousse, S., Kissel, C., Yiou, P., Eiríksson, J., Knudsen, K.L., Jansen, E., Turon, J.L., 2008a. Decadal variability of sea surface temperatures off North Iceland over the last 2000 years. Earth Planet. Sci. Lett. 268, 137–142. doi:10.1016/j.epsl.2008.01.011.

Sicre, M.A., Yiou, P., Eiríksson, J., Ezat, U., Guimbaut, E., Dahhaoui, I., Knudsen, K.L., Jansen, E., Turon, J.L., 2008b. A 4500-year reconstruction of sea surface temperature variability at decadal time-scales off North Iceland. Quat. Sci. Rev. 27, 2041–2047. doi:10.1016/j.quascirev.2008.08.009.

Sinclair, D.J., Williams, B., Allard, G., Ghaleb, B., Fallon, S., Ross, S.W., Risk, M., 2011. Reproducibility of trace element profiles in a specimen of the deep-water bamboo coral *Keratoisis* sp. Geochim. Cosmochim. Acta 75, 5101–5121. doi:10.1016/j.gca.2011.05.012.

Sinclair, D.J., Kinsley, L.P.J., McCulloch, M.T., 1998. High resolution analysis of trace elements in corals by laser ablation ICP-MS. Geochim. Cosmochim. Acta 62, 1889–1901.

Sinclair, D., Sherwood, O., Risk, M., Hillaire-Marcel, C., Tubrett, M., Sylvester, P., McCulloch, M., Kinsley, L., 2005. Testing the reproducibility of Mg/Ca profiles in the deep-water coral *Primnoa resedaeformis*: putting the proxy through its paces. Cold-Water Corals Ecosyst. 1039–1060. doi:10.1007/3-540-27673-4_52.

Smith, J.E., Schwarcz, H.P., Risk, M.J., McConnaughey, T.A., Keller, N., 2000. Paleotemperatures from deep-sea corals: Overcoming "vital effects". Palaios 15, 25–32.

Smith, S. V., Buddemeier, R.W., Redalje, R.C., Houck, J.E., 1979. Strontium-calcium thermometry in coral skeletons. Science. 204, 404–407.

Soldati, A.L., Jacob, D.E., Glatzel, P., Swarbrick, J.C., Geck, J., 2016. Element substitution by living organisms: The case of manganese in mollusc shell aragonite. Sci. Rep. 6, 1–9. doi:10.1038/srep22514.

Spielhagen, R.F., Werner, K., Sørensen, S.A., Zamelczyk, K., Kandiano, E., Budeus, G., Husum, K., Marchitto, T.M., Hald, M., 2011. Enhanced modern heat transfer to the Arctic by warm Atlantic water. Science. 331, 450–453.

Stecher, H. a., Krantz, D.E., Lord, C.J., Luther, G.W., Bock, K.W., 1996. Profiles of strontium and barium in *Mercenaria mercenaria* and *Spisula solidissima* shells. Geochim. Cosmochim. Acta 60, 3445–3456. doi:10.1016/0016-7037(96)00179-2.

Steingrímsson, S.A., Thórarinsdóttir, G., 1995. Age structure, growth and size at sexual maturity in ocean quahog, *Arctica islandica* (Mollusca: Bivalvia), off NW-Iceland. ICES Document CM 1995/K: 54 17 pp.

Stott, K.J., Austin, W.E.N., Sayer, M.D.J., Weidman, C.R., Cage, a. G., Wilson, R.J.S., 2010. The potential of *Arctica islandica* growth records to reconstruct coastal climate in north west Scotland, UK. Quat. Sci. Rev. 29, 1602–1613. doi:10.1016/j.quascirev.2009.06.016.

Strahl, J., Brey, T., Philipp, E.E.R., Thorarinsdóttir, G., Fischer, N., Wessels, W., Abele, D., 2011. Physiological responses to self-induced burrowing and metabolic rate depression in the ocean quahog *Arctica islandica*. J. Exp. Biol. 214, 4223–4233. doi:10.1242/jeb.055178.

Strahl, J., Dringen, R., Schmidt, M.M., Hardenberg, S., Abele, D., 2011. Metabolic and physiological responses in tissues of the long-lived bivalve *Arctica islandica* to oxygen deficiency. Comp. Biochem. Physiol. - A Mol. Integr. Physiol. 158, 513–519. doi:10.1016/j.cbpa.2010.12.015.

Strom, A., Francis, R.C., Mantua, N.J., Miles, E.L., Peterson, D.L., 2005. Preserving low-frequency climate signals in growth records of geoduck clams (Panopea abrupta). Palaeogeogr. Palaeoclimatol. Palaeoecol. 228, 167–178. doi:10.1016/j.palaeo.2005.03.048.

Takesue, R.K., van Geen, A., 2004. Mg/Ca, Sr/Ca, and stable isotopes in modern and Holocene *Protothaca staminea* shells from a northern California coastal upwelling region. Geochim. Cosmochim. Acta 68, 3845–3861. doi:10.1016/j.gca.2004.03.021.

Taylor, A.C., 1976. The cardiac responses to shell opening and closure in the bivalve *Arctica islandica* (L.). J. Exp. Biol. 64, 751–759.

Teichert, S., Freiwald, A., 2014. Polar coralline algal $CaCO_3$-production rates correspond to intensity and duration of the solar radiation. Biogeosciences 11, 833–842. doi:10.5194/bg-11-833-2014.

Theede, H., Ponat, A., Hiroki, K., Schlieper, C., 1969. Studies on the resistance of

marine bottom invertebrates to oxygen-deficiency and hydrogen sulphide. Mar. Biol. 2, 325–337. doi:10.1007/BF00355712.

Thompson, I., Jones, D.S., Dreibelbis, D., 1980. Annual internal growth banding and life-history of the ocean quahog *Arctica islandica* (Mollusca, Bivalvia). Mar. Biol. 57, 25–34.

Thorarinsdóttir, G.G., Jacobson, L.D., 2005. Fishery biology and biological reference points for management of ocean quahogs (*Arctica islandica*) off Iceland. Fish. Res. 75, 97–106. doi:10.1016/j.fishres.2005.04.010.

Thorarinsdóttir, G.G., Steingrímsson, S.A., 2000. Size and age at sexual maturity and sex ratio in ocean quahog, *Arctica islandica* (Linnaeus, 1767), off northwest iceland. J. Shellfish Res. 19, 943–947. doi:10.2983/035.029.0302

Treble, P., Shelley, J.M.G., Chappell, J., 2003. Comparison of high resolution sub-annual records of trace elements in a modern (1911–1992) speleothem with instrumental climate data from southwest Australia. Earth Planet. Sci. Lett. 216, 141–153. doi:10.1016/S0012-821X(03)00504-1.

Turekian, K.K., Cochran, J.K., Nozaki, Y., Thompson, I., Jones, D.S., 1982. Determination of shell deposition rates of *Arctica islandica* from the New York Bight using natural ^{228}Ra and ^{228}Th and bomb-produced ^{14}C. Limnol. Oceanogr. 27, 737–741. doi:10.1371/journal.pone.0070106.

Urey, H.C., Lowenstam, H. a., Epstein, S., McKinney, C.R., 1951. Measurement of paleotemperatures and temperatures of the upper Cretaceous of England, Denmark, and the southeastern United States. Bull. Geol. Soc. Am. 62, 399–416. doi:10.1130/0016-7606(1951)62[399:MOPATO]2.0.CO;2.

Valdimarsson, H., Malmberg, S., 1999. Near-surface circulation in Icelandic waters derived from satellite tracked drifters. Rit Fiskid. 16, 23–39.

Vander Putten, E., Dehairs, F., Keppens, E., Baeyens, W., 2000. High resolution distribution of trace elements in the calcite shell layer of modern *Mytilus edulis*: Environmental and biological controls. Geochim. Cosmochim. Acta 64, 997–1011.

Visbeck, M., 2002. The ocean's role in Atlantic climate variability. Science 297, 2223–2224. doi:10.1175/2009JCLI2778.1.

Wanamaker, A.D., Kreutz, K.J., Wilson, T., Borns, H.W., Introne, D.S., Feindel, S., 2008. Experimentally determined Mg/Ca and Sr/Ca ratios in juvenile bivalve calcite for *Mytilus edulis*: Implications for paleotemperature reconstructions. Geo-Marine Lett. 28, 359–368. doi:10.1007/s00367-008-0112-8.

Wanamaker, A.D., Kreutz, K.J., Schöne, B.R., Maasch, K. A., Pershing, A.J., Borns, H.W., Introne, D.S., Feindel, S., 2009. A late Holocene paleo-productivity record in the western Gulf of Maine, USA, inferred from growth histories of the long-lived ocean quahog (*Arctica islandica*). Int. J. Earth Sci. 98, 19–29. doi:10.1007/s00531-008-0318-z.

Wanamaker, A.D., Kreutz, K.J., Schöne, B.R., Introne, D.S., 2011. Gulf of Maine shells reveal changes in seawater temperature seasonality during the Medieval Climate Anomaly and the Little Ice Age. Palaeogeogr. Palaeoclimatol. Palaeoecol. 302, 43–51. doi:10.1016/j.palaeo.2010.06.005.

Wanamaker Jr, A.D., Butler, P.G., Scourse, J.D., Heinemeier, J., Eiríksson, J., Knudsen, K.L., Richardson, C.A., 2012. Surface changes in the North Atlantic meridional overturning circulation during the last millennium. Nat. Commun. 3, 237–252. doi:10.1038/ncomms1901.

Wanner, H., Brönnimann, S., Casty, C., Gyalistras, D., Luterbacher, J., Schmutz, C., Stephenson, D.B., Xoplaki, E., 2001. North Atlantic Oscillation – Concepts and studies. Surv. Geophys. 22, 321–382. doi:10.1023/A:1014217317898.

Warter, V., Müller, W., 2017. Daily growth and tidal rhythms in Miocene and modern giant clams revealed via ultra-high resolution LA-ICPMS analysis – A novel methodological approach towards improved sclerochemistry. Palaeogeogr. Palaeoclimatol. Palaeoecol. 465, 362–375. doi:10.1016/j.palaeo.2016.03.019.

Weidman, C.R., Jones, G.A., Kyger, 1994. The long-lived mollusk *Arctica islandica*: A new paleoceanographic tool for the reconstruction of bottom temperatures for the continental shelves of the northern North Atlantic Ocean. J. Geophys. Res. 99, 18,305-18,314. doi:10.1029/94JC01882.

Weiner, S., Dove, P.M., 2003. An overview of biomineralization processes and the problem of the vital effect. *In:* Dove, P.M., Weiner, S., deYoreo, J.J. (Eds.). Biomineralization. Reviews in Mineralogy and Geochemistry, 54, 1–29. doi:10.2113/0540001.

Wigley, T.M.L., Briffa, K.R., Jones, P.D., 1984. On the average value of correlated time series, with applications in dendroclimatology and hydrometeorology. J. Clim. Appl. Meteorol. 23, 201–213. doi:10.1175/1520-0450(1984)023<0201:OTAVOC>2.0.CO;2.

Winter, J.E., 1969. Über den Einfluß der Nahrungskonzentration und anderer Faktoren auf Filtrierleistung und Nahrungsausnutzung der Muscheln *Arctica islandica* und Modiolus modiolus. Mar. Biol. 4, 87–135. doi:10.1007/BF00347037.

Wit, J.C., De Nooijer, L.J., Wolthers, M., Reichart, G.J., 2013. A novel salinity proxy based on na incorporation into foraminiferal calcite. Biogeosciences 10, 6375–6387. doi:10.5194/bg-10-6375-2013.

Witbaard, R., Duineveld, G.C.A., De Wilde, P.A.W.J., 1997. A long-term growth record derived from *Arctica islandica* (Mollusca, Bivalvia) from the Fladen Ground (northern North Sea). J. Mar. Biol. Assoc. United Kingdom 77, 801–816. doi:10.1017/S0025315400036201.

Witbaard, R., Duineveld, G.C.A., de Wilde, P.A.W.J., 1999. Geographical differences in growth rates of *Arctica islandica* (Mollusc: Bivalvia) from the North Sea and adjacent waters. J. Mar. Biol. Assoc. United Kingdom 79, 907–915.

Witbaard, R., Jenness, M.I., Van Der Borg, K., Ganssen, G., 1994. Verification of annual growth increments in *Arctica islandica* L. from the North Sea by means of oxygen and carbon isotopes. Netherlands J. Sea Res. 33, 91–101. doi:10.1016/0077-7579(94)90054-X.

Witbaard, R., 1996. Growth variations in *Arctica islandica* L. (Mollusca): a reflection of hydrography-related food supply. ICES J. Mar. Sci. 53, 981–987.

Wooller, M., Wang, Y., Axford, Y., 2008. A multiple stable isotope record of Late Quaternary limnological changes and chironomid paleoecology from northeastern Iceland. J. Paleolimnol. 40, 63–77. doi:10.1007/s10933-007-9144-8.

Woollings, T., Hoskins, B., Blackburn, M., Hassell, D., Hodges, K., 2010. Storm track sensitivity to sea surface temperature resolution in a regional atmosphere model. Clim. Dyn. 35, 341–353. doi:10.1007/s00382-009-0554-3.

Zerefos, C.S., Tetsis, P., Kazantzidis, A., Amiridis, V., Zerefos, S.C., Luterbacher, J., Eleftheratos, K., Gerasopoulos, E., Kazadzis, S., Papayannis, A., 2014. Further evidence of important environmental information content in red-to-green ratios as depicted in paintings by great masters. Atmos. Chem. Phys. 14, 2987–3015. doi:10.5194/acp-14-2987-2014.

Appendix

Curriculum vitae

The curriculum vitae is not displayed for reasons of data protection.

Peer-reviewed publications

Marali, S., Schöne, B.R., Mertz-Kraus, R., Griffin, S.M., Wanamaker, A.D., Butler, P.G., Holland, H.A., Jochum, K.P., 2017 (in press). Reproducibility of trace element time-series (Na/Ca, Mg/Ca, Mn/Ca, Sr/Ca, and Ba/Ca) within and between specimens of the bivalve *Arctica islandica* – A LA-ICP-MS line scan study. Palaeogeogr. Palaeoclimatol. Palaeoecol. doi:10.1016/j.palaeo.2016.11.024.

Marali, S., Schöne, B.R., Mertz-Kraus, R., Griffin, S.M., Wanamaker, A.D., Matras, U., Butler, P.G., 2017. Ba/Ca ratios in shells of *Arctica islandica* – Potential environmental proxy and crossdating tool. Palaeogeogr. Palaeoclimatol. Palaeoecol. 465, 347–361. doi:10.1016/j.palaeo.2015.12.018.

Lindauer, S., Marali, S., Schöne, B.R., Uerpmann, H.-P., Kromer, B., Hinderer, M. 2017 (in press). Investigating the local reservoir effect and stable isotopes of shells from South-East Arabia. Radiocarbon, doi:10.1017/RDC.2016.80.

Marali, S., Schöne, B.R., 2015. Oceanographic control on shell growth of *Arctica islandica* (Bivalvia) in surface waters of Northeast Iceland – Implications for paleoclimate reconstructions. Palaeogeogr. Palaeoclimatol. Palaeoecol. 420, 138–149. doi:10.1016/j.palaeo.2014.12.016.

Holland, H. A., Schöne, B.R., Marali, S., Jochum, K.P., 2014. History of bioavailable lead and iron in the Greater North Sea and Iceland during the last millennium – A bivalve sclerochronological reconstruction. Mar. Pollut. Bull. 87, 104–116. doi:10.1016/j.marpolbul.2014.08.005.

Marali, S., Wisshak, M., López Correa, M., Freiwald, A., 2013. Skeletal microstructure and stable isotope signature of three bathyal solitary cold-water corals from the Azores. Palaeogeogr. Palaeoclimatol. Palaeoecol. 373, 25–38. doi:10.1016/j.palaeo.2012.06.017.

Conference contributions

Oral presentations

Marali, S., Schöne, B.R., 2015. Oceanographic conditions govern shell growth of *Arctica islandica* (Bivalvia) in surface waters off Northeast Iceland. 10th Geophysical Research Abstracts 17, EGU2015-6318-2, EGU General Assembly 2015, 12-17 April 2015, Vienna, Austria.

Marali, S., Wisshak, M., López Correa, M., Montagna, P., McCulloch, M., Freiwald, A., 2010. Skeletal and geochemical properties of scleractinian cold-water corals from the Azores. 2nd International Sclerochronology conference, July 2010, Mainz, Germany.

Posters

Schöne, B.R, Holland, H.A., Marali, S., Jochum, K.P., 2014. History of bioavailable lead and iron in the greater North Sea and Iceland during the last millennium – A story told by bivalves. Geological Society of America, Annual Meeting Vancouver 2014, 43-11, 210.

Marali, S., Schöne, B.R, 2013. A sclerochronological analysis of the bivalve *Arctica islandica* from northeastern Iceland. 3rd International Sclerochronology Conference, ISC2013, May 2013, Caernarfon, UK.

Marali, S., Wisshak, M., López Correa, M., Freiwald, A., 2012. Aragonitic cold-water corals as geochemical archives of ocean temperature. 100th Annual meeting of the German Paleontological Society, September 2012, Berlin, Germany.

Marali, S., Wisshak, M., López Correa, M., Montagna, P., McCulloch, M., Freiwald, A., 2012. Major and trace elements in recent solitary cold-water corals from the Azores archipelago.- 5th International Deep-Sea Coral Symposium, April 2012, Amsterdam, Netherlands.